TECHNISCHE UNIVERSITÄT MÜNCHEN

Lehrstuhl für Physiologie

Molecular pathomechanisms of ABCA3 mutations causing interstitial lung disease in children

Eva Kaltenborn

Vollständiger Abdruck der von der Fakultät Wissenschaftszentrum Weihenstephan für Ernährung, Landnutzung und Umwelt der Technischen Universität München zur Erlangung des akademischen Grades eines

Doktors der Naturwissenschaften

genehmigten Dissertation.

Vorsitzender: Univ.-Prof. Dr. D. Langosch

Prüfer der Dissertation:

1. Priv.-Doz. Dr. S. E. Ulbrich
2. apl. Prof. Dr. M. Griese
   (Ludwig-Maximilians-Universität München)
3. Univ.-Prof. Dr. H. Witt

Die Dissertation wurde am 20.08.2012 bei der Technischen Universität München eingereicht und durch die Fakultät Wissenschaftszentrum Weihenstephan für Ernährung, Landnutzung und Umwelt am 27.05.2013 angenommen.

Acknowledgments

I am very grateful to my supervisor Prof. Dr. med. Matthias Griese (Group Pneumology I, Research Center Kubus, Dr. von Hauner Children's Hospital) for providing an interesting PhD project. He always allowed for great scientific freedom, respected my ideas and supported the work in progress with helpful scientific discussions.

I would like to thank the late Prof. Heinrich H. D. Meyer for his interest in my PhD thesis and for his constructive criticism inspite of his severe disease. I also would like to thank PD Susanne E. Ulbrich and Prof. Heiko Witt for their interest in my thesis and their willingness to act as reviewers of my thesis on short notice.

I thank Prof. Karl-Klaus Conzelmann from the LMU Gene Center for his cooperation and Dr. Laetitia Fragnet for her excellent introduction into handling RSV and for her help with the virus experiments. I also thank Prof. Matthias Ochs for his cooperation with the TEM images, Dr. Gerhard Liebisch for his cooperation with the mass spectrometric lipid analysis, and Dr. Philipp Pagel for the processing of the raw microarray data.

I wish to thank our Postdocs Sunčana Kern and Ralf Zarbock for their help with my projects, always inspiring scientific discussions and very fun times in the lab.

Susan Franke, Traudl Wesselak and Sabrina Frixel I would like to thank for supporting talks, very enjoyable coffee breaks and all the fun times outside of Kubus.

I thank Kathrin Schiffl, Karin Idzikowski, Claudia Bräu-Heberger and Andrea Schams for excellent technical assistance during my PhD time.

I thank Manuel J. Deutsch for providing the method to analyze lipid droplets and for all the other helpful advices and discussions.

I am grateful to Corinna for proofreading my thesis and to her, Julia and Sonja for their friendship.

Many thanks to all co-workers from the Kubus labs for providing a very nice working atmosphere.

Special thanks to my boyfriend Frederik and to my parents for all their love, for their patience and for their support and assistance during my PhD time.

Index of contents

Index of figures

Index of tables

1 Summary

ABCA3 is a surfactant lipid transporter expressed in alveolar type II cells (ATII) where it is localized to the outer membrane of lamellar bodies. Defects in ABCA3 cause respiratory distress in newborns and interstitial lung disease (ILD) in older children and adults. However, the precise cellular disease-causing mechanisms are so far unknown.

In this thesis, A549 cells which serve as model system for ATII were stably transfected with vectors coding for ABCA3-WT and the clinically relevant mutations p.Q215K and p.E292V. ABCA3 mutations reduced the expression of epithelial proteins such as the ATII marker surfactant protein C (SP-C) as well as the cell adhesion molecules E-cadherin and ZO-1 while simultaneously upregulating the expression of the mesenchyme-associated proteins SNAI1, ET-1, MMP-2 and TGF-β1. Moreover, phosphorylation of Src kinase was increased in these cells. Infection with the respiratory syncytial virus (RSV) potentiated most of the observed effects and induced a phenotype resembling fibroblasts as well as phosphorylation of ERK and JNK kinases in cells harboring ABCA3 mutations. Therefore, RSV infection as a second hit induces a process resembling epithelial-mesenchymal transition (EMT) depending on the presence of ABCA3 mutations, thereby leading to decreased epithelial integrity and function, possibly mediated by signaling via TGF-β1, Src, ERK and JNK.

Since ABCA3 is a lipid transporter, the cellular lipid profiles were investigated and some differences between A549 cells harboring ABCA3-WT and mutations were observed. Besides, ABCA3 mutations induced accumulation of enlarged lipid droplets which are storage vesicles for neutral lipids, i.e. cholesterol esters. Concordantly, the absolute amount of cholesterol esters was elevated in cells harboring ABCA3 mutations. Moreover, expression of ABCA1, a cholesterol transporter involved in reverse cholesterol transport to HDL, was increased in ABCA3-mutant cell lines. Additionally, ABCA3 mutations induced a strong reduction of TLR-3 and TLR-4 expression as well as IL-6 and IL-8 expression and secretion. In line with these results, NF-κB activity was decreased in these cells. Cells harboring ABCA3 mutations were also less susceptible to stimulation with *Pseudomonas aeruginosa* LPS.

In conclusion, ABCA3 mutations strongly impair normal alveolar epithelial cell function by interfering with the epithelial integrity and cellular cholesterol homeostasis and by reducing the production of pro-inflammatory mediators. These results may present a mechanism by which ABCA3 mutations predispose to the development of ILD.

1 Zusammenfassung

ABCA3 ist ein Surfactantlipidtransporter, der in alveolaren Typ II Zellen (ATII) exprimiert wird und dort in der äußersten Membran von Lamellarkörperchen lokalisiert ist. ABCA3-Defekte verursachen ein Atemnotsyndrom bei Neugeborenen sowie interstitielle Lungenerkrankungen (ILD) in älteren Kindern und Erwachsenen. Die zugrundeliegenden Mechanismen sind bisher unbekannt.

In dieser Arbeit wurden A549 Zellen als Modellsystem für ATII genutzt und stabil mit Vektoren, welche für ABCA3-WT und die klinisch-relevanten Mutationen p.Q215K und p.E292V kodieren, transfiziert. ABCA3-Mutationen verringerten die Expression epithelialer Proteine, wie die des ATII Markers Surfactantprotein C (SP-C) sowie die der Zelladhäsionsproteine E-Cadherin und ZO-1, und führten gleichzeitig zu gesteigerter Expression der Mesenchym-assoziierten Proteine SNAI1, ET-1, MMP-2 und TGF-β1. Zusätzlich führten ABCA3-Mutationen zu einer verstärkten Phosphorylierung der Kinase Src in diesen Zellen. Eine Infektion mit dem Respiratorisches Syncytial Virus (RSV) verstärkte die meisten beobachteten Effekte und induzierte zudem einen Fibroblasten-ähnlichen Phänotyp sowie die Phosphorylierung der Kinasen ERK und JNK in Zellen mit ABCA3-Mutationen. Eine RSV-Infektion als zusätzlicher Krankheitsfaktor führt daher zu einem Prozess, welcher der Epithel-Mesenchym-Transition (EMT) ähnelt und von einer Prädisposition mit ABCA3-Mutationen abhängig ist. Durch die EMT kommt es zu einer Abnahme der epithelialen Integrität und Funktion, was vermutlich durch TGF-β1, Src, ERK und JNK-abhängige Signalwege vermittelt wird.

Da ABCA3 ein Lipidtransporter ist, wurden die zellulären Lipidzusammensetzungen untersucht und es wurden einige Änderungen zwischen Zellen mit ABCA3-WT und Mutationen festgestellt. Zudem verursachten ABCA3-Mutationen eine Ansammlung von vergrößerten Lipidtröpfchen, in welchen Neutrallipide wie Cholesterinester abgelagert werden. Damit übereinstimmend war die absolute Menge an Cholesterinestern in Zellen mit ABCA3-Mutationen gesteigert. Außerdem war die Expression von ABCA1, einem Cholesterintransporter, der an reversem Cholesterintransport zu HDL beteiligt ist, in ABCA3-Mutationszelllinien erhöht. Zusätzlich induzierten ABCA3-Mutationen eine starke Abnahme der TLR-3 und TLR-4 Expression sowie der IL-6 und IL-8 Expression und Sezernierung. Im Einklang mit diesen Ergebnissen war die NF-κB-Aktivität in den ABCA3-Mutationszellen vermindert. Des Weiteren waren Zellen, in denen ABCA3-

Mutationen exprimiert wurden, weniger anfällig gegenüber einer Stimulation mit *Pseudomonas aeruginosa* LPS.

Aus den oben genannten Ergebnissen kann geschlussfolgert werden, dass ABCA3-Mutationen die epitheliale Zellfunktion stark beeinträchtigen, indem sie die epitheliale Integrität sowie die zelluläre Cholesterinhomöostase stören und die Produktion pro-inflammatorischer Mediatoren verringern. Diese Ergebnisse könnten einen Mechanismus darstellen, durch den ABCA3-Mutationen zum Auslösen einer ILD beitragen können.

2 Introduction

2.1 Alveolar cells and surfactant

In the lung, air is conducted by the bronchial system to approximately 300 million alveolar sacs for gas exchange [1]. The alveoli are lined by highly specialized cells, the alveolar type I (ATI) and type II (ATII) cells (Figure 2.1 A). The flattened, non-dividing ATI cells comprise more than 90 % of the alveolar surface and are important for gas exchange between the air in the alveolar space and the alveolar capillaries. The cuboidal ATII cells are only present in fewer numbers compared to ATI cells and they are specialized for storage and secretion of surfactant into the alveolar space. Surfactant is a highly surface active material, which prevents alveolar collapse at the end of expiration by lowering the surface tension. Surfactant is composed of approximately 90 % lipids and 10 % proteins (mainly surfactant proteins (SP)-A, SP-B, SP-C, SP-D, as well as serum derived proteins) [2, 3]. Most of the surfactant lipids are phospholipids (PL) and the main phospholipid species present are phosphatidylcholin (PC) and phosphatidylglycerol (PG) [4]. The most abundant phospholipid in human surfactant is dipalmitoyl-PC (DPPC, ~ 40 % of total PC) [4]. Next to phospholipids, surfactant also consists of some neutral lipids (~10 %), the most abundant being cholesterol [2].

Besides being important for the proper structural organization of surfactant after secretion into the alveolar space, the surfactant proteins SP-A and SP-D have important functions in the immunological defense by means of opsonization of microorganisms, binding and capture of bacterial toxins and activation of immune cells [2]. SP-A was shown to bind both the respiratory syncytial virus (RSV) F and G-proteins, thereby increasing RSV uptake by monocytes, and SP-A knockout mice were found to have impaired clearance of RSV from the lungs [5-7]. SP-D is capable of binding to the viral G-protein and inhibiting RSV infection [8]. The hydrophobic proteins SP-B and SP-C both increase the adsorption rate of phospholipids at the liquid-air interface, thereby accelerating the formation of a surface-active film [2].

In ATII, surfactant lipids as well as SP-B and SP-C are stored in specialized organelles, the lamellar bodies (LBs). The 150 ± 30 LBs per ATII cell are thought to originate from endosomes/lysosomes by redistribution of phospholipids and fusion, resulting in formation of immature, intermediate multivesicular bodies (MVBs) and composite bodies (Figure 2.1 B) [9, 10]. LBs consist of tightly packed membranes organized in a concentric fashion [9]. Deficiencies in surfactant protein B lead to the formation of MVBs which are not

processed into mature LBs and do not store functional surfactant while defects in SP-C do not impair LB biogenesis [11-13]. Transport of surfactant lipids into the LB is likely mediated by ABC-transporters, especially ABCA3 [14].

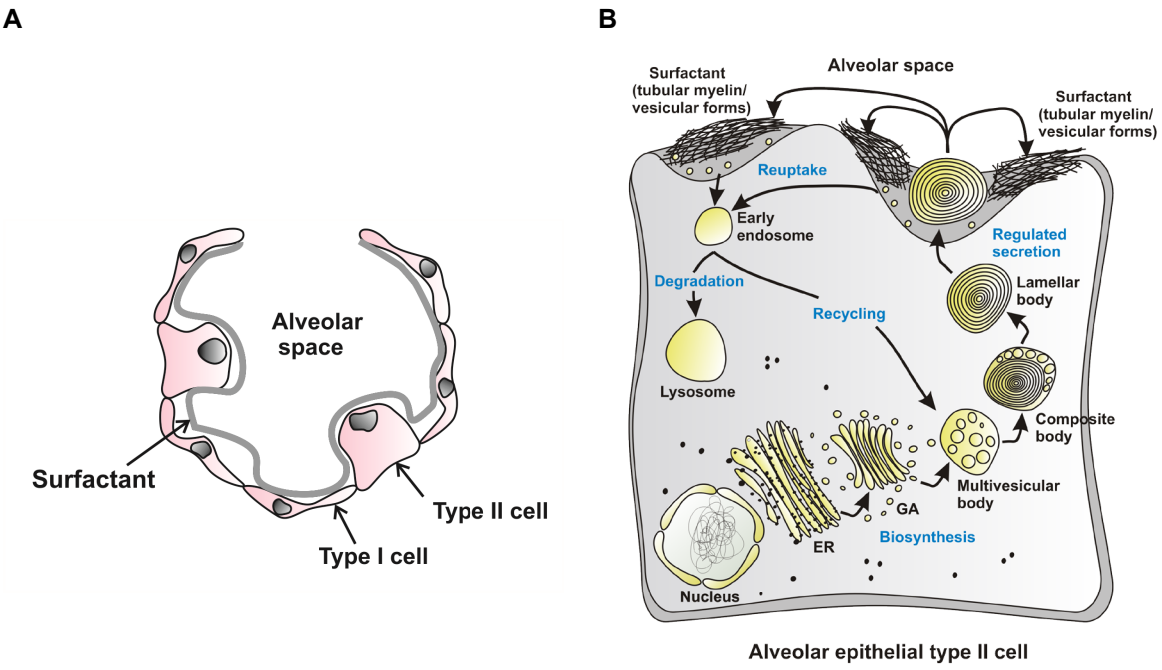

Figure 2.1: Model of a pulmonary alveolus (A), and of lamellar body biogenesis and surfactant secretion in ATII cells (B).
Figures adapted from Sunčana Kern.

Fusion of LBs with the plasma membrane and subsequent secretion of stored surfactant components is regulated by a variety of stimuli including the mechanical stretching of ATII cells, as results from the intake of breath [10]. In the rat lung, an average of 15 LBs is secreted from ATII cells per hour [15]. After secretion of surfactant components into the alveolar space, they organize into defined forms, either tubular myelin or vesicular structures, depending on the presence of surfactant lipids and proteins or physical conditions during respiration [1]. From the highly ordered tubular myelin lattice, phospholipids can easily adsorb to the liquid-air interface to form a functional surfactant film [2]. Surfactant from the alveolar space can either be recycled into type II pneumocytes or it can be taken up by alveolar macrophages, with both mechanisms being precisely regulated to maintain appropriate surfactant levels at all times.

Besides being the sole source for storage and secretion of pulmonary surfactant, ATII cells have several other important functions. In case of lung injury, they might transdifferentiate into ATI to repair damage to the alveolar epithelium [16]. Additionally, ATII cells express pattern recognition receptors which are activated in response to invasion of respiratory

pathogens [17]. The subsequent receptor induced intracellular signaling causes expression and secretion of pro-inflammatory cytokines and chemokines, leading in turn to an immune response involving activation of leukocytes which help clearing the pathogens from the lung.

2.2 Interstitial lung diseases in children and adults

Interstitial lung diseases (ILD), also known as diffuse parenchymal lung diseases (DPLD), encompass a heterogeneous group of chronic respiratory disorders of both known and unknown causes and are characterized by significant morbidity and mortality [18, 19]. The known causes include antigens (bird, fungi) in case of exogen allergic pneumonitis, some respiratory infections like Mycoplasma or Hepatitis C virus, or other environmental toxins like beryllium or cigarette smoke; however, the majority of the disease cases are idiopathic [20]. ILDs in children (chILDs) are very rare compared to adult ILDs with an estimated prevalence of 0.36 cases / 100 000 in Ireland and the UK and an incidence of 0.13 cases / 100 000 in Germany [18, 21]. It was suggested to consider pediatric ILD as a syndrome characterized by tachypnea, crackles, hypoxemia and/or diffuse infiltrates on chest radiograph [22]. ILD in older children has more resemblance to ILD in adults compared to ILD in infants. In contrast to adult idiopathic interstitial pneumonias (IIPs), a comprehensive classification of pediatric ILD was not available until recently, when a committee of experts in the field established a new classification scheme for ILD in children from 0-2 years [19, 23]. The disorders affecting these children were classified into two groups, (1) disorders more prevalent in infancy and (2) disorders occurring at all ages. Disorders more prevalent in infancy include “diffuse developmental disorders”, “growth abnormalities reflecting deficient alveolarization”, “specific conditions of undefined etiology”, such as neuroendocrine cell hyperplasia of infancy and pulmonary interstitial glycogenosis and “surfactant dysfunction disorders”, caused by mutations in *SFTPB*, *SFTPC, NKX1 (TTF-1)* and *ABCA3* [19]. Disorders which occur at all ages relate to “systemic diseases”, to the “immune intact host”, to the “immunocompromised host” and to “disorders masquerading as ILD”.

ILD-associated diseases in general are characterized by inflammatory responses and fibrotic changes in the interstitium between the epithelial and endothelial basement membranes as well as in the distal airways and vessels [23]. The idiopathic interstitial pneumonias in adults comprise amongst others idiopathic pulmonary fibrosis (IPF), nonspecific interstitial pneumonia (NSIP) and desquamative interstitial pneumonia (DIP)

[23]. Patients with IPF are usually above the age of 50, have an abnormal pulmonary function with impaired gas exchange and >80 % present with cough, dyspnea and Velcro-type end-inspiratory crackles on chest auscultation and additionally, almost all have abnormal chest radiographs [20]. 25-50 % of the IPF patients suffer from clubbing. IPF is believed to result from injury to the alveolar epithelium and basement membrane with impaired re-epithelialization and with production as well as secretion of excess amounts of extracellular matrix (ECM) components by fibroblasts. Viral infections, including herpes virus, hepatitis C virus, Epstein-Barr virus and cytomegalovirus, have been implicated in the initiation and exacerbation of IPF [24, 25].

2.3 RSV

The respiratory syncytial virus is one of the most common respiratory pathogens infecting almost all children up to the age of two at least once. RSV infection is a common cause for pediatric bronchiolitis and pneumonia [26]. RSV belongs to the family of *Paramyxoviridae*, subfamily *Pneumovirinae*, which are enveloped viruses with a non-segmented, negative-sense single-stranded RNA genome [27]. The RSV genome is composed of 10 genes coding for 11 proteins [27, 28]. Three of these proteins, the fusion (F), the attachment (G) and the small hydrophobic (SH) protein are located in the lipid envelope surrounding the virion and are responsible for virus attachment and entry into the host cell (Figure 2.2). The nucleocapsid (N) protein, the phosphoprotein (P) and the large (L) polymerase protein are needed for viral replication. Moreover, the virus genome encodes for the envelope associated matrix (M) protein, two M2 proteins and two non-structural proteins (NS1, NS2).

RSV infection of cell or tissue cultures might induce the formation of large cytopathic syncytia, depending on the tissue or cell type, hence the virus name [29]. Expression of the viral fusion protein as well as cytokeratin 17 in the infected host cells are implicated in syncytia formation, however the precise mechanisms have not yet been identified [27, 30, 31].

The RSV infection usually has a mild to moderate outcome in otherwise healthy subjects but does not result in prolonged immunity so that lifelong re-infections are possible [32, 33]. The estimated mortality from primary RSV infection among otherwise healthy children is 0.005 to 0.020 % [33]. However in some children, the elderly, transplant recipients, the immuno-compromised or patients with severe lung disease, RSV may cause severe, life-threatening forms of lower respiratory tract infection [33, 34]. Viral replication

in immunocompromised individuals for example may continue for month after initial contact with RSV [35, 36].

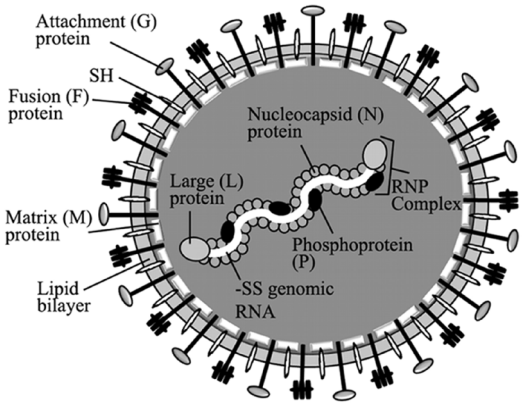

Figure 2.2: RSV structure.
Figure from Empey 2010 [37].

RSV infection induces expression or intracellular re-localization of several toll-like receptors (TLRs), including TLR-2, TLR-3, TLR-4 and TLR-6 [38-40]. The viral F protein for example was shown to interact with TLR-4 which sensitizes lung epithelial cells subsequent to LPS-dependent bacterial stimulation [39, 41]. Activation of the endosomally located TLR-3 was found to be regulated by double-stranded RNA which is synthesized as an intermediate during RSV replication [40]. TLR activation subsequently induces intracellular signaling pathways, leading to increased release of pro-inflammatory and immunoregulatory cytokines and chemokines from alveolar cells, some of which are implicated in chemotaxis and recruitment of eosinophils and neutrophils to the site of infection [27]. In cell culture model systems, RSV induced gene expression of RANTES, MIP-1α, IL-6, IL-8, IL-11, IL-1β, TNF-α and IFN-α and -β as soon as 4 h after virus inoculation [42]. The primary chemokine secreted from lung epithelial cells for attraction of neutrophils is IL-8 [42]. The first 6 days after inoculation, neutrophil invasion of the airways was observed in RSV infected mice. Monocyte numbers reached maximum between days 3 to 11 after RSV infection, whereas overall low lymphocyte numbers peaked around day 11 in bronchial alveolar lavage fluid (BALF) of RSV infected mice [43].

2.4 ABC-transporters

ABC transporters make up one of the biggest protein families and are ubiquitously expressed in bacteria, plants and animals [44, 45]. Under the expense of ATP hydrolysis, they transport a wide variety of substances, including lipids, ions, carbohydrates and xenobiotics, across otherwise impermeable biological membranes [46].

Functional ABC transporters are usually composed of four domains, two transmembrane domains (TMDs) which allow for recognition and transport of the substrate, and two nucleotide binding domains (NBDs) which bind and hydrolyze ATP [44]. All domains may be expressed on separate polypeptides with the subunits interacting by means of non-covalent binding, or two or more domains may be present on one polypeptide chain to form one single protein (Figure 2.3) [44].

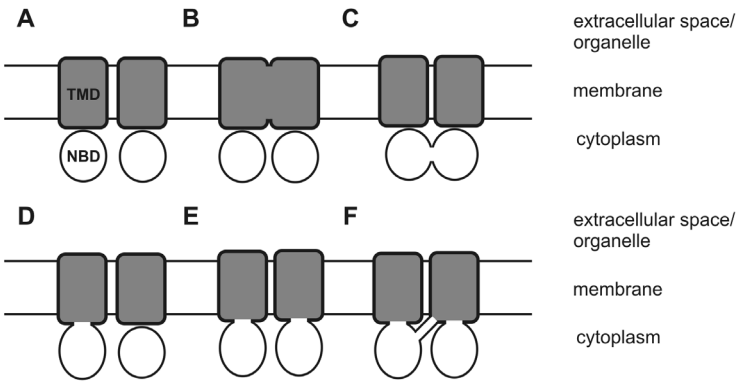

Figure 2.3: Possible organization of transmembrane domains (TMD) and nucleotide binding domains (NBD) of ABC transporters.
TMD – transmembrane domaine (dark grey), NBD – nucleotide binding domain (white); figure adapted from [44] and [46].

The TMD architecture typically consists of six membrane-spanning helices [46]. As there are two TMDs required for ABC-transporter function, a functional transporter contains a minimum of 12 transmembrane helices. In contrast to the TMDs, the NBDs of all known ABC transporters contain conserved sequences, leading to more than 30 % sequence identity [47]. Next to the Walker A and Walker B motifs also found in other ATPases, ABC transporters possess an unique, so-called signature-motif (LSGGQ, C-Loop) which is located between the Walker A and B motifs [45, 47, 48].

Without bound nucleotide, isolated NBDs were shown to exist in monomeric form; ATP-binding induced dimerization [44]. Even though the structures of some of the prokaryotic ABC transporters and the murine ABCB1 homolog have been solved by x-ray

crystallography (Figure 2.4), the molecular mechanisms of substrate recognition as well as substrate transport still remain largely unknown [49-51] .

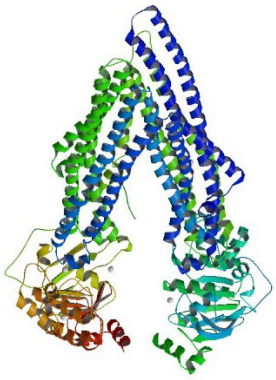

Figure 2.4: Cristallographic structure of the murine ABCB1 [51].
TMDs – dark blue and green (PDB-ID: 3g5u).

In mammalians, to date 49 ABC transporters, each with a defined substrate specifity, have been identified and grouped into 7 classes labeled from A to G according to sequence and structure similarities and phylogenetic analysis [52]. Human ABC transporter domains are either expressed on one single polypeptide or as half-transporters consisting of a TMD and a NBD with the need to homo- or hetero-oligomerize for full transporter function (Figure 2.3 E, F) [53]. Table 2.1 gives an overview of tissue expression, transported substrates and function, and associated diseases of selected human ABC transporters.

ABC transporters in humans have been shown to be involved in a variety of important physiological functions, such as multidrug resistance (MDR), antigen processing and presentation (TAP), or ion transport in the lung (CFTR/ABCC7) [54-56].

Originally, three ABC transporters were found to be involved in MDR of cultured tumor cells, namely ABCB1 (MDR1), ABCC1 (MRP1), and ABCG2 (BCRP) [57]. Recently however, also other ABC transporters of the ABCC/MRP class have been implicated in the transport of xenobiotics, thereby conferring cellular resistance to many clinically relevant drugs [57]. This is of importance especially for the field of cancer therapy, as these multi-drug resistance proteins are able to dispose of toxic chemotherapeutics. MDR is also found in prokaryotes. Bacteria employ several mechanisms that confer resistance to antibiotics, including the active export of the drugs by ABC transporters, thereby increasing the need to continuously develop new therapeutics to cure bacterial infectious diseases [58].

Table 2.1: Tissue expression, subtrates / functions and associated diseases from selected human ABC transporters.

Gene	Alias	Tissue expression	Substrate/Function	Associated diseases
ABCA1	ABC1	ubiquitous	PS, SPM, PC, (hydroxy) cholesterol	Tangier disease, familial hypoalphalipoproteinemia
ABCA2	ABC2	brain	choelsterol, ceramides, PE, PS, SM	
ABCA3	ABC3, ABCC	lung, brain, nerve, kidney and others	Transport of surfactant lipids, cholesterol	neonatal surfactant deficiency, RDS, ILD
ABCA4	ABCR	retinal photoreceptors	N-retinylidene-PE	Stargardt macular degeneration, retinitis pigmentosa, age-related macular degeneration
ABCA7		brain, skin, myelolymphatic system	cholesterol, PC, ceramides	
ABCA12		keratinocytes	GluCer	Harlequin ichthyosis
ABCB1	Pgp/MDR1	brain, kidney, liver, placenta	multidrug resistance	
ABCB2	TAP1	all cells	peptide transport (antigen presentation)	
ABCB3	TAP2	all cells	peptide transport (antigen presentation)	
ABCB4	PGY3	liver, bile, placenta, canicular membrane	PC transport	progressive familial intrahepatic cholestasis
ABCC1	MRP1	lung, testes, PBMC	drug resistance	
ABCC6	MRP6	liver, kidney	organic anions	Pseudoxanthoma elasticum
ABCC7	CFTR	lung, gut, exocrine organs	ion transport	Cystic fibrosis
ABCD1	ALD	peroxisomes	long-chain fatty acids	Adrenoleukodystrophy
ABCG1	ABC8/White	ubiquitous	cholesterol, PC, SM, hydroxy-cholesterol	
ABCG2	ABCP/MXR/ BCRP	placenta, intestine	toxins, drug resistance	
ABCG5	White2	liver, gastro-intestinal tract	cholesterol, plant sterols	β-sitosterolemia
ABCG8		liver, gastro-intestinal tract	cholesterol, plant sterols	β-sitosterolemia

PS – phosphatidylserine, SPM – sphingomyelin, PC – phosphatidylcholine, PE – phosphatidyl-ethanolamine, GluCer – Glucosylceramide, RDS – respiratory distress syndrome, ILD – interstitial lung disease. Table adapted from [52] + [59].

2.4.1 The ABCA family

The ABCA subfamily is one of the biggest ABC transporter subgroups, with to date 12 identified members [60]. All ABCA transporters are full transporters and most of them are expressed in a variety of tissues (Table 2.1) [61]. They often transport phospholipids and cholesterol, such as ABCA1 or ABCA3. Several members of the ABCA subfamily are implicated in the development of hereditary diseases [52]. ABCA1 is a well described transporter of the group and it was shown to be involved in cellular cholesterol efflux to apolipoprotein A-I (ApoA-I) in the process of reverse cholesterol transport [62]. ApoA-I is the major protein component of HDL in plasma. Defects in ABCA1 are implicated in a higher risk for the development of atherosclerosis [63, 64]. Dysfunctions caused by defects in ABCA1 include Tangier disease (TD) [65]. Patients with Tangier disease present with almost complete absence of plasma HDL, have an increased susceptibility to

atherosclerosis and suffer from phenotypic changes such as enlarged tonsils and splenomegaly due to accumulation of cholesterol esters [66]. Another member of the A family involved in genetic diseases, ABCA4, is exclusively expressed in the retinal rod and cone photoreceptors, and defects in ABCA4 induce Stargardt syndrome, one of the most common hereditary retinal dystrophies [67].

2.4.2 ABCA3

ABCA3 is a 1704 amino-acid long full ABC-transporter found in a variety of organs and tissues (Table 2.2) and is strongly expressed in ATII cells in the lung [68]. The human ABCA3 gene comprises 80 kb of genomic DNA and is localized on chromosome 16p13.3 [69, 70].

Table 2.2: Expressed sequence tags (ESTs) for ABCA3.

Pool name	Transcripts per million	Spot intensity	Gene EST	Total EST	Pool name	Transcripts per million	Spot intensity	Gene EST	Total EST
adipose tissue	76		1 /	13106	mammary gland	6		1 /	153271
adrenal gland	0		0 /	33197	mouth	0		0 /	67052
ascites	74		3 /	40015	muscle	9		1 /	107715
bladder	0		0 /	29757	nerve	63		1 /	15768
blood	0		0 /	123478	ovary	9		1 /	102051
bone	0		0 /	71655	pancreas	13		3 /	214812
bone marrow	0		0 /	48801	parathyroid	0		0 /	20539
brain	55		61 /	1100989	pharynx	0		0 /	41328
cervix	20		1 /	48171	placenta	3		1 /	280825
connective tissue	13		2 /	149255	prostate	47		9 /	189345
ear	0		0 /	16212	salivary gland	0		0 /	20155
embryonic tissue	9		2 /	215722	skin	18		4 /	210574
esophagus	0		0 /	20209	spleen	0		0 /	53952
eye	80		17 /	211054	stomach	51		5 /	96619
heart	22		2 /	89626	testis	15		5 /	330442
intestine	34		8 /	234472	thymus	0		0 /	81131
kidney	23		5 /	211777	thyroid	21		1 /	47473
larynx	0		0 /	24145	tonsil	0		0 /	16999
liver	4		1 /	207743	trachea	19		1 /	52413
lung	59		20 /	336974	umbilical cord	0		0 /	13680
lymph	0		0 /	44270	uterus	12		3 /	232878
lymph node	0		0 /	91610	vascular	19		1 /	51780

Table generated from the NCBI - Expressed Sequence Tags database.

ABCA3 is found in the limiting membrane of lamellar bodies and is thought to be involved in LB biogenesis and homeostasis of pulmonary surfactant [14, 71, 72]. ABCA3 most likely transports surfactant lipids from the cytosol to the inner membranes of LBs for storage and secretion [73]. Similar to surfactant proteins SP-B and SP-C, ABCA3 expression can be induced by the thyroid transcription factor-1 (TTF-1) *in vitro* [68, 74, 75]. Homozygous inactivation of the murine ABCA3 gene leads to death of the mice within one hour after birth, while heterozygous mice develop normally [76]. Conditional deletion of ABCA3 in mice caused the majority of mice to die shortly after birth [77]. In

the surviving mice, an altered surfactant lipid composition was observed as well as a decrease in mRNAs controlling fatty acid and PC metabolism.

To date, more than 100 homozygous or (compound) heterozygous splice site, frame-shift or missense mutations in the *ABCA3* gene have been identified. ABCA3 mutations cause respiratory distress syndrome (RDS) in the newborn or ILD in children and adults, depending on the mutation's severity, other genetic predispositions and environmental factors [70, 78, 79]. In one case, usual interstitial pneumonitis (UIP), the histologic pattern of IPF, was detected in a 15 year old boy with ABCA3 mutation [80]. Varying with age, DIP and NSIP histopathological patterns were found in children with ABCA3 mutations [70, 81]. The precise molecular mechanisms that connect ABCA3 mutations to fibrosing lung disease have so far not been identified. Defects in ABCA3 may impair LB biogenesis and may lead to formation of electron-dense bodies with central or peripheral core structures or rudimentary multi-lamellar structures (Table 2.3) [70, 76, 78]. ABCA3 mutations increase the phospholipid / protein ratio as well as the surface tension but decrease the relative amounts of phosphatidylcholine in BAL fluid from affected individuals [69]. Moreover, it was shown that heterozygosity for ABCA3 mutations modifies the severity of lung disease associated with the p.I73T mutation in the SP-C gene [82]. *In vitro*, ABCA3 protein mutations were shown to either mislocalize to the ER (type I, trafficking defect) or to correctly localize to the LB but having an impaired functionality due to reduced ATP-hydrolysis activity (type II, functional defect) [83]. Some ABCA3 mutations are more common than others. The mutation p.E292V, causing a functional defect, has an estimated prevalence of 1:314 in the Norway population and 1:276 in the Missouri population [84]. For two mutations, p.Q215K and p.E292V, the histological pattern and LB structure in patient samples as well as the molecular characteristics in comparison to the ABCA3-WT protein are outlined in Table 2.3.

Table 2.3: Histological pattern, LB structures and molecular characteristics induced by ABCA3 mutations.

ABCA3 model/mutation	Histological pattern	LB structure	Molecular characteristics
WT 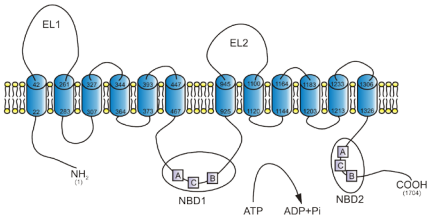 		- concentric membranes, no inclusions 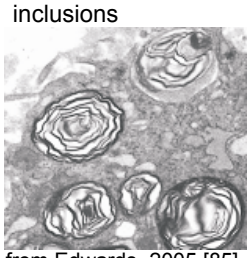 from Edwards, 2005 [85] 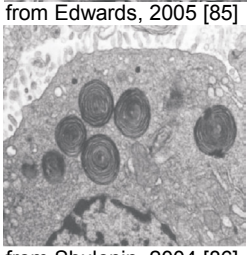 from Shulenin, 2004 [86]	- 150/190 kDa molecular weight forms - localizes to LB - functional lipid transporter [83]
p.Q215K 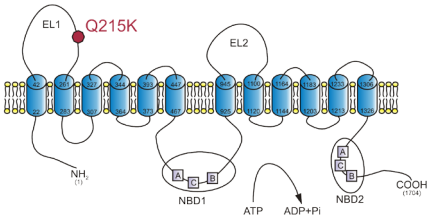 	- pneumocyte hyperplasia [78] - interstitial thickening, enlargement of alveolar septa (NSIP) [78] - accumulation of alveolar macrophages (DIP) [78] - intraalveolar accumulation of granular, eosinophilic material (PAP) [78] - low (absent) ABCA3 expression in ATII [78]	- fewer, smaller inclusions compared to WT - "fried-egg" appearance, electron-dense bodies with electron-dense peripheraly placed inclusions 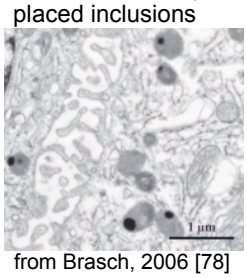 from Brasch, 2006 [78]	- only 190 kDa molecular weight form - localizes to ER - decreased epithelial markers - increased mesenchymal markers - other lipid transporters increased - reduced SP-C
p.E292V 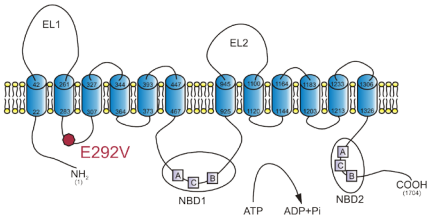 	- pneumocyte hyperplasia [70] - interstitial thickening [70] - lobular remodeling [70] -accumulation of PAS-positive material (PAP) - accumulation of alveolar macrophages [70] -cholesterol clefts [70] - lymphocytic inflammation [70]	most likely similar to p.Q215K/other ABCA3 mutations: -fewer, smaller inclusions compared to WT - "fried-egg" appearance, possibly densely-packed concentric membranes, electron-dense eccentrically placed inclusions	- 150/190 kDa molecular weight forms - decreased epithelial markers - localizes to LB - impaired lipid transport function [83] - other lipid transporters increased - reduced SP-B and/or SP-C [81]

ABCA3 models were adapted from Sunčana Kern. The histological patterns show a high variability in different patients even with the same mutation. PAP – pulmonary alveolar proteinosis, NSIP – non-specific interstitial pneumonitis, DIP – desquamative interstitial pneumonia.

2.5 EMT

Epitehlial mesenchymal transition (EMT) is a plastic process by which epithelial cells lose cell-cell adhesions and the attachment to the basement membrane while gaining mesenchymal properties and a mesenchymal phenotype [87, 88]. To date, three types of EMT have been identified: type I epithelial-mesenchymal transition of primitive epithelia during early embryogenesis, type II epithelial-mesenchymal transition of secondary epithelia, i.e. in developed lungs or kidneys, and type III carcinoma-metastatic transitions of carcinoma cells during tumor invasion and metastasis [87]. For demostration of EMT in *in vitro* cell culture models, *in vivo* mouse models or in patient samples, a variety of biomarkers have been identified [87]. Most of these biomarkers are common to all three EMT subtypes and they mostly can be classified into four groups: cell surface markers, transcription factors, cytoskeletal markers and extracellular proteins [87]. In the following, biomarkers of type II EMT, especially in consideration of EMT of alveolar type II cells, are further defined (reviewed in [87]). Loss of the cell surface marker and adhesion protein E-cadherin is a key event in EMT [88]. E-cadherin is found in adherens junctions, promoting Ca^{2+}-depending cell-cell contacts [89]. Another epithelial marker is the tight junction protein ZO-1, located on the cytoplasmic leaf of the plasmamembrane in tight junctions [90]. Mesenchymal cell surface markers, which increase during EMT, include N-cadherin and OB-cadherin as well as several integrins [87, 91-93]. Fibroblast-specific protein 1 (FSP-1), α-SMA, vimentin and β-catenin belong to the mesenchymal cytoskeletal markers that are upregulated during EMT [87, 94, 95]. After EMT, increased amounts of the ECM proteins type I and III collagens as well as fibronectin and matrix metalloproteases (MMPs) are observed [87, 88, 96]. Concurrently, the expression of type IV collagen, an ECM protein of the basement membrane underlying and anchoring the epithelium, is supposed to decrease during EMT [87, 97]. While EMT takes place, a variety of nuclear transcription factors are induced to regulate expression of mesenchymal (and epithelial) genes, including SNAI1 and SNAI2, ZEB1, Twist, LEF-1 and FOXC2 [87, 98-101]. Also, the cytoskeletal β-catenin functions as a transcription factor after nuclear translocation [102]. Accompanying these changes in protein expression is a phenotypic transition into an elongated, fibroblastic cell shape which involves loss of apical-basal polarity and acquisition of front-to-end polarity as well as rearrangement of the cell's cytoskeleton and gain of migratory properties [103].

EMT processes can be induced by a variety of exogenous and endogenous stimuli, including growth factors, ECM components such as collagens, respiratory infections or protein defects. A very potent EMT mediator is transforming growth factor β (TGF-β), which has been shown to induce EMT in a variety of cell lines [96, 104, 105]. Type II EMT has been observed in a variety of tissues (including eye, kidney, lung, liver) and has been extensively investigated in lung and kidney cells [88, 106-108].

For SP-C it has recently been shown that mutations in the protein might induce EMT through ER stress-related mechanisms [109, 110]. In a mouse model with a conditionally expressed SP-C mutation, the expression of the SP-C mutation alone did not induce tissue remodelling. However, an additional stimulus, such as bleomycin, lead to the development of fibrosis in challenged mice [111].

2.5.1 Transdifferentiation

Another type of cellular plasticity is metaplasia, also known as transdifferentiation. Transdifferentiation indicates the conversion from one fully differentiated cell type to another, as observed for the transformation of type II pneumocytes to type I pneumocytes in remodeling and repair of the alveolar epithelia after lung injury [16, 112].

2.6 EMT and fibrosis

Fibrosis in general is characterized by an abnormal gain of connective tissue, leading to rigidification, scarring and eventually loss of function of the affected tissue. The main components of the connective tissue are extracellular matrix (ECM) constituents, especially collagen fibers. ECM constituents are mainly secreted by fibroblasts. Recently it has been proposed that fibroblasts and myofibroblasts in the lung may originate from EMT of lung epithelial cells [103]. Using a transgenic reporter model, it was shown that kidney fibroblasts were derived from epithelial cells during renal fibrogenesis [113]. Isolated ATII cells from IPF patients were shown to express mesenchymal markers and undergo EMT when grown on fibronectin but not on Matrigel/Collagen [114]. However, EMT in the lung has so far mostly been demonstrated in *in vitro* cell cultures. Evidence of EMT in patient samples is so far limited to the immunohistochemical colocalization of both, epithelial as well as acquired mesenchymal markers in alveolar cells [115]. As biopsy material from affected individuals only represents a snapshot of the disease state, it may be that patients need to be sampled and monitored longitudinally over time to conclusively show involvement of EMT in the development of fibrosis. So far, the involvement of EMT in

lung fibrosis has most reliably been demonstrated in *in vivo* mouse models with transgenic modification to express a reporter gene exclusively in lung epithelial cells to monitor transition into fibroblasts [115].

2.7 Aim of the thesis

Defects in ABCA3 cause respiratory distress in newborns and interstitial lung disease in older children and adults with variable onset and progression. The precise cellular disease-causing mechanisms are so far unknown. Therefore, this thesis aimed to identify some of the underlying molecular pathomechanisms. As alveolar epithelial type II cells have a variety of functions, the cellular homeostasis might be perturbed on various stages. Defects in ABCA3 might interfere with the ATII function as surfactant producing cells, with the ATII involvement in the host defense against pathogens or they might change the cells plastic behaviour. Therefore, several hypotheses were investigated: 1) do ABCA3 mutations render the alveolar epithelial cells more susceptible to phenotypic changes, i.e. epithelial-mesenchymal transition, 2) do ABCA3 mutations interfere with the ATII lipid homeostasis, and 3) do RSV infection and bacterial LPS have differential effects on cells harboring ABCA mutations, as respiratory infections or other toxic environmental agents might initiate or excacerbate the ILD in affected individuals ("second hit").

In this thesis, some of the above mentioned cellular functions were investigated by using a cell culture model system for alveolar type II cells which was stably transfected to yield cells with stable and strong expression and synthesis of ABCA3-WT protein as well as the two clinically relevant ABCA3 mutations p.Q215K and p.E292V.

3 Material and Methods

3.1 Materials

Laboratory instruments

Axiovert 135 Fluorescence microscope	Zeiss, Jena, Germany
Cell Culture Bench Safe 2020	Thermo Scientific, Waltham, USA
Cool Centrifuge 5417R	Eppendorf, Hamburg, Germany
Cryo container	Nalgene, Rochester, USA
Developing Cassette	GE Healthcare, Freiburg, Germany
Developer Machine CP 1000	AGFA, Mortsel, Belgium
FLUOstar Optima	BMG Labtech, Offenburg, Germany
Freezer -20 °C	Liebherr, Kirchdorf, Germany
Freezer -80 °C	Thermo Scientific, Waltham, USA
Thermo Block TBD-120	Kisker, Steinfurt, Germany
High Performance Centrifuge Avanti J-30I	Beckman Coulter, Krefeld, Germany
Icycler Real-Time PCR System	Bio-Rad, Munich, Germany
Incubator HeraCell	Heraeus, Hanau, Germany
Liquid Nitrogen Tank	German-Cryo, Jücken, Germany
Megafuge 1.0 R	Heraeus, Hanau, Germany
Mikrotiter Plate Reader Ht III Type 12600	Anthos, Krefeld, Germany
Nanodrop	Thermo Scientific, Waltham, USA
Neubauer Counting Chamber	Brand, Berlin, Germany
pH-Meter CG 840	Schott, Mainz, Germany
Photometer	Amersham Biosciences
Pipettes (2.5 µl, 10 µl, 20 µl, 100 µl, 200 µl, 1000 µl)	Eppendorf, Hamburg, Germany
PowerEase 500 Power Supply EI8700	Life Technologies, Carlsbad, USA
Shaker Excella E24	New Brunswick Scientific
Stratalinka 2400 UV-Crosslinker	Stratagene, Waldbronn, Germany
Systec D65 Autoclave	Systec, Wettenberg, Germany
T1 Thermocycler	Biometra, Göttingen, Germany
Table Centrifuge	Labnet, Edison, USA
Water Bath	Julabo, Seelbach, Germany
Xcell SureLock Minicell Chamber (EI 0001)	Invitrogen, Karlsruhe, Germany
Xcell II Blot Module EI9051	Invitrogen, Karlsruhe, Germany

Disposables

Black/White F96 Microwell plates	Nunc, Langenselbold, Germany
Cell culture dish (100 mm)	Corning Incorporated, Corning, USA
Cell culture flasks (T-25, T-75)	BD, Heidelberg, Germany

Cell culture plates (96-, 24-well, 12-well, 6-well)	Corning Incorporated, Corning, USA
Centrifugation tubes (10 ml)	Sarstedt, Nümbrecht, Germany
Centrifugation tubes (15 ml, 50 ml)	BD, Heidelberg, Germany
Cryogenic vials (1.8 ml)	Nunc, Langenselbold, Germany
Filter Tips (2.5 µl, 10 µl, 100 µl, 1000 µl)	Sarstedt, Nümbrecht, Germany
Immobilon P PVDF membrane	Millipore, Billerica, USA
Microscope cover glasses	G. Menzel, Braunschweig, Germany
Microscope slides	G. Menzel, Braunschweig, Germany
Maxisorp 96-well ELISA plates	Nunc, Langenselbold, Germany
NuPAGE Novex 10 % Bis-Tris Gel	Invitrogen, Karlsruhe, Germany
NuPAGE Novex 3-8 % Tris-Acetate	Invitrogen, Karlsruhe, Germany
NuPAGE Novex 7 % Tris-Acetate	Invitrogen, Karlsruhe, Germany
Optical adhesive films	R&D systems, Wiesbaden, Germany
PCR Stripes	Brand, Wertheim, Germany
Pipette tips (2.5 µl, 10 µl, 20 µl, 200 µl, 1000 µl)	Eppendorf, Hamburg, Germany
Reaction tubes (0.5, 1.5 ml, 2 ml)	Eppendorf, Hamburg, Germany
Real time PCR Plates 96 well	Peqlab, Erlangen, Germany
Radiographic Film	GE Healthcare, Freiburg, Germany
Serological pipettes (2 ml, 5 ml, 10 ml, 25 ml)	Corning Incorporated, Corning, USA
Single use cuvettes (UVette 220-1600 nm)	Eppendorf, Hamburg, Germany

Kits

Amplex Red Cholesterol Kit (cat. # A12216)	Molecular probes, Karlsruhe, Germany
Bio-Plex Pro Human Cytokines Group I 6-Plex	Bio-Rad, Munich, Germany
Dual-Luciferase Reporter Assay System	Promega, Mannheim, Germany
ECL Chemiluminescence solution	GE Healthcare, Freiburg, Germany
High Pure RNA Isolation Kit (cat. # 11828665001)	Roche, Grenzach-Wyhlen, Germany
Human CCL5/RANTES DuoSet ELISA Development kit	R&D systems, Wiesbaden, Germany
Human CXCL8/IL-8 DuoSet ELISA Development kit	R&D systems, Wiesbaden, Germany
Human Endothelin-1 Quantikine ELISA kit	R&D systems, Wiesbaden, Germany
Human GM-CSF Quantikine ELISA kit	R&D systems, Wiesbaden, Germany
Human IL-6 DuoSet ELISA Development kit	R&D systems, Wiesbaden, Germany
Human MMP-2 Quantikine ELISA kit	R&D systems, Wiesbaden, Germany
Human TGF-β1 DuoSet ELISA Development kit	R&D systems, Wiesbaden, Germany
IQ SYBR Green Supermix	Bio-Rad, Munich, Germany
NucleoBond Plasmid DNA Purification Endotoxinfree	Macherey-Nagel, Düren, Germany
ProLong Gold Antifade mounting medium with DAPI	Invitrogen, Karlsruhe, Germany
QIAquick Gel Extraction Kit 50	Qiagen, Hilden, Germany
QIAquick PCR Purification Kit 50	Qiagen, Hilden, Germany
QIAprep Spin Miniprep Kit 50	Qiagen, Hilden, Germany
QuantiTect Reverse Transcription kit (cat. # 205313)	Qiagen, Hilden, Germany

QuickChange® Site-Directed Mutagenesis Kit (cat. # 200518)	Stratagene, Waldbronn, Germany
VenorGeM® Mycoplasmen-test (cat. # 11-1025)	Minerva Biolabs, Berlin, Germany
Vecta Shield Hardset Mounting Medium with DAPI	Vector Labs, Burlingame, USA
Vybrant Alexa Fluor 488 Lipid Raft Labeling Kit (cat. # V-34403)	Molecular Probes, Karlsruhe, Germany

Chemicals

Agarose GTQ	Roth, Karlsruhe, Germany
Ampicillin	Fluka, St. Louis, USA
Bovine serum albumine (BSA)	Paesel + Lorei, Duisberg, Germany
Bromophenol blue	Sigma-Aldrich, Steinheim, Germany
Calcium chloride	Merck, Darmstadt, Germany
Calyculin A	Cell Signaling, Danvers, USA
Coelanterazine (native; *cat.* # s053)	Synchem, Felsberg, Germany
Collagen R (2 mg/ml, sterile)	Serva, Heidelberg, Germany
Dimethyl sulfoxide (DMSO)	Roth, Karlsruhe, Germany
Dipotassium hydrogen phosphate (K_2HPO_4)	Merck, Darmstadt, Germany
Disodium hydrogen phosphate (Na_2HPO_4)	Merck, Darmstadt, Germany
Dithiothreitol (DTT)	Merck, Darmstadt, Germany
Ethylendiamintetraacid (EDTA)	Sigma-Aldrich, Steinheim, Germany
Ethanol	Merck, Darmstadt, Germany
Ethidiumbromide	Fluka, St. Louis, USA
Glacial acetic acid	Merck, Darmstadt, Germany
Glutaraldehyd	Fluka, St. Louis, USA
Glycerol	Merck, Darmstadt, Germany
2-Glycerophosphate-disodium salt	Serva, Heidelberg, Germany
HEPES (2-(4-(2-Hydroxyethyl)-1-piperazinyl)-ethansulfonsäure)	Merck, Darmstadt, Germany
Hydrochlorid acid (HCl)	Merck, Darmstadt, Germany
Hydrogen peroxide (H_2O_2)	Merck, Darmstadt, Germany
Igepal CA630 (cat. # I-3021)	Sigma-Aldrich, Steinheim, Germany
Isopropanol	Merck, Darmstadt, Germany
Kanamycin	Sigma-Aldrich, Steinheim, Germany
Magnesium chloride ($MgCl_2$)	Merck, Darmstadt, Germany
Magensium sulfate ($MgSO_4$)	Merck, Darmstadt, Germany
Methanol	Merck, Darmstadt, Germany
3-(4,5-Dimethylthiazol-2-yl)-2,5-diphenyltetrazoliumbromid (MTT) (cat. # M6494)	Invitrogen, Karlsruhe, Germany
Paraformaldehyde	Merck, Darmstadt, Germany
Potassium chloride (KCl)	Merck, Darmstadt, Germany
Potassium dihydrogen phosphate (KH_2PO_4)	Merck, Darmstadt, Germany
Saponin (cat. # 4185.1)	Roth, Karlsruhe, Germany
Sodium chloride (NaCl)	Merck, Darmstadt, Germany

Sodium deoxycholate	Sigma-Aldrich, Steinheim, Germany
Sodium dodecyl sulphate	Sigma-Aldrich, Steinheim, Germany
Sodium fluoride (NaF)	Sigma-Aldrich, Steinheim, Germany
Sodium hydroxide (NaOH)	Merck, Darmstadt, Germany
Sucrose	Merck, Darmstadt, Germany
β-Mercaptoethanol	Sigma-Aldrich, Steinheim, Germany
Tris (2-amino-2-hydroxymethl-1,3-propandiol)	Applichem, Darmstadt, Germany
Triton-X 100	Sigma-Aldrich, Steinheim, Germany
Tween-20	Sigma-Aldrich, Steinheim, Germany

Enzymes/markers

MB Taq DNA-Polymerase	Minerva Biolabs, Berlin, Germany
Lambda DNA/HindIII Marker	Promega, Mannheim, Germany
Novex Sharp Pre-stained Protein Standard	Invitrogen, Karlsruhe, Germany
KpnI	NEB, Frankfurt/Main, Germany
XhoI	NEB, Frankfurt/Main, Germany

Plasmids

pELAM-Luc	Gift: M.J. Fenton, NIH, Bethesda, USA
pMET-Luc	Gift: AG Rudolph, Kubus
pRLTK (E2241)	Promega, Mannheim, Germany
pUB6	Invitrogen, Karlsruhe, Germany
pUB6/hABCA3-HA WT	Prepared by M. Woischnik

Celltypes/Bacterial strains/Virus strains

Type	*catalog #*	*company*
A549	*ACC-107*	DSMZ, Braunschweig, Germany
DH5α	*18265017*	Invitrogen, Karlsruhe, Germany
RSV strain A2	*VR-1540*	ATCC, Manassas, USA
Vero	*CCL-81*	ATCC, Manassas, USA

Cell culture media, buffers and reagents

Blasticidin (cat. # ant-bl-1)	Invivogen, San Diego, USA
ExGen 500 *in vitro* Transfection Reagent	Fermentas, St. Leon-Rot, Germany
Fetal bovine serum (FBS) “Gold”	PAA lab. GmbH, Pasching, Austria
Phosphate buffered saline (PBS)	PAA lab. GmbH, Pasching, Austria
Quantum 286	PAA lab. GmbH, Pasching, Austria
RPMI 1640	PAA lab. GmbH, Pasching, Austria
Trypan blue solution	PAA lab. GmbH, Pasching, Austria
Trypsin-EDTA (1x)	PAA lab. GmbH, Pasching, Austria

Buffers and solutions

PBS-T (adjust pH to 7.4)

NaCl	136.9 mM
KCl	2.7 mM
Na_2HPO_4	10. mM
KH_2PO_4	1.8 mM
Tween	0.1 %

TBS-T

Tris pH 7.5	50 mM
NaCl	150 mM
Tween	0.1 %

Radio immunoprecipitation (RIPA) buffer

Tris pH 8	50 mM
EDTA	5 mM
sodium chloride	0.15 M
Triton-X 100	1 %
sodium deoxycholate	0.5 %
SDS	0.1 %
Complete protease inhibitor cocktail (Roche)	1x

Lysis buffer (buffer A)

Hepes pH 7.9	10 mM
KCl	10 mM
$MgCl_2$	1.5 mM
EDTA	1 mM
DTT	1 mM
Igepal	0.6 %
Protease-/Phosphataseinhibitors	
Protease inhibitor cocktail (Sigma) (cat. # P-8340)	1 µg/ml
NaF	25 mM
Glycerophosphate	50 mM
Calyculin A	1 %

Nuclear extraction buffer (buffer B)

Hepes pH 7.9	20 mM
NaCl	420 mM
$MgCl_2$	1.5 mM
EDTA	1 mM
DTT	1 mM
Glycerol	25 %
Protease-/Phosphataseinhibitors	
Protease inhibitor cocktail (Sigma)	1 µg/ml
NaF	25 mM
Glycerophosphate	50 mM
Calyculin A	1 %

SDS-lysis buffer

Tris pH 7,4	0.1 mM
SDS	0.2 %
EDTA	1 mM

Amplex Red Solution (in 1x reaction buffer)

Amplex Red	300 µM
HRP	2 U/ml
Cholesterinoxidase	2 U/ml
Cholesterinesterase	0.2 U/ml

EM fixative

HEPES pH 7.35	0.15 M
Paraformaldehyde	1.5 %
Glutaraldehyde	1.5 %

Transfer buffer for western blotting

Transfer buffer (Invitrogen)	1x
MeOH	10 %

TAE buffer (10x), pH 8.5

Tris base	0.4 M
Glacial acetic acid	0.2 M
EDTA	0.01 M

Loading buffer for Agarose gel electrophoresis (5x)

Tris-HCl pH 7.5	10 mM
Sucrose	40 %
Bromphenolblue	0,25 mg/ml
EDTA	50 mM

Ready to use buffers and solutions

Bio-Rad Protein Assay (cat. # 500-0006)	Bio-Rad, Munich, Germany
NuPAGE LDS sample buffer (4x)	Invitrogen, Karlsruhe, Germany
NuPAGE MES Running buffer (20x)	Invitrogen, Karlsruhe, Germany
NuPAGE MOPS Running buffer (20x)	Invitrogen, Karlsruhe, Germany
NuPAGE Tris-Acetat Running buffer (20x)	Invitrogen, Karlsruhe, Germany
NuPAGE Transfer buffer (20x)	Invitrogen, Karlsruhe, Germany
TMB ELISA Peroxidase Substrate (cat. # UP664780)	Uptima, Montlucon, France
Western Blot Stripping Buffer (cat. # 21059)	Thermo Scientific, Waltham, USA

Point mutagenesis primers

Gene	mutation	Forward (5'-3')	Reverse (5'-3')
ABCA3	p.Q215K	GGCCGTG**A**AGCATGCTGTGGAC	GTCCACAGCATGCT**T**CACGGCC
ABCA3	p.E292V	GGAGGCTGAAGG**T**GTACATGCGC	GCGCATGTAC**A**CCTTCAGCCTCC

qPCR Primers

Gene name	Abbr.	Forward Primer (5'-3')	Reverse Primer (5'-3')
Hypoxanthine phosphoribosyltransferase 1	HPRT	CATTGTAGCCCTCTGTGTGC	CTGACCAAGGAAAGCAAAGTCTG
β-actin	ACTB	CGCGAGAAGATGACCC	ATTGCCAATGGTGATGAC
E-cadherin	CDH1	CCTGAAGTGACTCGTAACGAC	CTCTGAGGAGTTCAGGGAGC
ATP-binding cassette, sub-family A (ABC1), member 3	ABCA3	CGGGAAGACCACGACTTT	GCTGCCGCACCTTTC
ATP-binding cassette, sub-family A (ABC1), member 1	ABCA1	GCAGATCATAGCCAAAAG	CCAGCCCTTGTTATTGA
Toll-like receptor 3	TLR3	GACTGAACTCCATCTCATGTCC	CCAATTGCGTGAAAACACCCTG
Toll-like receptor 4	TLR4	GCCTTCCTCTCCTGCGTGAG	AGGCTCCCAGGGCTAAACTC
Interleukin 6 (interferon, beta 2)	IL6	CCTTCTCCACAAGCGCCTTC	CTGAGATGCCGTCGAGGATG
Interleukin 8	IL8	TCTTGGCAGCCTTCCTGATT	TCCAGACAGAGCTCTCTTCCATC
Colony stimulating factor 2 (granulocyte-macrophage) (GM-CSF)	CSF2	AGCATGTGAATGCCATCC	CTGGCCATCATGGTCAAGG
Chemokine (C-C motif) ligand 5 (RANTES)	CCL5	CACCCTGCTGCTTTGCCTAC	GTTGATGTACTCCCGAACCC
Alpha smooth muscle actin (α-SMA)	ACTA2	CGACCGAATGCAGAAGGAG	GCTGATCCACATCTGCTGG
Endothelin 1	EDN1	GCCAAAAAGACAAGAAGTGC	CTTCCTCTCACTAACTGCTGA
S100 calcium binding protein A4 (FSP-1)	S100A4	TCTCTCCTCAGCGCTTCTTC	TGAGCTTGAACTTGTCACCC
Transforming growth factor, beta 1	TGFB1	TACCTGAACCCGTGTTGCTC	GATAACCACTCTGGCGAGTC
Surfactant protein C	SFTPC	GGCCTCGTGGTGTATGAC	TGGCCCAGCTTAGACGTA
Matrix metallopeptidase 2 (gelatinase A)	MMP2	GAGCACTCCCAAGACCCT	AGTCCGCCAAATGAACC
Mitogen-activated protein kinase 14 (p38)	MAPK14	CGAGCGTTACCAGAACCTGT	TTTTCGCATGAATGATGGAC
Glycogen synthase kinase 3 beta	GSK3B	GAGTGATCATGTCAGGGCG	CCACTGTTGTCACCTTGCTG
Snail homolog 1 (Drosophila)	SNAI1	CTTCTCTAGGCCCTGGCTG	CATCTGAGTGGGTCTGGAGG
Snail homolog 2 (Drosophila)	SNAI2	TCGGACCCACACATTACCTT	GCAGTGAGGGCAAGAAAAAG
Collagen, type I, alpha I	COL1A1	GATGTGCCACTCTGACT	GGGTTCTTGCTGATG
Collagen, type III, alpha I	COL3A1	GTGGTAGCCCTGGTGAGA	GGGGGTCCTGGGTTAC
SMAD family member 2	SMAD2	CATCGGAAGAGGAAGGAACA	TGTTCTTACCAAAGGCAGCA
SMAD family member 3	SMAD3	AACACCAAGTGCATCACCAT	GTAGCTCGTGGTGGCTGT

Abbr. – abbreviation.

Antibodies

For western blot analysis

Antibody	*catalog #*	*company*
ABCA3	*HPA007884*	Sigma-Aldrich, St. Louis, USA
ABCA1	*ab18180*	Abcam, Cambridge, UK
α-SMA	*ab5694*	Abcam, Cambridge, UK
ATF-6	*PRS3683*	Sigma-Aldrich, St. Louis, USA
β-actin (HRP-conjugated)	*sc-47778 (C4)*	Santa Cruz, Heidelberg, Germany
BiP	*3177*	Cell Signaling, Danvers, USA
Calnexin	*sc-6465 (C20)*	Santa Cruz, Heidelberg, Germany
E-cadherin	*MAB1838*	R&D systems, Wiesbaden, Germany
phospho-ERK1/2	*4370*	Cell Signaling, Danvers, USA
ERK1/2	*4695*	Cell Signaling, Danvers, USA
RSV fusion protein	*MAB8262X*	Millipore, Billerica, USA
HA-tag	*1 867 423*	Roche, Grenzach-Wyhlen, Germany
IRE1α	*3294*	Cell Signaling, Danvers, USA
phospho-JNK1/2	*4668*	Cell Signaling, Danvers, USA
JNK1/2	*9258*	Cell Signaling, Danvers, USA
PERK	*3192*	Cell Signaling, Danvers, USA
phospho-Smad2	*3108*	Cell Signaling, Danvers, USA
phospho-Smad3	*9520*	Cell Signaling, Danvers, USA
Smad2	*5339*	Cell Signaling, Danvers, USA
Smad3	*9523*	Cell Signaling, Danvers, USA
Vimentin	*V6389*	Sigma-Aldrich, St. Louis, USA
ZO-1	*5406*	Cell Signaling, Danvers, USA
Mouse IgG (HRP-conjugated)	*AP124P*	Millipore, Billerica, USA
Rabbit IgG (HRP-conjugated)	*111-036-045*	Dianova, Hamburg, Germany

For immunofluorescence staining

Antibody	*catalog #*	*company*
α-Tubulin	*BM753S*	Acris Antibodies, Herford, Germany
EEA1	*SP5141P*	Acris Antibodies, Herford, Germany
LAMP3 (CD63)	*CBL553*	Chemicon, Millipore, Billerica, USA
Ubiquitin	*PW8810*	Biomol, Hamburg, Germany
Mouse Alexa Fluor 488	*A11017*	Molecular probes, Carlsbad, USA
Mouse Alexa Fluor 555	*A21425*	Molecular probes, Carlsbad, USA
Rabbit Alexa Fluor 488	*A11070*	Molecular probes, Carlsbad, USA
Rabbit Alexa Fluor 555	*A21430*	Molecular probes, Carlsbad, USA
Rat Alexa Fluor 488	*A21208*	Molecular probes, Carlsbad, USA
Rat Alexa Fluor 555	*A21434*	Molecular probes, Carlsbad, USA

ABCA1, BiP, calnexin – same antibodies were used as for western blot analysis.

3.2 Methods

3.2.1 Cell culture and transfection

A549 cells were maintained in RPMI 1640 medium supplemented with 10 % FBS gold at 37 °C with 5 % CO_2. Plasmids encoding HA-tagged ABCA3-WT and mutant ABCA3 were constructed as previously described [116]. A549 cells were transfected with the *pUB6-ABCA3-WT* / *Q215K* / *E292V* vectors using ExGene 500 according to the manufacturer's protocol. 24 h post transfection, selection of stable cells was started by addition of 6 µg/ml Blasticidin. Single cell clones were obtained by transferring single cells into the wells of a 96-well plate. For experiments, cells were seeded into well plates and grown for 48 h in RPMI supplemented with 0.1 or 10 % FBS.

3.2.2 Virus production and infection

Interferon-free virus stocks of human RSV strain A2 were prepared from Vero cell monolayers infected at a multiplicity of 0.1 as described [117]. After growth at 37 °C in a 5 % CO_2 atmosphere, virus was released by freezing and thawing the cell monolayers. Cell debris was removed by centrifugation at 2 500 x g for 20 min at 4 °C. Infectious virus titers were determined on Vero cells by endpoint dilution and counting of infected cell foci stained for indirect immunofluorescence with an RSV F-specific monoclonal antibody. Non-transfected and *pUB6-ABCA3* transfected A549 cells were plated at 250 000 cells into 6-well plates and RSV was added to yield a MOI of 3. Cells were harvested for preparing cell lysates or RNA isolation and cell culture supernatants were collected for ELISA 48 h after infection.

3.2.3 Immunoblot

Cells in 6-well plates were rinsed once with PBS and subsequently lysed in the wells with RIPA buffer. The lysate was centrifuged for 30 min at 1 000 x g and 4 °C. The protein concentration of the post-nuclear supernatant (= whole cell lysate) was determined with the BioRad protein assay (Bradford assay) using BSA as protein standard. 15-30 µg of cell lysates in 4x LDS buffer containing 50 mM DTT were heated for 10 min at 70 °C and subsequently loaded onto NuPage Mini Bis-Tris or Tris-Acetate gels. Following gel electrophoresis, proteins were blotted to PVDF-membranes. After transfer, membranes were blocked with 5 % skim milk or BSA in TBS-T. Membranes were incubated over night with primary antibodies in blocking solution. After washing the membranes three times with TBS-T, HRP-conjugated secondary antibodies were applied 1 h at room

temperature. Detection was performed using ECL reagent. Where necessary, membranes were stripped with Restore buffer and restained as stated above.

3.2.4 Cell fractionation

10^6 cells were seeded in 10 cm dishes and grown for 48 h. Cells were washed once with cold PBS and scraped into 1.5 ml PBS. After centrifuging for 5 min at 3 900 x g, cells were lysed for 15 min using 400 µl of lysis buffer A. The lysate was centrifuged for 1 min at 18 000 x g and 4 °C. The supernatant was collected (= cell lysate) and the pellet was resuspended in 50 µl of nuclear extraction buffer B, incubated on ice for 15 min and centrifuged for 10 min at 18 000 x g, 4 °C. The supernatant was collected (= nuclear extract) and the protein concentrations of cell lysate and nuclear extract were determined using the Bio-Rad protein assay. Immunoblots were carried out as stated above.

3.2.5 MTT (cell proliferation) assay

7 500 cells were seeded in a total volume of 100 µl per well into 96-well plates and grown for 4 to 120 h. Subsequently, 3-(4,5-Dimethylthiazol-2-yl)-2,5-diphenyltetrazolium-bromid (MTT) dissolved in PBS was added to the wells to yield a final concentration of 500 µg/ml. The MTT reagent is a yellow, water soluble dye which is converted to a purple, non-water soluble formazan by metabolically active cells. After two hours of incubation, the MTT containing cell culture supernatants were carefully replaced by 200 µl DMSO per well. The plates were placed on a shaker at 150 rpm for 15 min to solubilize the formazan crystals. Optical density was determined at 540 nm and backround corrected at 650 nm. RPMI 1640 medium containing 10 % FBS was used as a control.

3.2.6 Real-time RT-PCR

Total RNA was collected from cells grown for 48 h in 6-well plates using the High Pure RNA Isolation Kit according to the manufacturer's instructions. RNA-concentrations were determined with a NanoDrop spectrophotometer. 1 µg of total RNA was transcribed into cDNA with the ReverseTect transcription kit. Real-time quantitative PCR (qPCR) was carried out on an icycler real-time PCR machine using SYBR green according to the manufacturer's instructions in 25 µl reaction volumes.

3.2.7 ELISA / Bioplex

Supernatants from cells grown for 48 h in 6-well plates were centrifuged at 2000 x g for 10 min to dispose of remaining cells and cell debris. IL-6, IL-8, GM-CSF and RANTES

were measured according to the manufacturer's protocol using ELISA DuoSet Development kits or a Bio-Plex Pro Human Cytokines Group I 6-Plex. TGF-β1 was measured using a R&D DuoSet ELISA Development kit according to the manufacturer's instructions. Both, pro- and activated, MMP-2 and endothelin-1 (ET-1) were detected using Quantikine ELISA kits. Supernatants containing infectious RSV were inactivated by UV (254 nm) crosslinking for 5 min in a Stratalinker 2400. ELISA / Bio-Plex results were normalized to the protein concentration of the corresponding cell lysate.

3.2.8 Immunofluorescence staining

Cells grown on glass coverslips in 12-well plates for 48 h were fixed with 4 % paraformaldehyde for 15 min at room temperature. Cells were permeabilized with 0.1 % Triton-X 100 for 10 min. Non-specific binding sites were blocked with 1 % BSA and 5 % FBS in PBS for 30 min. Labelling with the primary antibodies was carried out for 1 h at room temperature. Cells were washed three times with PBS and subsequently stained with the appropriate Alexa Fluor secondary antibodies. After washing three times with PBS, cells were mounted on microscope slides with ProLong Gold antifade reagent with DAPI. Objects were viewed with a Zeiss Axiovert 135 microscope and images were taken with a Zeiss AxioCam MR camera and the Axiovision 3.1 software.

3.2.9 Secreted luciferase assay

75 000 cells per well were seeded into 24-well plates and grown for 24 h. Cells were transfected with the pMetLuc-plasmid (gift from AG Rudolph) using ExGen 500 according to the manufacturer's protocol. After 24 to 48 h cell growth, supernatants were collected. Luciferase activity was detected via luminescence detection at a Wallac photometer through addition of 100 µl of a 100 µmol/ml coelanterazine solution (in PBS) per well.

3.2.10 NF-κB determination – dual luciferase assay

50 000 cells were seeded into each wells of a 24-well plate and grown for 24 h prior to transfection. Cells were transfected with 0.5 µg pELAM-Luc and 0.1 µg pRLTK using ExGen 500 according to the manufacturer's protocol and medium was exchanged in all wells 24 h after transfection. Transfected cells were grown for a total of 48 h and subsequently harvested and analyzed with the Dual luciferase kit. Briefly, cells were lysed with 100 µl per well of 1x passive lysis buffer on a shaker for 15 min. Luminescence of both luciferases in 20 µl lysates was detected using a Fluostar photometer by sequential

addition of each 75 µl LAR II and Stop&Glo reagent per well of a white 96-well microplate.

3.2.11 Mass spectrometric lipid / cholesterol determination

Cells were seeded at 250 000 or 500 000 cells per well into 6-well plates and grown for 48 h in Quantum 286 medium. Cells were washed with PBS three times and lysed with 0.5 ml of 0.1 % SDS. The lysate was transferred to a fresh tube and 0.5 ml H_2O were used to wash each well and were subsequently combined with the corresponding lysate. Protein concentrations were measured using the bicinchoninic acid (BCA) protein assay. Cell lysates were sent on dry ice to Dr. Gerhard Liebisch (Institut für Klinische Chemie und Laboratoriumsmedizin des Universitätsklinikums Regensburg, Germany) for electrospray ionization tandem mass spectrometry (ESI-MS/MS) analysis [118, 119].

3.2.12 Cholesterol determination with the Amplex Red Cholesterol Kit

Cells were plated at 200 000 cells per well into 6-well plates and grown for 48 h. After two washes with PBS, either 1) cells were lysed with SDS-buffer or 2) lipids and cholesterol were extracted using isopropanol and cells were lysed subsequently with NaOH. For 1), cells were lysed for 15 min at room temperature with 0.5 ml/well SDS-buffer (0.2 % SDS, 1 mM EDTA in 0.1 M Tris pH 7.4). The lysate was transferred to a tube and the corresponding well was rinsed with 0.5 ml of 0.1 M Tris pH 7.4 containing 1 mM EDTA, which was then combined with the lysate. For 2), lipids/cholesterol were extracted for 30 min at room temperature using 0.5 ml isopropanol per well. The extract was transferred to tubes and the remaining cells were lysed with 1 ml 1 M NaOH for 2 min on a shaker. Protein concentrations of cell lysates were determined using the BCA assay.

The Amplex Red assay was carried out according to the manufacturer's protocol. Briefly, an 8-point cholesterol standard (ranging from 0 to 8 µg/ml) in assay buffer was prepared. The cholesterol containing samples were diluted 1:5 in assay buffer, and a 10 µM H_2O_2 solution was prepared (positive control). The Amplex Red solution was prepared with cholesterol esterase to detect total cholesterol or without cholesterol esterase to detect free cholesterol. 50 µl of Amplex Red solution were added to the wells of a black microplate containing 50 µl of each standard and samples as well as controls in duplicates. After 30 min incubation protected from light at 37 °C, fluorescence was excited at 542 nm and emission was detected at 590 nm.

3.2.13 Transmission electron microscopy

Collagen gels were prepared from Collagen R Solution (0.2 %). 230 µl Collagen R solution were distributed evenly on the bottom of a well of a 12-well plate. 53.4 µl of 10 x MEM containing 0.11 M NaOH were added to each well. Plates were incubated for 60 min at room temperature. 10 000 cells were seeded into wells that were either non-coated or coated with Collagen gels and grown for 96 hours. Cells grown in non-coated wells were trypsinized, washed once with PBS and covered with 1 ml of EM-fixative. Collagen gels containing cells were transferred to 1.5 ml tubes and 1 ml of EM-fixate was added. Fixed cells were sent to Prof. Dr. med. Matthias Ochs (Institut für Funktionelle und Angewandte Anatomie, Medizinische Hochschule Hannover, Germany) for electron microscopic analysis.

3.2.14 Microarray hybridization and data analysis

After collection of total RNA with the High Pure RNA Isolation Kit, 2 µg of each sample were submitted to IMGM Laboratories Munich (Martinsried, Germany) for microarray analysis. At IMGM, the RNA-integrity number (RIN), an index for the quality of the RNA samples, was determined using a 2100 Bioanalyzer (Agilent Technologies). All samples were analyzed using RNA 6000 Nano LabChip Kits (Agilent Technologies). Subsequently, 100 ng of total RNA per sample were reversely transcribed into cDNA and then converted into Cyanine-3 labeled cRNA by *in-vitro* transcription (Low Input Quick-Amp Labeling Kit One-Color, Agilent Technologies). 825 ng of cyanine-3-labeled cRNA were fragmented and prepared for one-color-based hybridization (Gene Expression Hybridization Kit, Agilent Technologies). Each single cRNA sample was hybridized at 65 °C for 17 h on separate Human GE Microarrays (8x60K, Agilent Technologies). Fluorescent signal intensities were detected with the Scan Control A.8.4.1 Software (Agilent Technologies) on an Agilent DNA Microarray Scanner and extracted from the images using Feature Extraction 10.7.3.1 Software (Agilent Technologies). Feature Extraction 10.7.3.1 was used for quality control and visualization of the performance of microarray analysis. Normalization and processing of the raw microarray data was perfomed by Dr. Philipp Pagel (Lehrstuhl für Genomorientierte Bioinformatik, TU München, Germany) with the R statistical language [120] using packages form the Bioconductor framework [121]. Analysis of differential expression was carried out with the limma package [122] which fits a linear model for each gene and computes a moderated t-statistic and its p-value [123]. limma is part of the Bioconductor project [121].

Adjustment for multiple testing was done using the method by Benjamini and Hochberg [124]. For pathway analysis, DAVID Bioinformatics Resources 6.7, a functional annotation tool freely available on the internet as online tool, was used [125, 126]. Gene lists of the normalized microarray comparisons with an adjusted P value below 0.05 and with $log_2FC < -1$ or $log_2FC > 1$ were uploaded. The gene lists contained plain Agilent IDs of regulated genes but no other informations, i.e. fold change or P values. A background list was created using all Agilent IDs form the microarray. Agilent IDs of the gene lists and background list were converted to DAVID IDs using the DAVID tool, thereby collapsing multiple probe IDs of the same gene to one DAVID ID. Functional annotation charts containing only KEGG pathways with an EASE score (P value) below 0.05 were exported and the fold changes and P values of the corresponding genes were assembled manually.

3.2.15 Statistics

Comparisons of multiple groups were done using one-way repeated measure ANOVA with Tukey's post hoc test. Results are presented as mean + S.E.M. from a minimum of three different experiments except stated otherwise. P-values below 0.05 were considered statistically significant. All tests were performed using GraphPad Prism 4.0 (GraphPad Software).

4 Results

4.1 Characterization of stably transfected A549 cells

4.1.1 Stable transfection and growth of A549 cells

A549 cells were stably transfected with pUB6-vectors coding for HA-tagged ABCA3-WT protein and ABCA3 with the mutations p.Q215K and p.E292V. qPCR revealed that ABCA3 mRNA expression of stably transfected A549 cells was increased between 4 to 8-fold compared to non-transfected cells (Figure 4.1). Transient expression of HA-tagged ABCA3-WT in A549 cells induced an approximate 600-fold increase of ABCA3 mRNA when compared with non-transfected A549 cells (data not shown).

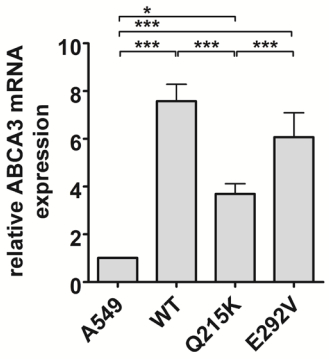

Figure 4.1: ABCA3 mRNA in stably transfected A549 cells.
Cells were grown for 48 h. RNA was isolated and analyzed by qPCR. Results were calculated relative to non-transfected A549 cells.
*P<0.05, ***P<0.001.

In western blot analysis of cell lysates from stably transfected cells using an antibody against the HA-tag, two bands were detected for ABCA3-WT and p.E292V at 150 and 190 kDa. For p.Q215K protein, only one band at 190 kDa was detected (Figure 4.2 A). Also in transiently transfected cells, two ABCA3 bands of 150 and 190 kDa were found for ABCA3-WT and p.E292V (Figure 4.2 C). Similar to stably transfected cells, only one protein form (190 kDa) was detected in case of p.Q215K. For both types of transfection, the ratio of the upper-to-lower ABCA3 band in ABCA3-WT and p.E292V cells was determined. As can be seen in Figure 4.2, the amount of the lower molecular weight form (150 kDa) was increased in stably transfected cells. Therefore, the upper-to-lower band ratio was decreased more than five-fold compared to transiently transfected ABCA3-WT and p.E292V cells. Also, the ratio of upper to lower band after stable transfection was decreased in p.E292V cells compared to ABCA3-WT cells. As expected, non-transfected A549 cells did not express HA-tagged ABCA3 protein (Figure 4.2 A, C).

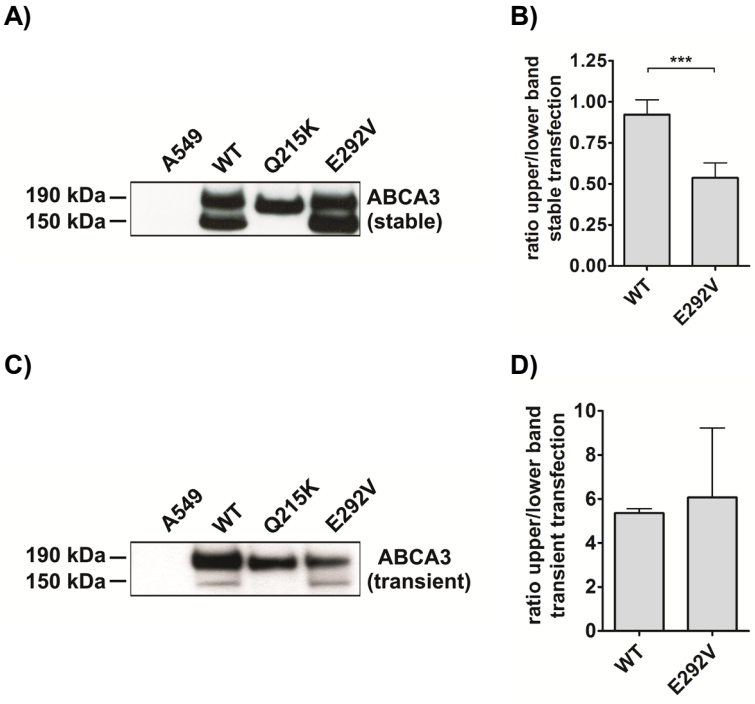

Figure 4.2: HA-tagged ABCA3 protein in stably and transiently transfected A549 cells.
A, B) Stably transfected cells were grown for 48 h. C, D) After cells had been grown for 24 h, they were transiently transfected and grown for another 48 h. A, C) Western blot of HA-tagged protein. B, D) The ratio of upper to lower band was calculated from densitometric analysis. ***P<0.001.

To verify equal growth rates of non-transfected and stably transfected A549 cells, the MTT proliferation assay was used. Between 0 and 72 h, the growth time used for normal experiments, no differences in cell growth were detected for all cells (Figure 4.3 A). At 96 h, proliferation was slightly increased in ABCA3-WT cells (Figure 4.3 B).

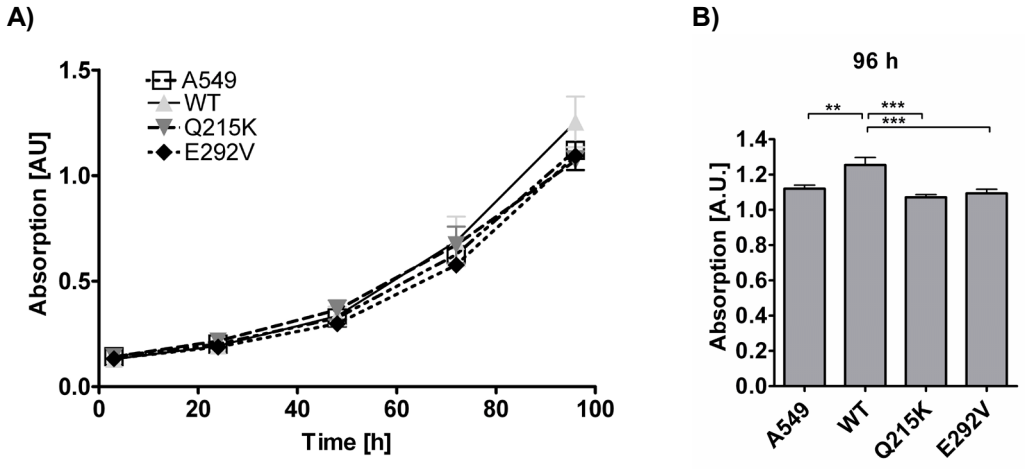

Figure 4.3: Effects of ABCA3 mutations on cell proliferation.
A) Growth curves at time points 4, 24, 48, 72 and 96 h. B) Comparison of cell density after 96 h cell growth. **P<0.01, ***P<0.001.

Next, the secretory capacity of non-transfected and stably transfected cells was investigated using an assay based on secretion of a renilla luciferase. Compared to non-transfected A549 cells, all stably transfected cells had a significantly decreased secretory

potential (Figure 4.4). Amongst the stably transfected cells, ABCA3-WT cells secreted the most luciferase, followed by p.Q215K cells. Cells transfected with the vector coding for ABCA3-p.E292V had the lowest secretory potential.

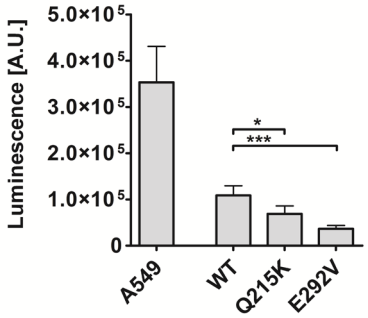

Figure 4.4: Effects of ABCA3 mutations on luciferase secretion.
Cells were grown for 48 h. P value was below 0.001 for all cells compared to A549 cells. *P<0.05, ***P<0.001.

4.1.2 Localization of ABCA3 in stably transfected cells and expression of ER chaperones

To determine the localization of WT and mutant ABCA3 in stably transfected A549 cells, co-immunofluorescence studies were performed. As shown in Figure 4.5 A, ABCA3-WT properly colocalized with LAMP3, a marker for lysosomes and lamellar bodies. ABCA3-WT and LAMP3 were stained in a ring-like fashion, consistent with their localization in the outer membrane of lamellar bodies. HA-tagged ABCA3-WT did not, or only to a very small extent, colocalize with the ER-chaperone calnexin (Figure 4.5 B). Similar was observed for the localization of p.E292V: p.E292V colocalized with LAMP3 and mostly did not localize with calnexin. On the other hand, the mutant ABCA3 p.Q215K colocalized with the ER chaperone calnexin and thus did not reach its final destination, the lamellar body. In addition, no colocalization was observed for the early endosomal marker EEA1 or for ubiqitin for WT and mutant ABCA3 (Figure 4.5 C, D).

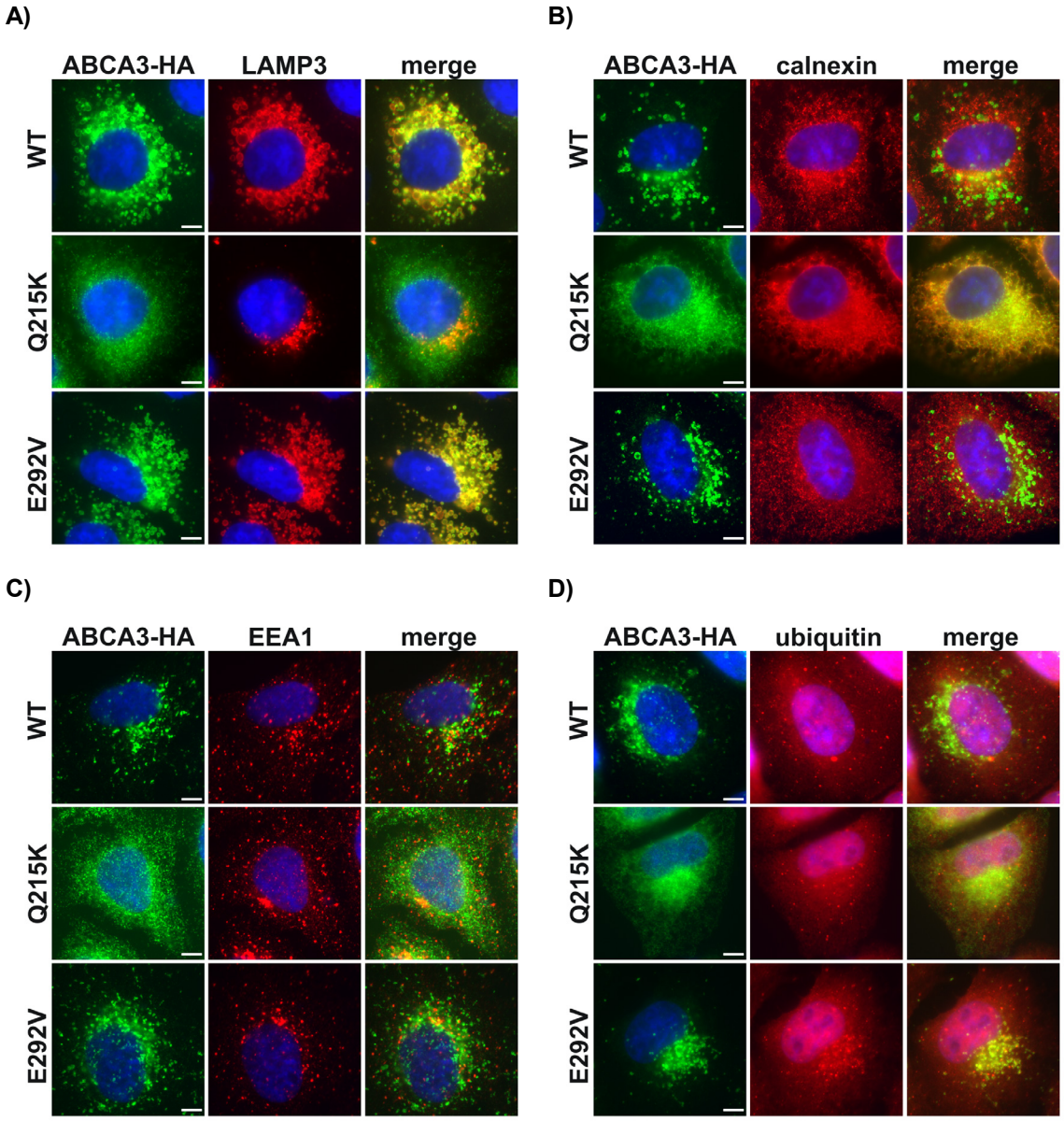

Figure 4.5: Immunofluorescence colocalization analysis of HA-tagged ABCA3 protein in stably transfected A549 cells.
Cells were grown for 48 h and HA-tagged ABCA3 (green) was costained with LAMP3 (A), calnexin (B), EEA1 (C) or ubiquitin (D). The merge images present the overlay from the green and red fluorescence. Scale bar 2.5 µm.

For the analysis of intracellular amounts of the ER chaperone calnexin, western immunoblots were performed. As can be seen in Figure 4.6, calnexin levels were similar in all cells.

Interestingly, when cells were co-stained for the HA-tag and the ER chaperone BiP, colocalization of BiP and ABCA3-WT protein as well as colocalization of BiP and p.E292V was observed in a ring-like fashion (Figure 4.7). No colocalization of BiP with p.Q215K was found.

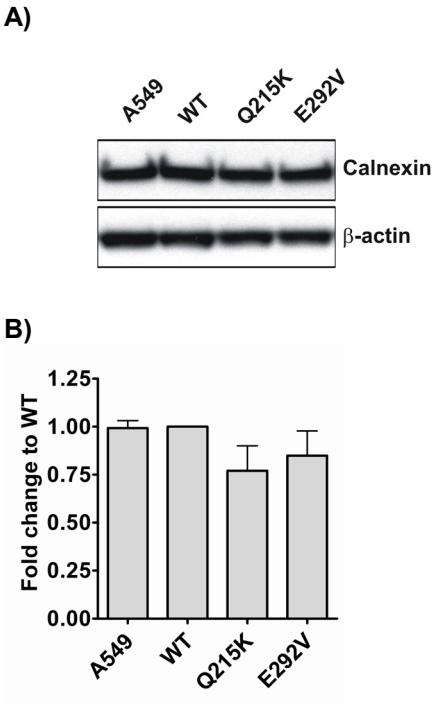

Figure 4.6: Effects of ABCA3 mutations on calnexin protein. Cells were grown for 48 h. A) Calnexin in western immunoblot. B) Densitometric analysis. Results were calculated relative to ABCA3-WT transfected cells. β-actin was used as loading control.

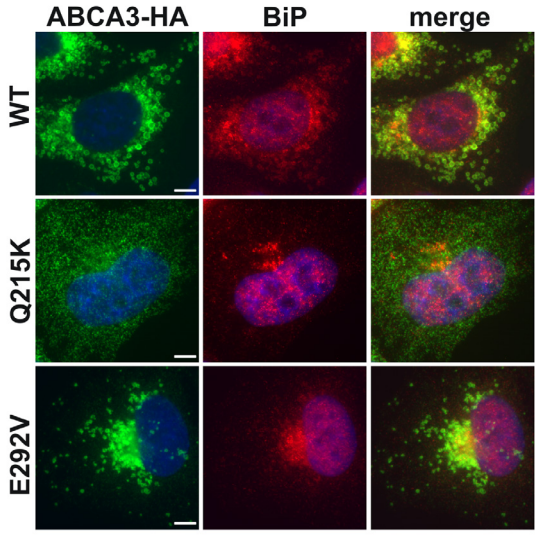

Figure 4.7: Immunofluorescence staining of the ER-chaperone BiP. Cells were grown for 48 h. Cells were stained for HA-tag (green) or BiP (red). Green and red fluorescence are overlayed in the merge image (right panels). Scale bar 2.5 µm.

Subsequently, western immunoblot was performed to determine intracellular amounts of BiP protein. As shown in Figure 4.8, cells expressing ABCA3-WT protein produced the most BiP protein, followed by non-transfected A549 cells. Cells harboring mutant ABCA3 had equally low amounts of BiP protein which were decreased by more than two-fold compared to ABCA3-WT cells.

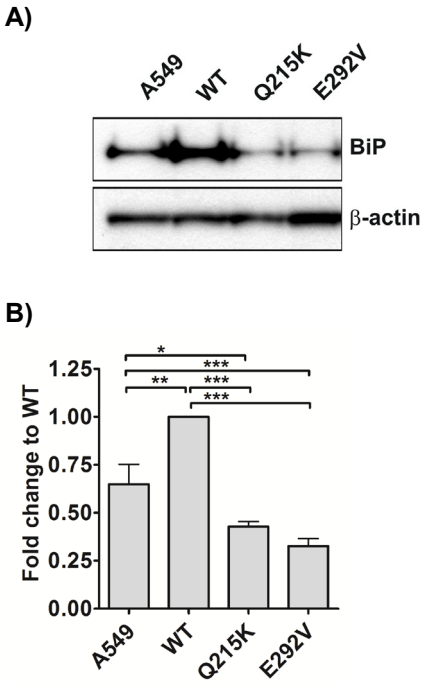

Figure 4.8: Effects of ABCA3 mutations on BiP protein.
Cells were grown for 48 h. A) Western immunoblot of BiP protein. B) Densitometric analysis. Results were calculated relative to ABCA3-WT transfected cells. β-actin was used as loading control. *P<0.05, **P<0.01, ***P<0.001.

4.1.3 Transmission electron microscopy

Cells were investigated by transmission electron microscopy (TEM) to evaluate the ultrastructural effects of ABCA3 mutations on lung epithelial cells. As can be seen in Figure 4.9 (left panels), the cellular integrity of the cell preparation was good. In non-transfected A549 control cells, only very few structures corresponding to lamellar bodies from ATII were detected (Figure 4.9 a, b). Expression of ABCA3-WT did not change the cellular ultrastructure compared to non-transfected A549 cells and did not induce increased lamellar body formation (Figure 4.9 c, d). ABCA3 mutant proteins p.E292V and especially p.Q215K induced extentions of the endoplasmic reticulum and formation of vesicles without visible content (Figure 4.9 e-h). An increase in the LB number was also not found in these cells.

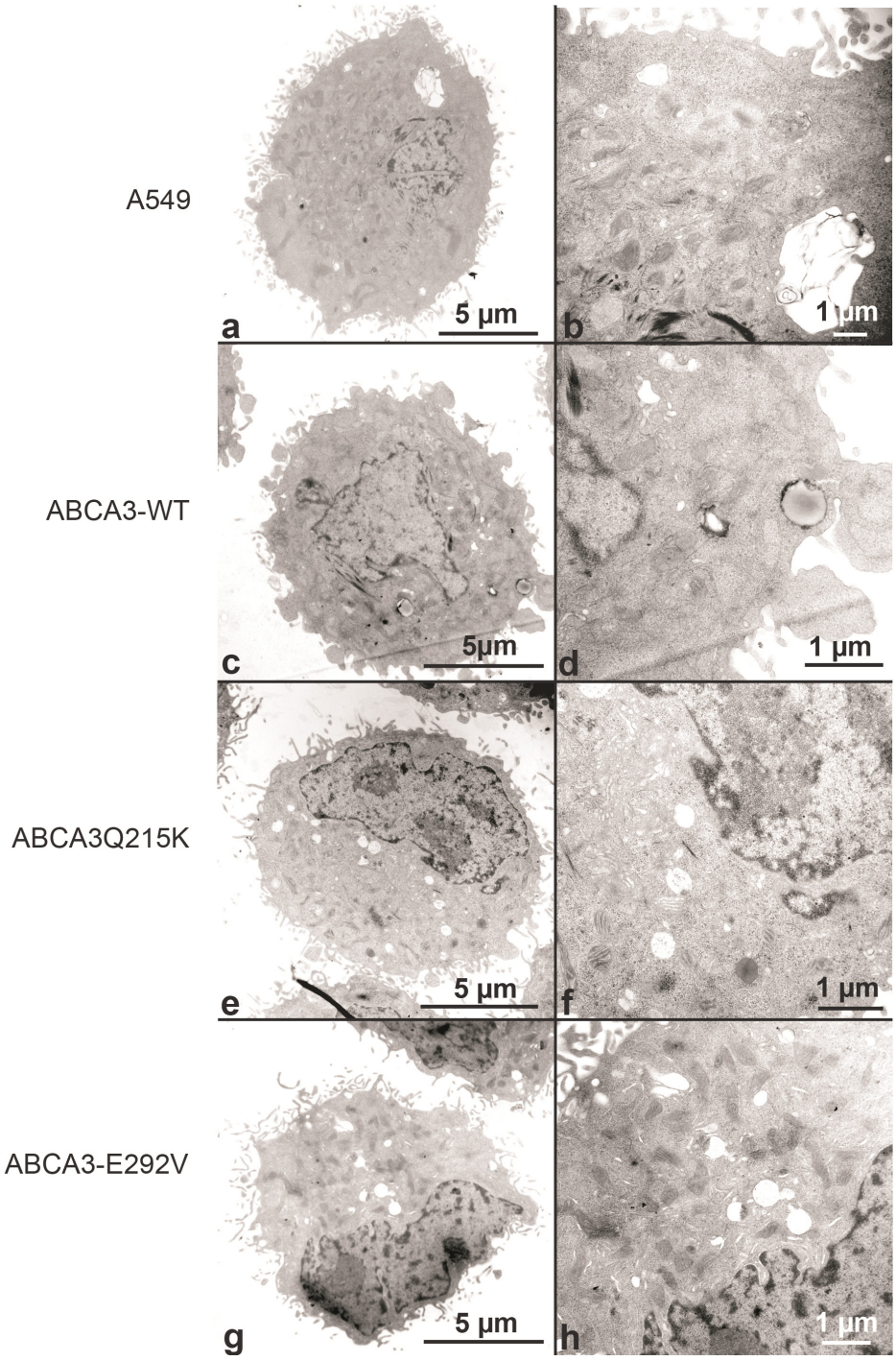

Figure 4.9: TEM representation of non-transfected A549 cells and cells harboring ABCA3-WT and mutations.
Left panels (a, c, e and g): overview of cells, right panels (b, d, f and h): detailed images of intracellular structures.

4.1.4 Expression of epithelial markers

To investigate the molecular effects of ABCA3 mutations on lung epithelial cells, first the expression of epithelial markers was analyzed. As shown in Figure 4.10, the mRNA of the ATII specific surfactant protein C (SP-C) was significantly decreased by three to four-fold

in cells harbouring ABCA3 mutations compared to ABCA3-WT and non-transfected A549 cells.

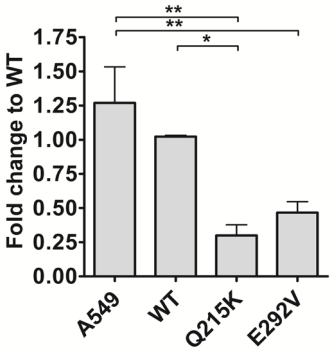

Figure 4.10: Effects of ABCA3 mutations on SP-C mRNA expression.
Cells were grown for 48 h. Results are calculated relative to ABCA3-WT cells.
*P<0.05, **P<0.01.

Next to SP-C, the expression of the cellular adhesion molecules E-cadherin, abundant in adherens junctions, and zonula occludens-1 (ZO-1), present in tight junctions, was investigated. E-cadherin was strongly decreased in cell lysates from cells with both ABCA3 mutations (Figure 4.11 A). ZO-1 was decreased almost three-fold in cells with p.Q215K mutation (Figure 4.11 B).

The results were supported by immunofluorescence studies. In ABCA3-WT cells, E-cadherin was properly and abundantly localized close to the cell surface (Figure 4.12 A). In p.Q215K cells, almost no E-cadherin was detected. Even though some E-cadherin was found in p.E292V cells, the adhesion molecule was not properly localized to the cell membrane but co-localized with the HA-tag of the ABCA3-p.E292V protein. ZO-1 was also detected on the cell surface in cells expressing ABCA3-WT and p.E292V (Figure 4.12 B). In p.Q215K cells, only very little ZO-1 was seen either on the cell surface or intracellularly, thus supporting the western immunoblot findings.

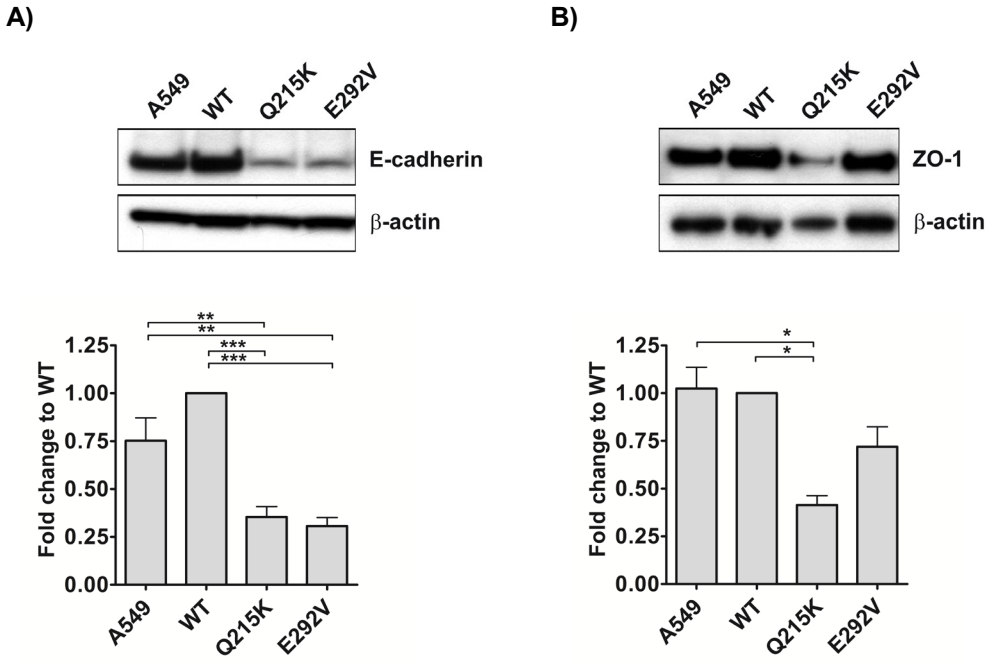

Figure 4.11: Effects of ABCA3 mutations on epithelial marker proteins.
Cells were grown for 48 h. A) E-Cadherin western immunoblot (top) and densitometric analysis (bottom). B) ZO-1 western immunoblot (top) and densitometric analysis (bottom). β-actin was used as loading control. Results were calculated relative to ABCA3-WT cells. *P<0.05, **P<0.01, ***P<0.001.

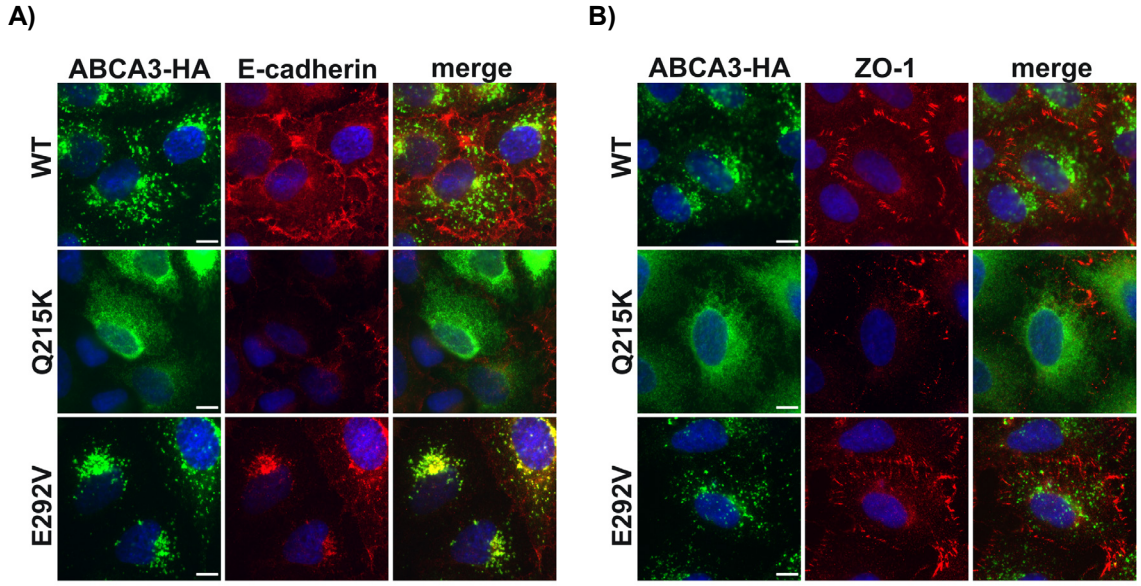

Figure 4.12: Immunofluorescence localization studies of epithelial markers in stably transfected A549 cells.
Cells were grown for 48 h. HA-tagged ABCA3-protein is presented in green. A) E-cadherin and B) ZO-1 staining (both red). The overlay of the red and green color is presented in the merge image. Scale bar 4 µm.

4.1.5 Expression of mesenchyme-associated markers

The transcription factor SNAI1 was shown to repress the expression of E-cadherin [127, 128]. Therefore, the presence of SNAI1 in nuclear extracts of stably transfected cells was

investigated. SNAI1 was significantly increased (more than four-fold) in nuclear extracts of p.Q215K cells compared to cells expressing ABCA3-WT (Figure 4.13). In p.E292V cells, SNAI1 was slightly, but not significantly upregulated.

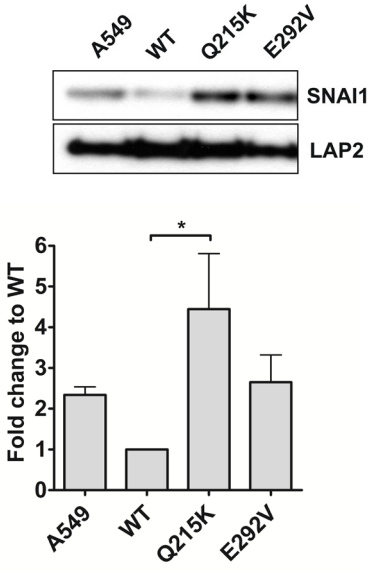

Figure 4.13: Effects of ABCA3 mutations on the SNAI1 transcription factor.
Cells were grown for 48 h. SNAI1 western immunoblot was performed with nuclear extracts. Results were calculated relative to ABCA3-WT cells. LAP2 was used as loading control. *P<0.05.

Elevated levels of endothelin-1 (ET-1), a 21-amino acid peptide, are found in patients with fibrosing lung diseases (scleroderma, pulmonary fibrosis) [129]. In cells expressing ABCA3 mutations, significantly two-fold increased ET-1 mRNA expression compared to ABCA3-WT cells was found (Figure 4.14). ET-1 mRNA was not significantly elevated in non-transfected A549 cells compared to cells transfected with the vector coding for ABCA3-WT protein. Similarly, ET-1 secretion into cell culture supernatants was elevated in all cells compared to ABCA3-WT cells (Figure 4.14 B).

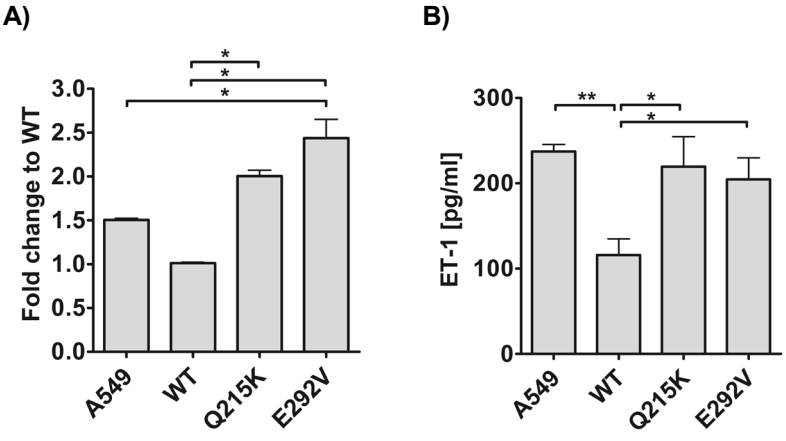

Figure 4.14: Effects of ABCA3 mutations on ET-1 mRNA expression and secretion.
Cells were grown for 48 h. A) ET-1 qPCR. Results were calculated relative to ABCA3-WT cells. B) ET-1 ELISA. *P<0.05, **P<0.01.

Matrix metalloproteases (MMPs) have also been shown to be upregulated in tissues from patients with fibrosing lung diseases. In cells harbouring the p.Q215K mutation, MMP-2 mRNA was significantly upregulated (Figure 4.15 A). Similarly, MMP-2 levels in supernatants of p.Q215K cells were significantly elevated more than eight-fold compared to all other cells (Figure 4.15 B). No MMP-2 was detected in supernatants from ABCA3-WT cells.

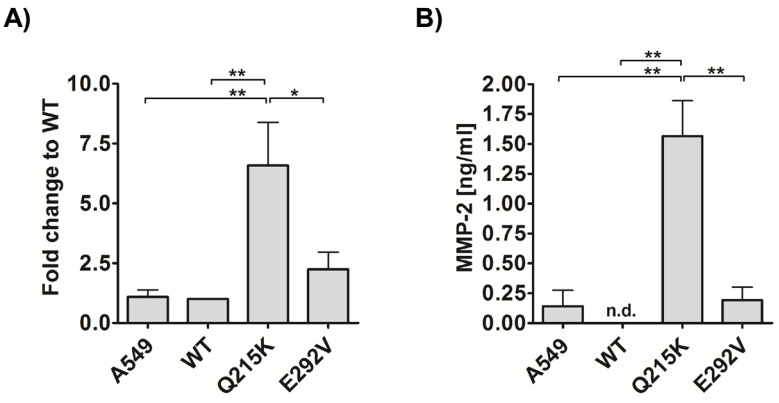

Figure 4.15: Effects of ABCA3 mutations on MMP-2 mRNA expression and secretion.
Cells were grown for 48 h. A) MMP-2 qPCR. Results were calculated relative to ABCA3-WT cells. B) MMP-2 ELISA. *P<0.05, **P<0.01.

To investigate which intracellular signals might be responsible for the upregulation of mesenchymal markers, the expression and secretion of the signaling molecule TGF-β1 was analyzed. mRNA levels of TGF-β1 were elevated in p.Q215K cells compared to ABCA3-WT and non-transfected A549 cells (Figure 4.16 A). These data were supported by ELISA measurements of secreted TGF-β1 protein in cell culture supernatants (Figure 4.16 B). TGF-β1 secretion was significantly elevated in cells harbouring p.Q215K mutant protein compared to all other cells.

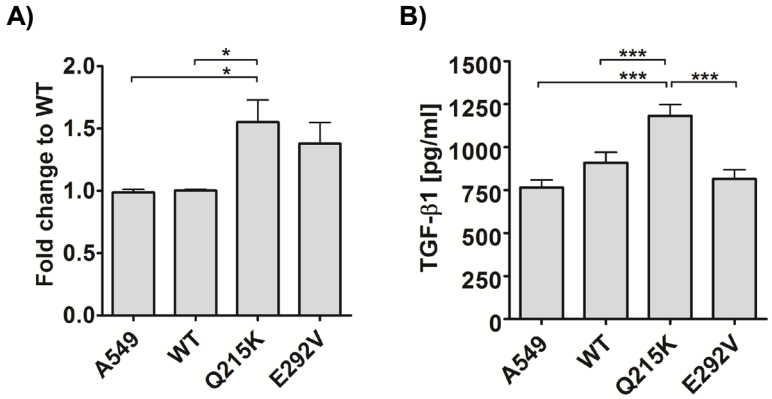

Figure 4.16: Effects of ABCA3 mutations on TGF-β1 mRNA expression and secretion.
Cells were grown for 48 h. A) TGF-β1 qPCR. Results were calculated relative to ABCA3-WT cells. B) TGF-β1 ELISA. Cells were grown in RPMI medium supple-mented with 0.1 % FBS. *P<0.05, ***P<0.001.

The tyrosine kinase Src was shown to signal in various cellular processes, including cell-matrix adhesion dynamics, regulation of the cytoskeleton and cell migration as well as

proliferation [130]. Therefore, the activation of Src by phosphorylation was investigated. In p.Q215K cells the ratio of phosphorylated Src to Src was significantly elevated compared to all other cells.

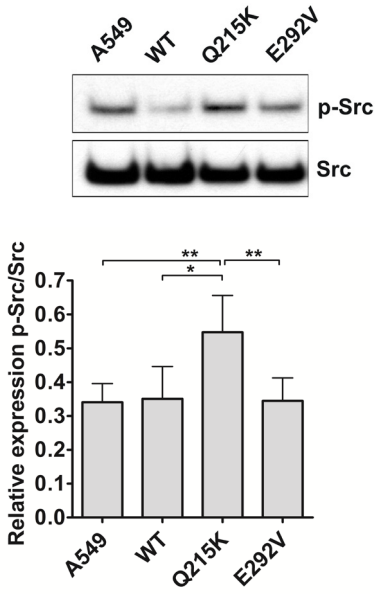

Figure 4.17: Effects of ABCA3 mutations on Src phosphorylation. Cells were grown for 48 h. Results were calculated from the ratio of phospho (p)-Src to Src. *P<0.05, **P<0.01.

4.1.6 Expression of ABCA1

Nonfunctional ABCA3 may influence the expression of other lipid transporters. Therefore, expression of ABCA1 was investigated. As shown in Figure 4.18, ABCA3 mutations significantly induced ABCA1 mRNA expression. Moreover, ABCA1 protein in cell lysates of cells harboring ABCA3 mutations was strongly increased.

In immunofluorescence studies, ABCA1 was not localized to the cell surface but was found to colocalize with HA-tagged ABCA3-WT protein and ABCA3-p.E292V (Figure 4.19). In p.E292V cells, more ABCA1 vesicles than ABCA3/ABCA1-positive vesicles were found. ABCA1 also seemed to be present in vesicular structures in p.Q215K cells. No colocalization was seen for p.Q215K and ABCA1.

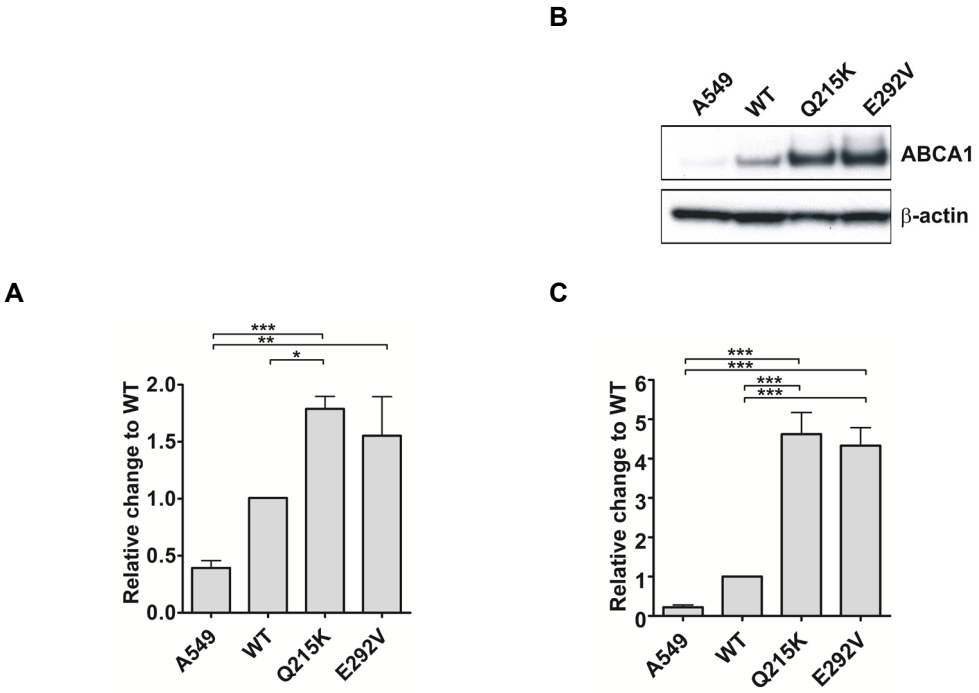

Figure 4.18: Effects of ABCA3 mutations on ABCA1 mRNA and protein.
Cells were grown for 48 h. A) ABCA1 qPCR. B, C) ABCA1 in western immunoblot. Results were calculated relative to ABCA3-WT cells. β-actin was used as loading control. *P<0.05, **P<0.01, ***P<0.001.

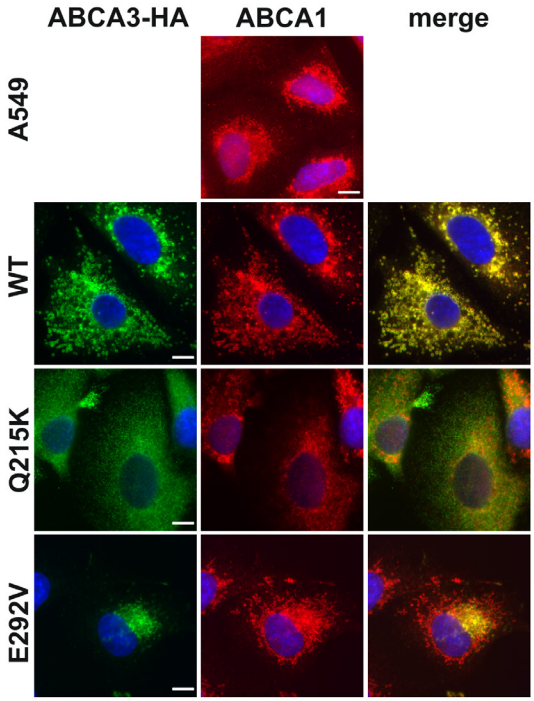

Figure 4.19: ABCA1 localization in stably transfected A549 cells.
Cells were grown for 48 h. The merge image is the overlay of the green (ABCA3-HA) and red (ABCA1) fluorescence. Scale bar 4 µm.

4.1.7 Cellular cholesterol content

Since ABCA3 and ABCA1, which was upregulated in cells harboring ABCA3 mutations, are proteins involved in the transport of lipids and / or cholesterol, the lipid and cholesterol content in cell lysates of stably transfected cells was determined. The total cholesterol was slightly elevated in p.Q215K cells compared to cells expressing ABCA3-WT (Figure 4.20 A, D). Similarly, also free cholesterol was slightly increased in p.Q215K cells compared to ABCA3-WT cells (Figure 4.20 B, E). In addition to free cholesterol, cells expressing ABCA3 mutations had significantly elevated levels of intracellular cholesterol esters compared to the non-transfected A549 control (Figure 4.20 F). Compared to ABCA3-WT cells, cholesterol esters were significantly elevated in p.Q215K mutant cells.

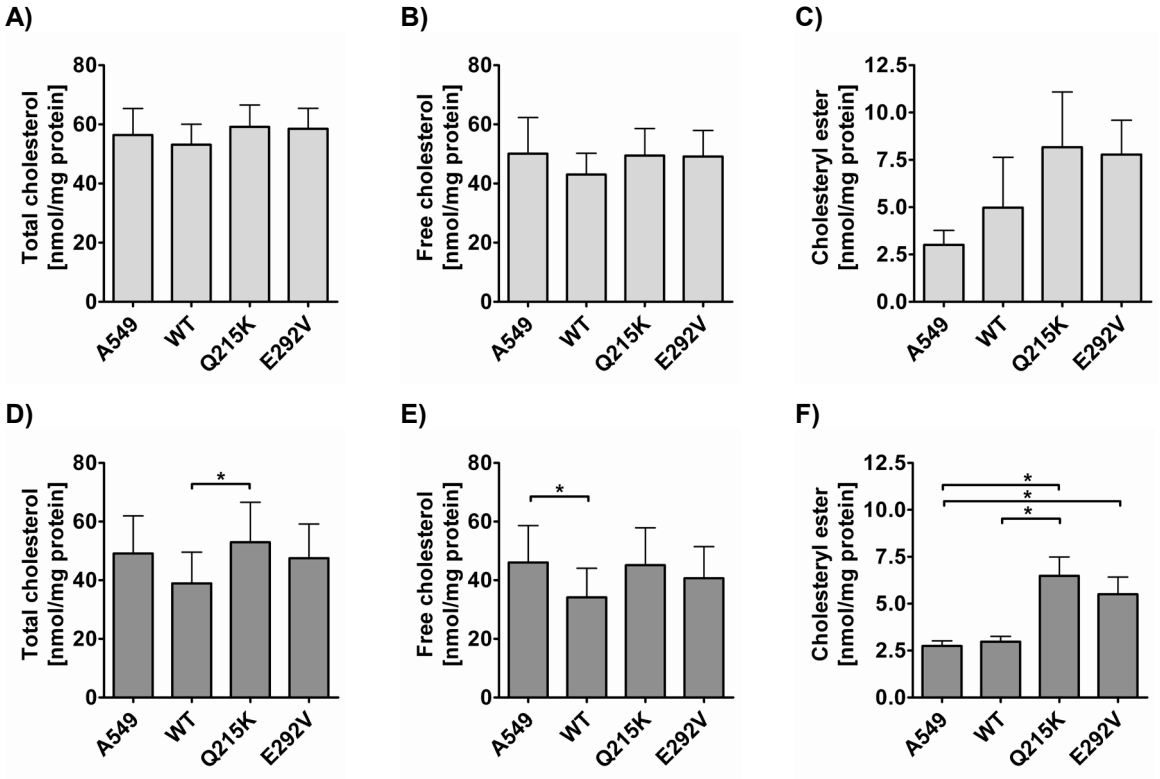

Figure 4.20: Cholesterol analysis.
Cells were grown for 48 h and either lysed with SDS or incubated with isopropanol for lipid extraction. With the Amplex-Red Kit, total (A) and free cholesterol (B) were determined, esterified cholesterol (C) being the difference of total cholesterol – free cholesterol. Using mass spectrometry, total cholesterol (D) was calculated from the sum of free cholesterol (E) + cholesterol ester (F). *P<0.05.

4.1.8 Oil Red O staining

Oil Red O staining was performed to investigate the intracellular distribution of lipid droplets. Oil Red O stains neutral lipids, i.e. cholesterol; therefore it can be used to visualize lipid storage vesicles. As can be seen in Figure 4.21, Oil Red O positive vesicles

were found distributed over the cytoplasm in all cells. In non-transfected A549 cells, almost two-fold more lipid droplets were stained when compared with all stably transfected cells (Figure 4.22 A). Cells harboring mutant ABCA3 had about the same amounts of Oil Red O positive droplets as ABCA3-WT cells. When the size of the lipid droplets was analyzed, it was found that the area of droplets in ABCA3-mutant cells and non-transfected A549 cells was increased by more than two-fold when compared with lipid vesicles in ABCA3-WT cells (Figure 4.22 B).

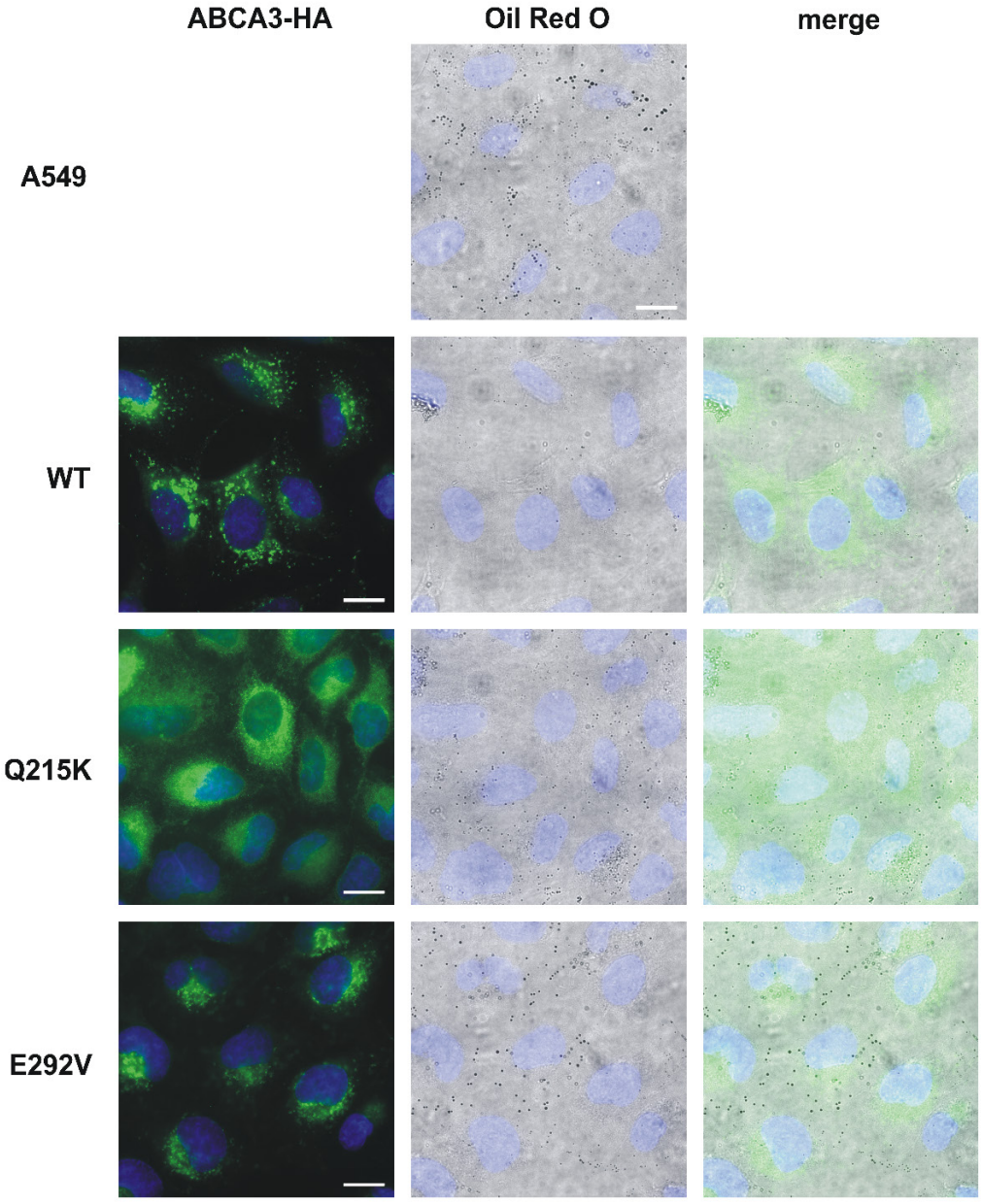

Figure 4.21: Oil Red O and ABCA3-HA staining in non-transfected and stably transfected A549 cells.
Cells were grown for 48 h. Lipid droplets were stained using Oil-red-O and HA-tagged ABCA3 protein was visualized by green fluorescence. The Oil Red O staining appears as black dots as the used microscope only records black-and-white images. Scale bar 8.5 µm.

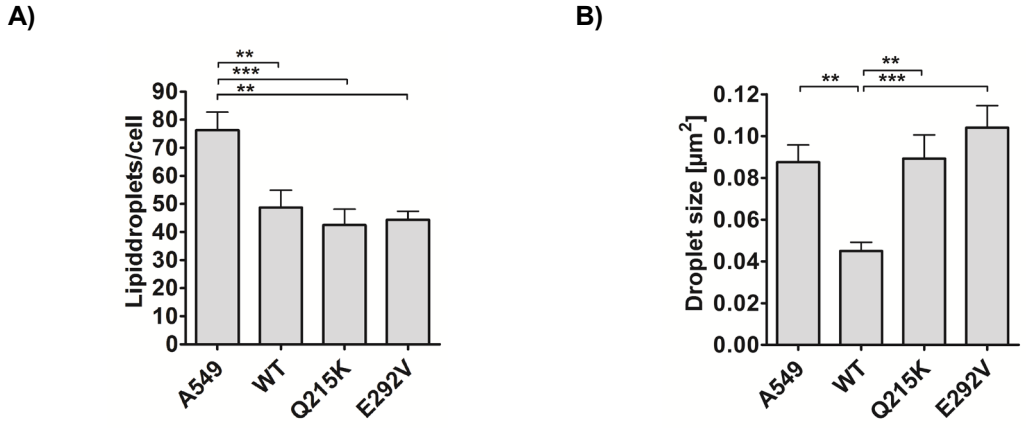

Figure 4.22: Effects of stable transfection and ABCA3 mutations on lipid droplet amount and size.
Cells were grown for 48 h on coverslips and stained with Oil-Red-O. A) Lipid droplet count per cell. B) Average lipid droplet size. At least six images per experiment and cell line from a total of three independent experiments were evaluated. **P<0.01, ***P<0.001.

4.1.9 Cellular lipid composition

To investigate the influence of ABCA3 mutations on the lipid metabolism of lung epithelial cells, the lipid composition of cell lysates was determined using mass spectrometry. As shown in Figure 4.23, the total lipid amount was slightly elevated in p.Q215K cells compared to ABCA3-WT cells. There were no significant differences detected between all other cells.

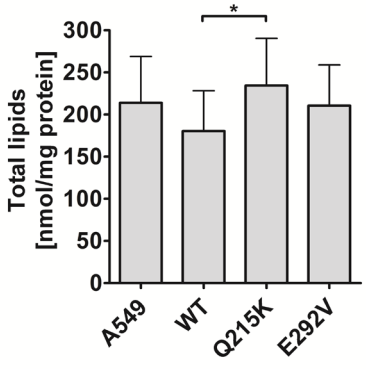

Figure 4.23: Total lipids in non-transfected and stably transfected A549 cells.
Cells were grown for 48 h and cell lysates were analyzed by mass spectrometry. Total lipids = phospholipids + ceramides + glucosyl ceramide + plasmenylethanolamine + cholesterol. *P<0.05.

The relative amounts of the analyzed lipid species in non-transfected A549 cells as well as in stably transfected A549 cells are presented in Figure 4.24. For most of the lipid species, no significant differences were detected. Relative to the total amounts of lipids, ABCA3-WT cells had significantly elevated levels of PE compared to all other cells. In p.Q215K cells, the relative amounts of dihydro-SPM, PG and glucosyl ceramides were elevated

compared to ABCA3-WT cells. Relative amounts of free cholesterol and PS were increased in non-transfected A549 cells, whereas relative amounts of SPM were increased in p.E292V cells when compared with ABCA3-WT cells.

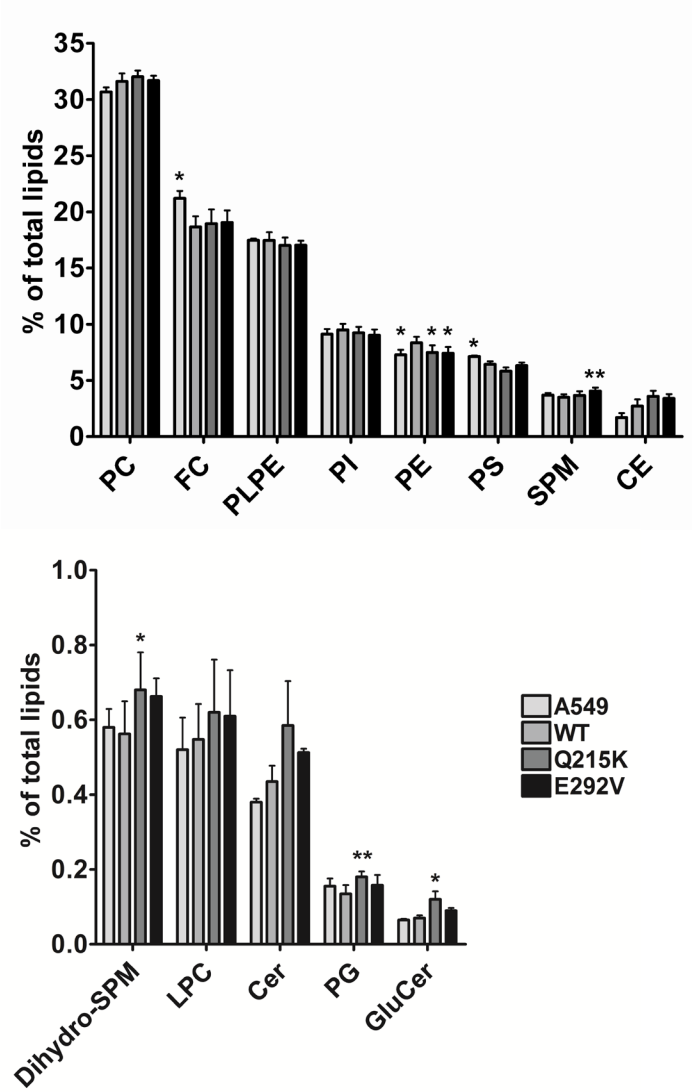

Figure 4.24: Relative amounts of lipid species in non-transfected and stably transfected A549 cells.
Cells were grown for 48 h and lipids in cell lysates were detected using mass spectrometry. Results are presented relative to the total cellular lipid amount. *P< 0.05, ** P<0.01 all compared to ABCA3-WT of the respective lipid species. PC – phosphatidylcholine, FC – free cholesterol, PLPE – plasmenylethanolamine, PI – phosphatidylinositol, PE – phosphatidylethalnolamine, PS – phosphatidylserine, SPM – sphingomyelin, CE – cholesterol ester, LPC – lyso-PC, Cer – ceramide, PG – phosphatidylglycerol, GluCer – glucocysyl ceramide.

In the following tables (Table 4.1, 4.2, 4.3 and 4.4), the absolute amount of each lipid species, the relative amount of the species compared to the total lipid amount, the relative amount of respective phospholipid (PL) species compared to the total PL amount, as well as the relative amount of analyzed subspecies compared to the corresponding lipid species (> 3 %) are presented. The following lipid species were accounted for as phospholipids:

phosphatidylcholine, phosphatidylinositol, phosphatidylethanolamine, phosphatidylserine, phosphatidylglycerol, sphingomyelin, dihydrosphingomyelin and lysophosphatidylcholine. Tables with all results are included in the supplement (section 7.1.1).

Overall, it can be seen that the relative distribution of lipid species does not vary much between non-transfected A549 cells, ABCA3-WT cells and ABCA3 mutant cells.

Table 4.1: Cellular lipid composition of PC, TC, CE and FC.

	A549 [mean±SD]	P (A549) ANOVA	WT [mean±SD]	Q215K [mean±SD]	P (p.Q215K) ANOVA	E292V [mean±SD]	P (p.E292V) ANOVA
PC [ng/mg protein]	65.38 ± 33.07	---	57.61 ± 31.61	75.24 ± 35.79	*	66.54 ± 29.66	---
PC (% of total lipids]	30.68 ± 0.81	---	31.61 ± 1.45	32.02 ± 1.12	---	31.68 ± 0.88	---
PC (% of PL]	51.86 ± 1.25	---	52.09 ± 1.54	53.63 ± 1.04	---	52.88 ± 0.88	---
PC 34:1 [% of total PC]	26.75 ± 1.90	---	25.38 ± 1.39	24.00 ± 2.03	---	25.18 ± 0.89	---
PC 32:1 [% of total PC]	18.16 ± 1.31	---	17.41 ± 2.65	14.26 ± 1.64	**	14.50 ± 2.00	**
PC 36:2 [% of total PC]	9.92 ± 0.79	---	11.59 ± 1.64	12.74 ± 1.54	---	11.94 ± 0.96	---
PC 34:2 [% of total PC]	7.85 ± 0.94	---	8.82 ± 1.53	9.99 ± 1.43	---	8.02 ± 0.65	---
PC 32:0 [% of total PC]	3.26 ± 0.51	*	4.14 ± 0.56	3.89 ± 0.17	---	4.50 ± 0.51	---
PC O 34:1 [% of total PC]	4.82 ± 0.41	*	3.87 ± 0.37	4.92 ± 0.62	**	5.15 ± 0.41	**
PC 36:1 [% of total PC]	4.28 ± 0.74	*	3.61 ± 0.93	3.99 ± 1.03	---	4.03 ± 0.81	---
PC 30:0 [% of total PC]	3.06 ± 0.53	*	3.41 ± 0.49	2.68 ± 0.38	***	3.18 ± 0.28	---
TC [nmol/mg protein]	49.15 ± 25.55	---	38.90 ± 21.37	52.94 ± 27.36	*	47.52 ± 23.33	---
TC[% of total lipids]	22.97 ± 0.77	---	21.55 ± 0.77	22.58 ± 2.31	---	22.56 ± 1.53	---
CE [nmol/mg protein]	3.08 ± 0.77	---	4.75 ± 3.58	7.78 ± 2.96	*	6.83 ± 2.94	*
CE [% of total lipids]	1.70 ± 0.79	---	2.72 ± 1.17	3.60 ± 0.97	---	3.39 ± 0.79	---
FC [nmol/mg protein]	46.07 ± 25.14	*	34.14 ± 19.81	45.15 ± 25.50	---	40.70 ± 21.53	---
FC [% of total lipids]	21.22 ± 1.30	*	18.67 ± 1.90	18.96 ± 2.52	---	19.05 ± 2.14	---
CE 18:1 [% of total CE]	28.73 ± 2.74	---	33.35 ± 6.64	37.70 ± 2.14	---	36.30 ± 2.99	---
CE 16:0 [% of total CE]	15.40 ± 1.01	---	14.40 ± 2.76	15.23 ± 2.39	---	16.60 ± 2.59	---
CE 16:1 [% of total CE]	13.20 ± 1.41	---	12.28 ± 2.00	11.98 ± 1.67	---	11.53 ± 1.79	---
CE 20:0 [% of total CE]	10.03 ± 2.34	---	7.68 ± 3.21	4.38 ± 0.59	---	4.85 ± 1.05	---
CE 18:2 [% of total CE]	5.63 ± 0.56	---	6.18 ± 1.55	5.43 ± 0.80	---	5.75 ± 0.85	---
CE 22:6 [% of total CE]	5.33 ± 1.35	---	4.85 ± 1.02	5.93 ± 0.33	---	4.90 ± 0.55	---
CE 18:0 [% of total CE]	5.75 ± 0.48	**	4.50 ± 0.49	4.23 ± 0.46	---	4.78 ± 0.62	---

All subspecies > 3% of the corresponding species are presented. SD - standard deviation, PL - phospholipid, PC - phosphatidylcholine, TC – total cholesterol, CE - cholesterol ester, FC - free cholesterol, P – P value compared to WT. *P<0.05, **P<0.01, ***P<0.001.

Table 4.2: Cellular lipid composition of PLPE and PI.

	A549 [mean±SD]	P (A549) ANOVA	WT [mean±SD]	Q215K [mean±SD]	P (p.Q215K) ANOVA	E292V [mean±SD]	P (p.E292V) ANOVA
PLPE [nmol/mg protein]	37.42 ± 19.26	---	30.48 ± 14.08	38.77 ± 16.19	---	35.36 ± 14.96	---
PLPE [% of total lipids]	17.49 ± 0.28	---	17.46 ± 1.45	17.01 ± 1.39	---	17.04 ± 0.78	---
PLPE 16:0/18:1 [% of total PLPE]	20.42 ± 1.11	*	16.80 ± 2.91	22.79 ± 2.62	**	20.97 ± 3.08	*
PLPE 16:0/20:4 [% of total PLPE]	12.11 ± 1.91	---	13.25 ± 3.63	9.89 ± 3.15	**	11.37 ± 2.19	---
PLPE 18:1/18:1 [% of total PLPE]	7.14 ± 0.79	---	8.78 ± 2.63	11.80 ± 3.63	---	10.34 ± 2.05	---
PLPE 16:0/20:3 [% of total PLPE]	6.16 ± 1.26	---	7.59 ± 2.41	4.35 ± 0.36	*	5.19 ± 0.40	---
PLPE 16:0/20:5 [% of total PLPE]	5.87 ± 1.26	---	5.79 ± 1.91	4.90 ± 1.77	---	5.10 ± 1.05	---
PLPE 16:0/22:6 [% of total PLPE]	8.32 ± 0.56	**	4.71 ± 2.08	2.94 ± 1.29	---	4.45 ± 1.62	---
PLPE 16:0/16:1 [% of total PLPE]	4.96 ± 1.28	---	4.51 ± 1.75	6.24 ± 2.56	*	4.71 ± 1.57	---
PLPE 16:0/18:2 [% of total PLPE]	5.14 ± 0.63	---	4.27 ± 0.55	5.62 ± 1.40	*	4.71 ± 0.64	---
PLPE 18:0/18:1 [% of total PLPE]	4.20 ± 0.77	---	3.76 ± 0.97	4.46 ± 0.94	*	5.13 ± 1.33	***
PLPE 18:0/20:4 [% of total PLPE]	3.05 ± 1.06	---	3.43 ± 1.86	2.46 ± 1.13	---	3.19 ± 1.67	---
PLPE 18:1/20:4 [% of total PLPE]	2.06 ± 0.26	*	3.43 ± 0.98	2.82 ± 0.76	---	2.88 ± 1.11	---
PI [ng/mg protein]	18.90 ± 8.64	---	16.50 ± 7.49	21.18 ± 8.87	*	18.55 ± 7.45	---
PI [% of total lipids]	9.11 ± 0.93	---	9.50 ± 1.08	9.23 ± 1.08	---	9.02 ± 1.04	---
PI (% of PL]	15.40 1.47	---	15.68 1.92	15.45 1.59	---	15.04 1.56	---
PI 38:3 [% of total PI]	26.13 ± 6.00	---	31.37 ± 8.74	23.12 ± 4.64	*	24.03 ± 3.41	*
PI 38:4 [% of total PI]	27.39 ± 3.71	---	24.18 ± 7.45	29.44 ± 6.72	---	28.10 ± 7.08	---
PI 34:0 [% of total PI]	23.91 ± 11.36	---	26.49 ± 11.24	22.04 ± 11.29	---	24.06 ± 10.79	---
PI 36:2 [% of total PI]	9.20 ± 0.41	---	10.46 ± 0.85	11.16 ± 1.51	---	11.19 ± 1.89	---
PI 36:1 [% of total PI]	4.91 ± 1.33	---	5.68 ± 1.20	4.69 ± 1.19	---	4.62 ± 0.62	---
PI 38:2 [% of total PI]	3.77 ± 0.70	---	4.52 ± 1.32	3.85 ± 1.51	---	4.40 ± 1.29	---
PI 38:5 [% of total PI]	5.05 ± 0.80	*	3.88 ± 1.42	6.68 ± 1.36	***	6.53 ± 0.97	***
PI 36:3 [% of total PI]	4.07 ± 0.89	---	3.79 ± 1.21	3.80 ± 1.14	---	3.60 ± 0.92	---

All subspecies > 3% of the corresponding species are presented. SD - standard deviation, PL - phospholipid, PLPE - plasmenylethanolamine, PI - phosphatidylinositol, P – P value compared to WT. *P<0.05, **P<0.01, ***P<0.001.

Table 4.3: Cellular lipid composition of PE, PS and SPM.

	A549 [mean±SD]	P (A549) ANOVA	WT [mean±SD]	Q215K [mean±SD]	P (p.Q215K) ANOVA	E292V [mean±SD]	P (p.E292V) ANOVA
PE [ng/mg protein]	16.108 ± 9.34	---	15.62 ± 9.34	18.24 ± 9.69	---	16.29 ± 8.97	---
PE [% of total lipids]	7.29 ± 0.86	*	8.35 ± 1.07	7.49 ± 1.29	*	7.41 ± 1.13	*
PE (% of PL)	12.32 ± 1.47	*	13.75 ± 1.62	12.49 ± 1.71	---	12.35 ± 1.70	*
PE 36:2 [% of total PE]	15.51 ± 0.93	---	19.45 ± 2.60	23.00 ± 3.58	---	21.33 ± 1.95	---
PE 38:4 [% of total PE]	12.58 ± 3.40	---	13.27 ± 4.18	11.69 ± 4.83	---	11.79 ± 4.72	---
PE 34:1 [% of total PE]	12.98 ± 0.49	*	11.53 ± 1.06	11.73 ± 0.99	---	11.69 ± 1.54	---
PE 36:1 [% of total PE]	8.36 ± 1.21	---	8.12 ± 1.08	7.78 ± 1.21	---	8.28 ± 1.23	---
PE 34:2 [% of total PE]	6.59 ± 1.81	---	6.67 ± 2.14	9.34 ± 2.98	**	6.88 ± 2.29	---
PE 38:5 [% of total PE]	5.47 ± 1.43	*	6.25 ± 1.68	6.20 ± 1.59	---	6.05 ± 1.82	---
PE O 40:3 [% of total PE]	6.81 ± 1.93	---	5.92 ± 1.94	4.94 ± 2.18	---	5.79 ± 2.33	---
PE 38:3 [% of total PE]	3.31 ± 0.48	---	4.03 ± 1.11	2.56 ± 0.23	*	3.15 ± 0.52	---
PE 36:3 [% of total PE]	2.83 ± 0.16	---	3.08 ± 0.17	3.35 ± 0.16	---	3.20 ± 0.20	---
PS [ng/mg protein]	15.36 ± 8.11	*	11.60 ± 6.31	13.78 ± 7.46	---	13.32 ± 6.56	---
PS [% of total lipids]	7.13 ± 0.20	*	6.44 ± 0.52	5.83 ± 0.66	---	6.32 ± 0.59	---
PS (% of PL)	12.05 ± 0.45	*	10.63 ± 0.99	9.80 ± 1.42	**	10.56 ± 1.21	*
PS 36:1 [% of total PS]	42.96 ± 1.12	*	48.51 ± 2.85	47.74 ± 2.96	---	49.23 ± 2.54	---
PS 34:1 [% of total PS]	15.61 ± 1.99	---	15.99 ± 1.66	16.49 ± 1.78	---	14.35 ± 2.11	*
PS 36:2 [% of total PS]	11.16 ± 0.73	---	12.46 ± 1.02	14.40 ± 1.11	*	14.05 ± 1.12	---
PS 40:7 [% of total PS]	9.79 ± 5.02	---	11.13 ± 5.44	9.15 ± 3.80	---	9.50 ± 3.81	---
PS 38:4 [% of total PS]	3.93 ± 0.91	---	4.67 ± 1.89	4.96 ± 1.76	---	3.90 ± 1.99	---
SPM [nmol/mg protein]	8.08 ± 4.60	---	6.53 ± 4.13	9.06 ± 5.85	---	8.83 ± 5.10	---
SPM [% of total lipids]	3.69 ± 0.40	---	3.50 ± 0.54	3.67 ± 0.73	---	4.05 ± 0.63	**
SPM (% of PL)	6.24 ± 0.73	---	5.78 ± 0.90	6.16 ± 1.27	---	6.78 ± 1.12	*
dih-SPM [nmol/mg protein]	1.27 ± 0.72	---	1.14 ± 0.84	1.76 ± 1.21	*	1.47 ± 0.83	---
dih-SPM [% of total lipids]	0.58 ± 0.10	---	0.57 ± 0.18	0.68 ± 0.20	---	0.66 ± 0.10	---
dih-SPM (% of PL)	0.98 ± 0.17	---	0.93 ± 0.27	1.13 ± 0.32	---	1.11 ± 0.16	---
SPM 16:0 [% of total SPM]	58.82 ± 2.01	***	46.23 ± 3.26	54.55 ± 2.45	***	52.07 ± 2.39	***
SPM 24:1 [% of total SPM]	13.37 ± 0.46	***	22.38 ± 2.08	16.75 ± 1.95	***	17.79 ± 1.45	**
SPM 24:0 [% of total SPM]	8.71 ± 2.23	***	11.49 ± 2.39	7.27 ± 1.92	***	8.23 ± 2.18	***
SPM 18:0 [% of total SPM]	2.23 ± 0.57	*	3.59 ± 0.53	3.72 ± 0.61	---	4.50 ± 0.49	---

All subspecies > 3 % of the corresponding species are presented. SD - standard deviation, PL - phospholipid, PE - phosphatidylethanolamine, PS - phosphatidylserine, SPM - sphingomyelin, dih – dihydro, P – P value compared to WT.*P<0.05, **P<0.01, ***P<0.001.

Table 4.4: Cellular lipid composition of LPC, Cer and PG.

	A549 [mean±SD]	P (A549) ANOVA	WT [mean±SD]	Q215K [mean±SD]	P (p.Q215K) ANOVA	E292V [mean±SD]	P (p.E292V) ANOVA
LPC [nmol/mg protein]	0.99 ± 0.34	---	0.86 ± 0.23	1.27 ± 0.46	---	1.13 ± 0.32	---
LPC [% of total lipids]	0.52 ± 0.17	---	0.55 ± 0.19	0.62 ± 0.28	---	0.61 ± 0.24	---
LPC (% of PL)	0.88 ± 0.28	---	0.90 ± 0.33	1.04 ± 0.47	---	1.02 ± 0.40	---
LPC 18:1 [% of total LPC]	45.57 ± 11.34	---	42.54 ± 12.83	46.41 ± 11.45	---	44.59 ± 11.34	---
LPC 16:0 [% of total LPC]	15.59 ± 5.97	---	15.64 ± 5.10	15.01 ± 5.63	---	15.69 ± 5.10	---
LPC 16:1 [% of total LPC]	10.93 ± 3.65	---	11.56 ± 4.93	11.11 ± 5.48	---	9.62 ± 4.19	---
LPC 18:0 [% of total LPC]	10.10 ± 8.01	---	10.67 ± 10.08	10.40 ± 8.24	---	12.17 ± 8.71	---
LPC 18:2 [% of total LPC]	3.28 ± 0.57	---	3.45 ± 0.76	3.62 ± 0.63	---	3.35 ± 0.66	---
Cer [nmol/mg protein]	0.82 ± 0.42	---	0.81 ± 0.52	1.44 ± 1.00	---	1.08 ± 0.48	---
Cer [% of total lipids]	0.38 ± 0.02	---	0.43 ± 0.08	0.58 ± 0.23	---	0.51 ± 0.02	---
GluCer [nmol/mg protein]	0.14 ± 0.07	---	0.14 ± 0.09	0.30 ± 0.20	*	0.20 ± 0.10	---
GluCer [% of total lipids]	0.07 ± 0.01	---	0.07 ± 0.01	0.12 ± 0.04	*	0.09 ± 0.01	---
Cer 24:1 [% of total Cer]	34.08 ± 3.18	**	42.99 ± 4.15	40.17 ± 6.90	---	36.63 ± 4.10	---
Cer 24:0 [% of total Cer]	39.58 ± 7.51	*	31.89 ± 8.48	30.04 ± 8.14	---	30.32 ± 6.22	---
Cer 16:0 [% of total Cer]	17.71 ± 3.87	---	15.15 ± 3.54	20.16 ± 2.44	**	21.21 ± 2.90	***
Cer 22:0 [% of total Cer]	3.21 ± 0.08	----	3.84 ± 0.20	3.79 ± 0.46	---	5.11 ± 0.39	***
Cer 23:0 [% of total Cer]	3.40 ± 0.32	---	3.01 ± 0.36	2.80 ± 0.19	---	2.99 ± 0.11	---
GluCer 24:1 [% of Glu Cer]	84.98 ± 2.87	**	90.41 ± 2.07	81.84 ± 1.90	***	83.99 ± 3.40	**
GluCer 16:0 [% of Glu Cer]	15.03 ± 2.87	**	9.59 ± 2.07	18.16 ± 1.90	***	16.01 ± 3.40	**
PG [ng/mg protein]	0.37 ± 0.26	*	0.28 ± 0.21	0.44 ± 0.26	***	0.37 ± 0.26	*
PG [% of total lipids]	0.16 ± 0.04	---	0.14 ± 0.05	0.18 ± 0.03	**	0.16 ± 0.06	---
PG (% of PL)	0.26 ± 0.07	---	0.22 ± 0.07	0.30 ± 0.04	**	0.26 ± 0.09	---
PG 34:1 [% of total PG]	83.43 ± 4.36	---	91.21 ± 10.92	65.55 ± 7.60	**	85.96 ± 10.11	---
PG 36:1 [% of total PG]	16.58 ± 4.36	---	6.37 ± 7.36	12.56 ± 5.17	---	10.49 ± 7.01	---

All subspecies > 3% of the corresponding species are presented. SD - standard deviation, PL - phospholipid, LPC - lysophosphatidylcholine, Cer - ceramide, GluCer - glucosyl ceramide, PG - phosphatidylglycine, P – P value compared to WT. *P<0.05, **P<0.01, ***P<0.001.

4.1.10 Expression of cytokines and TLRs

To investigate whether ABCA3 mutations influence the expression of selected cytokines and toll-like receptors, mRNA levels were quantified by real-time PCR. Secreted proteins in cell culture supernatants were analyzed by ELISA and Bioplex.

IL-6 mRNA was significantly downregulated in all cells compared to ABCA3-WT cells (Figure 4.25 A). Moreover, secreted IL-6 was significantly decreased in cells expressing ABCA3 mutations (Figure 4.25 C). Similarly, secreted IL-8 was significantly decreased in cells harboring ABCA3 mutants compared to ABCA3-WT cells and non-transfected control cells (Figure 4.25 D). IL-8 mRNA expression was also markedly, albeit not significantly, reduced (Figure 4.25 B).

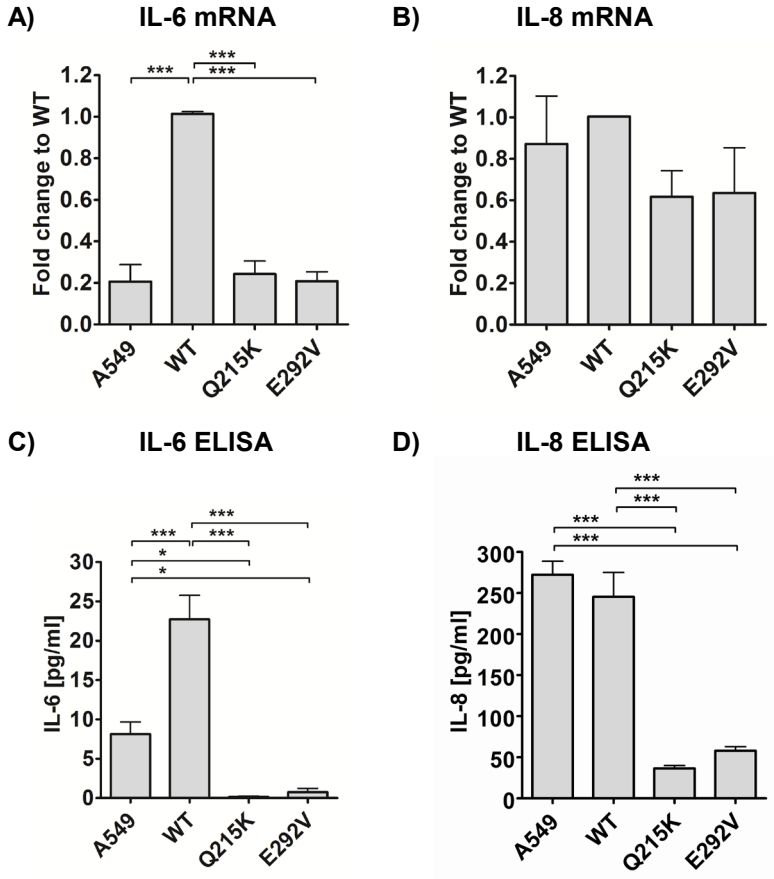

Figure 4.25: Effects of ABCA3 mutations on cytokine expression and secretion.
Cells were grown for 48 h. A,B) IL-6 and IL-8 mRNA expression. Results were calculated relative to ABCA3-WT cells. B,D) IL-6 and IL-8 ELISA.
*P<0.05, ***P<0.001.

Next to IL-6 and IL-8, the mRNA expression of GM-CSF and RANTES (CCL5) was also analyzed. GM-CSF deficiency is implicated in the development of pulmonary alveolar proteinosis (PAP). RANTES is a chemokine often upregulated in the presence of virus. No significant differences in either GM-CSF or RANTES mRNA levels between cell lines were found (Figure 4.26 and 4.27 A). Secretion of GM-CSF and RANTES into cell culture

supernatants was measured as well; however, for GM-CSF, secretion was below the detection limit of the applied method.

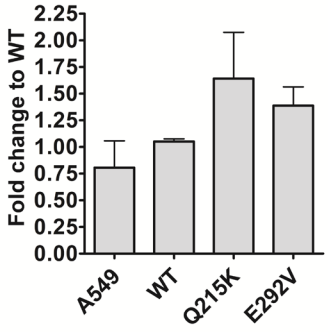

Figure 4.26: Effects of ABCA3 mutations on GM-CSF mRNA expression.
Cells were grown for 48 h. Results were calculated relative to ABCA-WT.

For RANTES, an increased secretion from ABCA3 mutant cells into cell culture supernatants was observed compared to ABCA3-WT cells and non-transfected A549 cells, with the differences between A549 cells and p.E292V cells being statistically significant (Figure 4.27 B).

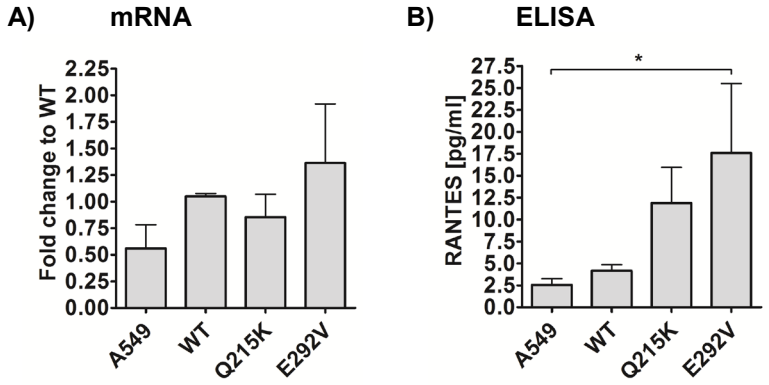

Figure 4.27: Effects of ABCA3 mutations on RANTES expression and secretion.
Cells were grown for 48 h.
A) RANTES mRNA. Results were calculated relative to ABCA3-WT cells.
B) RANTES ELISA. P<0.05.

TLR-3 and TLR-4 are receptors for viral double-stranded RNA (dsRNA) and bacterial lipopolysaccharides (LPS), respectively. TLR-3 and TLR-4 mRNA expression was significantly decreased in cells harboring the ABCA3 mutations p.Q215K and p.E292V compared to ABCA3-WT cells (Figure 4.28).

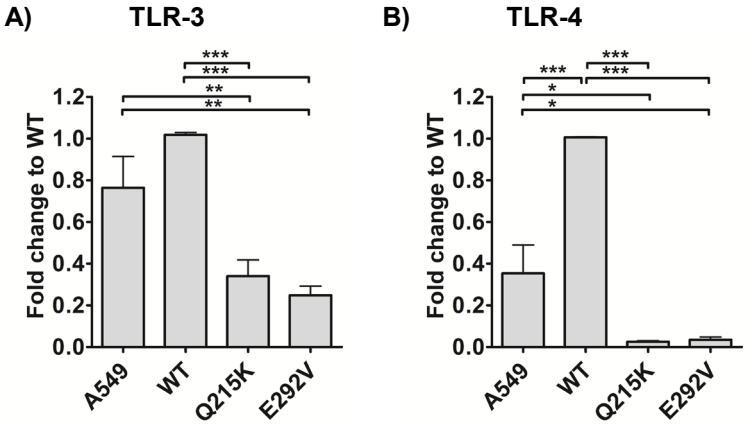

Figure 4.28: Effects of ABCA3 mutations on toll-like receptor expression.
Cells were grown for 48 h. qPCR analysis of TLR-3 (A) and TLR-4 (B). Results were calculated relative to ABCA3-WT cells. *P<0.05, **P<0.01, **P<0.001.

Signaling through TLRs often induces activation the transcription factor NF-κB which in turn leads to transcription of specific cytokines. A dual luciferase assay was employed to analyze whether NF-κB activation in cell lysates of stably transfected cells with ABCA3 mutations was changed in the same pattern as the investigated cytokines and TLRs. As shown in Figure 4.29 A, NF-κB activation was significantly decreased in p.Q215K and p.E292V cells compared to ABCA3-WT cells. Subsequently, cells were stimulated with TNF-α to check for functional NF-κB activation. All cells were successfully stimulated with TNF-α and NF-κB was activated at least two-fold compared to the corresponding non-treated samples (Figure 4.29 B). The strongest NF-κB activation after TNF-α treatment was observed in p.Q215K cells.

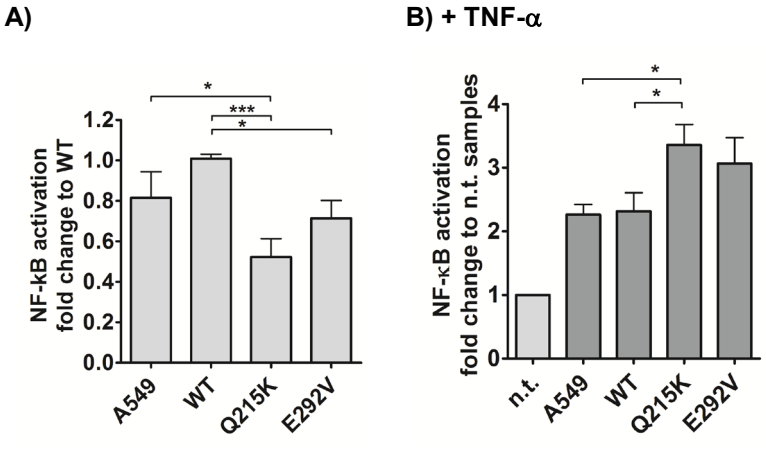

Figure 4.29: Effects of ABCA3 mutations on NF-κB activation.
Cells were grown for 48 h. A) Basal NF-κB activation. Results were calculated relative to ABCA3-WT. B) NF-κB activation after TNF-α stimulation. Results were calculated relative to the corresponding non-treated (n.t.) samples; P value was below 0.001 in all cells when compared to n.t.. *P<0.05, ***P<0.001.

4.2 RSV infection

Respiratory infections may initiate or aggravate ILDs. The respiratory syncytial virus (RSV) is the most common respiratory pathogen in young infants. To investigate the effect of respiratory infections on lung epithelial cells harboring ABCA3 mutations, non-transfected and stably transfected A549 cells were infected with RSV.

4.2.1 RSV replication

Virus growth was determined between 0 to 72 h after infection. Virus titers were the same after 0 and 24 h (data not shown). Virus growth after 48 and 72 h was similar in all cells investigated; no significant differences were observed (Figure 4.30). Therefore, molecular changes in cells harboring ABCA3 mutations are not due to unequal virus load.

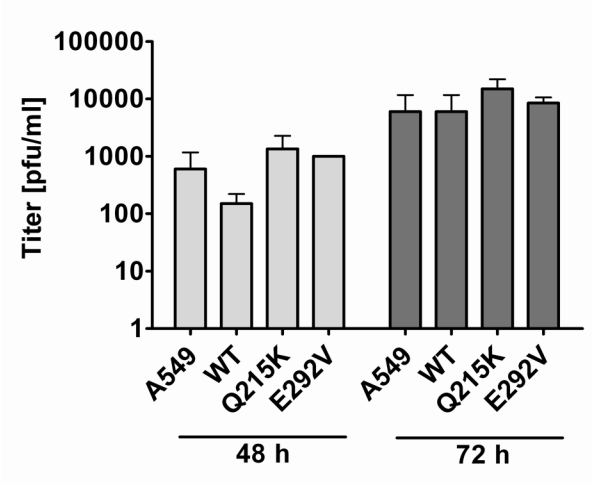

Figure 4.30: Virus growth in non-transfected and stably transfected cells.
Cells were infected with RSV strain A2 (MOI 3) and titers were determined after 48 and 72 h cell growth.

RSV-infected cells can be visualized by immunostaining of the RSV structural F-protein. As can be seen in Figure 4.31, 48 h after initial RSV infection, a considerable fraction of all cells were infected.

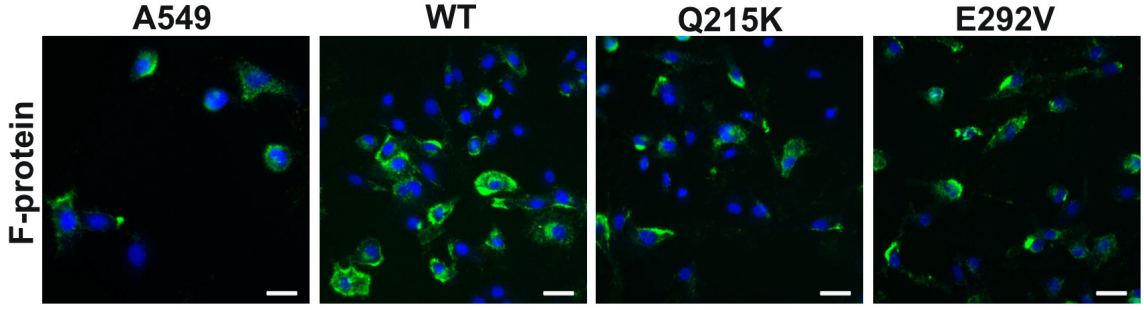

Figure 4.31: Immunofluorescence visualization of RSV-infection.
Cells were grown for 48 h in the presence of RSV (MOI 3). Cells were stained for RSV F-protein (green) and nuclei were visualized using Hoechst (blue). Scale bar 15 µm.

When cells were examined using brightfield microscopy, the shape of the cells harboring ABCA3 mutations drastically changed after RSV infection (Figure 4.32). The former cobblestone-like appearing cells became elongated, and they often also had elongated outgrowths. Moreover, the cells harboring ABCA3 mutations, especially p.Q215K, did not grow in a confluent monolayer any longer. The cell shape of non-transfected A549 and ABCA3-WT cells changed slightly as well; however, the cells still grew in a confluent monolayer and almost no elongated outgrowths were observed.

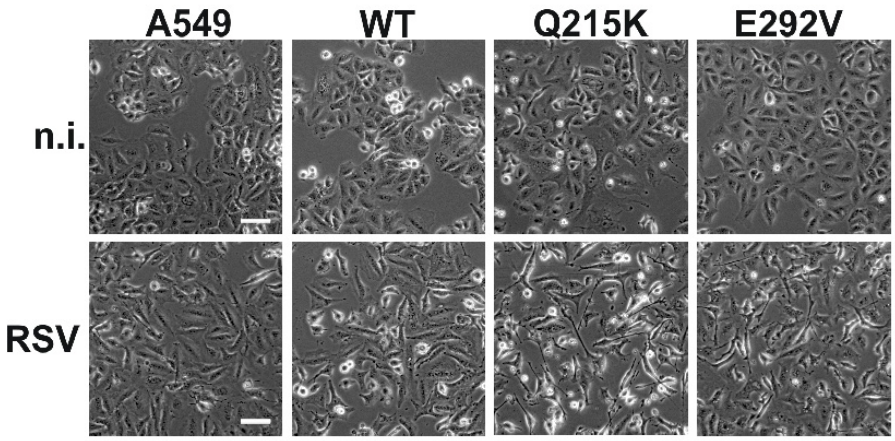

Figure 4.32: Effect of RSV infection on the cell morphology.
Cells were grown for 48 h in the presence of RSV (MOI 3). Scale bar 30 µm.

α-tubulin is a part of the cytoskeleton and α-tubulin staining was used to visualize intracellular arrangement of microtubules after RSV infection. In non-infected cells, microtubules were distributed in a non-organized fashion in all cells (Figure 4.33 A). RSV infection lead to a more ordered and almost parallel arrangement of microtubules in p.Q215K and p.E292V cells, probably to support the elongated cell shape and the cellular outgrowths (Figure 4.33 B).

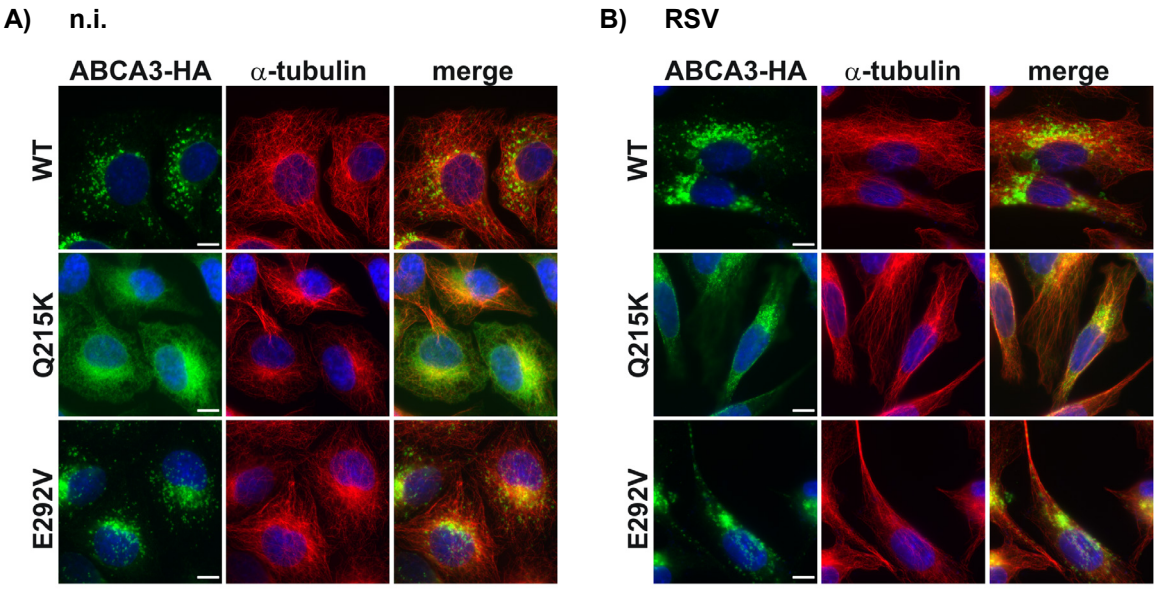

Figure 4.33: Effect of RSV infection on intracellular α-tubulin distribution.
Cells were grown for 48 h in the absence (A) or presence (B) of RSV (MOI 3). Cells were stained for α-tubulin (red), HA-tagged ABCA3 (green) and DAPI (blue). The merge image presents the oevelay from the green and red fluorescences. Scale bar 4 µm.

4.2.2 Effect of RSV infection on expression of epithelial markers

SP-C mRNA levels were downregulated in all cells after RSV-infection (Figure 4.34 B). However, compared to ABCA3-WT and A549 control cells, SP-C mRNA was significantly decreased in cells harboring ABCA3 mutations (Figure 4.34 A).

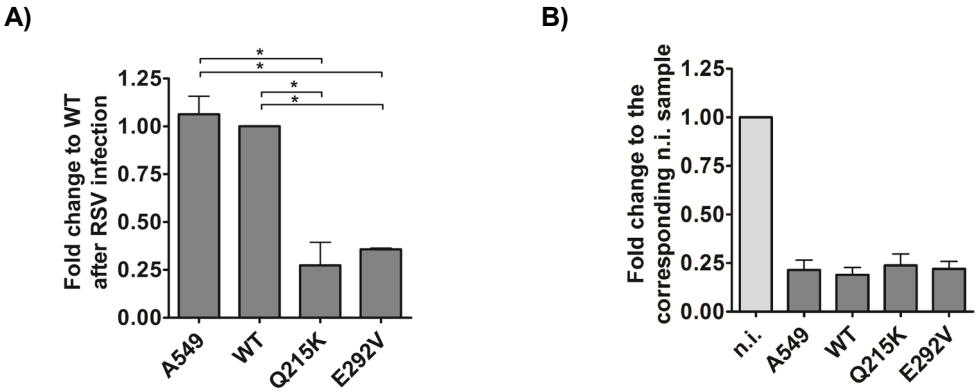

Figure 4.34: Effect of RSV infection on SP-C mRNA.
Cells were infected with RSV (MOI 3) and grown for 48 h. A) Fold change in SP-C mRNA expression after RSV infection relative to ABCA3-WT cells. B) Fold change to the corresponding non-infected (n.i.) sample after RSV infection. P value was below 0.001 for all cells compared to n.i.. *P<0.05.

After RSV infection, synthesis of the epithelial cell adhesion molecule E-cadherin was strongly decreased more than five-fold in cells harboring the ABCA3 mutations p.Q215K

and p.E292V compared to ABCA3-WT cells (Figure 4.35 A, C). No RSV-induced changes were observed in ABCA3-WT cells and non-transfected A549 cells. Therefore the differences between ABCA3-WT cells and cells transfected with mutant ABCA3 were further enhanced by RSV infection (Figure 4.35 B).

Contrary to E-cadherin, RSV infection induced reduction of ZO-1 protein in ABCA3 p.Q215K and E292V cells as well as in cells transfected with ABCA3-WT (Figure 4.36 A, C). However, the observed differences were not significant.

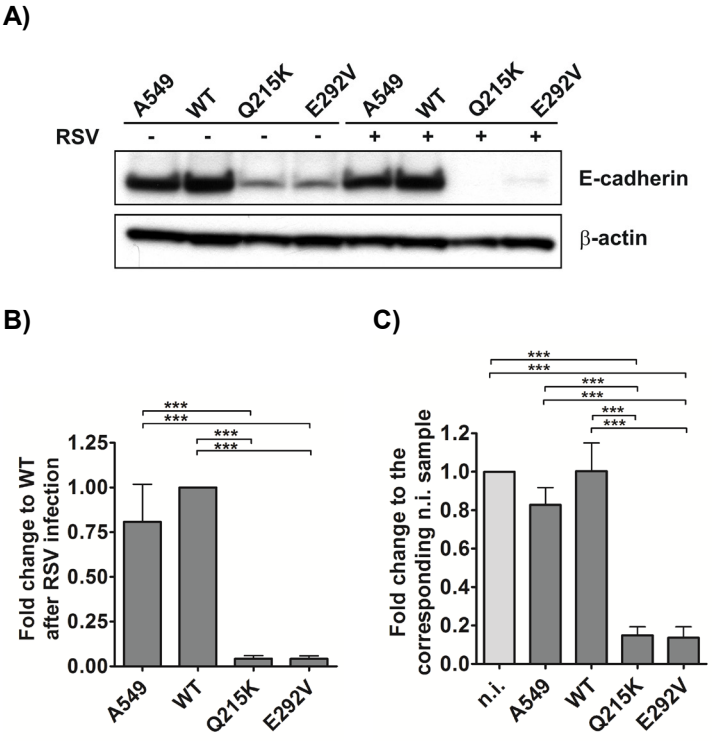

Figure 4.35: Effect of RSV infection on E-cadherin protein.
Cells were grown for 48 h in the presence of RSV (MOI 3). A) Western immunoblot of E-cadherin. β-actin was used as loading control. The left part (absence of RSV) of the western blot was already presented in Figure 4.11 A. B) Fold change in E-cadherin protein relative to ABCA3-WT cells after RSV infection. C) Fold change to the corresponding non-infected (n.i.) sample after RSV infection. ***P<0.001.

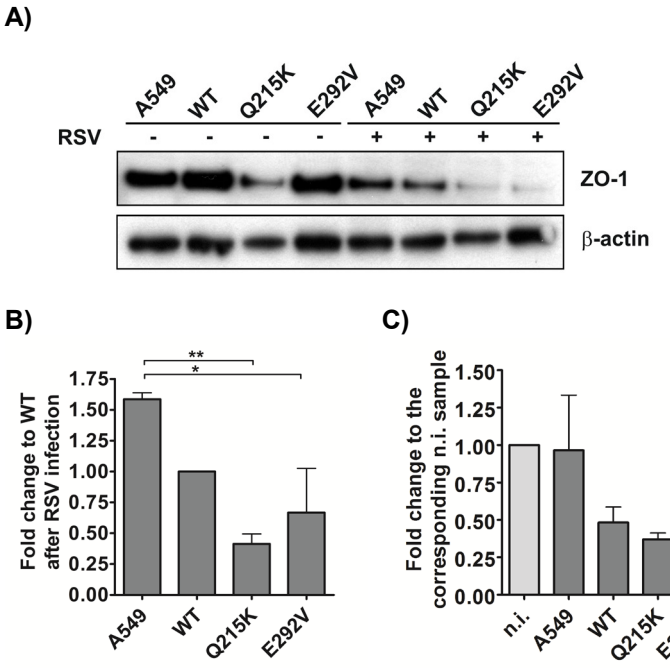

Figure 4.36: Effect of RSV infection on ZO-1 protein. Cells were grown for 48 h in the presence of RSV (MOI 3). A) Western immunoblot of ZO-1. β-actin was used as loading control. The left part (absence of RSV) of the western blot was already presented in Figure 4.11 B. B) Fold change relative to ABCA3-WT after RSV infection. C) RSV-induced change relative to the corresponding non-infected (n.i.) sample. *P<0.05, **P<0.01.

4.2.3 Effect of RSV infection on expression of mesenchymal markers

The mesenchymal SNAI transcription factors have been shown to repress expression of epithelial markers and their mRNA levels have been shown to inversely correlate with the mRNA of E-cadherin [127, 128]. As presented in Figure 4.37 A, SNAI1 mRNA was significantly increased in p.Q215K cells compared to ABCA3-WT cells after RSV infection. Also in p.Q215K cells, an approximate 4-fold change in SNAI1 mRNA was observed compared to the non-infected state, therefore being the only significant increase (Figure 4.37 B).

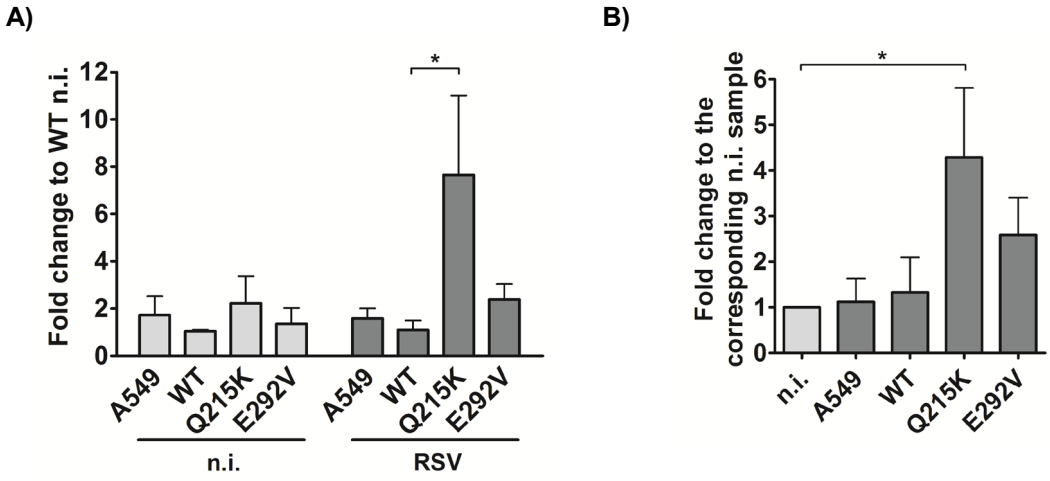

Figure 4.37: Effect of RSV infection on SNAI1 expression.
Cells were grown for 48 h in the presence or absence of RSV (MOI 3). A) Fold changes in SNAI1 mRNA relative to non-infected (n.i.) ABCA3-WT cells. B) RSV-induced changes in SNAI1 mRNA relative to the corresponding n.i. samples. *P<0.05.

Similar to SNAI1 mRNA, SNAI2 mRNA levels of p.Q215K cells were significantly increased after RSV infection compared to the corresponding non-infected sample (Figure 4.38 B). Moreover, SNAI2 mRNA in p.Q215K cells was significantly elevated compared to non-transfected A549 cells and p.E292V cells after virus infection (Figure 4.38 A).

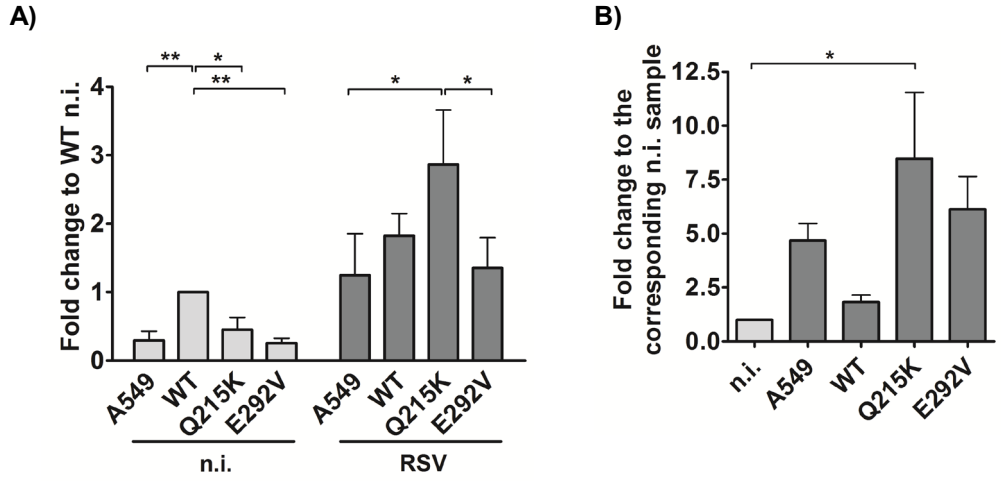

Figure 4.38: Effect of RSV infection on SNAI2 expression.
Cells were grown for 48 h in the presence or absence of RSV (MOI 3). A) Fold changes in SNAI2 mRNA relative to non-infected (n.i.) ABCA3-WT cells. B) RSV-induced changes relative to the corresponding n.i. samples. *P<0.05, **P<0.01.

Collagens are part of the extracellular matrix. Collagen type I is a structural component of the connective tissue and mainly secreted by fibroblasts. Therefore, the collagen type I mRNA expression before and after RSV infection was investigated. As can be seen in Figure 4.39 B, collagen type I mRNA levels of p.Q215K cells were significantly elevated after RSV infection. No collagen type I mRNA induction was observed for all other cells.

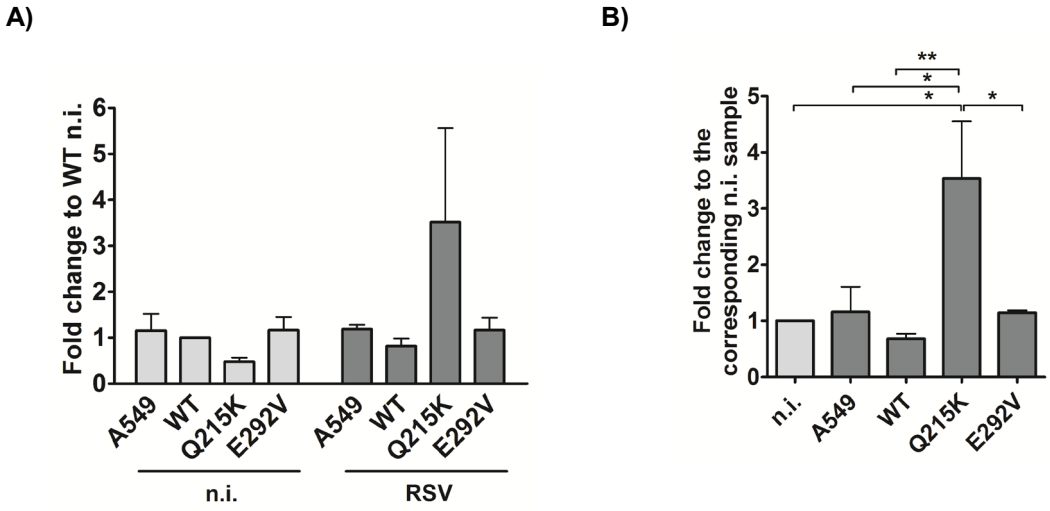

Figure 4.39: Effect of RSV infection on collagen type I expression.
Cells were grown for 48 h in the presence or absence of RSV (MOI 3). A) Fold changes in collagen type I mRNA relative to non-infected (n.i.) ABCA3-WT cells. B) RSV-induced changes relative to the corresponding n.i. samples. *P<0.05, **P<0.01.

Expression of the mesenchymal markers vimentin and α-SMA was investigated next. As shown in Figure 4.40, no differences were observed for either α-SMA or vimentin in western immunoblot analysis.

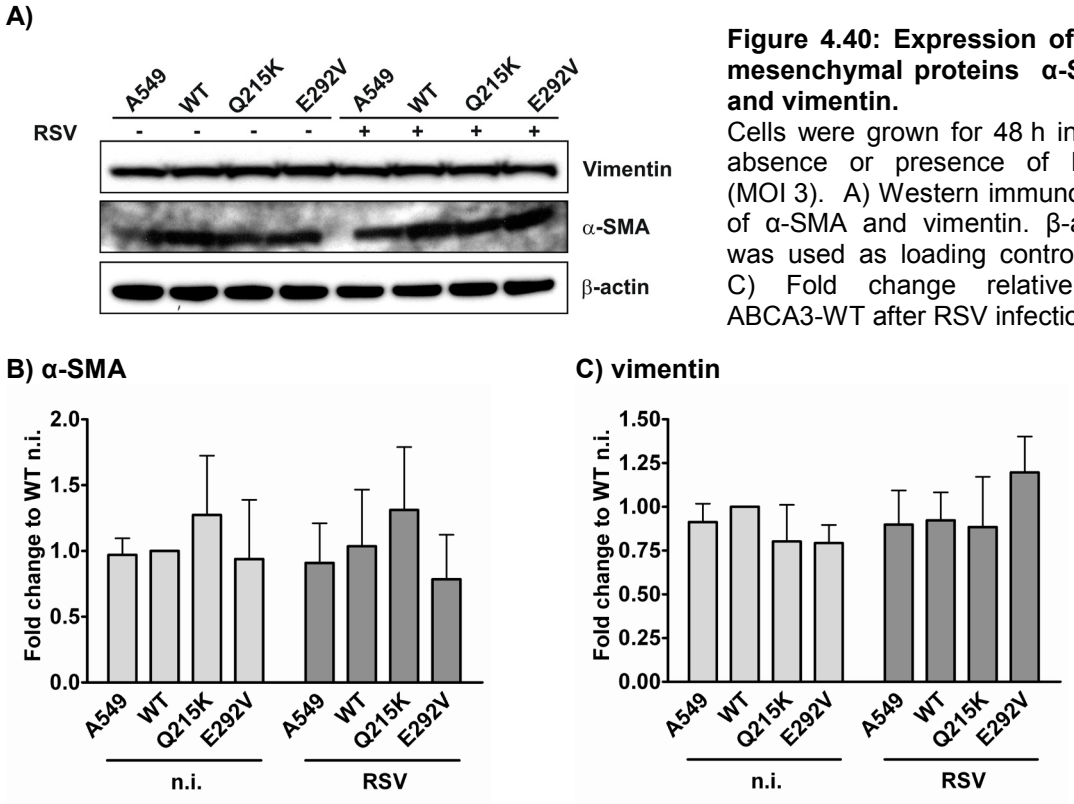

Figure 4.40: Expression of the mesenchymal proteins α-SMA and vimentin.
Cells were grown for 48 h in the absence or presence of RSV (MOI 3). A) Western immunoblot of α-SMA and vimentin. β-actin was used as loading control. B, C) Fold change relative to ABCA3-WT after RSV infection.

4.2.4 Effect of RSV infection on TGF-β1 and MMP-2 expression and secretion

Next, it was investigated whether RSV infection affects TGF-β mRNA and protein secretion. TGF-β mRNA was significantly elevated in cells harboring the p.Q215K mutation compared to non-transfected A549 cells as well as ABCA3-WT cells after RSV infection (Figure 4.41 A). RSV infection induced expression of TGF-β1 mRNA compared to the corresponding non-infected sample in p.Q215K cells; however the changes were not significant (Figure 4.41 B).

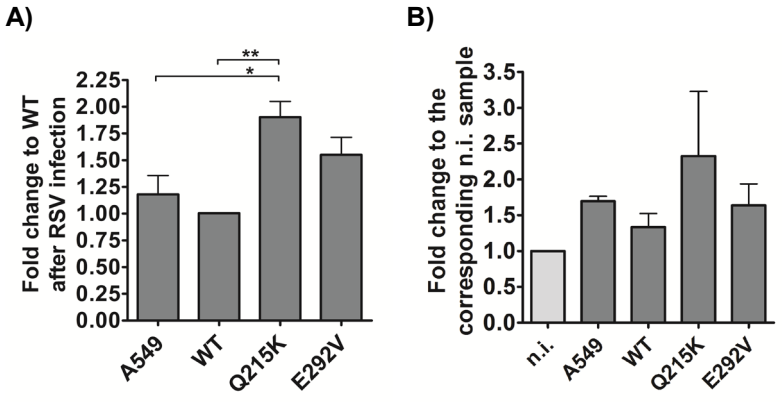

Figure 4.41: Effect of RSV infection on TGF-β1 expression.
Cells were infected with RSV (MOI 3) and grown for 48 h. A) Fold change in TGF-β1 mRNA relative to ABCA3-WT cells after RSV infection. B) RSV-induced changes relative to the corresponding non-infected (n.i.) samples. *P<0.05, **P<0.01.

Prior to the analysis of cell culture supernatants from RSV infected cells, the supernatants needed to be UV-inactivated to dispose of infectious virus particles. UV-inactivation however had a negative effect on the supernatants' protein content, leading to a reduction in the amount of TGF-β1 by more than two-fold compared to the non-UV treated sample (Figure 4.42 A, exemplarily shown for ABCA-WT cells). When both, non-infected as well as RSV infected supernatants, were UV-inactivated and subsequently analyzed for TGF-β1 secretion, a significant increase in TGF-β1 protein induced by RSV infection was observed in all cells (Figure 4.41 B). The strongest TGF-β1 secretion was found for p.Q215K cells (Figure 4.42 B).

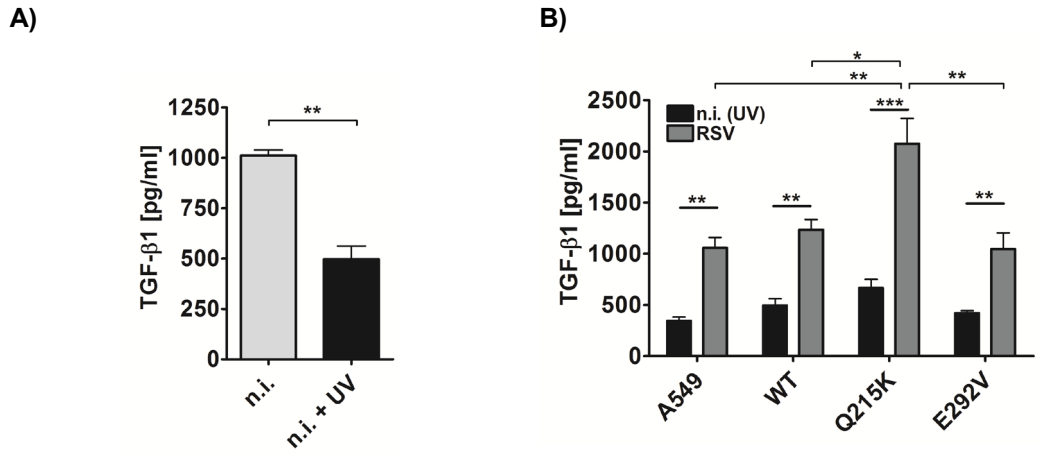

Figure 4.42: Effects of UV-inactivation and RSV infection on secreted TGF-β1.
Cells were RSV-infected and grown for 48 h. Supernatants were collected and UV-inactivated. A) Effect of UV-inactivation on secreted TGF-β1 in cell culture supernatants of ABCA3-WT cells, P=0.0055. B) RSV-induced changes on TGF-β1 secretion; all supernatants were UV-inactivated. *P<0.05, **P<0.01, ***P<0.001.

Similar to TGF-β1, secreted MMP-2 was affected by UV-inactivation. After UV-inactivation, MMP-2 could solely be detected in cell culture supernatants from p.Q215K cells (Figure 4.43 C). In all other supernatants, secreted MMP-2 was decreased below the detection limit. After RSV infection, MMP-2 mRNA was significantly elevated in p.Q215K cells compared to non-transfected A549 cells and ABCA3-WT cells (Figure 4.43 A). Even though RSV infection increased MMP-2 mRNA in all cells with ABCA3 mutations, a significant effect was only observed for p.E292V (Figure 4.43 B).

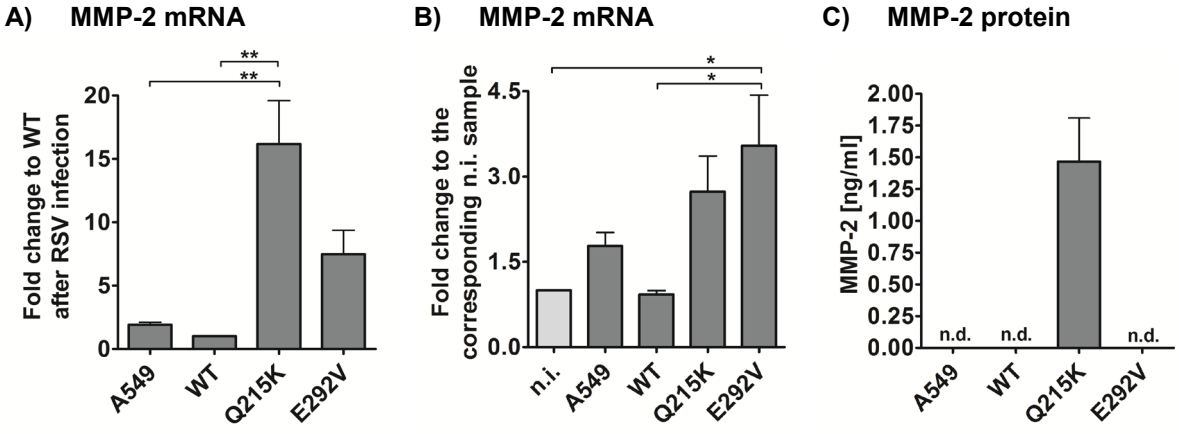

Figure 4.43: Effect of RSV-infection on MMP-2 expression and secretion.
Cells were infected with RSV (MOI 3) and grown for 48 h. A) Fold change in MMP-2 mRNA relative to ABCA3-WT cells after RSV infection. B) RSV-induced changes relative to the corresponding non-infected (n.i.) samples. C) MMP-2 secretion after RSV infection, samples were UV-inactivated. *P<0.05, **P<0.01.

4.2.5 Effect of RSV infection on phosphorylation of Src kinase

RSV infection induced phosphorylation of the tyrosine kinase Src in all cells (Figure 4.44 A, C). However, phosphorylation of Src in p.Q215K cells was significantly elevated compared to all other cells (Figure 4.44 A, B).

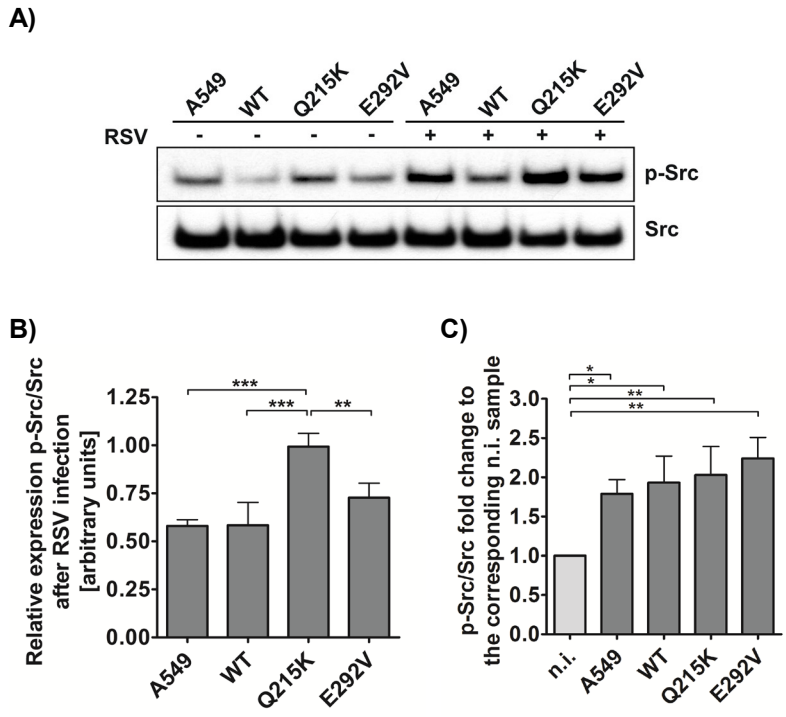

Figure 4.44: Effect of RSV infection on Src phosphorylation. Cells were grown for 48 h in the presence or absence of RSV (MOI 3). A) Western immunoblot of phosphorylated (p)-Src and total Src protein. The left part (in the absence of RSV) was already presented in Figure 4.17. B) Ratio of p-Src to Src after RSV infection. C) RSV-induced changes in the p-Src to Src ratio relative to the corresponding non-infected (n.i.) samples. *P<0.05, **P<0.01, ***P<0.001.

4.2.6 Effects of ABCA3 mutations and RSV infection on Smad2/3 phosphorylation

Smad2 and Smad3 are downstream effectors of TGF-β signaling. As ABCA3 mutations and RSV infection induce TGF-β1 secretion, the phosphorylation state of Smad2 and Smad3 was investigated. As presented in Figure 4.45, no Smad2/3 or phospho-Smad2/3 regulation was detected in the absence of RSV, therefore also no changes in the phospho-Smad to total Smad ratios were found. RSV infection induced a reduction of both Smad2 and phospho-Smad2 proteins as well as of Smad3 and to a lesser extend of phospho-Smad3 protein in cell lysates of ABCA3-mutant cells (Figure 4.45 A). Therefore, no significant differences in the ratios of phospho-Smad to Smad were detected after RSV infection (Figure 4.45 B, C). However, as the decrease in Smad3 was stronger compared to the decrease in phosphorylated Smad3 in p.Q215K cells, the fold change in the p-Smad3/Smad3 ratio was significant when compared to the corresponding non-infected sample (Figure 4.45 D).

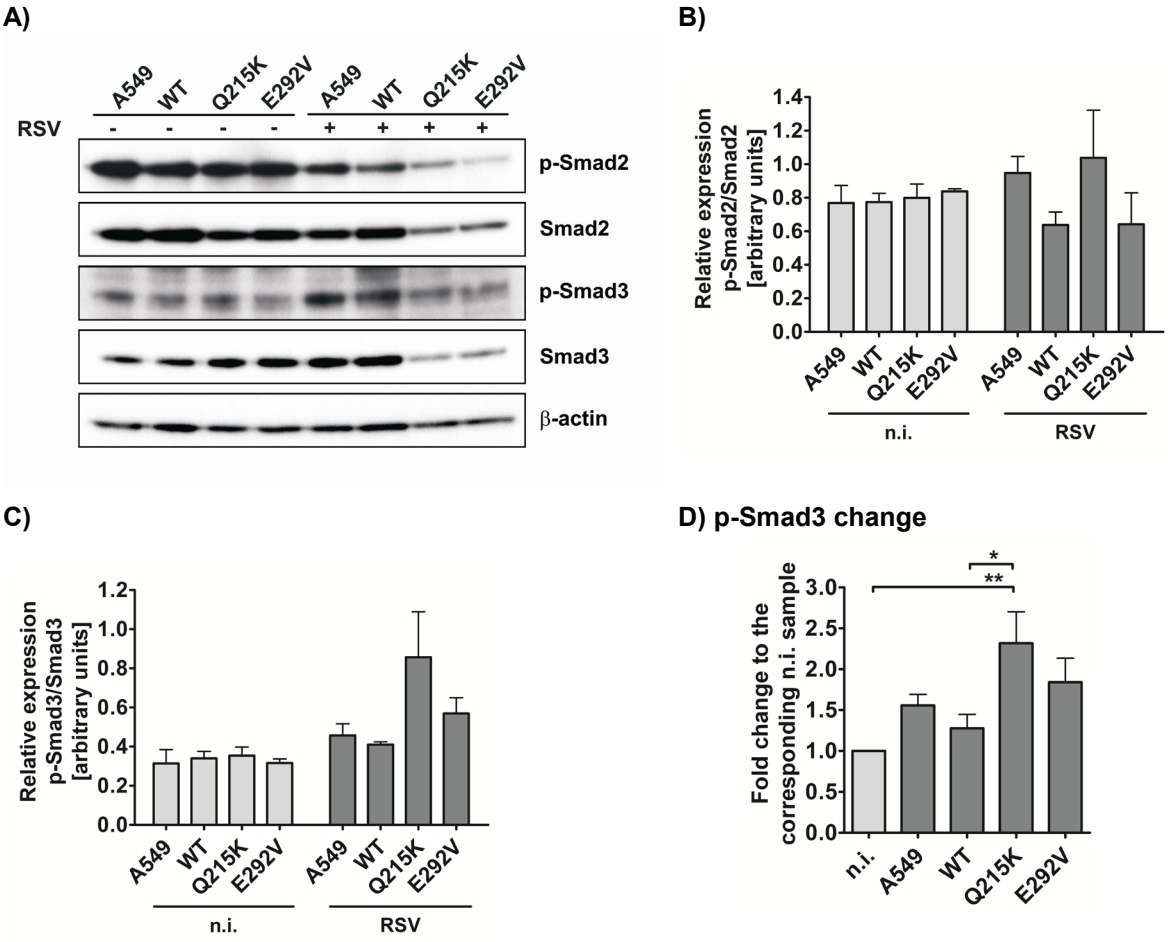

Figure 4.45: Effects of ABCA3 mutations and RSV infection on phosphorylation of Smad proteins.
Cells were grown for 48 h in the absence or presence of RSV. A) Proteins were detected by western immunoblots of RIPA cell lysates. β-actin was used as loading control. B) Ratio of p-Smad2/Smad2. C) Ratio of p-Smad3/Smad3. D) Fold change in the p-Smad3/Smad3 ratio after RSV infection relative to the corresponding non-infected (n.i.) sample. *P<0.05, **P<0.01.

4.2.7 Effects of ABCA3 mutations and RSV infection on phosphorylation of the MAP kinases ERK1/2 and JNK1/2

Next to the canonical Smad pathway, TGF-β may activate other intracellular signaling molecules, such as mitogen-activated protein kinases (MAPKs) [131]. Therefore, the phosphorylation state of the MAP kinases ERK and JNK was investigated by western immunoblots. The antibodies that were used recognized both the 42 kDa (ERK2) and 44 kDa (ERK1) form of ERK as well as the 46 kDa (JNK1) and 54 kDa (JNK2) form of JNK. In the presence of RSV, the ratios of phospho-ERK1/2 to total ERK1/2 as well as of phospho-JNK1/2 to total JNK1/2 in cells harboring the ABCA3 mutant p.Q215K were significantly elevated when compared with ABCA3-WT and non-transfected A549 cells (Figure 4.46 and 4.47).

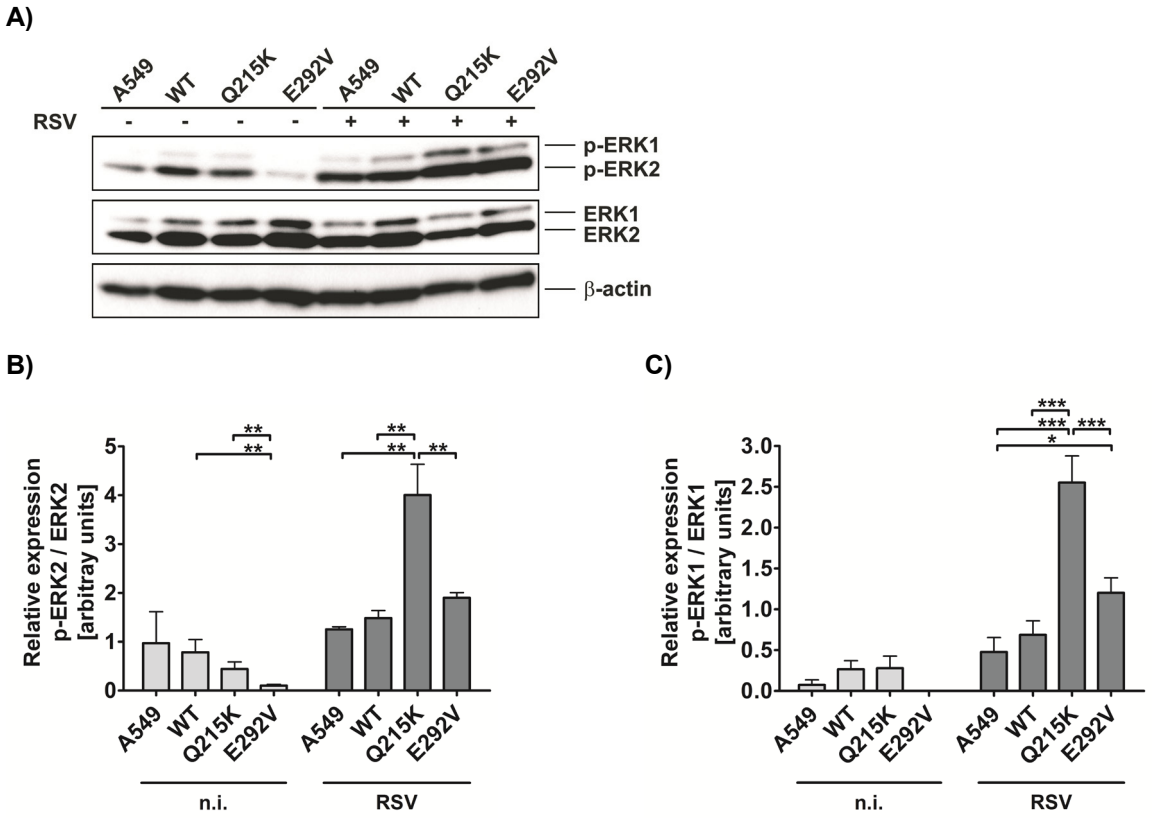

Figure 4.46: Effects of ABCA3 mutations and RSV infection on phosphorylation of MAPKs EKR1 and ERK2.
Cells were grown for 48 h in the absence or presence of RSV. A) Proteins were detected by western immunoblots of RIPA cell lysates. β-actin was used as loading control. B) Ratio of p-ERK2 / ERK2. C) Ratio of p-ERK1 / ERK1. n.i. – non-infected. *P<0.05, **P<0.01, ***P<0.001.

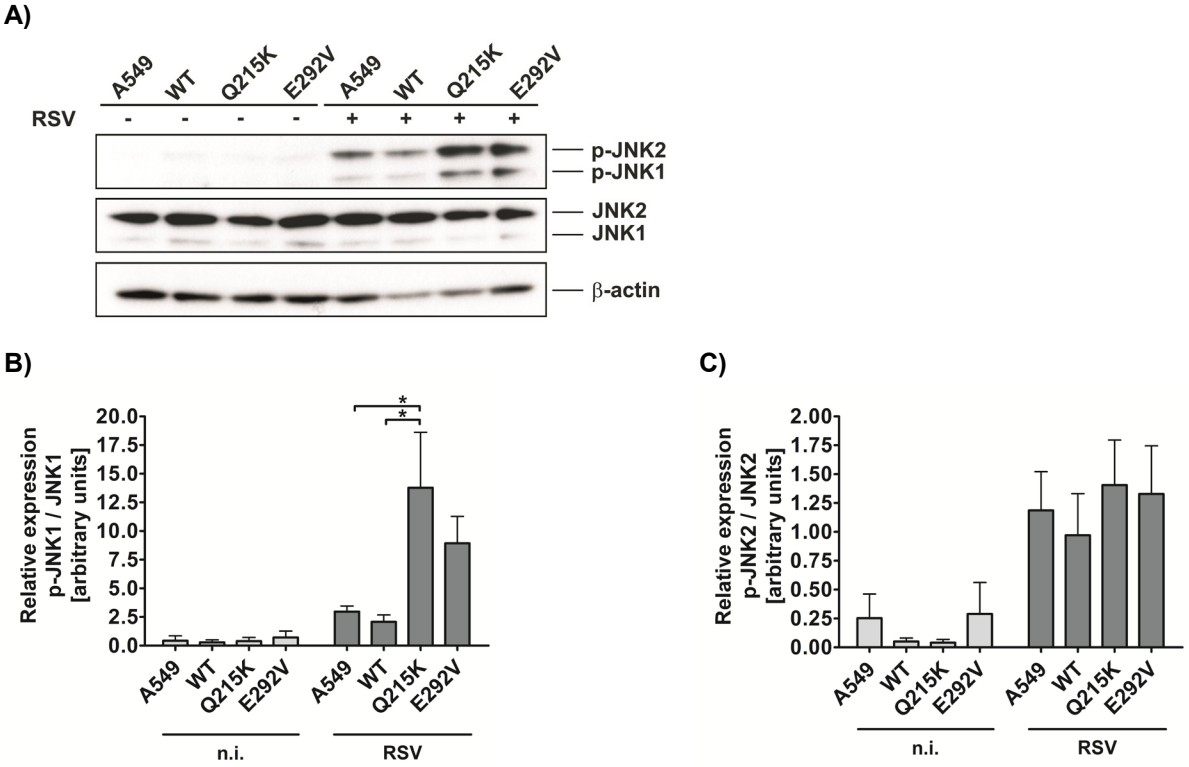

Figure 4.47: Effects of ABCA3 mutations and RSV infection on phosphorylation of MAPKs JNK1 and JNK2.
Cells were grown for 48 h in the absence or presence of RSV. A) Proteins were detected by western immunoblots of RIPA cell lysates. β-actin was used as loading control. B) Ratio of p-JNK1 / JNK1 and C) ratio of p-JNK2 / JNK2 after densitometric analysis. n.i. – non-infected. *P<0.05.

4.2.8 Effects of ABCA3 mutations and RSV infection on ER stress and UPR markers

To investigate if RSV infection imposes additional stress on stably transfected A549 cells, ER-stress markers as well as markers of the unfolded protein response (UPR) were analyzed in cell lysates. In Figure 4.48, the effects of RSV infection on the ER chaperone BiP are presented. Even though a significant increase in cells harboring mutant ABCA3 compared to the corresponding non-infected samples was observed after RSV infection (Figure 4.48 C), BiP protein was still decreased in p.Q215K and p.E292V cells when compared with ABCA3-WT cells (Figure 4.48 B).

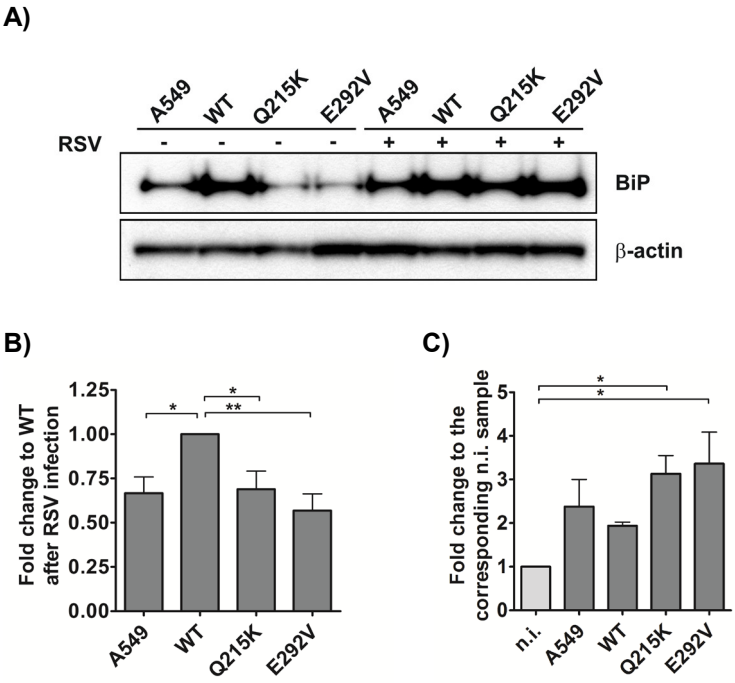

Figure 4.48: Effect of RSV infection on the ER chaperone BiP.
Cells were grown for 48 h in the presence or absence of RSV (MOI 3). A) Western immunoblot of BiP protein. β-actin was used as loading control. The left part (in the absence of RSV) was already presented in Figure 4.8. B) Fold change of BiP protein relative to ABCA3-WT cells after RSV infection. C) RSV-induced changes relative to the corresponding non-infected (n.i.) samples. *P<0.05, **P<0.01.

PERK, IRE1α and ATF-6 bind to BiP and are sensors of ER stress located in the ER membrane. Upon elevated ER stress, BiP dissociates from the sensors IRE1, PERK and ATF-6 [132]. BiP dissociation leads to IRE1 dimerization, subsequent autophosphorylation and activation of its RNase function to splice the transcription factor XBP1 to its active form [132]. Similarly, PERK dimerizes after dissociation of BiP which leads to activation as a kinase by autophosphorylation and subsequent phosphorylation of the translation initiation factor 2 (eIF2), thereby rendering eIF2 inactive [132]. Upon BiP dissocation, ATF-6 is released to be cleaved at the Golgi which activates its function as a transcription factor [132].

In the non-infected state, PERK protein was slightly decreased in cells harboring ABCA3 mutations (Figure 4.49 B). No increase of PERK was observed after RSV infection (Figure 4.49).

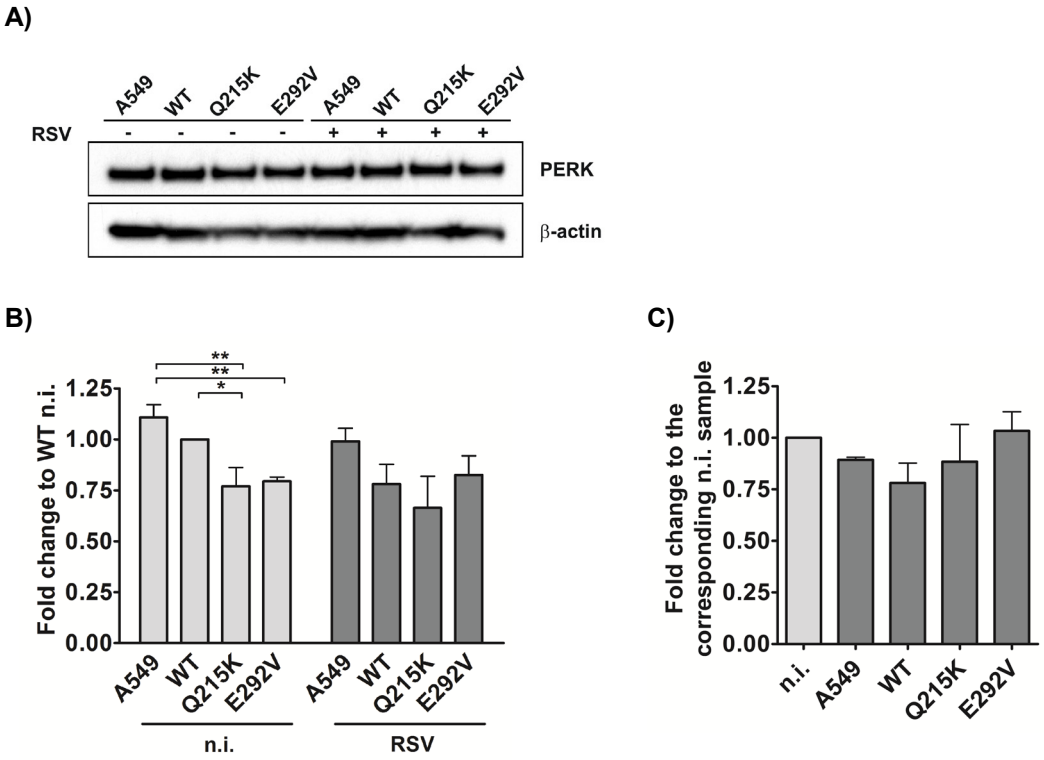

Figure 4.49: Effect of RSV infection on the UPR marker PERK.
Cells were grown for 48 h in the presence or absence of RSV (MOI 3). A) Western immunoblot of PERK protein. β-actin was used as loading control. B) Fold change of PERK protein relative to ABCA3-WT cells after RSV infection. C) RSV-induced changes relative to the corresponding non-infected (n.i.) samples. *P<0.05, **P<0.01.

Similarly, IRE1α was present in equal levels in the non-infected state, except IRE1α in p.E292V cells was significantly decreased compared to ABCA3-WT and non-transfected A549 cells (Figure 4.50 A, B). RSV infection lead to an increase in IRE1α expression; however the changes to the corresponding non-infected samples were only significant for p.E292V cells (Figure 4.50 C). The total amount of IRE1α was still lowest for p.E292V after RSV infection.

ATF-6 could only be detected in its activated, cleaved form after RSV infection in all cells (Figure 4.51 A). Compared to A549 and ABCA3-WT cells, ATF-6 was significantly elevated in p.E292V cells (Figure 4.51 B). For p.Q215K, a trend for elevated ATF-6 was observed after RSV infection; however the changes compared to non-transfected A549 and ABCA3-WT cells were not significantly different.

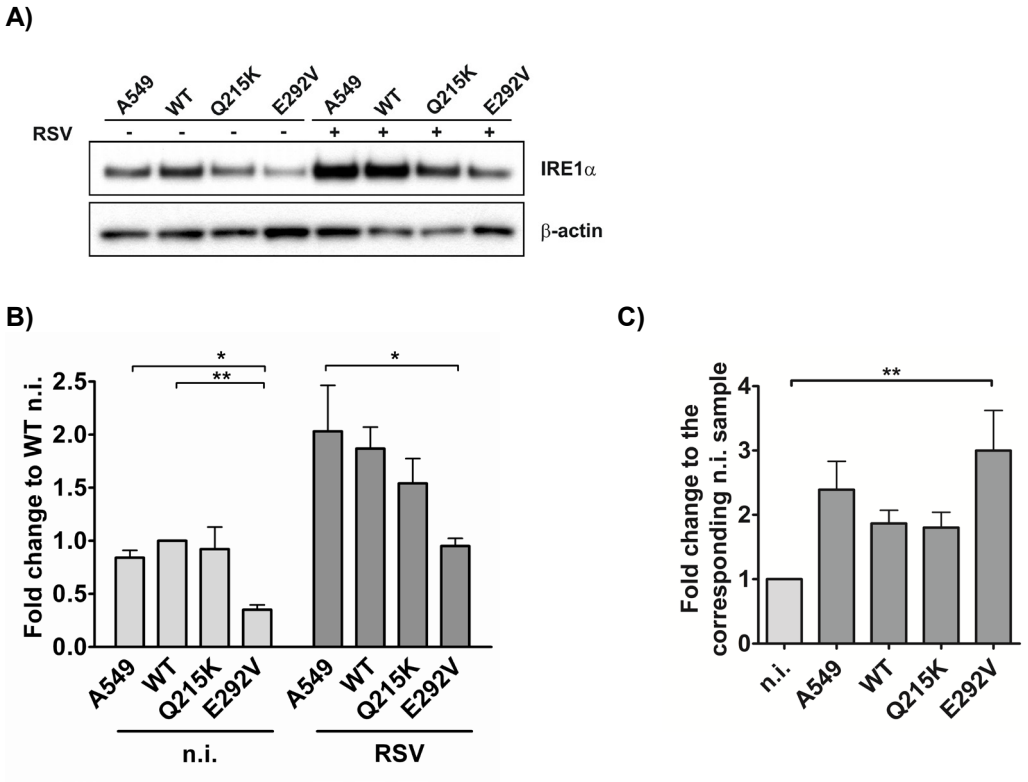

Figure 4.50: Effect of RSV infection on the UPR marker IRE-1α.
Cells were grown for 48 h in the presence or absence of RSV (MOI 3). A) Western immunoblot of IRE-1α protein. β-actin was used as loading control. B) Fold change of IRE-1α protein relative to ABCA3-WT cells after RSV infection. C) RSV-induced changes relative to the corresponding non-infected (n.i.) samples. *P<0.05, **P<0.01.

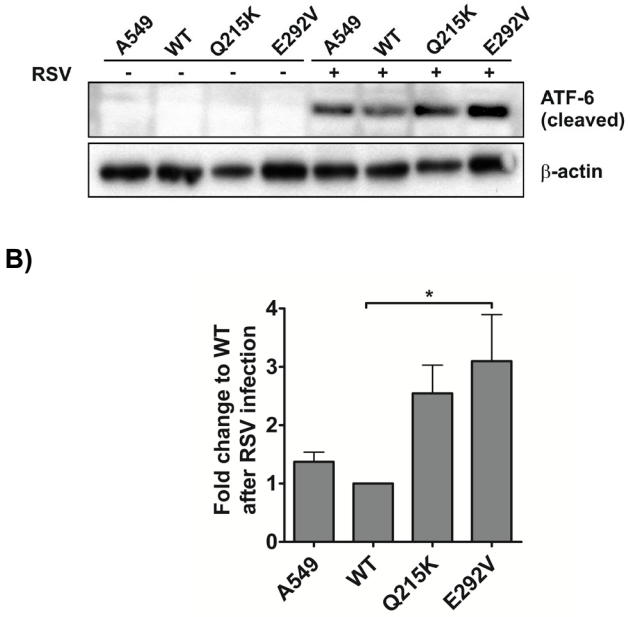

Figure 4.51: Effect of RSV infection on the UPR marker ATF-6.
Cells were grown for 48 h in the presence or absence of RSV (MOI 3).
A) Western immunoblot of ATF-6 protein. β-actin was used as loading control. B) Fold change of ATF-6 protein relative to ABCA3-WT cells after RSV infection. *P<0.05.

4.2.9 Effect of RSV infection on ABCA1

RSV infection strongly induced ABCA1 protein in A549 cells (Figure 4.52 A, C). In A549 cells harboring mutant ABCA3, no RSV induced changes were observed. Compared to ABCA3-WT cells, ABCA1 was still highest in p.Q215K cells and lowest in non-transfected A549 cells.

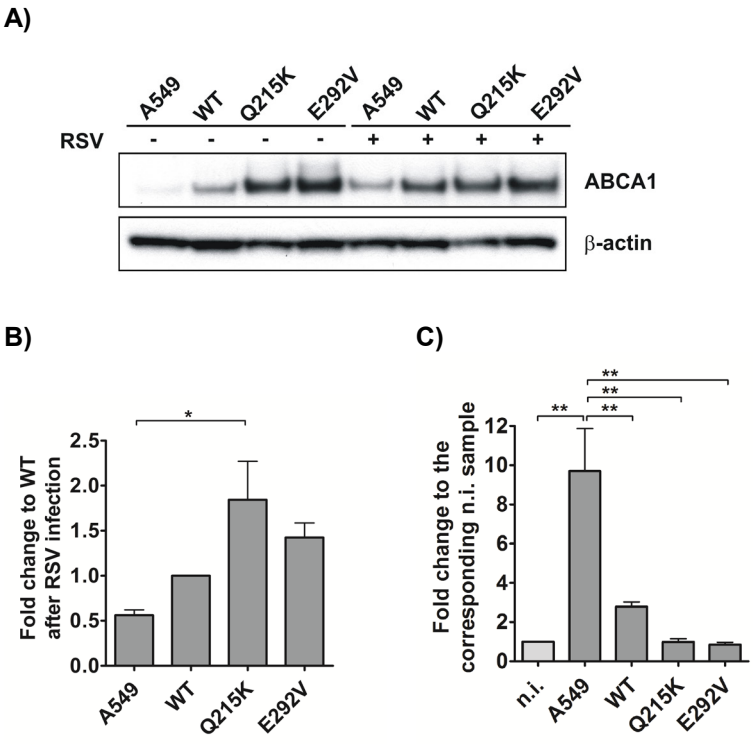

Figure 4.52: Effect of RSV infection on ABCA1.
Cells were grown for 48 h in the presence or absence of RSV (MOI 3). A) Western immuno-blot of ABCA1 protein. β-actin was used as loading control. The left part (absence of RSV) was already presented in Figure 4.18. B) Fold change of ABCA1 protein relative to ABCA3-WT cells after RSV infection. C) RSV-induced changes relative to the corresponding non-infected (n.i.) samples. *P<0.05, **P<0.01.

4.2.10 Effect of RSV infection on expression of cytokines and toll-like receptors

RSV infection induced secretion of IL-6 into cell culture supernatants of all cells (Figure 4.53 B). The strongest increase in IL-6 secretion was seen in supernatants from ABCA3 mutant cells. In absolute terms, IL-6 secretion was still highest in ABCA3-WT cells, with significant differences to p.Q215K cells and p.E292V cells (Figure 4.53 A).

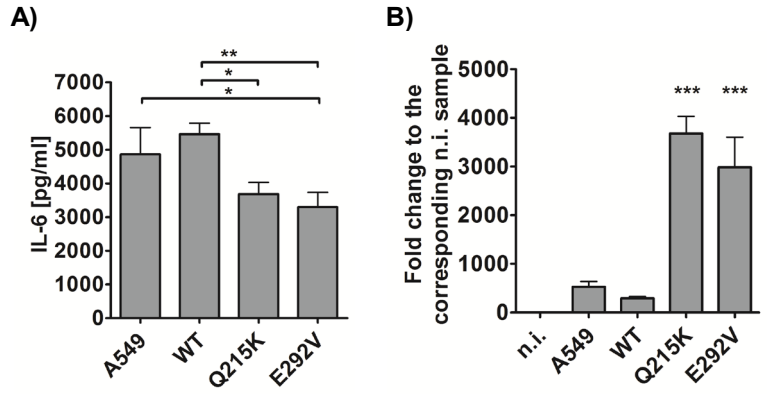

Figure 4.53: Effect of RSV infection on IL-6 secretion. Cells were RSV-infected (MOI 3) and grown for 48. A) IL-6 ELISA. *P<0.05, **P<0.01. B) RSV-induced fold change of secreted IL-6 relative to the corresponding non-infected (n.i.) sample. P value was below 0.001 compared to the corresponding n.i. samples /A549 / WT.

As observed for IL-6, IL-8 secretion after 48 h of RSV infection was elevated in all cells and the strongest increase was seen for cells harboring ABCA3 mutations (Figure 4.54 B). However, compared to non-transfected A549 and ABCA3-WT cells, IL-6 and IL-8 secretion was still decreased in ABCA3 mutant cells (Figure 4.53 A and 4.54 A).

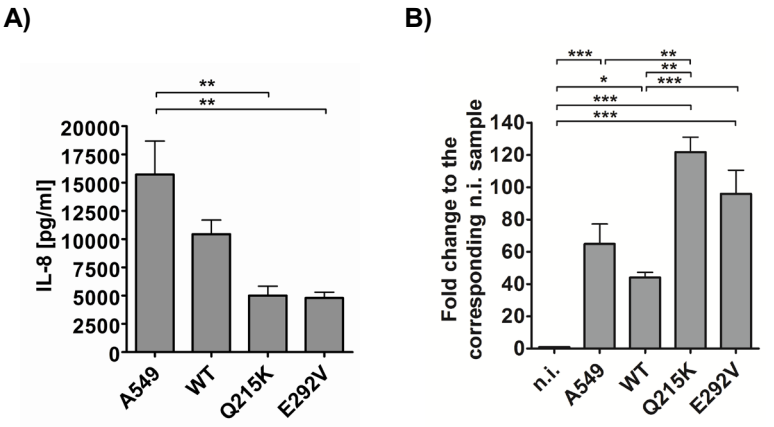

Figure 4.54: Effect of RSV infection on IL-8 secretion. Cells were RSV-infected and grown for 48 h. A) IL-8 ELISA. B) RSV-induced fold change of secreted IL-8 relative to the corresponding non-infected (n.i.) sample. *P<0.05, **P<0.01, ***P<0.001.

GM-CSF, which could not be detected in the non-infected state, was measured after RSV infection. p.Q215K cells secreted the lowest amounts of GM-CSF into the cell culture supernatants; however no significant differences were observed (Figure 4.55). RSV infection therefore induced GM-CSF secretion; however there is no information on the fold-change, as there are no values for the non-infected state available.

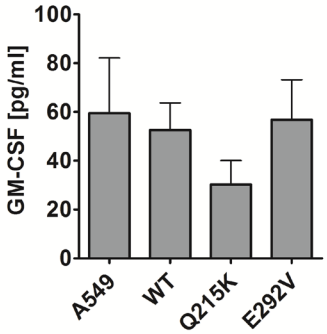

Figure 4.55: GM-CSF secretion after RSV infection.
Cells were grown for 48 h in the presence of RSV (MOI 3).

Similar to the other cytokines measured, RANTES secretion was also upregulated by RSV infection (Figure 4.56 B). RANTES levels were lowest for p.Q215K cells and highest for p.E292V cells (Figure 4.56 A).

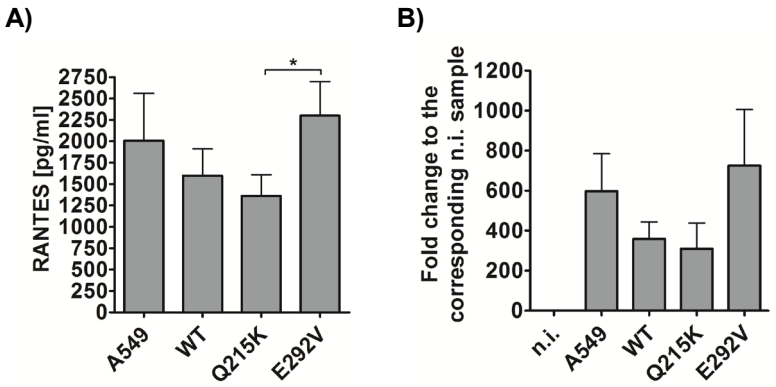

Figure 4.56: Effect of RSV infection on RANTES secretion.
Cells were RSV-infected and grown for 48h. A) RANTES ELISA. B) RSV-induced fold change relative to the corresponding non-infected (n.i.) sample. *P<0.05.

Next to cytokines, TLR-3 and TLR-4 expression were also analyzed after RSV infection. Even though both receptor mRNAs were induced by RSV infection, the strongest induction was observed for TLR-3 with a more than 17-fold change in non-transfected A549 cells (Figure 4.57 B and 4.58 B). mRNA levels in ABCA3 mutant cells were lower compared to non-transfected A549 or ABCA3-WT cells (Figure 4.57 A and 4.58 A).

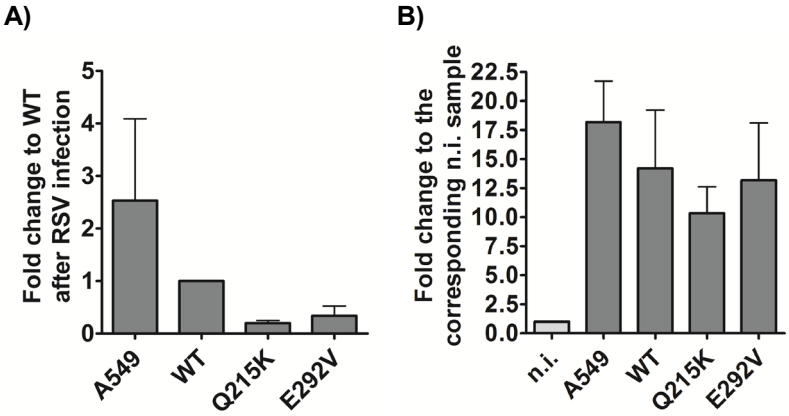

Figure 4.57: Effect of RSV infection on TLR-3 expression.
Cells were grown for 48 h in the presence of RSV (MOI 3). A) Fold change in TLR-3 mRNA calculated relative to ABCA3-WT cells after RSV infection. B) RSV-induced change relative to the corresponding non-infected (n.i.) samples.

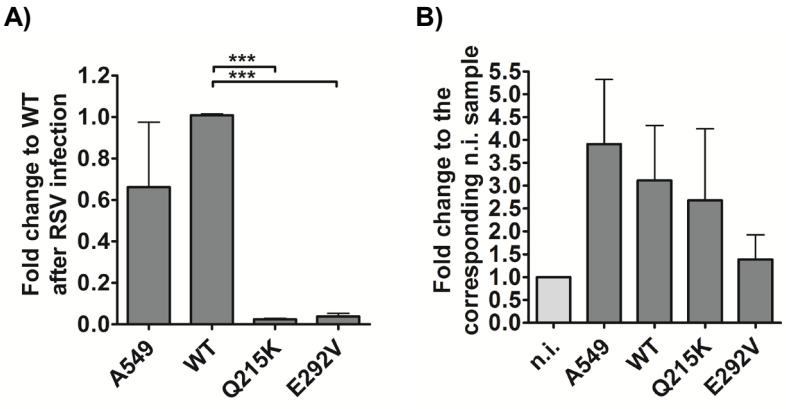

Figure 4.58: Effect of RSV infection on TLR-4 expression.
Cells were grown for 48 h in the presence of RSV (MOI 3). A) Fold change in TLR-4 mRNA calculated relative to ABCA3-WT cells after RSV infection. B) RSV-induced change relative to the corresponding non-infected (n.i.) samples. ***P<0.001.

To show that the observed effects on cytokine secretion were mediated by RSV, the virus was UV-inactivated prior to infection. UV-inactivation disrupts viral RNA and therefore inhibits virus replication inside of host cells. However, the virus can still be recognized by cellular receptors. As shown in Figure 4.59, IL-6 and IL-8 secretion after RSV infection were decreased more than two-fold in A549 and ABCA3-WT cells when the virus was UV-inactivated beforehand. In cells harboring ABCA3 mutations, IL-6 secretion was only slightly reduced (Figure 4.59 A). IL-8 secretion from ABCA3 mutant cells decreased in the same pattern as from non-transfected A549 and ABCA3-WT cells (Figure 4.59 B).

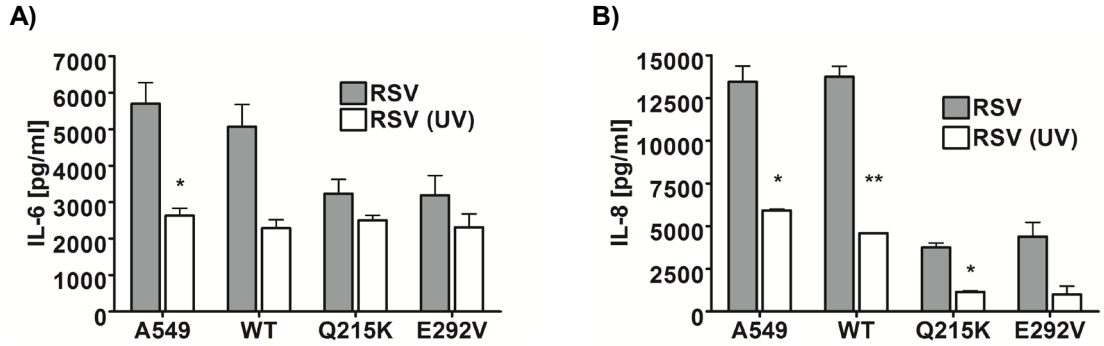

Figure 4.59: Effect of UV-inactivation of RSV on cytokine secretion.
Cells were grown for 48 h in the presence of RSV or UV-inactivated RSV. A) IL-6, B) IL-8 secretion into cell culture supernatants. Data from two independent experiments. *P<0.05, **P<0.01 compared to the corresponding RSV sample according to the unpaired students t-test.

4.3 LPS stimulation

LPS is an endotoxin on the outer membrane of gram-negative bacteria which is released when the bacteria break down. To simulate bacterial infection in the lung, stably transfected cells were stimulated with LPS from the respiratory pathogen *Pseudomonas aeruginosa*.

4.3.1 Effect of LPS stimulation on cytokine secretion and TLR expression

As shown in Figure 4.60 B), LPS stimulation induces IL-6 mRNA more than 14-fold in ABCA3-WT cells. No stimulation was seen for ABCA3 mutant cell. Similar was observed for IL-6 secretion (Figure 4.60 D). In absolute values, IL-6 secretion after LPS stimulation was highest in ABCA3-WT cells and lowest in cells harboring ABCA3 mutations.

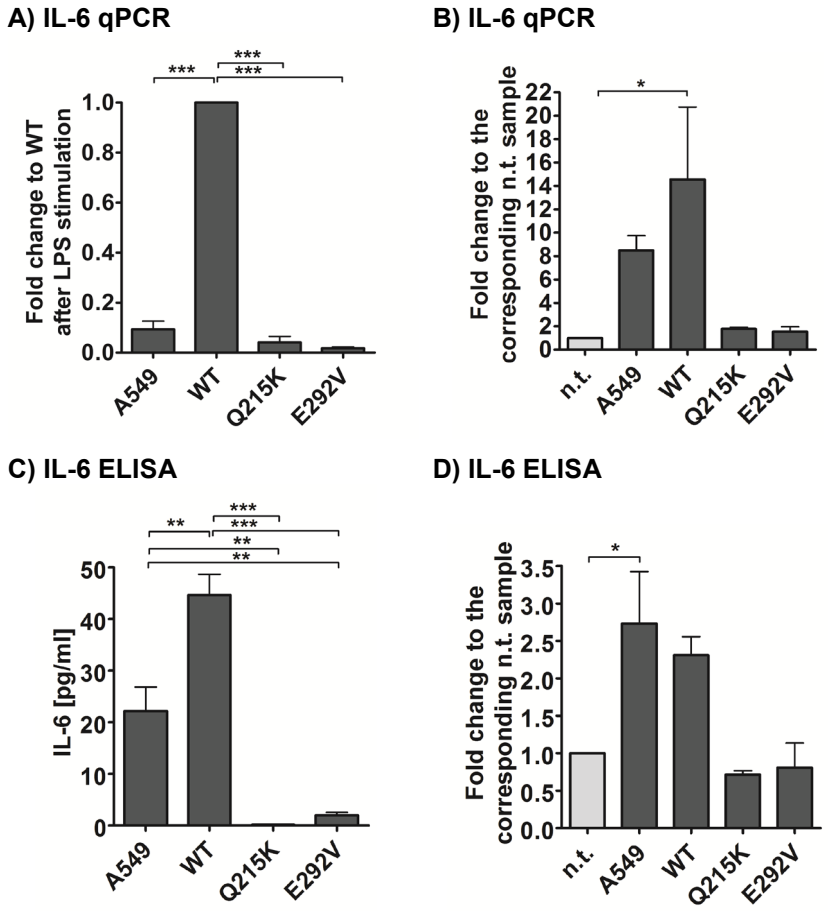

Figure 4.60: Effect of LPS stimulation on IL-6 expression and secretion.
Cells were grown for 48 h in the presence of 10 µg/ml *P. aeruginosa* LPS. IL-6 mRNA expression relative to stimulated ABCA3-WT cells (A) and absolute IL-6 secretion (C) are presented. LPS-induced fold changes in IL-6 mRNA (B) and secreted protein (D) were calculated relative to the corresponding non-treated (n.t.) samples.
*P<0.05, **P<0.01, ***P<0.001.

Similarly, IL-8 mRNA was upregulated and IL-8 secretion was increased in response to LPS stimulation in non-transfected A549 cells as well as in cells harboring ABCA3-WT (Figure 4.61 B, D). The LPS induced mRNA increase was stronger than the induced

cytokine secretion. In ABCA3 mutant cells, IL-8 mRNA expression and IL-8 secretion were induced only approximately two-fold. Therefore, the differences in absolute amounts of secreted IL-8 between ABCA3-WT and ABCA3 mutant cells were further increased (Figure 4.61 C). IL-8 secretion was approximately eight-fold reduced in ABCA3 mutant cells compared to cells harboring ABCA3-WT. Compared to RSV infection; LPS stimulation was less potent for induction of IL-6 and IL-8 secretion (compare Figure 4.53 and 4.54).

LPS stimulation did not affect TLR-3 and TLR-4 expression, as presented in Figure 4.62 (B, D). TLR-3 and TLR-4 mRNA were still strongly decreased in ABCA3 mutant cells compared to ABCA3-WT cells (Figure 4.62 A, C).

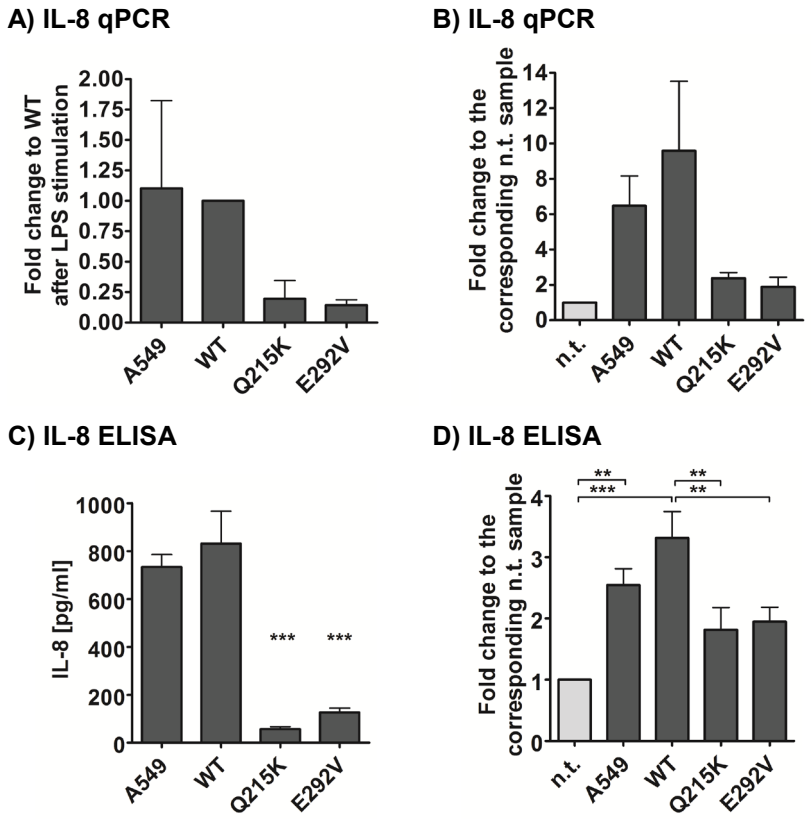

Figure 4.61: Effect of LPS stimulation on IL-8 expression and secretion.
Cells were grown for 48 h in the presence of 10 µg/ml *P. aeruginosa* LPS. IL-8 mRNA expression relative to stimulated ABCA3-WT cells (A) and absolute IL-8 secretion (C) are presented. LPS-induced fold changes in IL-8 mRNA (B) and secreted protein (D) were calculated relative to the corresponding non-treated (n.t.) samples. **P<0.01, ***P<0.001.

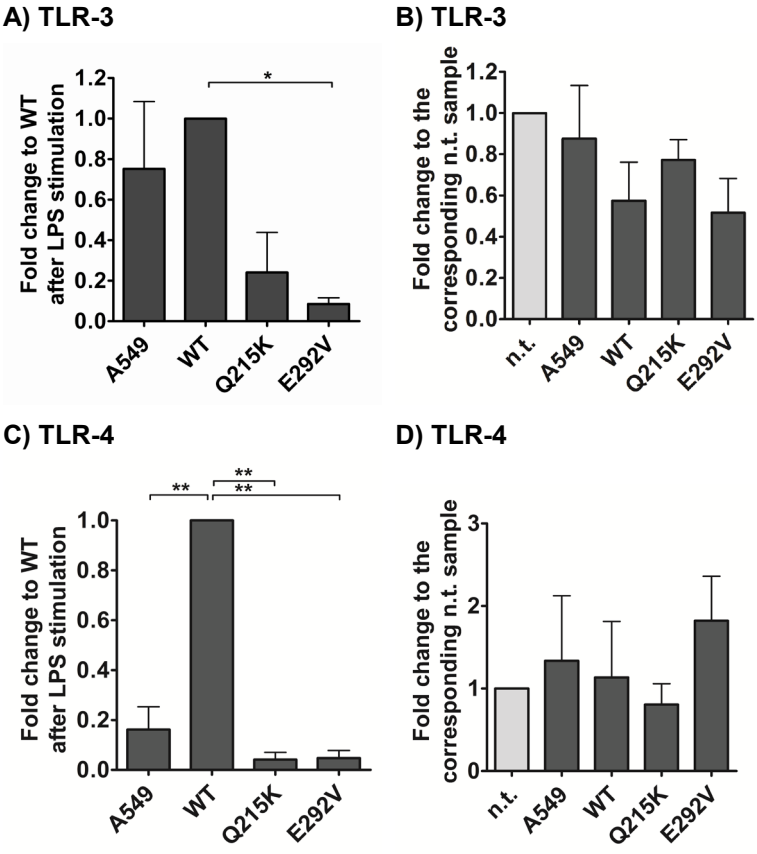

Figure 4.62: Effect of LPS stimulation on toll-like receptor expression.
Cells were grown for 48 h in the presence of 10 µg/ml *P. aeruginosa* LPS. TLR-3 (A) and TLR-4 (C) mRNA expression were calculated relative to stimulated ABCA3-WT cells. LPS-induced fold changes in TLR-3 (B) and TLR-4 (D) mRNA are presented relative to the corresponding non-treated (n.t.) samples. *P<0.05, **P<0.01.

4.4 Microarray analysis

Microarray analysis is a method which can be used to identify sets of differentially expressed genes across the whole genome. In this study, mRNA from non-transfected A549 and ABCA3-WT cells as well as p.Q215K and p.E292V cells, grown in the absence or presence of RSV, was analyzed for differentially expression by microarray analysis. In total, five comparisons were conducted: p.Q215K and p.E292V cells vs. ABCA3-WT cells, RSV-infected p.Q215K and p.E292V cells vs. RSV-infected ABCA3-WT cells and lastly RSV-infected cells compared to non-infected cells.

Fold changes (FC) derived from microarray analysis should correlate with qPCR fold changes from the corresponding genes investigated independently. Correlation analysis for mRNA fold changes from qPCR and microarray analysis from p.Q215K and p.E292V cells compared to ABCA3-WT cells are presented in Figure 4.63. Both correlations were significant with P<0.0001.

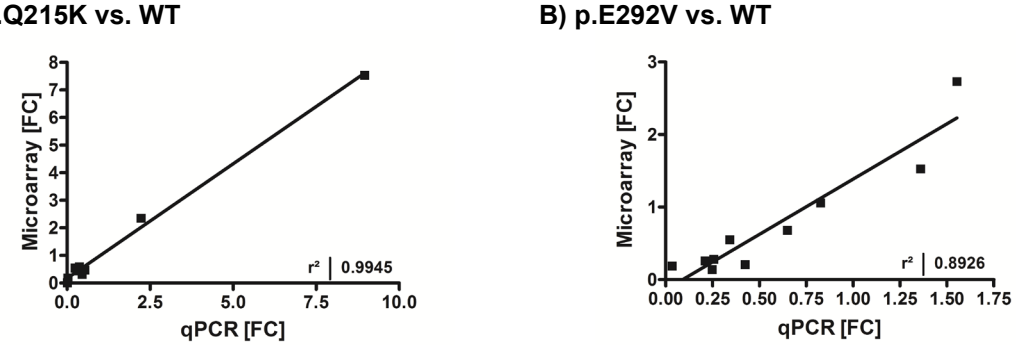

Figure 4.63: Correlation analysis of qPCR and microarray data by linear regression.
A) p.Q215K vs. WT, B) p.E292V vs. WT. Data from 10 genes was analyzed. r^2: Pearson correlation quotient (assuming Gaussian distribution).

In the following tables, the top 15 down- and upregulated genes according to the normalized microarray data of the respective comparisons are presented. The genes are ranked according to the log_2FC. Genes strongly upregulated in the absence of RSV in both p.Q215K and p.E292V cells include CES1, CXCR4, RAB42, PRKCDBP, HYI, RIPPLY2, STXBP6, CHST2, TRPM2, SLCO2B1, SDR4E1, CES1P2, and UGT8 (Table 4.5 and 4.7). Strongly downregulated genes in p.Q215K and p.E292V include CEACAM6, HNF1A, SLC1A3, TM4SF4, CEACAM7, FXYD2, FGB, PCSK1, SETBP1, KRT20, FGA, VCAN, and MUC5B.

Table 4.5: Top 15 up- and downregulated genes of p.Q215K vs. WT, ranked according to log_2FC.

Gene Name	Description	log_2FC	adj.P.Val
		downregulated	
RPS4Y1	ribosomal protein S4, Y-linked 1	-12,70	1,23E-22
RPS4Y2	ribosomal protein S4, Y-linked 2	-12,40	1,23E-22
NCRNA00230A	non-protein coding RNA 230A	-10,30	9,19E-14
DDX3Y	DEAD (Asp-Glu-Ala-Asp) box polypeptide 3, Y-linked, transcript variant 1	-9,40	3,63E-21
USP9Y	ubiquitin specific peptidase 9, Y-linked	-7,78	9,89E-21
CEACAM6	carcinoembryonic antigen-related cell adhesion molecule 6	-7,73	2,57E-15
CDH2	cadherin 2, type 1, N-cadherin (neuronal)	-7,51	1,20E-11
HNF1A	HNF1 homeobox A	-7,12	2,30E-12
EIF1AY	eukaryotic translation initiation factor 1A, Y-linked	-7,07	8,57E-19
CYorf15B	chromosome Y open reading frame 15B	-7,03	4,73E-12
PRY2	PTPN13-like, Y-linked 2	-6,90	2,37E-11
SLC1A3	solute carrier family 1 (glial high affinity glutamate transporter), member 3, transcript variant 1	-6,61	3,30E-10
TM4SF4	transmembrane 4 L six family member 4	-6,58	5,73E-10
CYorf15A	chromosome Y open reading frame 15A	-6,47	9,49E-16
CEACAM7	carcinoembryonic antigen-related cell adhesion molecule 7	-6,11	1,03E-11
		upregulated	
CES1	carboxylesterase 1, transcript variant 1	8,75	9,89E-21
CXCR4	chemokine (C-X-C motif) receptor 4, transcript variant 1	7,30	3,93E-13
RAB42	RAB42, member RAS oncogene family, transcript variant 2	6,76	1,00E-06
PRKCDBP	protein kinase C, delta binding protein	6,19	2,69E-19
HYI	hydroxypyruvate isomerase (putative), transcript variant 3	6,11	6,63E-15
CES1	carboxylesterase 1, transcript variant 3	5,86	1,01E-13
FAM159B	family with sequence similarity 159, member B	5,58	4,45E-08
GPR109B	G protein-coupled receptor 109B	5,41	8,11E-14
RIPPLY2	ripply2 homolog (zebrafish)	5,14	4,63E-14
STXBP6	syntaxin binding protein 6 (amisyn)	4,94	1,52E-12
CHST2	carbohydrate (N-acetylglucosamine-6-O) sulfotransferase 2	4,88	3,97E-12
TRPM2	transient receptor potential cation channel, subfamily M, member 2	4,86	1,94E-10
ATL1	atlastin GTPase 1, transcript variant 2	4,79	3,40E-11
HYI	hydroxypyruvate isomerase (putative), transcript variant 1	4,72	6,03E-12
SLCO2B1	solute carrier organic anion transporter family, member 2B1, transcript variant 1	4,70	2,84E-08

FC – fold change, adj. P val - adjusted P value corrected for multiple testing.

For pathway analysis, Agilent IDs of regulated genes with a $log_2FC < 1$ or a $log_2FC > 1$ and an adjusted P value below 0.05 (corrected for multiple testing) were uploaded to DAVID Bioinformatics Resources 6.7, a Functional Annotation Tool [125, 126]. As background, all Agilent IDs from the Agilent 8x60k microarray were uploaded. Agilent identifiers recognized by DAVID were converted to DAVID IDs. Multiple probes of the same gene were collapsed to one DAVID ID. Functional annotation charts displaying only KEGG pathways with an EASE score (P value) of 0.05 and below were exported (Table 4.6, 4.8, 4.10, 4.12 and 4.14). Regulated genes according to regulated KEGG pathways are presented in the supplement (section 7.1.2).

For p.Q215K vs. WT, 1720 genes with DAVID ID and for p.Q215K vs. WT in the presence of RSV, 2031 genes with DAVID ID were found to be regulated.

For p.Q215K vs. WT, 14 regulated KEGG pathways with an EASE score below 0.05 were found using DAVID (Table 4.6). All regulated pathways included both up- and downregulated genes. The pathways include steroid hormone biosynthesis (with 9 down- and 5 upregulated genes), cytokine-cytokine receptor interactions (with 25 down- and 19

upregulated genes), cell-adhesion molecules (with 15 down- and 8 upregulated genes), ECM-receptor interactions (with 8 down- and 7 upregulated genes) as well as ABC transporters (with 3 down- and 10 upregulated genes). To the upregulated genes of the ABC transporter pathway belong ABCA1, ABCA5, ABCA6, and ABCG4 and to the downregulated genes belongs CFTR (section 7.1.2.1).

Table 4.6: Regulated KEGG pathways of p.Q215K vs. WT.

KEGG pathway	Term	count down	count up	P value	Fold Enrichment
hsa00140	Steroid hormone biosynthesis	9	5	5,06E-04	2,90
hsa00982	Drug metabolism - Cytochrome P450	10	6	8,62E-04	2,54
hsa00980	Metabolism of xenobiotics by cytochrome P450	10	6	8,62E-04	2,54
hsa04610	Complement and coagulation cascades	13	3	3,54E-03	2,23
hsa00150	Androgen and estrogen metabolism	7	4	3,83E-03	2,78
hsa00830	Retinol metabolism	7	6	4,52E-03	2,45
hsa04060	Cytokine-cytokine receptor interaction	25	19	5,09E-03	1,52
hsa04514	Cell adhesion molecules (CAMs)	15	8	1,31E-02	1,75
hsa04080	Neuroactive ligand-receptor interaction	25	12	1,49E-02	1,47
hsa04621	NOD-like receptor signaling pathway	7	7	1,89E-02	1,99
hsa04670	Leukocyte transendothelial migration	10	12	2,42E-02	1,71
hsa04512	ECM-receptor interaction	8	7	2,77E-02	1,84
hsa02010	ABC transporters	3	10	3,21E-02	2,19
hsa00983	Drug metabolism	7	2	3,63E-02	2,28

1720 genes with DAVID IDs were found to be regulated.
Count down/up – number of down- and upregulated genes in the respective pathway.

Table 4.7: Top 15 up- and downregulated genes of p.E292V vs. WT, ranked according to log_2FC.

Gene Name	Description	log_2FC	adj.P.Val
		downregulated	
FGG	fibrinogen gamma chain, transcript variant gamma-A	-7,15	2,22E-12
SLC1A3	solute carrier family 1 (glial high affinity glutamate transporter), member 3, transcript variant 1	-6,90	3,07E-10
LCN2	lipocalin 2	-6,50	3,23E-10
ADAMTS9	ADAM metallopeptidase with thrombospondin type 1 motif, 9	-6,20	9,71E-13
TM4SF4	transmembrane 4 L six family member 4	-6,13	2,07E-09
FXYD2	FXYD domain containing ion transport regulator 2, transcript variant b	-5,89	1,71E-15
HNF1A	HNF1 homeobox A	-5,86	4,50E-11
SLPI	secretory leukocyte peptidase inhibitor	-5,81	6,45E-14
CEACAM6	carcinoembryonic antigen-related cell adhesion molecule 6	-5,80	8,85E-14
CEACAM3	carcinoembryonic antigen-related cell adhesion molecule 3	-5,73	2,91E-11
FGB	fibrinogen beta chain, transcript variant 1	-5,66	1,01E-14
PCSK1	proprotein convertase subtilisin/kexin type 1	-5,65	2,77E-10
NTRK3	neurotrophic tyrosine kinase, receptor, type 3, transcript variant 1	-5,61	8,52E-15
PCSK1	proprotein convertase subtilisin/kexin type 1, transcript variant 1	-5,49	9,19E-08
CFI	complement factor I	-5,42	3,85E-12
		upregulated	
CES1	carboxylesterase 1, transcript variant 1	8,99	3,20E-20
CDH19	cadherin 19, type 2	7,84	1,33E-17
CES1	carboxylesterase 1, transcript variant 3	6,35	6,26E-14
HYI	hydroxypyruvate isomerase (putative), transcript variant 3	6,22	8,53E-15
RAB42	RAB42, member RAS oncogene family, transcript variant 2	6,14	4,13E-06
TRPM2	transient receptor potential cation channel, subfamily M, member 2	6,12	1,82E-11
PART1	prostate androgen-regulated transcript 1, transcript variant 2, non-coding RNA	5,37	8,96E-13
CES1P2	carboxylesterase 1 pseudogene 2, non-coding RNA	5,09	1,52E-11
SLCO2B1	solute carrier organic anion transporter family, member 2B1, transcript variant 1	5,08	1,62E-08
HYI	hydroxypyruvate isomerase (putative), transcript variant 1	5,06	4,45E-12
GREM1	gremlin 1 (GREM1), transcript variant 1	4,58	1,97E-11
PRKCDBP	protein kinase C, delta binding protein	4,56	4,48E-17
SERPINI1	serpin peptidase inhibitor, clade I member 1, transcript variant 1	4,37	2,11E-10
STXBP6	syntaxin binding protein 6 (amisyn)	4,31	1,40E-11
HS6ST2	heparan sulfate 6-O-sulfotransferase 2, transcript variant L	4,30	3,78E-06

FC – fold change, adj. P val - adjusted P value corrected for multiple testing.

For p.E292V vs. WT, 1233 genes with DAVID ID and for p.E292V vs. WT in the presence of RSV, 1370 genes with DAVID ID were found to be regulated.
For p.E292V vs. WT, 18 KEGG pathways were found to be regulated (Table 4.8). They include cytokine-cytokine receptor interaction (with 27 down- and 9 upregulated genes), steroid hormone biosynthesis (with 11 down- and 2 upregulated genes) and TLR signaling pathway (with 9 down- and 4 upregulated genes).

Table 4.8: Regulated KEGG pathways of p.E292V vs. WT.

KEGG pathway	Term	count down	count up	P value	Fold Enrichment
hsa04060	Cytokine-cytokine receptor interaction	27	9	1,86E-04	1,91
hsa00980	Metabolism of xenobiotics by cytochrome P450	15	1	2,10E-04	3,25
hsa00140	Steroid hormone biosynthesis	11	2	2,47E-04	3,65
hsa00982	Drug metabolism - Cytochrome P450	14	1	8,07E-04	3,02
hsa00983	Drug metabolism - other enzymes	9	2	9,30E-04	3,70
hsa00053	Ascorbate and aldarate metabolism	7	0	1,97E-03	5,93
hsa04621	NOD-like receptor signaling pathway	9	4	2,27E-03	2,70
hsa00830	Retinol metabolism	10	2	2,40E-03	3,03
hsa04610	Complement and coagulation cascades	12	1	2,65E-03	2,66
hsa04670	Leukocyte transendothelial migration	7	10	2,94E-03	2,24
hsa00512	O-Glycan biosynthesis	6	4	3,56E-03	3,79
hsa00150	Androgen and estrogen metabolism	9	1	4,02E-03	3,33
hsa00500	Starch and sucrose metabolism	7	2	1,26E-02	3,06
hsa04640	Hematopoietic cell lineage	8	4	1,82E-02	2,19
hsa00040	Pentose and glucuronate interconversions	6	0	1,91E-02	4,56
hsa04514	Cell adhesion molecules (CAMs)	9	6	3,07E-02	1,83
hsa00590	Arachidonic acid metabolism	7	2	3,56E-02	2,32
hsa04620	Toll-like receptor signaling pathway	9	4	3,66E-02	1,90

1233 genes with DAVID IDs were found to be regulated.
Count down/up – number of down- and upregulated genes in the respective pathway.

There were 10 KEGG pathways with an EASE score below 0.05 that were regulated in both comparisons p.Q215K vs. WT and p.E292V vs. WT, namely steroid hormone biosynthesis, drug metabolism by cytochrome P450, metabolism of xenobioticx by cytochrome P450, complement and coagulation cascades, retinol metabolism, cytokine-cytokine receptor interactions, cell adhesion molecules, NOD-like receptor interactions, leukocyte transendothelial migration and drug metabolism by other enzymes (compare Table 4.6 and 4.8).

In the presence of RSV infection, genes strongly downregulated in p.Q215K as well as in p.E292V cells included HNF1A, CEACAM6, FGG, ARMCX1, CEACAM7, RM4SF4, TLR4, NTRK3, CCL28, VCAN, and MIA2. RAB42, CES1, HYI, PRKCDBP, CES1P2, PCDH7, and CXCR7 belonged to the genes strongly upregulated in p.Q215K and p.E292V cells grown in the presence of RSV (compare Table 4.9 and 4.11).

Table 4.9: Top 15 up- and downregulated genes of p.Q215K vs. WT in the presence of RSV, ranked according to log_2FC.

Gene Name	Description	log_2FC	adj.P.Val
		downregulated	
RPS4Y1	ribosomal protein S4, Y-linked 1	-11,90	6,08E-23
RPS4Y2	ribosomal protein S4, Y-linked 2	-11,70	6,08E-23
DDX3Y	DEAD (Asp-Glu-Ala-Asp) box polypeptide 3, Y-linked, transcript variant 1	-9,65	4,33E-22
NCRNA00230A	non-protein coding RNA 230A	-9,37	6,31E-14
HNF1A	HNF1 homeobox A	-8,22	4,23E-14
CYorf15B	chromosome Y open reading frame 15B	-8,03	1,95E-13
USP9Y	ubiquitin specific peptidase 9, Y-linked	-7,87	1,85E-21
CEACAM6	carcinoembryonic antigen-related cell adhesion molecule 6	-6,89	2,99E-15
EIF1AY	eukaryotic translation initiation factor 1A, Y-linked	-6,66	5,16E-19
KDM5D	lysine (K)-specific demethylase 5D, transcript variant 2	-6,41	5,37E-11
TRIM31	tripartite motif-containing 31	-6,18	1,23E-09
PRY2	PTPN13-like, Y-linked 2	-6,13	1,82E-11
FGG	gamma chain (FGG), transcript variant gamma-A	-5,89	7,29E-10
ZFY	zinc finger protein, Y-linked, transcript variant 1	-5,81	2,81E-17
SHROOM3	shroom family member 3	-5,80	8,56E-17
		upregulated	
RAB42	RAB42, member RAS oncogene family, transcript variant 2	8,40	1,31E-08
CES1	carboxylesterase 1, transcript variant 1	7,51	1,87E-20
HYI	hydroxypyruvate isomerase (putative), transcript variant 3	6,89	3,81E-16
CES1	carboxylesterase 1, transcript variant 3	6,33	8,93E-15
CLDN14	claudin 14, transcript variant 1	6,32	7,26E-10
UGT8	UDP glycosyltransferase 8, transcript variant 2	5,38	1,75E-10
HYI	hydroxypyruvate isomerase (putative), transcript variant 1	5,13	4,37E-13
OTUD7A	OTU domain containing 7A	5,13	7,80E-09
ATL1	atlastin GTPase 1, transcript variant 2	5,10	4,21E-13
PRKCDBP	protein kinase C, delta binding protein	5,00	1,10E-18
ADAMTS6	ADAM metallopeptidase with thrombospondin type 1 motif, 6	5,00	9,35E-10
KIF5C	kinesin family member 5C	4,96	2,90E-14
CES1P2	carboxylesterase 1 pseudogene 2, non-coding RNA	4,79	3,51E-12
RIPPLY2	ripply2 homolog (zebrafish)	4,69	3,04E-14
FAM159B	family with sequence similarity 159, member B	4,69	5,88E-08

FC – fold change, adj. P val - adjusted P value corrected for multiple testing.

RSV-infected p.Q215K cells induced the regulation of 9 KEGG pathways when compared with RSV infected ABCA3-WT cells (Table 4.10).

Table 4.10: Regulated KEGG pathways of p.Q215K vs. WT in the presence of RSV.

KEGG pathway	Term	count down	count up	P value	Fold Enrichment
hsa04060	Cytokine-cytokine receptor interaction	28	20	2,25E-03	1,52
hsa04610	Complement and coagulation cascades	14	3	4,87E-03	2,08
hsa04110	Cell cycle	21	6	8,50E-03	1,68
hsa03030	DNA replication	10	1	1,22E-02	2,37
hsa04672	Intestinal immune network for IgA production	8	5	1,83E-02	2,05
hsa05217	Basal cell carcinoma	7	6	3,47E-02	1,89
hsa04512	ECM-receptor interaction	7	9	3,68E-02	1,72
hsa04514	Cell adhesion molecules (CAMs)	12	10	4,61E-02	1,54
hsa05200	Pathways in cancer	30	21	4,83E-02	1,28

2031 genes with DAVID IDs were found to be regulated.
Count down/up – number of down- and upregulated genes in the respective pathway.

Table 4.11: Top 15 up- and downregulated genes of p.E292V vs. WT in the presence of RSV, ranked according to log_2FC.

Gene Name	Description	log_2FC	adj.P.Val
		downregulated	
ADAMTS9	ADAM metallopeptidase with thrombospondin type 1 motif, 9	-8,26	3,67E-14
HNF1A	HNF1 homeobox A	-7,29	1,44E-12
FGG	fibrinogen gamma chain, transcript variant gamma-A	-6,47	2,26E-09
PCSK1	proprotein convertase subtilisin/kexin type 1, transcript variant 1	-6,02	1,31E-10
ALOX5	arachidonate 5-lipoxygenase	-5,95	4,92E-11
DCLK1	doublecortin-like kinase 1, transcript variant 1	-5,85	6,34E-12
TMEM139	transmembrane protein 139	-5,70	3,91E-11
CA9	carbonic anhydrase IX	-5,52	2,64E-07
NTRK3	neurotrophic tyrosine kinase, receptor, type 3, transcript variant 3	-5,40	1,20E-17
BMP4	bone morphogenetic protein 4, transcript variant 1	-5,31	2,82E-10
FGA	fibrinogen alpha chain, transcript variant alpha	-5,31	2,09E-07
ARMCX1	armadillo repeat containing, X-linked 1	-5,08	4,03E-08
C7orf29	chromosome 7 open reading frame 29	-5,07	9,53E-10
CEACAM6	carcinoembryonic antigen-related cell adhesion molecule 6	-4,99	1,18E-12
TM4SF4	transmembrane 4 L six family member 4	-4,97	2,49E-08
		upregulated	
CES1	carboxylesterase 1, transcript variant 1	8,48	7,96E-20
RAB42	RAB42, member RAS oncogene family, transcript variant 2	7,87	2,29E-07
CES1	carboxylesterase 1, transcript variant 3	7,62	1,15E-14
HYI	hydroxypyruvate isomerase (putative), transcript variant 3	6,65	4,36E-15
CDH19	cadherin 19, type 2	6,26	1,68E-16
CES1P2	carboxylesterase 1 pseudogene 2, non-coding RNA	5,83	2,92E-12
TRPM2	transient receptor potential cation channel, subfamily M, member 2	5,26	1,25E-10
HYI	hydroxypyruvate isomerase (putative), transcript variant 1	4,70	1,13E-11
CXCR7	chemokine (C-X-C motif) receptor 7	4,66	8,23E-14
PCDH7	protocadherin 7, transcript variant a	4,46	1,68E-06
UGT8	UDP glycosyltransferase 8, transcript variant 2	4,44	1,64E-08
PART1	prostate androgen-regulated transcript 1, transcript variant 2, non-coding RNA	4,33	1,28E-11
LGI2	leucine-rich repeat LGI family, member 2	4,28	4,60E-10
PGBD5	piggyBac transposable element derived 5	4,16	4,19E-10
KIF5C	kinesin family member 5C	4,14	1,92E-12

FC – fold change, adj. P val - adjusted P value corrected for multiple testing.

When comparing p.E292V vs. ABCA3-WT cells in the presence of RSV, 8 pathways were found to be regulated (Table 4.12).

Table 4.12: Regulated KEGG pathways of E292V vs. WT in the presence of RSV.

KEGG pathway	Term	count down	count up	P value	Fold Enrichment
hsa04610	Complement and coagulation cascades	14	2	6,72E-04	2,63
hsa04060	Cytokine-cytokine receptor interaction	20	20	7,99E-04	1,70
hsa04514	Cell adhesion molecules (CAMs)	9	11	4,87E-03	1,96
hsa04062	Chemokine signaling pathway	13	15	1,77E-02	1,60
hsa04360	Axon guidance	9	11	2,64E-02	1,67
hsa04623	Cytosolic DNA-sensing pathway	7	3	3,12E-02	2,21
hsa04640	Hematopoietic cell lineage	5	8	3,51E-02	1,90
hsa04670	Leukocyte transendothelial migration	7	9	4,54E-02	1,69

1370 genes with DAVID IDs were found to be regulated.
Count down/up – number of down- and upregulated genes in the respective pathway.

KEGG Pathways with an EASE score < 0.05 regulated in both p.Q215K and p.E292V cells compared to ABCA3-WT cells in the presence of RSV include cytokine-cytokine receptor interactions, complement and coagulation cascades and cell adhesion molecules (compare Table 4.10 and 4.12).

In Table 4.13, the top 15 up- and downregulated genes of the comparison RSV-infected cells vs. non-infected cells are presented.

Table 4.13: Top 15 up- and downregulated genes of RSV-infected vs. non-infected cells, ranked according to log_2FC.

Gene Name	Description	log_2FC	adj.P.Val
		downregulated	
LRP2	low density lipoprotein receptor-related protein 2	-6,29	1,91E-13
KRT4	keratin 4	-4,15	1,00E-14
TRIM67	tripartite motif-containing 67	-4,02	7,86E-16
ANXA13	annexin A13, transcript variant 2	-3,76	3,75E-09
HLA-DMB	major histocompatibility complex, class II, DM beta	-3,70	7,50E-17
CBLN2	cerebellin 2 precursor	-3,51	5,24E-12
KRT4	keratin 4	-3,49	1,91E-14
CPLX2	complexin 2, transcript variant 1	-3,47	9,80E-18
PRR15L	proline rich 15-like	-3,41	9,22E-14
ST6GAL2	ST6 beta-galactosamide alpha-2,6-sialyltranferase 2, transcript variant 1	-3,37	2,75E-19
CPLX2	complexin 2, transcript variant 1	-3,35	6,48E-21
VAV3	vav 3 guanine nucleotide exchange factor, transcript variant 1	-3,20	1,32E-14
RAB26	RAB26, member RAS oncogene family	-3,19	1,36E-19
BCAS1	breast carcinoma amplified sequence 1	-3,19	3,46E-12
PROC	protein C (inactivator of coagulation factors Va and VIIIa)	-3,18	3,12E-09
		upregulated	
CCL3	chemokine (C-C motif) ligand 3	14,90	2,05E-23
CCL3L3	chemokine (C-C motif) ligand 3-like 3	12,30	3,01E-16
CCL5	chemokine (C-C motif) ligand 5	11,70	1,00E-22
IL29	interleukin 29 (interferon, lambda 1)	11,70	6,53E-19
CSF3	colony stimulating factor 3 (granulocyte)	11,20	1,73E-24
IL29	interleukin 29 (interferon, lambda 1)	11,20	2,34E-21
IL28B	interleukin 28B (interferon, lambda 3)	10,60	3,08E-23
ZBTB32	zinc finger and BTB domain containing 32	10,60	5,24E-19
CCL4	chemokine (C-C motif) ligand 4, transcript variant 1	10,20	6,57E-25
OASL	2'-5'-oligoadenylate synthetase-like (OASL), transcript variant 1	9,98	3,18E-22
RSAD2	radical S-adenosyl methionine domain containing 2	9,95	3,89E-27
MMP1	matrix metallopeptidase 1 (interstitial collagenase), transcript variant 1	9,62	4,24E-18
IFI27	interferon, alpha-inducible protein 27, transcript variant 2	9,39	9,61E-23
IL28A	interleukin 28A (interferon, lambda 2)	9,31	3,18E-22
IFI44	interferon-induced protein 44	9,26	2,54E-17

FC – fold change, adj. P val - adjusted P value corrected for multiple testing.

RSV infection induced the regulation of a total of 14 KEGG pathways with an EASE score below 0.05 when compared with non-infected cells (Table 4.14). Interestingly, these pathways either contained mostly upregulated genes (such as the the pathway cytokine-cytokine receptor interactions, JAK-STAT signaling pathway, TLR signaling pathway or cytosolic DNA-sensing pathway) or they contain mostly downregulated genes (such as Cell cycle or DNA replication). RSV therefore induces the expression of cytokines, chemokines, cytokine and toll-like receptors as well as other molekules needed for the host cells to fight against viral infection while simultaniously decreasing cellular proliferation by impairing the cell cycle and inhibiting DNA replication.

Table 4.14: Regulated KEGG pathways of RSV-infected cells vs. non-infected cells.

KEGG pathway	Term	count down	count up	P value	Fold Enrichment
hsa04060	Cytokine-cytokine receptor interaction	6	81	5,32E-13	2,09
hsa04630	Jak-STAT signaling pathway	3	40	3,22E-05	1,85
hsa04620	Toll-like receptor signaling pathway	2	28	1,55E-04	2,00
hsa04612	Antigen processing and presentation	5	20	3,33E-04	2,07
hsa04621	NOD-like receptor signaling pathway	1	21	8,03E-04	2,08
hsa04610	Complement and coagulation cascades	7	16	1,04E-03	2,04
hsa04640	Hematopoietic cell lineage	3	22	2,20E-03	1,91
hsa04110	Cell cycle	30	3	4,19E-03	1,62
hsa04623	Cytosolic DNA-sensing pathway	0	16	7,86E-03	2,01
hsa03030	DNA replication	13	0	1,17E-02	2,12
hsa04062	Chemokine signaling pathway	7	34	1,39E-02	1,43
hsa04622	RIG-I-like receptor signaling pathway	1	16	1,84E-02	1,80
hsa04650	Natural killer cell mediated cytotoxicity	2	26	3,22E-02	1,47
hsa05322	Systemic lupus erythematosus	26	9	4,77E-02	1,50

2583 genes with DAVID IDs were found to be regulated.
Count down/up – number of down- and upregulated genes in the respective pathway.

5 Discussion

ABCA3 mutations may induce respiratory distress syndrome in newborns or interstitial lung disease in children or older patients. Mutations in the *ABCA3* gene may impair the protein's transport function. Since ABCA3 is involved in the transport of surfactant lipids and the biogenesis of lamellar bodies, a nonfunctional protein may interfere with alveolar type II cell homeostasis. However, the exact mechanisms by which ABCA3 mutations cause RDS or ILD remain to be investigated.

In the present study, a cell culture model for alveolar type II cells was used to analyze the impact of ABCA3 mutations on lung epithelial cells. A549 cells are human lung epithelial adenocarcinoma cells and they are a well described and widely used model system for ATII [133-138].

5.1 Cellular characteristics of cells harboring ABCA3-WT and mutations

5.1.1 ABCA3 processing

Studies on ABCA3 expression in native lung tissue reported different findings on ABCA3 molecular weights. Yamano et al. found that a 150 kDa protein is predominat in the native lung. However, transient transfection also induces expression of a higher molecular weight form (190 kDa) [71]. Brasch et al. reported strong ABCA3 expression with molecular sizes of 150 and 190 kDa in lung tissue from a healthy control [78]. Solely a 180 kDa or 190 kDa ABCA3 form was found in studies conducted on rat or mouse lungs, respectively [68, 72]. The 150 kDa form was reported to be the cleavage product of the 190 kDa form [139]. Proteolytic cleavage of the N-terminus takes place inside multivesicular bodies / LBs and is likely mediated by cysteine proteases [139].

Stable transfection of A549 cells with the modified pUB6 vector coding for HA-tagged ABCA3-WT as well as the ABCA3 mutations p.Q215K and p.E292V lead to stable overexpression of ABCA3 mRNA. In concordance with the literature, ABCA3-WT and p.E292V proteins were found in two different forms, 150 and 190 kDa [140]. p.Q215K was only present in the higher molecular weight (190 kDa) protein form. This is in agreement with its localization to the ER, since proteolytic processing does not take place before the lamellar body / lysosomal compartment along the secretory pathway [139]. Both, transient or stable transfection of HA-tagged ABCA3-WT and p.E292V into A549

cells induced expression of both molecular weight forms. Compared to transient transfection, stable transfection of A549 cells lead to increased expression of the 150 kDa form, indicating that the strong overexpression during transient transfection leads to an overload of the cellular processing and trafficking apparatus. It remains to be investigated which of the forms represents the active transporter.

5.1.2 Cellular growth

Metabolically active cells convert 3-(4,5-dimethylthiazol-2-yl)-2,5-diphenyl tetrazolium-bromide (MTT) to the purple product 1-(4,5-dimethylthiazol-2-yl)-3,5-diphenyl formazan which can be photometrically detected [141]. The extent of MTT reduction through intracellular NEM-sensitive flavin oxidases and subsequent formazan accumulation therefore is a measure for cell viability and proliferation [142]. Cellular proliferation might be impaired by several factors, including accumulation of toxic metabolic products, cellular stress or treatment with medication or other substances. In the present study, the MTT proliferation assay was performed to exclude that aberrant cellular growth rates were responsible for observed diffenrences in experiments. For normal experiments, stably transfected cells were grown for 48 h. During this period of time, similar growth curves with no significant differences were obtained for all investigated cell lines. Therefore, stable transfection of A549 cells does not impair proliferation of the single cell clones.

5.1.3 Cellular secretory capacity

Sorting of proteins for different cellular organelles, the plasmamembrane or the extracellular space begins as early as the protein reaches the ER during translation. The proteins' posttranslational processing, incorporation into cellular membranes, sorting and trafficking to their final destinations are all part of the secretory pathway. Determination of the cellular secretory capacity using secretion of luciferases also gives insight into the cellular stress level [143]. Compared to non-transfected A549 cells, secretion of luciferase was impaired in all stably transfected cells, implying that stable transfection may increase intracellular stress. Overexpression of ABCA3-WT or mutations seems to interfere with the secretory pathway of stably transfected cells, possibly through increased translation, protein folding, trafficking and degradation. Within the group of ABCA3 transfected cells, ABCA3-WT cells had the strongest secretory capacity, followed by p.Q215K cells. The lowest secretory capacity was observed for p.E292V cells, indicating that trafficking of mutant ABCA3 to the MVBs / LBs, while it lacks full functionality, poses a strong insult on intracellular processes.

5.1.4 ABCA3 localization

Functional ABCA3 protein localizes to the outer membrane of lamellar bodies, lysosome derived organelles [71]. In cell culture model systems, colocalization with LAMP3 is a criterion for correct cellular ABCA3 trafficking to lysosomal / LB-associated compartments [73, 83, 116, 139]. In this study, ABCA3-WT protein properly colocalized with the lysosomal / lamellar body marker LAMP3 (CD63), as did ABCA3-p.E292V. For p.E292V, it has already been reported that its lipid transport function is moderately impaired and its catalytic ATP hydrolysis cycle is aberrant compared to the ABCA3-WT protein [140]. The p.Q215K mutant does not localize to LAMP3-positive intracellular vesicles but instead colocalizes with the ER marker calnexin, suggesting ER-retention due to a misfolding or trafficking defect. Since the p.Q215K protein is not trafficked to the lysosome-associated organelles and is retained in the ER, it most likely lacks a functional ATP hydrolysis cycle. The ABCA3 mutations analyzed in this thesis therefore represent both, a type I trafficking defect possibly leading to fatal surfactant deficiency, as well as a type II functional defect accompanied by impaired ATP hydrolysis, which may cause ILD in children or adults. No increased colocalization of ABCA3-WT or mutations with the early-endosomal marker EEA1 or ubiquitin was observed. Also, the cellular distribution and abundance of these markers was similar in all cell lines, suggesting that ABCA3-WT or mutants are not recruited to the early endosomal compartment or are aberrantly marked for degradation by ubiquitin.

5.1.5 Expression of ER chaperones calnexin and BiP

Expression of mutant proteins can elevate the cellular stress response, which can be detected by increased amounts of ER chaperones such as calnexin or BiP [116, 144]. However, in contrast to transiently transfected cells, cells stably expressing mutated proteins other than ABCA3 can adapt to chronic ER stress imposed by misfolded or mislocalized protein and therefore no elevation of ER chaperones can be detected [145]. In accordance with this, calnexin and BiP protein were not elevated in ABCA3-mutant cells in the present study. However, elevated levels of BiP were found in ABCA3-WT compared to all other cells. These results are in concordance with proteomic analyses of rat lung lamellar bodies [146, 147]. ER chaperones may not only be ER-resident but can be found in other cellular compartments. Ridsdale et al. reported that proteins normally located in the ER are enriched in lamellar bodies from the rat lung and that BiP was actually found in the limiting membrane of lamellar bodies [146]. Possibly, BiP (among

other ER proteins) is involved in the biogenesis of LBs or LB-associated organelles and therefore is increased in cells with ABCA3-WT protein which was shown to induce lamellar body biogenesis [148, 149]. BiP localization in the outer membrane of lamellar bodies is also in agreement with the observed partly colocalization of BiP with ABCA3-WT and p.E292V, which localize to LAMP3-positive vesicles in a ring-like fashion.

5.1.6 Ultrastructural analysis

A549 cells grown to confluent monolayers are supposed to have abundant amounts of intracellular lamellar bodies or, if not present, transfection of A549 cells with ABCA3 can induce formation of LB-like structures [73, 137, 150]. Also, transgenic expression of ABCA3 in HEK293 cells, which are of non-lung origin, induced formation of lamellar-body like structures [148, 151]. Electron microscopic analysis of stably transfected and non-transfected A549 cells in this study revealed that the ER lumen was enlarged in cells expressing ABCA3 mutations p.Q215K and p.E292V, thus indicating increased intracellular activity, possibly in connection with misfolding and mislocalization. Since ABCA3 protein is involved in LB biogenesis, increased amounts of LBs were expected in cells stably transfected with ABCA3-WT. However, only very few LBs were found in non-transfected A549 cells and overexpression of ABCA3-WT protein did not induce additional formation of LBs. As expected, also expression of mutant ABCA3 protein did not induce LB biogenesis.

5.2 Characterization of epithelial and mesenchymal markers

5.2.1 Loss of epithelial markers in cells harboring ABCA3 mutations

SP-C is a surfactant specific protein, produced exclusively by differentiated alveolar epithelial type II cells [152]. Diminished expression of SP-C, as observed in cells harboring ABCA3 mutations, is in line with functional impairment and loss of differentiated epithelial cell characteristics. This loss of epithelial characteristics includes the loss / derangement of the epithelial adhesion protein E-cadherin which is the main structural component of adherens junctions and critical for cell-cell contacts [153]. E-cadherin downregulation, as well as the observed reduction of ZO-1, result in reduced cell-cell adhesion and a subsequent destabilization of the epithelial architecture.

Additionally, decreased levels of mature SP-C protein in immunohistochemistry staining of lung tissue [78] and in lavage samples from patients (compound) heterozygote for the ABCA3 mutations p.Q215K and p.E292V were found (data not shown). This supports the

in vitro findings of this study that *ABCA3* mutations induce loss of epithelial cell differentiation, thereby functionally impairing the alveolar type II cells [154].

5.2.2 Gain of mesenchymal markers in cells harboring ABCA3 mutations

A central role in the regulation of E-cadherin expression has been attributed to the transcription factors SNAI1 and SNAI2 that operate as repressors of the E-cadherin gene as well as other genes involved in cellular adhesion [128, 155]. SNAI1 may also induce the expression of different mesenchymal genes [128]. In concordance with the observed loss of E-cadherin, SNAI1 protein amount was elevated in nuclear extracts from cells with ABCA3 mutations [154].

Endothelin-1 (ET-1) is a 21 amino-acid peptide hormone with roles in fibrosis, cell proliferation and vasoconstriction [156]. In the lung, ET-1 can be secreted by epithelial, endothelial and mesenchymal cells [156]. Elevated amounts of ET-1 have been found in tissues and BALF from patients with fibrosing lung diseases [157-159]. In addition to upregulation of the mesenchymally expressed SNAI1, ET-1 mRNA expression and protein secretion were increased in cells harboring ABCA3 mutations [154].

MMPs degrade components of the extracellular matrix (ECM) and have been observed to be increased in samples from patients with fibrosing lung diseases [160, 161]. The gelatinase MMP-2 is constitutively expressed in fibroblasts and endothelial cells, and the basement membrane constituents type IV collagen and laminin belong to its substrates [162, 163]. MMP-2 frequently localizes to collagen type IV and disrupted basement membranes in lungs of patients with idiopathic pulmonary fibrosis [163]. Degradation of the basement membrane may cause the adherent epithelia to lose integrity. MMPs also cleave the extracellular domain of E-cadherin, leading to a loss of cell-cell adhesion [164]. Moreover, by degrading ECM, MMP activity may result in the release of growth factors like TGF-β1 and PDGF sequestered in the ECM [165]. In cells with *ABCA3* mutations, especially those with p.Q215K, MMP-2 mRNA and protein secretion were strongly elevated [154].

5.2.3 Upregulation of TGF-β secretion and Src phosphorylation in cells harboring ABCA3 mutations

TGF-β1 is a pluripotent molecule important for processes such as cell proliferation, differentiation, and tissue regeneration. It is secreted by different cell types in response to a

variety of stimuli [96, 166]. TGF-β1 is synthesized as an inactive precursor. Activation of the biologically inactive form can be achieved by a number of different pathways, including pH changes, proteases, or integrins [167, 168]. For MMP-2 it was shown that it can proteolytically activate the TGF-β1 precursor [169]. TGF-β1 can promote loss of epithelial features by activating, amongst others, the SNAI1 transcriptional repressor, thereby inhibiting E-cadherin synthesis [170]. Treatment of A549 cells with TGF-β can increase MMP-2 mRNA and its activation [171]. Both TGF-β1 production and secretion were increased in cells expressing the ABCA3 p.Q215K mutation [154].

Src is a non-receptor membrane-associated tyrosine kinase and its signaling function is required for rearrangement of the cytoskeleton, cell differentiation, cellular adhesion, motility, and migration [130, 172]. Signal transduction via Src can be initiated by its interaction with receptor tyrosine kinases or adhesion molecules [173]. Activated Src kinase induces signaling pathways that eventually lead to destabilization of the epithelial adhesion molecule E-cadherin and is therefore linked to loss of epithelial architecture [174]. In cells with the p.Q215K mutation, increased phosphorylation of Src was found [154].

Taken together, these results show that mutations in ABCA3 activate mechanisms leading to loss of epithelial differentiation which is associated with an impairment of the epithelial cell function.

5.3 ABCA1 expression, cholesterol content and lipid profile

5.3.1 ABCA1 expression

As ABCA3, ABCA1 also belongs to the class A family of ABC transporters and is described to have important functions in phospholipid and cholesterol efflux [64]. Intracellularly, ABCA1 was shown to be localized both in the plasma membrane as well as inside endosomal / lysosomal vesicles [175]. Though ABCA1 was found to localize to the plasma membrane in this study, it was localized predominantly to intracellular vesicles in all stably transfected cells (and non-transfected A549 cells). For ABCA3-WT and p.E292V, partly colocalization with ABCA1 was observed. ABCA1 expression is regulated on different levels: through small molecules like the second messenger cyclic AMP (cAMP), through nuclear receptors, including liver-X receptors (LXRs), retinoic-X receptor (RXR) and peroxisome proliferator-activated receptors (PPARs), and through posttranscriptional modulation of ABCA1 activity [176]. Among the LXR mediated

regulation, crosstalk with immune regulatory pathways is possible [177]. Pro-inflammatory cytokines were shown to reduce ABCA1 expression whereas the anti-inflammatory TGF-β1 positively affected ABCA1 translation and transcription [178-180]. ABCA1 mRNA and protein were increased in cells harboring ABCA3 mutations compared to ABCA3-WT cells. ABCA1 might be upregulated in cells with ABCA3 mutations to compensate for non-functional ABCA3 induced intracellular lipid or cholesterol accumulation.

5.3.2 Cellular cholesterol content

Intracellularly, cholesterol is found in free (FC) or esterified (CE) form. Cholesterol esters serve as storage form for excess cholesterol and can also be easily transported by lipoproteins. As too much free cholesterol is toxic for the cell, it is converted to cholesterol ester by the acyl-CoA cholesterol acyl transferase (ACAT) in the ER [181, 182] or it may be effluxed to apoA1 by ABCA1 [64]. Free cholesterol is found in cellular membranes and modifies the fluidity of the lipid bilayer. High amounts of free cholesterol are located to lipid rafts, specialized areas of the plasma membrane where receptors are predominantly localized and accumulated for efficient signal transduction into the cell's cytoplasm. ABCA3 knockout mice ($ABCA3^{-/-}$) did not affect cholesterol levels in the lung compared to their healthy littermates [183]. Also, stable transfection of HEK cells with vectors coding for ABCA3-WT or p.N568D did not induce changes in the amounts of total cholesterol [73]. In the present study, the total cholesterol was increased 1.3 and 1.2-fold in cells harboring ABCA3-p.Q215K and p.E292V compared to ABCA3-WT cells, respectively. Similarly, significantly more free and esterified cholesterol were found in p.Q215K cells compared to ABCA3-WT cells. The increased amounts of FC or CE in cells harboring ABCA3 mutations might result from the impaired ABCA3 transporter function. It can be speculated that increased FC may lead to accumulation of oxidation products. These may in turn activate the LXR receptor which might be responsible for increased ABCA1 expression and also reduced expression of cytokines (compare section 5.4).

5.3.3 Formation of lipid droplets

Neutral lipids (i.e. triacylglycerides and cholesterol) are stored intracellularly in lipid droplets [184]. Neutral triacylglycerides are the source for phosphatidylcholine (PC) synthesis by ATII. One of the mechanisms for PC synthesis involves hydrolysis of neutral lipid in lipid droplets by the lysophosphatitylcholine acyltransferase (LPCAT1) [185]. Also, next to phosphatidylcholine and phosphatidylglycerol, neutral lipids (especially cholesterol) are a minor component of lung surfactant. Mutated ABCA3 might interfere

with the lipid metabolism of epithelial cells and might cause accumulation of neutral lipids; therefore intracellular lipid storage vesicles were visualized and quantitated using Oil-Red-O, which only binds to neutral lipids. Compared to non-transfected A549 cells, stable transfection lead to reduced amounts of Oil-Red-O positive lipid droplets in all cells. Reduction of the absolute amount of cellular neutral lipid deposits can be either achieved by the lipid transport capacity of ABCA3 itself or by compensatory upregulation of other lipid transporter in ABCA3-mutant cells. Lipid droplet sizes were significantly smaller in ABCA3-WT cells compared to all other cells. Functional ABCA3 protein therefore seems to induce the strongest clearance of neutral lipids in lung epithelial cells. These results are in concordance with the elevated amounts of esterified cholesterol in cells harboring ABCA3 mutations, as esterified cholesterol is intracellularly stored in lipid droplets and might therefore account for the increased lipid droplet size in these cells.

5.3.4 Cellular lipid composition

In a study by Matsumura et al. it was shown that HEK293 cells expressing ABCA3-WT had the highest phosphocholine lipid content compared to cells harboring different ABCA3 mutants; however, cellular cholesterol was not changed [140]. In this thesis, the total lipid content, as determined by mass spectrometry, was elevated in p.Q215K cells. Therefore, most lipidspecies were elevated as well. Total lipids were normalized to the total protein of the respective cell lysate. The cellular lipid content should be proportional to the total cellular protein, since the total protein content is a measure for the cell number. Differences in protein concentrations however, for example reduced protein in p.Q215K cells, induced higher normalized lipid concentrations, possibly due to high background signals. Therefore, relative fractions of the total lipid amount were calculated for each lipid species to compare if stable transfection induces changes in lipid distribution among all species. For the phospholipids PC, PI, and PS, no differences were observed in the relative lipid amounts. Relative lipid amounts in p.Q215K cells were elevated for dihydro-SPM, PG and GluCer. ABCA3-WT cells had elevated relative amounts of PE. However, the changes in relative lipid composition were only very small. Since cellular fractionation was not established in the laboratory, the lipid analysis could only be performed on whole cell lysates. However, the lipid composition of the whole cell and of the lamellar body differ from each other [137]. Supernatants with secreted lipids were not analyzed as the addition of fetal bovine serum, which contains large amounts of lipids, to the growth medium interfered with the mass spectrometric detection and the cells did not grow without serum. Moreover, serum deprivation might also change the normal cellular lipid metabolism as the

serum supplements for nutrients. For investigation of the cell culture supernatants, preparation of a complete growth medium with labeled lipids would have been necessary. Also, as electron microscopic analysis revealed, the A549 cells used for this study did not have lamellar bodies or even LB-like structures. Therefore, the effect of non-functional or functional ABCA3 on the lipid composition of A549 cells is not clear.

In concordance with the literature, the most abundant phospholipid in A549 cells was PC [137]. However, it was reported already in 1980, that the PL composition of A549 cells and primary rat alveolar type II cells differ strongly from each other [135]. Of the PC subspecies in non-transfected and transfected A549 cells, the most abundant was PC 34:1, followed by PC 32:1. The most abundant phospholipid of surfactant usually is DPPC (PC 32:0) [186], which was only present in minor PC concentrations (< 5 %) in the total cell lysates of non-transfected and transfected A549 cells. However, the total cellular lipid content, as measured in total cell lysates, does not resemble that of secreted surfactant, therefore it is hard to make a comparison between these two. Lyso-PC was slightly, but not significantly upregulated in A549 cells harboring ABCA3 mutations. Lyso-PC can induce upregulation of LXR-α and ABCA1 [187]. Relative to the total lipids, ceramides were slightly and glucosyl-ceramides significantly elevated in p.Q215K cells when compared with ABCA3-WT cells. Ceramides are bioactive sphingolipids involved in regulation of cellular processes such as cell growth, differentiation, stress response and cell viability [188]. Ceramides can be synthesized via several pathways including from sphingomyelins (SPMs) using sphingomyelinase or *de novo* [188]. Several sphingomyelin subspecies were elevated in cells harboring ABCA3 mutations when compared with ABCA3-WT cells. Similar to ceramides, SPMs function in cellular processes including cell cycle and cellular stress [189]. Moreover, it is an important component of lipid raft microdomains in cellular membranes [189].

5.4 Cytokine and toll-like receptor expression

Besides being responsible for gas exchange, synthesis of pulmonary surfactant and maintaining a regenerative capacity, alveolar epithelial cells are under constant exposure to viral and bacterial pathogens and therefore have important functions in immune defense [190, 191]. Even though the pathogen load is high in the lungs, lung epithelial cells do not have a constitutively increased inflammatory response. Alveolar epithelial cells express several pathogen recognition receptors (PRRs, i.e. toll like receptors TLR-2 and TLR-4) on their cell surface [192, 193] and intracellularly (TLR-3) [194]. TLR-4 recognizes gram-

negative bacterial LPS, TLR-2 reacts to binding of ligands from gram-positive bacteria, viruses or fungi and TLR-3 recognizes viral double-stranded (ds) RNA. Upon bacterial or viral infection, cytokines such as IL-6, IL-8, GM-CSF or RANTES (CCL5) are secreted into the extracellular space to attract macrophages or leukocytes and to initiate the clearing of pathogens [33]. Biopsies from CF-patients or cell-lines harboring CFTR mutation ΔF508 were shown to express decreased amounts of plasma membrane TLR-4 [195-197] and to secrete less IL-6 and IL-8 compared to corresponding cells in which the CFTR defect was corrected [195]. Also, LPS responsiveness was decreased in cells with CFTR defect [195]. The underlying mechanisms have yet to be determined. It was also shown that TLR4 receptor deficiency causes pulmonary emphysema [198]. In the present study, basal TLR-3 and TLR-4 mRNA expression were strongly impaired in cells harboring the ABCA3 mutations p.Q215K and p.E292V. Concordantly, NF-κB activation as well as cytokine secretion was decreased in p.Q215K and p.E292V cells compared to cells expressing ABCA3-WT protein. Contrary, TLR-6 mRNA was elevated in p.Q215K cells according to microarray results. TLR6 has an expression pattern similar to TLR1 and is mostly localized in the plasma membrane of monocytes, where it colocalizes with TLR-2 [199].

One possible connection between mutations in ABCA3 and the aberrant immunological profile they induce might be provided by the compensatory upregulation of ABCA1 in cells with ABCA3 defect. ABCA1 was shown to have immunomodulatory functions in macrophages by selectively removing free cholesterol from lipid rafts, thereby reducing TLR trafficking to lipid rafts [200]. Also, plasma levels of chemokines and cytokines were increased in ABCA1 deficient mice injected with LPS, suggesting an attenuation of immune responses mediated by functional ABCA1 [201]. Moreover, ABCA1 knockout mice exhibit increased infiltration of inflammatory cells in a variety of tissues [202]. Therefore, the immunomodulatory capacity of ABCA1 reduces the inflammatory response of immune cells and possibly other cells with ABCA1 expression.

Another possibility how mutations in ABCA3 might cause a reduction of TLR expression and cytokine secretion in lung epithelial cells is by excess cholesterol accumulation. Cholesterol accumulation leads to formation of oxysterols which were shown to induce LXR activation [203-205]. LXR activation reduces NF-κB activity [206]. Less NF-κB activity might impair cytokine secretion and therefore lead to a decreased inflammatory response in the affected cells or tissues.

5.5 RSV infection

Acute infections with respiratory viruses have been implicated in exacerbations of interstitial lung diseases [207]. RSV is a common pathogen in infants, children and adults and possibly capable of deteriorating the pulmonary condition of patients harboring *ABCA3* mutations. Mice deficient for SP-C were shown to be more susceptible to RSV [208]. To address this issue, the effect of RSV on cells expressing ABCA3 mutations was investigated.

5.5.1 Effect of RSV infection on expression of epithelial and mesenchymal markers

RSV infection induced a marked loss of epithelial cell adhesion proteins E-Cadherin, ZO-1 and SP-C and lead to profound morphological changes as well as to increased expression of the mesenchyme-asscociated molecules collagen type I, SNAI1, SNAI2, MMP-2 and TGF-β1 in p.Q215K; nonetheless, a substantial gain of the mesenchymal markers α-SMA and vimentin was not detected in these cells. However, it is not surprising that α-SMA is not present in A549 cells, since even in fibroblasts, only a subset of cells, the myofibroblasts, express this protein [88]. Similarly, vimentin may not be suitable as a marker for EMT, as it is expressed in various cell types and not specific for fibroblastoid cells. Moreover, its expression is subject to a variety of insults [87, 88]. Interestingly, Morbini et al. observed only expression of some, but not all, of the markers classically associated with EMT in samples from patients with UIP, supporting the results of the present study that not all of the investigated markers were upregulated in cells with ABCA3 mutations [209]. In addition, different subsets of markers can be expected to be regulated in different cell types. The results also seem to be in concordance with a study that described that TGF-β1 driven EMT is dependent on ECM components, since cellular growth on fibronectin was sufficient to induce EMT via integrin-mediated pathways [115]. In the *in vitro* cell culture system used for this study, cells did only grow in cell culture treated plastic dishes in the absence of ECM proteins.

5.5.2 ABCA3 mutations and RSV infection induce EMT

The alterations in cell morphology, the loss of epithelial cell properties and function, and the gain of some mesenchymal characteristics that were observed suggest that RSV infection induces a process resembling epithelial-mesenchymal transition (EMT) in cells harboring ABCA3 mutations (Figure 5.1) [154]. Since its characteristics were dependent

on the expression of ABCA3 mutations, it is termed “ABCA3-associated EMT”. Several other viruses, especially gamma herpes viruses like Epstein-Barr Virus (EBV) or Herpesvirus-8, have been implicated in exacerbation of ILD and have been shown to induce EMT via diverse signaling pathways [25, 207, 210, 211]. Epstein-Barr virus is more often found in the lungs of patients with idiopathic pulmonary fibrosis compared to healthy controls and EBV latent membrane protein 1 can induce EMT, employing a variety of signaling pathways, including Twist, extracellular signal-regulated kinase (ERK), NF-κB or SNAI1 [210, 212-214]. Moreover, EBV infection of alveolar epithelial cells increases TGF-β1 expression [215]. A γ-herpes virus was shown to lead to progressive interstitial fibrosis in interferon-γ-receptor knockout mice and also to induce EMT via Twist signaling [211, 216]. TGF-β1 was activated by means of MMP-2 induction after EMT in cytomegalovirus (CMV) infected renal epithelial cells [217] and the hepatitis C virus core protein can induce EMT in cholangiocarcinoma cells [218]. However, RSV infection has not yet been implicated to be involved in EMT processes and in the development of fibrosing lung diseases. Therefore, it is suggested that genetic predisposition of epithelial cells due to ABCA3 mutations creates a permissive environment for the development of EMT, a process further promoted and potentiated by RSV infection. During EMT, alveolar epithelial cells lose their polarity and proteins important for maintaining cellular adhesions to the basement membrane and other cells, and gain mesenchymal as well as migratory properties [103]. Most importantly, EMT affects the functionality of alveolar epithelial cells, impairing their ability to produce and secrete surfactant.

Loss of epithelial cell differentiation may therefore be the molecular basis for the association of ABCA3 with ILD, which is characterized by varying degrees of inflammation and fibrotic changes of the lung parenchyma [219]. In some cases, ABCA3 defects may also lead to premature development of pulmonary fibrosis as suggested by a report from Young et al. who found the UIP pattern of pulmonary fibrosis in a 15-year-old boy who had mutations in ABCA3 [80].

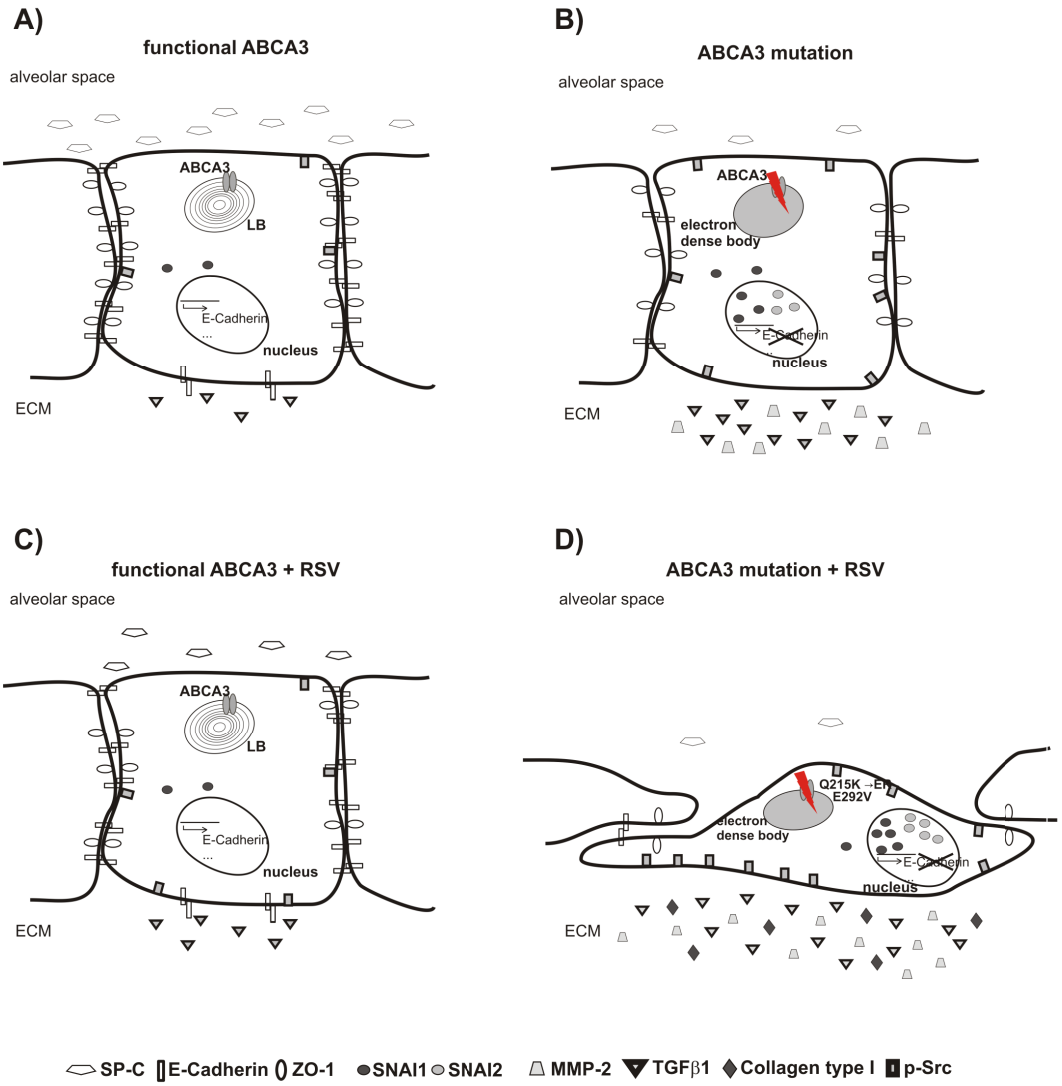

Figure 5.1: Overview of RSV-induced epithelial and mesenchymal changes in cells harboring ABCA3 mutations.
A) Functional ABCA3, B) ABCA3 mutation, C) functional ABCA3 in the presence of RSV, and D) ABCA3 mutation in the presence of RSV. RSV infection of cells harboring ABCA3 mutations induces a process that resembles EMT.

5.5.3 Effects of ABCA3 mutations and RSV infection on ER-stress and UPR markers

Elevated ER-stress, whether induced by the ER stressors tunicamycin and thapsigargin or the expression of mutant SP-C, was sufficient to induce EMT in lung epithelial cells [109, 110]. However, from the data derived in this study, it can be concluded that the observed processes did not depend upon increased ER-stress since no elevated expression of the ER chaperone BiP and the UPR-markers IRE1α, PERK and ATF-6 was found in cells harboring ABCA3 mutations when compared with ABCA3-WT cells. Quite the contrary, the ER stress and UPR marker proteins were less abundantly expressed in A549 cells

stably transfected with *ABCA3* mutations compared to non-transfected A549 or ABCA3-WT transfected cells. RSV infection elevated ER stress as indicated by the presence of the cleaved UPR protein ATF-6. However, this effect was independent of the presence or absence of mutant ABCA3. Thus, ABCA3 mutations do not lead to increased ER stress when stably expressed in A549 cells and ER-stress can therefore not account for the loss of epithelial characteristics and morphological changes as well as acquisition of mesenchymal markers [154].

5.5.4 ABCA3- and RSV-induced signaling pathways

EMT processes in many *in vitro* cell lines and animal models are often mediated by TGF-β and subsequent activation of downstream intracellular signaling, including the canonical Smad pathways [96, 115, 131]. In this study, elevated secretion of TGF-β1 was found in p.Q215K cells, both in the absence and presence of RSV. However, the amounts of phosphorylated Smad as well as the total Smad proteins decreased after RSV infection in cells harboring ABCA3 mutations. Activation of Smad-signaling therefore does not account for the processes that were observed in this study. Other (TGF-β-mediated) cellular signaling mechanisms might involve MAP kinase pathways. Recently it was reported that activation of MAPK by TGF-β receptors in lipid rafts is required for epithelial cell plasticity [220]. Moreover, TGF-β stimulation can induce activation of the MAP kinase ERK which might lead to disintegration of cell-matrix adhesions and disassembly of adherens junctions [221, 222]. It was also reported that ERK and JNK are able to mediate EMT in epithelial cells [223, 224]. Additionally, TGF-β1 might induce downregulation of E-cadherin by activation of SNAI1 transcription [225], which might also affect expression of other epithelial and mesenchymal proteins. Other possible cellular signaling molecules for EMT mediation include the tyrosine kinase Src. Phosphorylation of Src kinases is required for activation of signaling pathways that then transmit signals to cellular components such as the nucleus or the cytoskeleton. Src kinase activity is crucial for the regulation of the turnover of cellular adhesions and for cellular motility since cells deficient for Src show a strong adhesion to the ECM, an impaired migrating ability and a decreased turnover of cellular adhesions [226]. The Src-kinase family member Fyn was strongly upregulated ($\log_2 FC = 4.4$) in cells harboring the ABCA3 mutation p.Q215K according to the microarray analysis. Fyn tyrosine kinase was shown to mediate E-cadherin downregulation induced by TGF-β [227]. In SP-C-mediated EMT, phosphorylation of Src kinase, as well as MAP kinases ERK and JNK, was elevated [109,

110]. Taken together, these data support a role for TGF-β, MAPK and Src signaling in ABCA3-associated EMT [154].

5.5.5 Effect of RSV infection on ABCA1 protein

In macrophages, stimulation with viral (influenza A) or bacterial pathogens (*E. coli*) can reduce ABCA1 expression via crosstalk between LXR and TLR signaling [228]. Upregulation of TLR-3/4 leads to an IRF3-mediated decrease in LXRα expression which in turn suppresses induction of the target gene ABCA1 [228]. Infection of macrophages with the human cytomegalovirus (hCMV) or HIV also reduced ABCA1 expression through different mechanisms [229, 230]. In this study, infection of A549 cells with RSV increased ABCA1 protein. However, RSV infection of cells harboring mutant ABCA3 had the opposite effect and decreased ABCA1 protein, thereby compensating for the former ABCA1 overexpression in these cells.

5.5.6 Effect of RSV infection on cytokine secretion and TLR expression

RSV infection of A549 cells leads to secretion of pro-inflammtory cytokines [231]. In accordance with the literature, increased secretion of IL-6, IL-8, RANTES and GM-CSF was observed after viral infection in this study. Additionally, TLR-3 and TLR-4 expression was upregulated to the same extent in all investigated cells; however, TLR-3 and TLR-4 mRNA levels in cells harboring ABCA3 mutations were still below mRNA levels of ABCA3-WT cells. Similar was observed for IL-6 and IL-8 secretion, as the basal concentration in cells with ABCA3 mutations were barely detectable and therefore RSV infection induced a stronger response; however, concentrations of secreted IL-6 and IL-8 were still below ABCA3-WT cells and non-transfected A549 cells. Decreased interleukin and TLR expression both in the absence and presence of virus might render the cells harboring ABCA3 mutations more susceptible to (further) respiratory infections. TLRs recognize invading pathogens and induce an immune response which in turn leads to secretion of interleukins and activation of immune cells. If the immune response is impaired, stronger or more frequent infections are possible. No significant differences were observed for GM-CSF or RANTES secretion when cells harboring ABCA3 mutations were compared with non-transfected A549 and ABCA3-WT cells. RSV infection also increased TGF-β1 secretion as already mentioned above, which was shown to arrest the cell cycle and therefore enhances replication of the virus in lung epithelial cells [232]. Virus counts of infected cells were similar, even though an upward trend was observed for p.Q215K cells.

5.5.7 UV-inactivation of RSV

For control purposes, cells were stimulated with UV-inactivated RSV. UV-inactivation is supposed to interfere with the virus' replication capabilities [233]. Compared to non-inactivated RSV, UV-inactivated virus led to decreased secretion of IL-6 and IL-8 in non-transfected A549 cells as well as in ABCA3-WT cells. However, the expression was not diminished and way above levels of non-infected cells. One possible explanation could be that the viral coat proteins can still be recognized by the host cell and the virus can even enter the host cell without being able to replicate, thereby initiating a (weaker) immune response. Another possibility arises from the method of virus production. RSV was propagated in Vero cells and after freezing of the Vero cells, all viruses were released into the supernatant presenting the new inoculum. During viral propagation, Vero cells themselves produce and secrete cytokines and other virus-related molecules into the cell culture supernatant. These molecules are still present in the virus inoculum used to infect A549 cells and might possibly initiate an immune response in these cells even though the RSV was UV-inactivated. For IL-8 secretion from neutrophils it has already been shown that secretion at high MOIs is induced independently of viral replication [234].

5.6 LPS stimulation

According to the literature, A549 cells were shown to be not responsive to bacterial LPS due to intracellular localization of TLR-4 [235]. RSV infection stimulates TLR-4 plasma membrane expression and sensitizes A549 cells to LPS exposure [41]. In the present study, A549 cells were responsive to stimulation with *P. aeruginosa* LPS. Concordant with earlier findings, the immunological response as measured by secretion of inflammatory cytokines IL-6 and IL-8 is weaker in response to LPS stimulation compared to RSV infection [41, 236]. Interestingly, stably transfected cells harboring ABCA3 mutations were less sensitive to LPS stimulation compared to ABCA3-WT transfected cells. Similar, cells harbouring CFTR mutations were shown to be less responsive to LPS [195]. TLR-3 and TLR-4 expressions were found not to be responsive to the *P. aeruginosa* LPS concentrations used in this study.

5.7 Microarray analysis

Microarray analysis can be used to identify genes or pathways that are regulated between different sets of samples, even though the mass of obtained data can be difficult to comprehend and integrate. There are several freely and commercially available softwares,

each processing through the data according to specific algorithms [126, 237]. In this study, pathway analysis was conducted with the DAVID bioinformatics tool, a freely available web-based software. As many genes were regulated in the different comparisons of gene sets, cut-offs for fold changes were arbitrarily set to FC > 2 (in both directions) and for adjusted P values below 0.05 to narrow down the regulated gene sets and to obtain more precise results in pathway analysis.

Several of the same genes were strongly regulated in both comparisons, p.Q215K vs. WT and p.E292V vs. WT. Of these, there are some of which the function of the gene product is not known so far or the gene products are usually found in other tissues than the lung (i.e. liver or kidney). Therefore, these proteins are less likely to be responsible for lung specific effects. Examples of these genes are HYI, a putative hydoxypyruvate isomerase, SDR42E1, RAB42 or HNF1A (hepatocyte nuclear factor 1) in the liver [238, 239]. The carboxylesterase 1 (CES1), a lypolytic enzyme involved in the hydrolysis of ester bonds usually expressed in the liver, was strongly upregulated in both comparisons ($log_2FC \geq 8.75$). CES1 was shown to increase size and density of intracellular lipid droplets, which is in agreement with the results of this study [240]. CES1 was still upregulated in both mutations when compared with WT after RSV infection ($log_2FC \geq 7.15$). The chemokine receptor CXCR4 was also among the strongly upregulated genes ($log_2FC \geq 3.78$). CXCR4 is implicated in migration of ATII, accompanied by upregulation of MMP-2 [241].

Pathways regulated in the comparisons p.Q215K/p.E292V vs. WT in the absence or presence of RSV include (besides others) cytokine-cytokine receptor interactions and the complement and coagulations cascades. Many of the genes of these pathways are downregulated, but there are also several upregulated genes that in a pathway would interfere with the downregulated genes. Therefore, the pathway regulation analysis is inconclusive.

It has already been reported that RSV infection has several effects on the host cell, including activation of innate immunity through TLR signalling [40, 41], activation of the NF-κB pathway [242], changes of the membrane lipid raft composition [243] and TGF-β1 mediated cell cycle arrest [232]. The effect of RSV on A549 cells as model for lung epithelial cells has already been extensively studied [231, 244, 245]. In concordance with the literature about viral infections, pathways involving recognition of viral pathogens (i.e. the TLR signalling pathway and the antigen processing and presentation pathway) or cytokine secretion and interaction (i.e. the cytokine-cytokine receptor interaction pathway)

were regulated and contained mostly upregulated genes. On the other hand, pathways involved in the cell cycle or DNA replication were also regulated but contained mostly downregulated genes, which is in agreement with previous reports that the cell cycle is arrested during RSV infection [232, 246].

5.8 Limitations of the system

A549 cells are often used as model system for alveolar type II cells. However, their suitability has long been under debate [137, 247, 248]. A549 cells are a tumor cell line derived from cancerous lung tissue in 1972 [249]. As epithelial tumor cells they express high amounts of the epithelial E-cadherin, but also of the mesenchymal vimentin, which is a contradiction in terms of pure epithelial origin. Publications as early as 1976 showed the existence of numerous lamellar bodies in these cells [134, 137]. However, in the electron microscopic images taken from non-transfected and ABCA3 transfected A549 cells, no lamellar bodies could be identified. Already in a study from 1984 it was reported that different clones of A549 cells may have different characteristics [133]. The cells used in this study were purchased from DSMZ but there may be other A549 cells circulating having other characteristics. Moreover, A549 cells mostly lack expression of TTF-1 which is a prerequisite for expression of surfactant proteins, including SP-C [250]. Indeed, only very small amounts of SP-C mRNA were found in A549 cells. However, introduction of ABCA3 mutations or RSV infection still decreased these low SP-C amounts even further. Also, the A549 cells used in this study already had basal ABCA3 expression. Cells transfected with mutant ABCA3 therefore expressed both, intrinsic probable functional ABCA3 as well as mutant ABCA3. The influence of the basal ABCA3 expression in non-transfected and ABCA3 mutant transfected cells is hard to estimate, as a functional assay was not yet established in the laboratory. Further studies could be improved by introducing an ABCA3 knockout into A549 cells.

5.9 Conclusion and Outlook

In summary, it was shown in this thesis that expression of ABCA3 mutations in lung epithelial cells results in a reduction of epithelial proteins important for cellular function, cellular adhesion and epithelial architecture as well as in increased expression of proteins associated with a mesenchymal phenotype. Moreover, ABCA3 mutations induced the expression of other (lipid) transporters and lead to intracellular accumulation of cholesterol esters as well as to formation of enlarged neutral lipid storage droplets. Additionally,

expression of ABCA3 mutations interfered with TLR-mediated immune responses. RSV infection induced pronounced changes in cell morphology and potentiated the observed effects on reduction of epithelial and acquisition of mesenchymal proteins in cells expressing ABCA3 mutations, thereby rendering the genetically predisposed epithelial cells even more prone to the loss of lung epithelial cell differentiation. Cells harbouring mutant ABCA3 were impaired in their response to LPS stimulation, which in the lung epithelium possibly might lead to interference with bacterial clearance as well as rendering the cells more susceptible to reinfection.

These findings offer some insights into the mechanisms by which ABCA3 mutations may cause ILD which have not been unraveled so far. ABCA3 mutations might disrupt epithelial integrity by impairing ATII function via TGF-β1, MAP kinase and Src dependent pathways. The ABCA3-mediated mechanisms that lead to a reduced inflammatory potential in cells harbouring ABCA3 mutations remain to be investigated. The results imply that individuals carrying *ABCA3* mutations have a genetic predisposition for functional impairment of the alveolar epithelium. Additional genetic or environmental factors, such as mutations in other genes or virus infection, might ultimately result in pathologic changes of the lung parenchyma consistent with the development of ILD.

Further experiments should be dedicated to identifying cellular mechanisms by which defects in ABCA3 lead to a profibrotic environment as well as a reduced expression of inflammatory mediators and if and how these two are connected. Possible hypothetical relationships between ABCA3 mutations and the observed cholesterol / lipid-related effects are presented in Figure 5.2. Most importantly, ABCA3 mutation-induced LXR activation has to be demonstrated. Also, the amount of cellular oxysterols, mediators of LXR activation, needs to be investigated. Additionally, protein expression of the pro-inflammatory prostaglandin synthase COX-2, which was shown to be regulated by LXR, as well as secretion of the COX-2 product prostaglandin E_2 (PGE_2) should be determined. PGE_2 has an inhibitory effect on fibroblast proliferation and migration as well as on collagen secretion and differentiation into myofibroblasts, and decreased levels of PGE_2 were found in patients with fibrosing lung diseases. Therefore, the effect of conditioned media from A549 cells harboring ABCA3-WT or mutations on proliferation and migration of human pulmonary fibroblasts needs to be investigated.

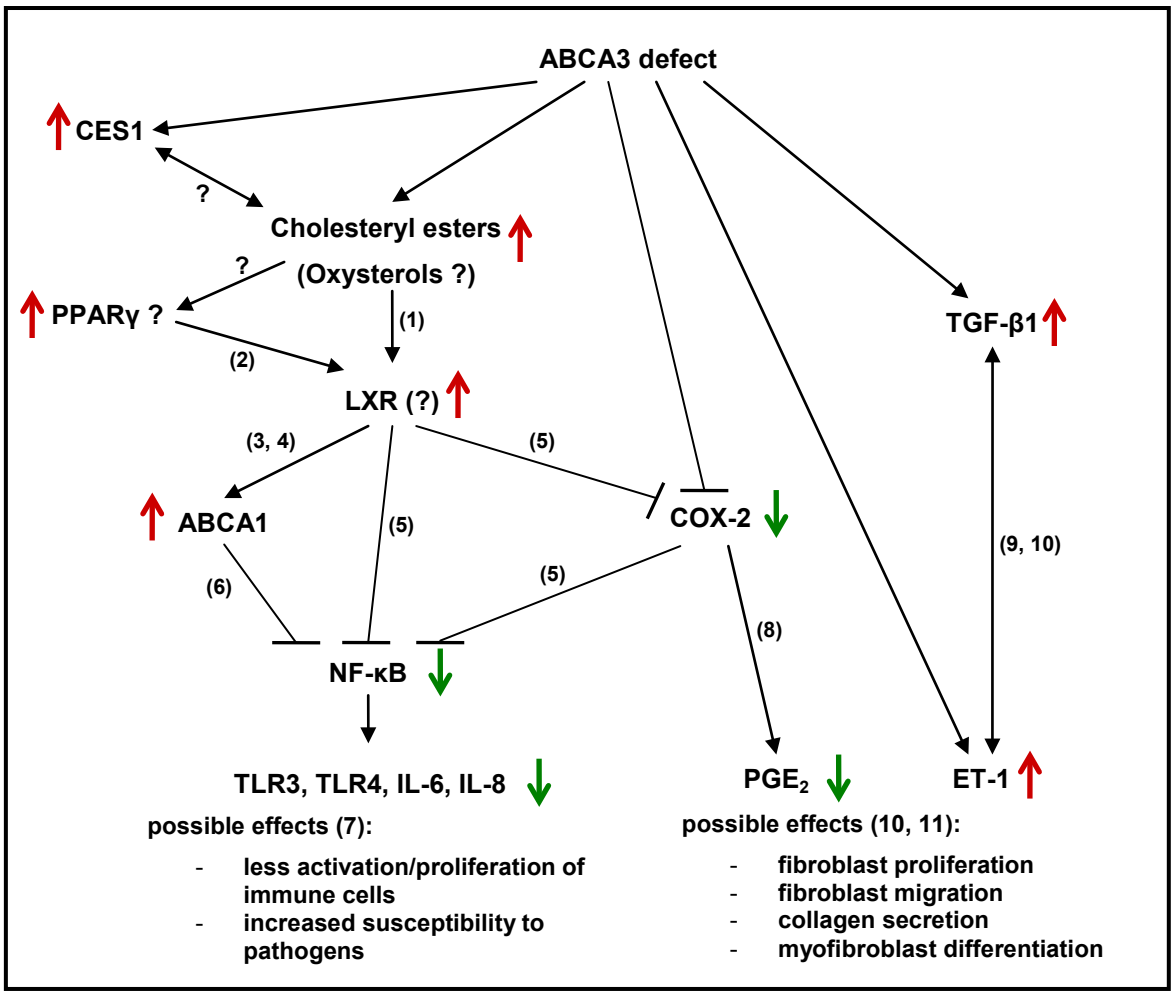

Figure 5.2: Schematic illustration of how ABCA3 mutations might induce fibrosing lung disease and / or reduce the cell's inflammatory mediators.
↑ - upregulation and ↓ - downregulation in cells harboring an ABCA3 mutation, ? - relationships which are so far unknown or have not yet been investigated in this thesis; →/↔ - activation and ⊥ - inhibition. References: (1) Janowski 1996 [203], (2) Chawla 2001 [251], (3) Repa 2000 [252], (4) Costet 2000 [253], (5) Joseph 2003 [206], (6) Zhu 2010 [200], (7) Greene 2005 [254], (8) Cui 2006 [255], (9) Jain 2007 [129], (10) Ross 2010 [156], (11) Bozyk 2011 [256].

6 References

1. Whitsett, J.A., Wert, S.E., and Weaver, T.E., *Alveolar surfactant homeostasis and the pathogenesis of pulmonary disease.* Annu Rev Med, 2010. **61**: p. 105-119.
2. Griese, M., *Pulmonary surfactant in health and human lung diseases: state of the art.* Eur Respir J, 1999. **13**(6): p. 1455-1476.
3. Lang, C.J., Postle, A.D., Orgeig, S., Possmayer, F., Bernhard, W., et al., *Dipalmitoylphosphatidylcholine is not the major surfactant phospholipid species in all mammals.* Am J Physiol Regul Integr Comp Physiol, 2005. **289**(5): p. R1426-1439.
4. Postle, A.D., Mander, A., Reid, K.B., Wang, J.Y., Wright, S.M., et al., *Deficient hydrophilic lung surfactant proteins A and D with normal surfactant phospholipid molecular species in cystic fibrosis.* Am J Respir Cell Mol Biol, 1999. **20**(1): p. 90-98.
5. Ghildyal, R., Hartley, C., Varrasso, A., Meanger, J., Voelker, D.R., et al., *Surfactant protein A binds to the fusion glycoprotein of respiratory syncytial virus and neutralizes virion infectivity.* J Infect Dis, 1999. **180**(6): p. 2009-2013.
6. Hickling, T.P., Malhotra, R., Bright, H., McDowell, W., Blair, E.D., et al., *Lung surfactant protein A provides a route of entry for respiratory syncytial virus into host cells.* Viral Immunol, 2000. **13**(1): p. 125-135.
7. LeVine, A.M., Gwozdz, J., Stark, J., Bruno, M., Whitsett, J., et al., *Surfactant protein-A enhances respiratory syncytial virus clearance in vivo.* J Clin Invest, 1999. **103**(7): p. 1015-1021.
8. Hickling, T.P., Bright, H., Wing, K., Gower, D., Martin, S.L., et al., *A recombinant trimeric surfactant protein D carbohydrate recognition domain inhibits respiratory syncytial virus infection in vitro and in vivo.* Eur J Immunol, 1999. **29**(11): p. 3478-3484.
9. Weaver, T.E., Na, C.L., and Stahlman, M., *Biogenesis of lamellar bodies, lysosome-related organelles involved in storage and secretion of pulmonary surfactant.* Semin Cell Dev Biol, 2002. **13**(4): p. 263-270.
10. Andreeva, A.V., Kutuzov, M.A., and Voyno-Yasenetskaya, T.A., *Regulation of surfactant secretion in alveolar type II cells.* Am J Physiol Lung Cell Mol Physiol, 2007. **293**(2): p. L259-271.
11. Clark, J.C., Wert, S.E., Bachurski, C.J., Stahlman, M.T., Stripp, B.R., et al., *Targeted disruption of the surfactant protein B gene disrupts surfactant homeostasis, causing respiratory failure in newborn mice.* Proc Natl Acad Sci USA, 1995. **92**(17): p. 7794-7798.
12. Stahlman, M.T., Gray, M.P., Falconieri, M.W., Whitsett, J.A., and Weaver, T.E., *Lamellar body formation in normal and surfactant protein B-deficient fetal mice.* Lab Invest, 2000. **80**(3): p. 395-403.
13. Glasser, S.W., Burhans, M.S., Korfhagen, T.R., Na, C.L., Sly, P.D., et al., *Altered stability of pulmonary surfactant in SP-C-deficient mice.* Proc Natl Acad Sci USA, 2001. **98**(11): p. 6366-6371.
14. Ban, N., Matsumura, Y., Sakai, H., Takanezawa, Y., Sasaki, M., et al., *ABCA3 as a lipid transporter in pulmonary surfactant biogenesis.* J Biol Chem, 2007. **282**(13): p. 9628-9634.
15. Young, S.L., Kremers, S.A., Apple, J.S., Crapo, J.D., and Brumley, G.W., *Rat lung surfactant kinetics biochemical and morphometric correlation.* J Appl Physiol, 1981. **51**(2): p. 248-253.

16. Danto, S.I., Shannon, J.M., Borok, Z., Zabski, S.M., and Crandall, E.D., *Reversible transdifferentiation of alveolar epithelial cells.* Am J Respir Cell Mol Biol, 1995. **12**(5): p. 497-502.
17. Rohmann, K., Tschernig, T., Pabst, R., Goldmann, T., and Dromann, D., *Innate immunity in the human lung: pathogen recognition and lung disease.* Cell Tissue Res, 2011. **343**(1): p. 167-174.
18. Griese, M., Haug, M., Brasch, F., Freihorst, A., Lohse, P., et al., *Incidence and classification of pediatric diffuse parenchymal lung diseases in Germany.* Orphanet journal of rare diseases, 2009. **4**: p. 26.
19. Deutsch, G.H., Young, L.R., Deterding, R.R., Fan, L.L., Dell, S.D., et al., *Diffuse lung disease in young children: application of a novel classification scheme.* Am J Respir Crit Care Med, 2007. **176**(11): p. 1120-1128.
20. Borchers, A.T., Chang, C., Keen, C.L., and Gershwin, M.E., *Idiopathic pulmonary fibrosis-an epidemiological and pathological review.* Clin Rev Allergy Immunol, 2011. **40**(2): p. 117-134.
21. Dinwiddie, R., Sharief, N., and Crawford, O., *Idiopathic interstitial pneumonitis in children: a national survey in the United Kingdom and Ireland.* Pediatr Pulmonol, 2002. **34**(1): p. 23-29.
22. Fan, L.L., Deterding, R.R., and Langston, C., *Pediatric interstitial lung disease revisited.* Pediatr Pulmonol, 2004. **38**(5): p. 369-378.
23. *American Thoracic Society/European Respiratory Society International Multidisciplinary Consensus Classification of the Idiopathic Interstitial Pneumonias.* Am J Respir Crit Care Med, 2002. **165**(2): p. 277-304.
24. Kottmann, R.M., Hogan, C.M., Phipps, R.P., and Sime, P.J., *Determinants of initiation and progression of idiopathic pulmonary fibrosis.* Respirology, 2009. **14**(7): p. 917-933.
25. Vannella, K.M. and Moore, B.B., *Viruses as co-factors for the initiation or exacerbation of lung fibrosis.* Fibrogenesis Tissue Repair, 2008. **1**(1): p. 2.
26. Wright, M. and Piedimonte, G., *Respiratory syncytial virus prevention and therapy: past, present, and future.* Pediatr Pulmonol, 2011. **46**(4): p. 324-347.
27. Easton, A.J., Domachowske, J.B., and Rosenberg, H.F., *Animal pneumoviruses: molecular genetics and pathogenesis.* Clin Microbiol Rev, 2004. **17**(2): p. 390-412.
28. Hacking, D. and Hull, J., *Respiratory syncytial virus--viral biology and the host response.* J Infect, 2002. **45**(1): p. 18-24.
29. Jordan, W.S., Jr., *Growth characteristics of respiratory syncytial virus.* J Immunol, 1962. **88**: p. 581-590.
30. Morton, C.J., Cameron, R., Lawrence, L.J., Lin, B., Lowe, M., et al., *Structural characterization of respiratory syncytial virus fusion inhibitor escape mutants: homology model of the F protein and a syncytium formation assay.* Virology, 2003. **311**(2): p. 275-288.
31. Domachowske, J.B., Bonville, C.A., and Rosenberg, H.F., *Cytokeratin 17 is expressed in cells infected with respiratory syncytial virus via NF-kappaB activation and is associated with the formation of cytopathic syncytia.* J Infect Dis, 2000. **182**(4): p. 1022-1028.
32. Hall, C.B., Walsh, E.E., Long, C.E., and Schnabel, K.C., *Immunity to and frequency of reinfection with respiratory syncytial virus.* J Infect Dis, 1991. **163**(4): p. 693-698.
33. Ogra, P.L., *Respiratory syncytial virus: the virus, the disease and the immune response.* Paediatr Respir Rev, 2004. **5 Suppl A**: p. S119-126.

34. Ramet, M., Korppi, M., and Hallman, M., *Pattern recognition receptors and genetic risk for rsv infection: value for clinical decision-making?* Pediatr Pulmonol, 2011. **46**(2): p. 101-110.
35. Whimbey, E., Couch, R.B., Englund, J.A., Andreeff, M., Goodrich, J.M., et al., *Respiratory syncytial virus pneumonia in hospitalized adult patients with leukemia.* Clin Infect Dis, 1995. **21**(2): p. 376-379.
36. Englund, J.A., Sullivan, C.J., Jordan, M.C., Dehner, L.P., Vercellotti, G.M., et al., *Respiratory syncytial virus infection in immunocompromised adults.* Ann Intern Med, 1988. **109**(3): p. 203-208.
37. Empey, K.M., Peebles, R.S., Jr., and Kolls, J.K., *Pharmacologic advances in the treatment and prevention of respiratory syncytial virus.* Clin Infect Dis, 2010. **50**(9): p. 1258-1267.
38. Murawski, M.R., Bowen, G.N., Cerny, A.M., Anderson, L.J., Haynes, L.M., et al., *Respiratory syncytial virus activates innate immunity through Toll-like receptor 2.* J Virol, 2009. **83**(3): p. 1492-1500.
39. Kurt-Jones, E.A., Popova, L., Kwinn, L., Haynes, L.M., Jones, L.P., et al., *Pattern recognition receptors TLR4 and CD14 mediate response to respiratory syncytial virus.* Nat Immunol, 2000. **1**(5): p. 398-401.
40. Groskreutz, D.J., Monick, M.M., Powers, L.S., Yarovinsky, T.O., Look, D.C., et al., *Respiratory syncytial virus induces TLR3 protein and protein kinase R, leading to increased double-stranded RNA responsiveness in airway epithelial cells.* J Immunol, 2006. **176**(3): p. 1733-1740.
41. Monick, M.M., Yarovinsky, T.O., Powers, L.S., Butler, N.S., Carter, A.B., et al., *Respiratory syncytial virus up-regulates TLR4 and sensitizes airway epithelial cells to endotoxin.* J Biol Chem, 2003. **278**(52): p. 53035-53044.
42. Welliver, R.C., Sr., *The immune response to respiratory syncytial virus infection: friend or foe?* Clin Rev Allergy Immunol, 2008. **34**(2): p. 163-173.
43. van Schaik, S.M., Obot, N., Enhorning, G., Hintz, K., Gross, K., et al., *Role of interferon gamma in the pathogenesis of primary respiratory syncytial virus infection in BALB/c mice.* J Med Virol, 2000. **62**(2): p. 257-266.
44. Linton, K.J. and Higgins, C.F., *The Escherichia coli ATP-binding cassette (ABC) proteins.* Mol Microbiol, 1998. **28**(1): p. 5-13.
45. Zolnerciks, J.K., Andress, E.J., Nicolaou, M., and Linton, K.J., *Structure of ABC transporters.* Essays Biochem, 2011. **50**(1): p. 43-61.
46. Higgins, C.F., *ABC transporters: from microorganisms to man.* Annu Rev Cell Biol, 1992. **8**: p. 67-113.
47. Hyde, S.C., Emsley, P., Hartshorn, M.J., Mimmack, M.M., Gileadi, U., et al., *Structural model of ATP-binding proteins associated with cystic fibrosis, multidrug resistance and bacterial transport.* Nature, 1990. **346**(6282): p. 362-365.
48. Al-Shawi, M.K., *Catalytic and transport cycles of ABC exporters.* Essays Biochem, 2011. **50**(1): p. 63-83.
49. Dawson, R.J. and Locher, K.P., *Structure of the multidrug ABC transporter Sav1866 from Staphylococcus aureus in complex with AMP-PNP.* FEBS Lett, 2007. **581**(5): p. 935-938.
50. Locher, K.P., Lee, A.T., and Rees, D.C., *The E. coli BtuCD structure: a framework for ABC transporter architecture and mechanism.* Science, 2002. **296**(5570): p. 1091-1098.
51. Aller, S.G., Yu, J., Ward, A., Weng, Y., Chittaboina, S., et al., *Structure of P-glycoprotein reveals a molecular basis for poly-specific drug binding.* Science, 2009. **323**(5922): p. 1718-1722.

52. Quazi, F. and Molday, R.S., *Lipid transport by mammalian ABC proteins.* Essays Biochem, 2011. **50**(1): p. 265-290.
53. Dean, M., Rzhetsky, A., and Allikmets, R., *The human ATP-binding cassette (ABC) transporter superfamily.* Genome Res, 2001. **11**(7): p. 1156-1166.
54. Abele, R. and Tampe, R., *The TAP translocation machinery in adaptive immunity and viral escape mechanisms.* Essays Biochem, 2011. **50**(1): p. 249-264.
55. Kim Chiaw, P., Eckford, P.D., and Bear, C.E., *Insights into the mechanisms underlying CFTR channel activity, the molecular basis for cystic fibrosis and strategies for therapy.* Essays Biochem, 2011. **50**(1): p. 233-248.
56. Sharom, F.J., *The P-glycoprotein multidrug transporter.* Essays Biochem, 2011. **50**(1): p. 161-178.
57. Slot, A.J., Molinski, S.V., and Cole, S.P., *Mammalian multidrug-resistance proteins (MRPs).* Essays Biochem, 2011. **50**(1): p. 179-207.
58. Chang, G., *Multidrug resistance ABC transporters.* FEBS Lett, 2003. **555**(1): p. 102-105.
59. Dean, M. *The human ATP-binding cassette (ABC) Transporter Superfamily [Internet]*. 2002. Bethesda (MD): National Center for Biotechnology Information (US); 18. November 2002. Available from: http://www.ncbi.nlm.nih.gov/books/NBK3/
60. Kaminski, W.E., Piehler, A., and Wenzel, J.J., *ABC A-subfamily transporters: structure, function and disease.* Biochim Biophys Acta, 2006. **1762**(5): p. 510-524.
61. Tusnady, G.E., Sarkadi, B., Simon, I., and Varadi, A., *Membrane topology of human ABC proteins.* FEBS Lett, 2006. **580**(4): p. 1017-1022.
62. Oram, J.F., *HDL apolipoproteins and ABCA1: partners in the removal of excess cellular cholesterol.* Arterioscler Thromb Vasc Biol, 2003. **23**(5): p. 720-727.
63. van Eck, M., Bos, I.S., Kaminski, W.E., Orso, E., Rothe, G., et al., *Leukocyte ABCA1 controls susceptibility to atherosclerosis and macrophage recruitment into tissues.* Proc Natl Acad Sci USA, 2002. **99**(9): p. 6298-6303.
64. Attie, A.D., *ABCA1: at the nexus of cholesterol, HDL and atherosclerosis.* Trends Biochem Sci, 2007. **32**(4): p. 172-179.
65. Oram, J.F., *Tangier disease and ABCA1.* Biochim Biophys Acta, 2000. **1529**(1-3): p. 321-330.
66. Kang, M.H., Singaraja, R., and Hayden, M.R., *Adenosine-triphosphate-binding cassette transporter-1 trafficking and function.* Trends Cardiovasc Med, 2010. **20**(2): p. 41-49.
67. Molday, R.S., Zhong, M., and Quazi, F., *The role of the photoreceptor ABC transporter ABCA4 in lipid transport and Stargardt macular degeneration.* Biochim Biophys Acta, 2009. **1791**(7): p. 573-583.
68. Stahlman, M.T., Besnard, V., Wert, S.E., Weaver, T.E., Dingle, S., et al., *Expression of ABCA3 in developing lung and other tissues.* J Histochem Cytochem, 2007. **55**(1): p. 71-83.
69. Garmany, T.H., Moxley, M.A., White, F.V., Dean, M., Hull, W.M., et al., *Surfactant composition and function in patients with ABCA3 mutations.* Pediatr Res, 2006. **59**(6): p. 801-805.
70. Doan, M.L., Guillerman, R.P., Dishop, M.K., Nogee, L.M., Langston, C., et al., *Clinical, radiological and pathological features of ABCA3 mutations in children.* Thorax, 2008. **63**(4): p. 366-373.
71. Yamano, G., Funahashi, H., Kawanami, O., Zhao, L.X., Ban, N., et al., *ABCA3 is a lamellar body membrane protein in human lung alveolar type II cells.* FEBS Lett, 2001. **508**(2): p. 221-225.

72. Mulugeta, S., Gray, J.M., Notarfrancesco, K.L., Gonzales, L.W., Koval, M., et al., *Identification of LBM180, a lamellar body limiting membrane protein of alveolar type II cells, as the ABC transporter protein ABCA3.* J Biol Chem, 2002. **277**(25): p. 22147-22155.
73. Matsumura, Y., Sakai, H., Sasaki, M., Ban, N., and Inagaki, N., *ABCA3-mediated choline-phospholipids uptake into intracellular vesicles in A549 cells.* FEBS Lett, 2007. **581**(17): p. 3139-3144.
74. DeFelice, M., Silberschmidt, D., DiLauro, R., Xu, Y., Wert, S.E., et al., *TTF-1 phosphorylation is required for peripheral lung morphogenesis, perinatal survival, and tissue-specific gene expression.* J Biol Chem, 2003. **278**(37): p. 35574-35583.
75. Minoo, P., Su, G., Drum, H., Bringas, P., and Kimura, S., *Defects in tracheoesophageal and lung morphogenesis in Nkx2.1(-/-) mouse embryos.* Dev Biol, 1999. **209**(1): p. 60-71.
76. Hammel, M., Michel, G., Hoefer, C., Klaften, M., Muller-Hocker, J., et al., *Targeted inactivation of the murine Abca3 gene leads to respiratory failure in newborns with defective lamellar bodies.* Biochem Biophys Res Commun, 2007. **359**(4): p. 947-951.
77. Besnard, V., Matsuzaki, Y., Clark, J., Xu, Y., Wert, S.E., et al., *Conditional deletion of Abca3 in alveolar type II cells alters surfactant homeostasis in newborn and adult mice.* Am J Physiol Lung Cell Mol Physiol, 2010. **298**(5): p. L646-659.
78. Brasch, F., Schimanski, S., Muhlfeld, C., Barlage, S., Langmann, T., et al., *Alteration of the pulmonary surfactant system in full-term infants with hereditary ABCA3 deficiency.* Am J Respir Crit Care Med, 2006. **174**(5): p. 571-580.
79. Bullard, J.E., Wert, S.E., and Nogee, L.M., *ABCA3 deficiency: neonatal respiratory failure and interstitial lung disease.* Semin Perinatol, 2006. **30**(6): p. 327-334.
80. Young, L.R., Nogee, L.M., Barnett, B., Panos, R.J., Colby, T.V., et al., *Usual interstitial pneumonia in an adolescent with ABCA3 mutations.* Chest, 2008. **134**(1): p. 192-195.
81. Bullard, J.E., Wert, S.E., Whitsett, J.A., Dean, M., and Nogee, L.M., *ABCA3 mutations associated with pediatric interstitial lung disease.* Am J Respir Crit Care Med, 2005. **172**(8): p. 1026-1031.
82. Bullard, J.E. and Nogee, L.M., *Heterozygosity for ABCA3 mutations modifies the severity of lung disease associated with a surfactant protein C gene (SFTPC) mutation.* Pediatr Res, 2007. **62**(2): p. 176-179.
83. Matsumura, Y., Ban, N., Ueda, K., and Inagaki, N., *Characterization and classification of ATP-binding cassette transporter ABCA3 mutants in fatal surfactant deficiency.* J Biol Chem, 2006. **281**(45): p. 34503-34514.
84. Garmany, T.H., Wambach, J.A., Heins, H.B., Watkins-Torry, J.M., Wegner, D.J., et al., *Population and disease-based prevalence of the common mutations associated with surfactant deficiency.* Pediatr Res, 2008. **63**(6): p. 645-649.
85. Edwards, V., Cutz, E., Viero, S., Moore, A.M., and Nogee, L., *Ultrastructure of lamellar bodies in congenital surfactant deficiency.* Ultrastruct Pathol, 2005. **29**(6): p. 503-509.
86. Shulenin, S., Nogee, L.M., Annilo, T., Wert, S.E., Whitsett, J.A., et al., *ABCA3 gene mutations in newborns with fatal surfactant deficiency.* N Engl J Med, 2004. **350**(13): p. 1296-1303.
87. Zeisberg, M. and Neilson, E.G., *Biomarkers for epithelial-mesenchymal transitions.* J Clin Invest, 2009. **119**(6): p. 1429-1437.
88. Willis, B.C. and Borok, Z., *TGF-beta-induced EMT: mechanisms and implications for fibrotic lung disease.* Am J Physiol Lung Cell Mol Physiol, 2007. **293**(3): p. L525-L534.

89. Janda, E., Nevolo, M., Lehmann, K., Downward, J., Beug, H., et al., *Raf plus TGFbeta-dependent EMT is initiated by endocytosis and lysosomal degradation of E-cadherin.* Oncogene, 2006. **25**(54): p. 7117-7130.
90. Fanning, A.S. and Anderson, J.M., *Zonula occludens-1 and -2 are cytosolic scaffolds that regulate the assembly of cellular junctions.* Ann N Y Acad Sci, 2009. **1165**: p. 113-120.
91. Shintani, Y., Fukumoto, Y., Chaika, N., Svoboda, R., Wheelock, M.J., et al., *Collagen I-mediated up-regulation of N-cadherin requires cooperative signals from integrins and discoidin domain receptor 1.* J Cell Biol, 2008. **180**(6): p. 1277-1289.
92. Schneider, D.J., Wu, M., Le, T.T., Cho, S.H., Brenner, M.B., et al., *Cadherin-11 contributes to pulmonary fibrosis: potential role in TGF-beta production and epithelial to mesenchymal transition.* FASEB J, 2012. **26**(2): p. 503-512.
93. Kim, K.K., Wei, Y., Szekeres, C., Kugler, M.C., Wolters, P.J., et al., *Epithelial cell alpha3beta1 integrin links beta-catenin and Smad signaling to promote myofibroblast formation and pulmonary fibrosis.* J Clin Invest, 2009. **119**(1): p. 213-224.
94. van der Velden, J.L., Guala, A.S., Leggett, S.E., Sluimer, J., Badura, E.C., et al., *Induction of a Mesenchymal Expression Program in Lung Epithelial Cells by Wnt/beta-catenin Requires the Presence of c-Jun N-Terminal Kinase 1.* Am J Respir Cell Mol Biol, 2012.
95. Zhou, B., Liu, Y., Kahn, M., Ann, D.K., Han, A., et al., *Interactions between beta-catenin and transforming growth factor-beta signaling pathways mediate epithelial-mesenchymal transition and are dependent on the transcriptional co-activator cAMP-response element-binding protein (CREB)-binding protein (CBP).* J Biol Chem, 2012. **287**(10): p. 7026-7038.
96. Kasai, H., Allen, J.T., Mason, R.M., Kamimura, T., and Zhang, Z., *TGF-beta1 induces human alveolar epithelial to mesenchymal cell transition (EMT).* RespirRes, 2005. **6**: p. 56.
97. Song, W., Jackson, K., and McGuire, P.G., *Degradation of type IV collagen by matrix metalloproteinases is an important step in the epithelial-mesenchymal transformation of the endocardial cushions.* Dev Biol, 2000. **227**(2): p. 606-617.
98. Jayachandran, A., Konigshoff, M., Yu, H., Rupniewska, E., Hecker, M., et al., *SNAI transcription factors mediate epithelial-mesenchymal transition in lung fibrosis.* Thorax, 2009. **64**(12): p. 1053-1061.
99. Merikallio, H., Kaarteenaho, R., Paakko, P., Lehtonen, S., Hirvikoski, P., et al., *Zeb1 and twist are more commonly expressed in metastatic than primary lung tumours and show inverse associations with claudins.* J Clin Pathol, 2011. **64**(2): p. 136-140.
100. Mani, S.A., Yang, J., Brooks, M., Schwaninger, G., Zhou, A., et al., *Mesenchyme Forkhead 1 (FOXC2) plays a key role in metastasis and is associated with aggressive basal-like breast cancers.* Proc Natl Acad Sci USA, 2007. **104**(24): p. 10069-10074.
101. Kim, K., Lu, Z., and Hay, E.D., *Direct evidence for a role of beta-catenin/LEF-1 signaling pathway in induction of EMT.* Cell Biol Int, 2002. **26**(5): p. 463-476.
102. Zhou, B., Buckley, S.T., Patel, V., Liu, Y., Luo, J., et al., *Troglitazone Attenuates TGF-beta1-Induced EMT in Alveolar Epithelial Cells via a PPARgamma-Independent Mechanism.* PLoS One, 2012. **7**(6): p. e38827.
103. Willis, B.C., duBois, R.M., and Borok, Z., *Epithelial origin of myofibroblasts during fibrosis in the lung.* Proc Am Thorac Soc, 2006. **3**(4): p. 377-382.

104. Miettinen, P.J., Ebner, R., Lopez, A.R., and Derynck, R., *TGF-beta induced transdifferentiation of mammary epithelial cells to mesenchymal cells: involvement of type I receptors.* J Cell Biol, 1994. **127**(6 Pt 2): p. 2021-2036.
105. Yang, J. and Liu, Y., *Dissection of key events in tubular epithelial to myofibroblast transition and its implications in renal interstitial fibrosis.* Am J Pathol, 2001. **159**(4): p. 1465-1475.
106. Liu, Y., *New insights into epithelial-mesenchymal transition in kidney fibrosis.* J Am Soc Nephrol, 2010. **21**(2): p. 212-222.
107. Li, H., Wang, H., Wang, F., Gu, Q., and Xu, X., *Snail involves in the transforming growth factor beta1-mediated epithelial-mesenchymal transition of retinal pigment epithelial cells.* PLoS One, 2011. **6**(8): p. e23322.
108. Pinzani, M., *Epithelial-mesenchymal transition in chronic liver disease: fibrogenesis or escape from death?* J Hepatol, 2011. **55**(2): p. 459-465.
109. Zhong, Q., Zhou, B., Ann, D.K., Minoo, P., Liu, Y., et al., *Role of endoplasmic reticulum stress in epithelial-mesenchymal transition of alveolar epithelial cells: effects of misfolded surfactant protein.* Am J Respir Cell Mol Biol, 2011. **45**(3): p. 498-509.
110. Tanjore, H., Cheng, D.S., Degryse, A.L., Zoz, D.F., Abdolrasulnia, R., et al., *Alveolar Epithelial Cells Undergo Epithelial-to-Mesenchymal Transition in Response to Endoplasmic Reticulum Stress.* J Biol Chem, 2011. **286**(35): p. 30972-30980.
111. Lawson, W.E., Cheng, D.S., Degryse, A.L., Tanjore, H., Polosukhin, V.V., et al., *Endoplasmic reticulum stress enhances fibrotic remodeling in the lungs.* Proc Natl Acad Sci USA, 2011. **108**(26): p. 10562-10567.
112. Borok, Z., Danto, S.I., Lubman, R.L., Cao, Y., Williams, M.C., et al., *Modulation of t1alpha expression with alveolar epithelial cell phenotype in vitro.* Am J Physiol, 1998. **275**(1 Pt 1): p. L155-164.
113. Iwano, M., Plieth, D., Danoff, T.M., Xue, C., Okada, H., et al., *Evidence that fibroblasts derive from epithelium during tissue fibrosis.* J Clin Invest, 2002. **110**(3): p. 341-350.
114. Marmai, C., Sutherland, R.E., Kim, K.K., Dolganov, G.M., Fang, X., et al., *Alveolar epithelial cells express mesenchymal proteins in patients with idiopathic pulmonary fibrosis.* Am J Physiol Lung Cell Mol Physiol, 2011. **301**(1): p. L71-78.
115. Kim, K.K., Kugler, M.C., Wolters, P.J., Robillard, L., Galvez, M.G., et al., *Alveolar epithelial cell mesenchymal transition develops in vivo during pulmonary fibrosis and is regulated by the extracellular matrix.* Proc Natl Acad Sci USA, 2006. **103**(35): p. 13180-13185.
116. Weichert, N., Kaltenborn, E., Hector, A., Woischnik, M., Schams, A., et al., *Some ABCA3 mutations elevate ER stress and initiate apoptosis of lung epithelial cells.* Resp Res, 2011. **12**: p. 4.
117. Schlender, J., Hornung, V., Finke, S., Gunthner-Biller, M., Marozin, S., et al., *Inhibition of toll-like receptor 7- and 9-mediated alpha/beta interferon production in human plasmacytoid dendritic cells by respiratory syncytial virus and measles virus.* J Virol, 2005. **79**(9): p. 5507-5515.
118. Leidl, K., Liebisch, G., Richter, D., and Schmitz, G., *Mass spectrometric analysis of lipid species of human circulating blood cells.* Biochim Biophys Acta, 2008. **1781**(10): p. 655-664.
119. Liebisch, G., Binder, M., Schifferer, R., Langmann, T., Schulz, B., et al., *High throughput quantification of cholesterol and cholesteryl ester by electrospray ionization tandem mass spectrometry (ESI-MS/MS).* Biochim Biophys Acta, 2006. **1761**(1): p. 121-128.

120. R Development Core Team, *R: A language and environment for statistical computing*, 2008, R Foundation for Statistical Computing: Vienna, Austria. 3-900051-07-0.
121. Gentleman, R.C., Carey, V.J., Bates, D.M., Bolstad, B., Dettling, M., et al., *Bioconductor: open software development for computational biology and bioinformatics.* Genome Biol, 2004. **5**(10): p. R80.
122. Smyth, G.K., *Linear models and empirical bayes methods for assessing differential expression in microarray experiments.* Stat Appl Genet Molec, 2004. **3**: p. Article3.
123. Smyth, G., *limma: Linear Models for Microarray Data*, in *Bioinformatics and Computational Biology Solutions Using R and Bioconductor*, R. Gentleman, et al., (eds). 2005, Springer New York. p. 397-420.
124. Benjamini, Y. and Hochberg, Y., *Controlling the False Discovery Rate: A Practical and Powerful Approach to Multiple Testing.* J R Stat Soc, 1995. **57**(1): p. 289-300.
125. Huang da, W., Sherman, B.T., and Lempicki, R.A., *Systematic and integrative analysis of large gene lists using DAVID bioinformatics resources.* Nat Protoc, 2009. **4**(1): p. 44-57.
126. Huang da, W., Sherman, B.T., and Lempicki, R.A., *Bioinformatics enrichment tools: paths toward the comprehensive functional analysis of large gene lists.* Nucleic Acids Res, 2009. **37**(1): p. 1-13.
127. Batlle, E., Sancho, E., Franci, C., Dominguez, D., Monfar, M., et al., *The transcription factor snail is a repressor of E-cadherin gene expression in epithelial tumour cells.* Nat Cell Biol, 2000. **2**(2): p. 84-89.
128. Cano, A., Perez-Moreno, M.A., Rodrigo, I., Locascio, A., Blanco, M.J., et al., *The transcription factor snail controls epithelial-mesenchymal transitions by repressing E-cadherin expression.* Nat Cell Biol, 2000. **2**(2): p. 76-83.
129. Jain, R., Shaul, P.W., Borok, Z., and Willis, B.C., *Endothelin-1 induces alveolar epithelial-mesenchymal transition through endothelin type A receptor-mediated production of TGF-beta1.* Am J Respir Cell Mol Biol, 2007. **37**(1): p. 38-47.
130. Guarino, M., *Src signaling in cancer invasion.* J Cell Physiol, 2010. **223**(1): p. 14-26.
131. Derynck, R. and Zhang, Y.E., *Smad-dependent and Smad-independent pathways in TGF-beta family signalling.* Nature, 2003. **425**(6958): p. 577-584.
132. Rutkowski, D.T. and Kaufman, R.J., *That which does not kill me makes me stronger: adapting to chronic ER stress.* Trends Biochem Sci, 2007. **32**(10): p. 469-476.
133. Balis, J.U., Bumgarner, S.D., Paciga, J.E., Paterson, J.F., and Shelley, S.A., *Synthesis of lung surfactant-associated glycoproteins by A549 cells: description of an in vitro model for human type II cell dysfunction.* Exp Lung Res, 1984. **6**(3-4): p. 197-213.
134. Lieber, M., Smith, B., Szakal, A., Nelson-Rees, W., and Todaro, G., *A continuous tumor-cell line from a human lung carcinoma with properties of type II alveolar epithelial cells.* Int J Cancer, 1976. **17**(1): p. 62-70.
135. Mason, R.J. and Williams, M.C., *Phospholipid composition and ultrastructure of A549 cells and other cultured pulmonary epithelial cells of presumed type II cell origin.* Biochim Biophys Acta, 1980. **617**(1): p. 36-50.
136. Nardone, L.L. and Andrews, S.B., *Cell line A549 as a model of the type II pneumocyte. Phospholipid biosynthesis from native and organometallic precursors.* Biochim Biophys Acta, 1979. **573**(2): p. 276-295.

137. Shapiro, D.L., Nardone, L.L., Rooney, S.A., Motoyama, E.K., and Munoz, J.L., *Phospholipid biosynthesis and secretion by a cell line (A549) which resembles type II aleveolar epithelial cells.* Biochim Biophys Acta, 1978. **530**(2): p. 197-207.
138. Smith, B.T., *Cell line A549: a model system for the study of alveolar type II cell function.* Am Rev Respir Dis, 1977. **115**(2): p. 285-293.
139. Engelbrecht, S., Kaltenborn, E., Griese, M., and Kern, S., *The surfactant lipid transporter ABCA3 is N-terminally cleaved inside LAMP3-positive vesicles.* FEBS Lett, 2010. **584**(20): p. 4306-4312.
140. Matsumura, Y., Ban, N., and Inagaki, N., *Aberrant catalytic cycle and impaired lipid transport into intracellular vesicles in ABCA3 mutants associated with nonfatal pediatric interstitial lung disease.* Am J Physiol Lung Cell Mol Physiol, 2008. **295**(4): p. L698-L707.
141. Mosmann, T., *Rapid colorimetric assay for cellular growth and survival: application to proliferation and cytotoxicity assays.* J Immunol Methods, 1983. **65**(1-2): p. 55-63.
142. Liu, Y., Peterson, D.A., Kimura, H., and Schubert, D., *Mechanism of cellular 3-(4,5-dimethylthiazol-2-yl)-2,5-diphenyltetrazolium bromide (MTT) reduction.* J Neurochem, 1997. **69**(2): p. 581-593.
143. Badr, C.E., Hewett, J.W., Breakefield, X.O., and Tannous, B.A., *A highly sensitive assay for monitoring the secretory pathway and ER stress.* PLoS One, 2007. **2**(6): p. e571.
144. Mulugeta, S., Nguyen, V., Russo, S.J., Muniswamy, M., and Beers, M.F., *A surfactant protein C precursor protein BRICHOS domain mutation causes endoplasmic reticulum stress, proteasome dysfunction, and caspase 3 activation.* Am J Respir Cell Mol Biol, 2005. **32**(6): p. 521-530.
145. Bridges, J.P., Xu, Y., Na, C.L., Wong, H.R., and Weaver, T.E., *Adaptation and increased susceptibility to infection associated with constitutive expression of misfolded SP-C.* J Cell Biol, 2006. **172**(3): p. 395-407.
146. Ridsdale, R., Na, C.L., Xu, Y., Greis, K.D., and Weaver, T., *Comparative proteomic analysis of lung lamellar bodies and lysosome-related organelles.* PLoS One, 2011. **6**(1): p. e16482.
147. Wang, P., Chintagari, N.R., Narayanaperumal, J., Ayalew, S., Hartson, S., et al., *Proteomic analysis of lamellar bodies isolated from rat lungs.* BMC Cell Biol, 2008. **9**: p. 34.
148. Cheong, N., Zhang, H., Madesh, M., Zhao, M., Yu, K., et al., *ABCA3 is critical for lamellar body biogenesis in vivo.* J Biol Chem, 2007. **282**(33): p. 23811-23817.
149. Cheong, N., Madesh, M., Gonzales, L.W., Zhao, M., Yu, K., et al., *Functional and trafficking defects in ATP binding cassette A3 mutants associated with respiratory distress syndrome.* J Biol Chem, 2006. **281**(14): p. 9791-9800.
150. Flamein, F., Riffault, L., Muselet-Charlier, C., Pernelle, J., Feldmann, D., et al., *Molecular and cellular characteristics of ABCA3 mutations associated with diffuse parenchymal lung diseases in children.* Hum Mol Genet, 2012. **21**(4): p. 765-775.
151. Nagata, K., Yamamoto, A., Ban, N., Tanaka, A.R., Matsuo, M., et al., *Human ABCA3, a product of a responsible gene for abca3 for fatal surfactant deficiency in newborns, exhibits unique ATP hydrolysis activity and generates intracellular multilamellar vesicles.* Biochem Biophys Res Commun, 2004. **324**(1): p. 262-268.
152. Mulugeta, S. and Beers, M.F., *Surfactant protein C: its unique properties and emerging immunomodulatory role in the lung.* Microb Infect, 2006. **8**(8): p. 2317-2323.

153. Lewis, J.E., Jensen, P.J., Johnson, K.R., and Wheelock, M.J., *E-cadherin mediates adherens junction organization through protein kinase C.* J Cell Sci, 1994. **107 (Pt 12)**: p. 3615-3621.
154. Kaltenborn, E., Kern, S., Frixel, S., Fragnet, L., Conzelmann, K.K., et al., *Respiratory syncytial virus potentiates ABCA3 mutation-induced loss of lung epithelial cell differentiation.* Hum Mol Genet (Oxford University Press), 2012. **21**(12): p. 2793-2806.
155. Hajra, K.M., Chen, D.Y., and Fearon, E.R., *The SLUG zinc-finger protein represses E-cadherin in breast cancer.* Cancer Res, 2002. **62**(6): p. 1613-1618.
156. Ross, B., D'Orleans-Juste, P., and Giaid, A., *Potential role of endothelin-1 in pulmonary fibrosis: from the bench to the clinic.* Am J Respir Cell Mol Biol, 2010. **42**(1): p. 16-20.
157. Uguccioni, M., Pulsatelli, L., Grigolo, B., Facchini, A., Fasano, L., et al., *Endothelin-1 in idiopathic pulmonary fibrosis.* J Clin Pathol, 1995. **48**(4): p. 330-334.
158. Reichenberger, F., Schauer, J., Kellner, K., Sack, U., Stiehl, P., et al., *Different expression of endothelin in the bronchoalveolar lavage in patients with pulmonary diseases.* Lung, 2001. **179**(3): p. 163-174.
159. Shahar, I., Fireman, E., Topilsky, M., Grief, J., Schwarz, Y., et al., *Effect of endothelin-1 on alpha-smooth muscle actin expression and on alveolar fibroblasts proliferation in interstitial lung diseases.* Int J Immunopharmacol, 1999. **21**(11): p. 759-775.
160. Suga, M., Iyonaga, K., Okamoto, T., Gushima, Y., Miyakawa, H., et al., *Characteristic elevation of matrix metalloproteinase activity in idiopathic interstitial pneumonias.* Am J Respir Crit Care Med, 2000. **162**(5): p. 1949-1956.
161. Ratjen, F., Hartog, C.M., Paul, K., Wermelt, J., and Braun, J., *Matrix metalloproteases in BAL fluid of patients with cystic fibrosis and their modulation by treatment with dornase alpha.* Thorax, 2002. **57**(11): p. 930-934.
162. Corbel, M., Belleguic, C., Boichot, E., and Lagente, V., *Involvement of gelatinases (MMP-2 and MMP-9) in the development of airway inflammation and pulmonary fibrosis.* Cell Biol Toxicol, 2002. **18**(1): p. 51-61.
163. Hayashi, T., Stetler-Stevenson, W.G., Fleming, M.V., Fishback, N., Koss, M.N., et al., *Immunohistochemical study of metalloproteinases and their tissue inhibitors in the lungs of patients with diffuse alveolar damage and idiopathic pulmonary fibrosis.* Am J Pathol, 1996. **149**(4): p. 1241-1256.
164. Yamashita, C.M., Dolgonos, L., Zemans, R.L., Young, S.K., Robertson, J., et al., *Matrix metalloproteinase 3 is a mediator of pulmonary fibrosis.* Am J Pathol, 2011. **179**(4): p. 1733-1745.
165. McCawley, L.J. and Matrisian, L.M., *Matrix metalloproteinases: they're not just for matrix anymore!* Curr Opin Cell Biol, 2001. **13**(5): p. 534-540.
166. Kelly, M., Kolb, M., Bonniaud, P., and Gauldie, J., *Re-evaluation of fibrogenic cytokines in lung fibrosis.* Curr Pharm Des, 2003. **9**(1): p. 39-49.
167. Barcellos-Hoff, M.H. and Dix, T.A., *Redox-mediated activation of latent transforming growth factor-beta 1.* Mol Endocrinol, 1996. **10**(9): p. 1077-1083.
168. Wipff, P.J. and Hinz, B., *Integrins and the activation of latent transforming growth factor beta1 - an intimate relationship.* Eur J Cell Biol, 2008. **87**(8-9): p. 601-615.
169. Wang, M., Zhao, D., Spinetti, G., Zhang, J., Jiang, L.Q., et al., *Matrix metalloproteinase 2 activation of transforming growth factor-beta1 (TGF-beta1) and TGF-beta1-type II receptor signaling within the aged arterial wall.* Arterioscler Thromb Vasc Biol, 2006. **26**(7): p. 1503-1509.

170. Peinado, H., Quintanilla, M., and Cano, A., *Transforming growth factor beta-1 induces snail transcription factor in epithelial cell lines: mechanisms for epithelial mesenchymal transitions.* J Biol Chem, 2003. **278**(23): p. 21113-21123.
171. Fujita, H., Sakamoto, N., Ishimatsu, Y., Kakugawa, T., Hara, S., et al., *Effects of doxycycline on production of growth factors and matrix metalloproteinases in pulmonary fibrosis.* Respiration, 2011. **81**(5): p. 420-430.
172. Thomas, S.M. and Brugge, J.S., *Cellular functions regulated by Src family kinases.* Annu Rev Cell Dev Biol, 1997. **13**: p. 513-609.
173. Giancotti, F.G. and Ruoslahti, E., *Integrin signaling.* Science, 1999. **285**(5430): p. 1028-1032.
174. Shen, Y., Hirsch, D.S., Sasiela, C.A., and Wu, W.J., *Cdc42 regulates E-cadherin ubiquitination and degradation through an epidermal growth factor receptor to Src-mediated pathway.* J Biol Chem, 2008. **283**(8): p. 5127-5137.
175. Neufeld, E.B., Remaley, A.T., Demosky, S.J., Stonik, J.A., Cooney, A.M., et al., *Cellular localization and trafficking of the human ABCA1 transporter.* J Biol Chem, 2001. **276**(29): p. 27584-27590.
176. Santamarina-Fojo, S., Remaley, A.T., Neufeld, E.B., and Brewer, H.B., Jr., *Regulation and intracellular trafficking of the ABCA1 transporter.* J Lipid Res, 2001. **42**(9): p. 1339-1345.
177. Zarubica, A., Trompier, D., and Chimini, G., *ABCA1, from pathology to membrane function.* Pflugers Arch, 2007. **453**(5): p. 569-579.
178. Panousis, C.G. and Zuckerman, S.H., *Interferon-gamma induces downregulation of Tangier disease gene (ATP-binding-cassette transporter 1) in macrophage-derived foam cells.* Arterioscler Thromb Vasc Biol, 2000. **20**(6): p. 1565-1571.
179. Lusis, A.J., *Atherosclerosis.* Nature, 2000. **407**(6801): p. 233-241.
180. Panousis, C.G., Evans, G., and Zuckerman, S.H., *TGF-beta increases cholesterol efflux and ABC-1 expression in macrophage-derived foam cells: opposing the effects of IFN-gamma.* J Lipid Res, 2001. **42**(5): p. 856-863.
181. Tabas, I., *Consequences of cellular cholesterol accumulation: basic concepts and physiological implications.* J Clin Invest, 2002. **110**(7): p. 905-911.
182. Guo, Y., Cordes, K.R., Farese, R.V., Jr., and Walther, T.C., *Lipid droplets at a glance.* J Cell Sci, 2009. **122**(Pt 6): p. 749-752.
183. Fitzgerald, M.L., Xavier, R., Haley, K.J., Welti, R., Goss, J.L., et al., *ABCA3 inactivation in mice causes respiratory failure, loss of pulmonary surfactant, and depletion of lung phosphatidylglycerol.* J Lipid Res, 2007. **48**(3): p. 621-632.
184. Bartz, R., Li, W.H., Venables, B., Zehmer, J.K., Roth, M.R., et al., *Lipidomics reveals that adiposomes store ether lipids and mediate phospholipid traffic.* J Lipid Res, 2007. **48**(4): p. 837-847.
185. Moessinger, C., Kuerschner, L., Spandl, J., Shevchenko, A., and Thiele, C., *Human lysophosphatidylcholine acyltransferases 1 and 2 are located in lipid droplets where they catalyze the formation of phosphatidylcholine.* J Biol Chem, 2011. **286**(24): p. 21330-21339.
186. Postle, A.D., Heeley, E.L., and Wilton, D.C., *A comparison of the molecular species compositions of mammalian lung surfactant phospholipids.* Comp Biochem Physiol, A: Mol Integr Physiol, 2001. **129**(1): p. 65-73.
187. Hou, M., Xia, M., Zhu, H., Wang, Q., Li, Y., et al., *Lysophosphatidylcholine promotes cholesterol efflux from mouse macrophage foam cells via PPARgamma-LXRalpha-ABCA1-dependent pathway associated with apoE.* Cell Biochem Funct, 2007. **25**(1): p. 33-44.

188. Kitatani, K., Idkowiak-Baldys, J., and Hannun, Y.A., *The sphingolipid salvage pathway in ceramide metabolism and signaling.* Cell Signal, 2008. **20**(6): p. 1010-1018.
189. Malewicz, B., Valiyaveettil, J.T., Jacob, K., Byun, H.S., Mattjus, P., et al., *The 3-hydroxy group and 4,5-trans double bond of sphingomyelin are essential for modulation of galactosylceramide transmembrane asymmetry.* Biophys J, 2005. **88**(4): p. 2670-2680.
190. Mason, R.J. and Williams, M.C., *Type II alveolar cell. Defender of the alveolus.* Am Rev Respir Dis, 1977. **115**(6 Pt 2): p. 81-91.
191. Fehrenbach, H., *Alveolar epithelial type II cell: defender of the alveolus revisited.* Resp Res, 2001. **2**(1): p. 33-46.
192. Armstrong, L., Medford, A.R., Uppington, K.M., Robertson, J., Witherden, I.R., et al., *Expression of functional toll-like receptor-2 and -4 on alveolar epithelial cells.* Am J Respir Cell Mol Biol, 2004. **31**(2): p. 241-245.
193. Thorley, A.J., Grandolfo, D., Lim, E., Goldstraw, P., Young, A., et al., *Innate immune responses to bacterial ligands in the peripheral human lung--role of alveolar epithelial TLR expression and signalling.* PLoS One, 2011. **6**(7): p. e21827.
194. Guillot, L., Le Goffic, R., Bloch, S., Escriou, N., Akira, S., et al., *Involvement of toll-like receptor 3 in the immune response of lung epithelial cells to double-stranded RNA and influenza A virus.* J Biol Chem, 2005. **280**(7): p. 5571-5580.
195. John, G., Yildirim, A.O., Rubin, B.K., Gruenert, D.C., and Henke, M.O., *TLR-4-mediated innate immunity is reduced in cystic fibrosis airway cells.* Am J Respir Cell Mol Biol, 2010. **42**(4): p. 424-431.
196. John, G., Chillappagari, S., Rubin, B.K., Gruenert, D.C., and Henke, M.O., *Reduced surface toll-like receptor-4 expression and absent interferon-gamma-inducible protein-10 induction in cystic fibrosis airway cells.* Exp Lung Res, 2011. **37**(6): p. 319-326.
197. Hauber, H.P., Tulic, M.K., Tsicopoulos, A., Wallaert, B., Olivenstein, R., et al., *Toll-like receptors 4 and 2 expression in the bronchial mucosa of patients with cystic fibrosis.* Can Respir J, 2005. **12**(1): p. 13-18.
198. Zhang, X., Shan, P., Jiang, G., Cohn, L., and Lee, P.J., *Toll-like receptor 4 deficiency causes pulmonary emphysema.* J Clin Invest, 2006. **116**(11): p. 3050-3059.
199. Nakao, Y., Funami, K., Kikkawa, S., Taniguchi, M., Nishiguchi, M., et al., *Surface-expressed TLR6 participates in the recognition of diacylated lipopeptide and peptidoglycan in human cells.* J Immunol, 2005. **174**(3): p. 1566-1573.
200. Zhu, X., Owen, J.S., Wilson, M.D., Li, H., Griffiths, G.L., et al., *Macrophage ABCA1 reduces MyD88-dependent Toll-like receptor trafficking to lipid rafts by reduction of lipid raft cholesterol.* J Lipid Res, 2010. **51**(11): p. 3196-3206.
201. Francone, O.L., Royer, L., Boucher, G., Haghpassand, M., Freeman, A., et al., *Increased cholesterol deposition, expression of scavenger receptors, and response to chemotactic factors in Abca1-deficient macrophages.* Arterioscler Thromb Vasc Biol, 2005. **25**(6): p. 1198-1205.
202. Yin, K., Liao, D.F., and Tang, C.K., *ATP-binding membrane cassette transporter A1 (ABCA1): a possible link between inflammation and reverse cholesterol transport.* Mol Med, 2010. **16**(9-10): p. 438-449.
203. Janowski, B.A., Willy, P.J., Devi, T.R., Falck, J.R., and Mangelsdorf, D.J., *An oxysterol signalling pathway mediated by the nuclear receptor LXR alpha.* Nature, 1996. **383**(6602): p. 728-731.

204. Lehmann, J.M., Kliewer, S.A., Moore, L.B., Smith-Oliver, T.A., Oliver, B.B., et al., *Activation of the nuclear receptor LXR by oxysterols defines a new hormone response pathway.* J Biol Chem, 1997. **272**(6): p. 3137-3140.
205. Zhao, C. and Dahlman-Wright, K., *Liver X receptor in cholesterol metabolism.* J Endocrinol, 2010. **204**(3): p. 233-240.
206. Joseph, S.B., Castrillo, A., Laffitte, B.A., Mangelsdorf, D.J., and Tontonoz, P., *Reciprocal regulation of inflammation and lipid metabolism by liver X receptors.* Nat Med, 2003. **9**(2): p. 213-219.
207. Mora, A.L. and Roman, J., *Virus-related interstitial lung disease*, in *Interstitial Lung Disease*, M.I. Schwarz and T.E. King, Jr., (eds). 2010, People's Medical Publishing House: Shelton, CT, USA. p. 251-265.
208. Glasser, S.W., Witt, T.L., Senft, A.P., Baatz, J.E., Folger, D., et al., *Surfactant protein C-deficient mice are susceptible to respiratory syncytial virus infection.* Am J Physiol Lung Cell Mol Physiol, 2009. **297**(1): p. L64-L72.
209. Morbini, P., Inghilleri, S., Campo, I., Oggionni, T., Zorzetto, M., et al., *Incomplete expression of epithelial-mesenchymal transition markers in idiopathic pulmonary fibrosis.* Pathol Res Pract, 2011.
210. Sides, M.D., Klingsberg, R.C., Shan, B., Gordon, K.A., Nguyen, H.T., et al., *The Epstein-Barr virus latent membrane protein 1 and transforming growth factor--beta1 synergistically induce epithelial--mesenchymal transition in lung epithelial cells.* Am J Respir Cell Mol Biol, 2011. **44**(6): p. 852-862.
211. Pozharskaya, V., Torres-Gonzalez, E., Rojas, M., Gal, A., Amin, M., et al., *Twist: a regulator of epithelial-mesenchymal transition in lung fibrosis.* PLoS One, 2009. **4**(10): p. e7559.
212. Horikawa, T., Yang, J., Kondo, S., Yoshizaki, T., Joab, I., et al., *Twist and epithelial-mesenchymal transition are induced by the EBV oncoprotein latent membrane protein 1 and are associated with metastatic nasopharyngeal carcinoma.* Cancer Res, 2007. **67**(5): p. 1970-1978.
213. Kong, Q.L., Hu, L.J., Cao, J.Y., Huang, Y.J., Xu, L.H., et al., *Epstein-Barr virus-encoded LMP2A induces an epithelial-mesenchymal transition and increases the number of side population stem-like cancer cells in nasopharyngeal carcinoma.* PLoS Path, 2010. **6**(6): p. e1000940.
214. Horikawa, T., Yoshizaki, T., Kondo, S., Furukawa, M., Kaizaki, Y., et al., *Epstein-Barr Virus latent membrane protein 1 induces Snail and epithelial-mesenchymal transition in metastatic nasopharyngeal carcinoma.* Br J Cancer, 2011. **104**(7): p. 1160-1167.
215. Malizia, A.P., Keating, D.T., Smith, S.M., Walls, D., Doran, P.P., et al., *Alveolar epithelial cell injury with Epstein-Barr virus upregulates TGFbeta1 expression.* Am J Physiol Lung Cell Mol Physiol, 2008. **295**(3): p. L451-460.
216. Mora, A.L., Woods, C.R., Garcia, A., Xu, J., Rojas, M., et al., *Lung infection with gamma-herpesvirus induces progressive pulmonary fibrosis in Th2-biased mice.* Am J Physiol Lung Cell Mol Physiol, 2005. **289**(5): p. L711-721.
217. Shimamura, M., Murphy-Ullrich, J.E., and Britt, W.J., *Human cytomegalovirus induces TGF-beta1 activation in renal tubular epithelial cells after epithelial-to-mesenchymal transition.* PLoS Path, 2010. **6**(11): p. e1001170.
218. Li, T., Li, D., Cheng, L., Wu, H., Gao, Z., et al., *Epithelial-mesenchymal transition induced by hepatitis C virus core protein in cholangiocarcinoma.* Ann Surg Oncol, 2010. **17**(7): p. 1937-1944.
219. Corvol, H., Flamein, F., Epaud, R., Clement, A., and Guillot, L., *Lung alveolar epithelium and interstitial lung disease.* Int J Biochem Cell Biol, 2009. **41**(8-9): p. 1643-1651.

220. Zuo, W. and Chen, Y.G., *Specific activation of mitogen-activated protein kinase by transforming growth factor-beta receptors in lipid rafts is required for epithelial cell plasticity.* Mol Biol Cell, 2009. **20**(3): p. 1020-1029.
221. Zhang, Y.E., *Non-Smad pathways in TGF-beta signaling.* Cell Res, 2009. **19**(1): p. 128-139.
222. Zavadil, J., Bitzer, M., Liang, D., Yang, Y.C., Massimi, A., et al., *Genetic programs of epithelial cell plasticity directed by transforming growth factor-beta.* Proc Natl Acad Sci USA, 2001. **98**(12): p. 6686-6691.
223. Xie, L., Law, B.K., Chytil, A.M., Brown, K.A., Aakre, M.E., et al., *Activation of the Erk pathway is required for TGF-beta1-induced EMT in vitro.* Neoplasia, 2004. **6**(5): p. 603-610.
224. Wang, J., Kuiatse, I., Lee, A.V., Pan, J., Giuliano, A., et al., *Sustained c-Jun-NH2-kinase activity promotes epithelial-mesenchymal transition, invasion, and survival of breast cancer cells by regulating extracellular signal-regulated kinase activation.* Mol Cancer Res, 2010. **8**(2): p. 266-277.
225. Cho, H.J., Baek, K.E., Saika, S., Jeong, M.J., and Yoo, J., *Snail is required for transforming growth factor-beta-induced epithelial-mesenchymal transition by activating PI3 kinase/Akt signal pathway.* Biochem Biophys Res Commun, 2007. **353**(2): p. 337-343.
226. Klinghoffer, R.A., Sachsenmaier, C., Cooper, J.A., and Soriano, P., *Src family kinases are required for integrin but not PDGFR signal transduction.* EMBO J, 1999. **18**(9): p. 2459-2471.
227. Kim, A.N., Jeon, W.K., Lim, K.H., Lee, H.Y., Kim, W.J., et al., *Fyn mediates transforming growth factor-beta1-induced down-regulation of E-cadherin in human A549 lung cancer cells.* Biochem Biophys Res Commun, 2011. **407**(1): p. 181-184.
228. Castrillo, A., Joseph, S.B., Vaidya, S.A., Haberland, M., Fogelman, A.M., et al., *Crosstalk between LXR and toll-like receptor signaling mediates bacterial and viral antagonism of cholesterol metabolism.* Mol Cell, 2003. **12**(4): p. 805-816.
229. Sanchez, V. and Dong, J.J., *Alteration of lipid metabolism in cells infected with human cytomegalovirus.* Virology, 2010. **404**(1): p. 71-77.
230. Mujawar, Z., Rose, H., Morrow, M.P., Pushkarsky, T., Dubrovsky, L., et al., *Human immunodeficiency virus impairs reverse cholesterol transport from macrophages.* PLoS Biol, 2006. **4**(11): p. e365.
231. Arnold, R., Humbert, B., Werchau, H., Gallati, H., and Konig, W., *Interleukin-8, interleukin-6, and soluble tumour necrosis factor receptor type I release from a human pulmonary epithelial cell line (A549) exposed to respiratory syncytial virus.* Immunology, 1994. **82**(1): p. 126-133.
232. Gibbs, J.D., Ornoff, D.M., Igo, H.A., Zeng, J.Y., and Imani, F., *Cell cycle arrest by transforming growth factor beta1 enhances replication of respiratory syncytial virus in lung epithelial cells.* J Virol, 2009. **83**(23): p. 12424-12431.
233. Loveys, D.A., Kulkarni, S., and Atreya, P.L., *Role of type I IFNs in the in vitro attenuation of live, temperature-sensitive vaccine strains of human respiratory syncytial virus.* Virology, 2000. **271**(2): p. 390-400.
234. Konig, B., Krusat, T., Streckert, H.J., and Konig, W., *IL-8 release from human neutrophils by the respiratory syncytial virus is independent of viral replication.* J Leukoc Biol, 1996. **60**(2): p. 253-260.
235. Tsutsumi-Ishii, Y. and Nagaoka, I., *Modulation of human beta-defensin-2 transcription in pulmonary epithelial cells by lipopolysaccharide-stimulated mononuclear phagocytes via proinflammatory cytokine production.* J Immunol, 2003. **170**(8): p. 4226-4236.

236. Xie, X.H., Law, H.K., Wang, L.J., Li, X., Yang, X.Q., et al., *Lipopolysaccharide induces IL-6 production in respiratory syncytial virus-infected airway epithelial cells through the toll-like receptor 4 signaling pathway.* Pediatr Res, 2009. **65**(2): p. 156-162.
237. Khatri, P. and Draghici, S., *Ontological analysis of gene expression data: current tools, limitations, and open problems.* Bioinformatics, 2005. **21**(18): p. 3587-3595.
238. Swenson, E.S., Guest, I., Ilic, Z., Mazzeo-Helgevold, M., Lizardi, P., et al., *Hepatocyte nuclear factor-1 as marker of epithelial phenotype reveals marrow-derived hepatocytes, but not duct cells, after liver injury in mice.* Stem Cells, 2008. **26**(7): p. 1768-1777.
239. Mossman, D. and Scott, R.J., *Long term transcriptional reactivation of epigenetically silenced genes in colorectal cancer cells requires DNA hypomethylation and histone acetylation.* PLoS One, 2011. **6**(8): p. e23127.
240. Blais, D.R., Lyn, R.K., Joyce, M.A., Rouleau, Y., Steenbergen, R., et al., *Activity-based protein profiling identifies a host enzyme, carboxylesterase 1, which is differentially active during hepatitis C virus replication.* J Biol Chem, 2010. **285**(33): p. 25602-25612.
241. Ghosh, M.C., Makena, P.S., Gorantla, V., Sinclair, S.E., and Waters, C.M., *CXCR4 regulates migration of lung alveolar epithelial cells through activation of Rac1 and matrix metalloproteinase-2.* Am J Physiol Lung Cell Mol Physiol, 2012. **302**(9): p. L846-856.
242. Fiedler, M.A., Wernke-Dollries, K., and Stark, J.M., *Mechanism of RSV-induced IL-8 gene expression in A549 cells before viral replication.* Am J Physiol, 1996. **271**(6 Pt 1): p. L963-971.
243. Yeo, D.S., Chan, R., Brown, G., Ying, L., Sutejo, R., et al., *Evidence that selective changes in the lipid composition of raft-membranes occur during respiratory syncytial virus infection.* Virology, 2009. **386**(1): p. 168-182.
244. Kong, X., San Juan, H., Kumar, M., Behera, A.K., Mohapatra, A., et al., *Respiratory syncytial virus infection activates STAT signaling in human epithelial cells.* Biochem Biophys Res Commun, 2003. **306**(2): p. 616-622.
245. van Diepen, A., Brand, H.K., Sama, I., Lambooy, L.H., van den Heuvel, L.P., et al., *Quantitative proteome profiling of respiratory virus-infected lung epithelial cells.* J Proteomics, 2010. **73**(9): p. 1680-1693.
246. Bian, T., Gibbs, J.D., Orvell, C., and Imani, F., *Respiratory Syncytial Virus Matrix Protein Induces Lung Epithelial Cell Cycle Arrest through a p53 Dependent Pathway.* PLoS One, 2012. **7**(5): p. e38052.
247. Rooney, S.A. and Gobran, L.I., *Alveolar lavage and lavaged lung tissue phosphatidylcholine composition during fetal rabbit development.* Lipids, 1977. **12**(12): p. 1050-1054.
248. Mason, R.J. and Dobbs, L.G., *Synthesis of phosphatidylcholine and phosphatidylglycerol by alveolar type II cells in primary culture.* J Biol Chem, 1980. **255**(11): p. 5101-5107.
249. Giard, D.J., Aaronson, S.A., Todaro, G.J., Arnstein, P., Kersey, J.H., et al., *In vitro cultivation of human tumors: establishment of cell lines derived from a series of solid tumors.* J Natl Cancer Inst, 1973. **51**(5): p. 1417-1423.
250. Kolla, V., Gonzales, L.W., Gonzales, J., Wang, P., Angampalli, S., et al., *Thyroid transcription factor in differentiating type II cells: regulation, isoforms, and target genes.* Am J Respir Cell Mol Biol, 2007. **36**(2): p. 213-225.
251. Chawla, A., Boisvert, W.A., Lee, C.H., Laffitte, B.A., Barak, Y., et al., *A PPAR gamma-LXR-ABCA1 pathway in macrophages is involved in cholesterol efflux and atherogenesis.* Mol Cell, 2001. **7**(1): p. 161-171.

252. Repa, J.J., Turley, S.D., Lobaccaro, J.A., Medina, J., Li, L., et al., *Regulation of absorption and ABC1-mediated efflux of cholesterol by RXR heterodimers.* Science, 2000. **289**(5484): p. 1524-1529.
253. Costet, P., Luo, Y., Wang, N., and Tall, A.R., *Sterol-dependent transactivation of the ABC1 promoter by the liver X receptor/retinoid X receptor.* J Biol Chem, 2000. **275**(36): p. 28240-28245.
254. Greene, C.M. and McElvaney, N.G., *Toll-like receptor expression and function in airway epithelial cells.* Arch Immunol Ther Exp (Warsz), 2005. **53**(5): p. 418-427.
255. Cui, X., Yang, S.C., Sharma, S., Heuze-Vourc'h, N., and Dubinett, S.M., *IL-4 regulates COX-2 and PGE2 production in human non-small cell lung cancer.* Biochem Biophys Res Commun, 2006. **343**(4): p. 995-1001.
256. Bozyk, P.D. and Moore, B.B., *Prostaglandin E2 and the pathogenesis of pulmonary fibrosis.* Am J Respir Cell Mol Biol, 2011. **45**(3): p. 445-452.

7 Supplement

7.1 Supplemental data tables

7.1.1 Lipid analysis

In the following data tables, the complete mass spectrometric lipid analysis results are presented.

Table 7.1: Cellular lipid composition of PC.

	A549 [mean±SD]	P (A549) ANOVA	WT [mean±SD]	Q215K [mean±SD]	P (p.Q215K) ANOVA	E292V [mean±SD]	P (p.E292V) ANOVA
PC [ng/mg protein]	65.38 ± 33.07	---	57.61 ± 31.61	75.24 ± 35.79	*	66.54 ± 29.66	---
PC (% of total lipids]	30.68 ± 0.81	---	31.61 ± 1.45	32.02 ± 1.12	---	31.68 ± 0.88	---
PC (% of PL]	51.86 ± 1.25	---	52.09 ± 1.54	53.63 ± 1.04	---	52.88 ± 0.88	---
PC 34:1 [% of total PC]	26.75 ± 1.90	---	25.38 ± 1.39	24.00 ± 2.03	---	25.18 ± 0.89	---
PC 32:1 [% of total PC]	18.16 ± 1.31	---	17.41 ± 2.65	14.26 ± 1.64	**	14.50 ± 2.00	**
PC 36:2 [% of total PC]	9.92 ± 0.79	---	11.59 ± 1.64	12.74 ± 1.54	---	11.94 ± 0.96	---
PC 34:2 [% of total PC]	7.85 ± 0.94	---	8.82 ± 1.53	9.99 ± 1.43	---	8.02 ± 0.65	---
PC 32:0 [% of total PC]	3.26 ± 0.51	*	4.14 ± 0.56	3.89 ± 0.17	---	4.50 ± 0.51	---
PC O 34:1 [% of total PC]	4.82 ± 0.41	*	3.87 ± 0.37	4.92 ± 0.62	**	5.15 ± 0.41	**
PC 36:1 [% of total PC]	4.28 ± 0.74	*	3.61 ± 0.93	3.99 ± 1.03	---	4.03 ± 0.81	---
PC 30:0 [% of total PC]	3.06 ± 0.53	*	3.41 ± 0.49	2.68 ± 0.38	***	3.18 ± 0.28	---
PC 32:2 [% of total PC]	2.31 ± 0.51	---	2.47 ± 0.84	2.53 ± 0.84	---	1.72 ± 0.32	*
PC O 32:1 [% of total PC]	2.33 ± 0.51	---	2.00 ± 0.37	2.11 ± 0.58	---	2.41 ± 0.55	---
PC 36:3 [% of total PC]	1.57 ± 0.04	*	1.99 ± 0.27	2.04 ± 0.43	---	1.91 ± 0.39	---
PC O 34:2 [% of total PC]	2.41 ± 0.43	*	1.91 ± 0.24	2.91 ± 0.61	***	2.59 ± 0.31	**
PC O 36:2 [% of total PC]	1.80 ± 0.04	---	1.58 ± 0.17	2.23 ± 0.20	***	2.18 ± 0.17	***
PC O 32:0 [% of total PC]	1.32 ± 0.05	---	1.23 ± 0.16	1.38 ± 0.21	---	1.62 ± 0.16	**
PC O 36:1 [% of total PC]	1.45 ± 0.18	**	1.14 ± 0.25	1.35 ± 0.27	*	1.47 ± 0.24	**
PC 38:2 [% of total PC]	0.94 ± 0.08	---	1.12 ± 0.12	1.13 ± 0.12	---	1.16 ± 0.19	---
PC 38:4 [% of total PC]	0.71 ± 0.13	*	1.00 ± 0.21	0.88 ± 0.30	---	0.95 ± 0.29	---
PC 36:4 [% of total PC]	0.83 ± 0.18	---	0.91 ± 0.32	0.78 ± 0.31	---	0.79 ± 0.26	---
PC 38:5 [% of total PC]	0.71 ± 0.21	---	0.87 ± 0.37	0.88 ± 0.30	---	0.93 ± 0.33	---
PC 38:3 [% of total PC]	0.64 ± 0.03	---	0.80 ± 0.08	0.73 ± 0.10	---	0.81 ± 0.15	---
PC 30:1 [% of total PC]	0.64 ± 0.15	---	0.71 ± 0.20	0.51 ± 0.13	*	0.37 ± 0.13	***
PC 34:3 [% of total PC]	0.61 ± 0.06	---	0.66 ± 0.08	0.68 ± 0.03	---	0.54 ± 0.04	*
PC 38:6 [% of total PC]	0.71 ± 0.24	---	0.56 ± 0.29	0.60 ± 0.27	---	0.73 ± 0.19	---
PC O 34:0 [% of total PC]	0.51 ± 0.03	---	0.47 ± 0.03	0.46 ± 0.06	---	0.54 ± 0.05	*
PC 40:6 [% of total PC]	0.43 ± 0.13	---	0.39 ± 0.23	0.45 ± 0.16	---	0.53 ± 0.13	---
PC 36:5 [% of total PC]	0.40 ± 0.14	---	0.37 ± 0.17	0.35 ± 0.14	---	0.34 ± 0.11	---
PC 38:1 [% of total PC]	0.35 ± 0.06	---	0.34 ± 0.11	0.28 ± 0.10	---	0.35 ± 0.08	---
PC O 30:0 [% of total PC]	0.31 ± 0.04	---	0.29 ± 0.04	0.29 ± 0.02	---	0.34 ± 0.07	---
PC O 36:4 [% of total PC]	0.26 ± 0.05	---	0.25 ± 0.01	0.28 ± 0.02	---	0.30 ± 0.03	---
PC 40:5 [% of total PC]	0.17 ± 0.02	---	0.20 ± 0.06	0.24 ± 0.07	---	0.29 ± 0.05	**
PC O 36:5 [% of total PC]	0.18 ± 0.02	---	0.18 ± 0.07	0.21 ± 0.03	---	0.21 ± 0.04	---
PC 40:4 [% of total PC]	0.13 ± 0.02	---	0.14 ± 0.02	0.12 ± 0.03	---	0.14 ± 0.03	---
PC O 30:1 [% of total PC]	0.13 ± 0.03	---	0.11 ± 0.01	0.10 ± 0.02	---	0.13 ± 0.03	---
PC 34:0 [% of total PC]	0.06 ± 0.05	---	0.05 ± 0.05	0.02 ± 0.02	---	0.15 ± 0.10	---
PC 36:0 [% of total PC]	0.04 ± 0.02	---	0.03 ± 0.02	0.02 ± 0.02	---	0.05 ± 0.02	---
PC alkyl [% of total PC]	15.49 ± 1.19	*	13.03 ± 0.63	16.23 ± 1.88	**	16.92 ± 1.05	***
PC saturated [% of total PC]	6.42 ± 0.99	*	7.63 ± 0.86	6.61 ± 0.40	*	7.87 ± 0.62	---
PC monounsaturated [% of total PC]	50.17 ± 1.47	---	47.46 ± 2.74	43.04 ± 2.33	*	44.42 ± 2.20	---
PC polyunsaturated [% of total PC]	27.92 ± 1.24	*	31.89 ± 2.67	34.12 ± 2.20	---	30.79 ± 1.60	---
PC sum of unsaturated [% of total PC]	78.09 ± 0.56	---	79.34 ± 1.35	77.16 ± 1.71	---	75.21 ± 0.87	*

SD – standard deviation, P – P-value compared to WT, PC – phosphatidylcholine. *P<0.05, **P<0.01, ***P<0.001.

Table 7.2: Cellular lipid composition of PLPE.

	A549 [mean±SD]	P (A549) ANOVA	WT [mean±SD]	Q215K [mean±SD]	P (p.Q215K) ANOVA	E292V [mean±SD]	P (p.E292V) ANOVA
PLPE [nmol/mg protein]	37.42 ± 19.26	---	30.48 ± 14.08	38.77 ± 16.19	---	35.36 ± 14.96	---
PLPE [% of total lipids]	17.49 ± 0.28	---	17.46 ± 1.45	17.01 ± 1.39	---	17.04 ± 0.78	---
PLPE 16:0/18:1 [% of total PLPE]	20.42 ± 1.11	*	16.80 ± 2.91	22.79 ± 2.62	**	20.97 ± 3.08	*
PLPE 16:0/20:4 [% of total PLPE]	12.11 ± 1.91	---	13.25 ± 3.63	9.89 ± 3.15	**	11.37 ± 2.19	---
PLPE 18:1/18:1 [% of total PLPE]	7.14 ± 0.79	---	8.78 ± 2.63	11.80 ± 3.63	---	10.34 ± 2.05	---
PLPE 16:0/20:3 [% of total PLPE]	6.16 ± 1.26	---	7.59 ± 2.41	4.35 ± 0.36	*	5.19 ± 0.40	---
PLPE 16:0/20:5 [% of total PLPE]	5.87 ± 1.26	---	5.79 ± 1.91	4.90 ± 1.77	---	5.10 ± 1.05	---
PLPE 16:0/22:6 [% of total PLPE]	8.32 ± 0.56	**	4.71 ± 2.08	2.94 ± 1.29	---	4.45 ± 1.62	---
PLPE 16:0/16:1 [% of total PLPE]	4.96 ± 1.28	---	4.51 ± 1.75	6.24 ± 2.56	*	4.71 ± 1.57	---
PLPE 16:0/18:2 [% of total PLPE]	5.14 ± 0.63	---	4.27 ± 0.55	5.62 ± 1.40	*	4.71 ± 0.64	---
PLPE 18:0/18:1 [% of total PLPE]	4.20 ± 0.77	---	3.76 ± 0.97	4.46 ± 0.94	*	5.13 ± 1.33	***
PLPE 18:0/20:4 [% of total PLPE]	3.05 ± 1.06	---	3.43 ± 1.86	2.46 ± 1.13	---	3.19 ± 1.67	---
PLPE 18:1/20:4 [% of total PLPE]	2.06 ± 0.26	*	3.43 ± 0.98	2.82 ± 0.76	---	2.88 ± 1.11	---
PLPE 18:1/16:1 [% of total PLPE]	2.20 ± 0.74	---	2.87 ± 0.85	3.87 ± 1.61	---	2.67 ± 0.81	---
PLPE 18:1/16:0 [% of total PLPE]	1.09 ± 0.05	*	2.37 ± 0.54	2.76 ± 0.87	---	2.55 ± 0.64	---
PLPE 18:1/18:2 [% of total PLPE]	1.77 ± 0.19	---	2.23 ± 0.34	2.37 ± 0.49	---	2.18 ± 0.36	---
PLPE 18:1/20:3 [% of total PLPE]	0.85 ± 0.28	*	1.42 ± 0.54	0.91 ± 0.22	---	0.91 ± 0.19	---
PLPE 18:0/20:5 [% of total PLPE]	1.35 ± 0.47	---	1.36 ± 0.72	0.97 ± 0.45	---	1.28 ± 0.51	---
PLPE 18:0/20:3 [% of total PLPE]	1.15 ± 0.04	---	1.31 ± 0.30	0.74 ± 0.17	*	1.09 ± 0.27	---
PLPE 18:1/20:5 [% of total PLPE]	0.81 ± 0.18	*	1.20 ± 0.33	0.94 ± 0.15	---	1.06 ± 0.30	---
PLPE 16:0/18:3 [% of total PLPE]	1.08 ± 0.38	---	1.16 ± 0.56	0.83 ± 0.18	---	0.85 ± 0.20	---
PLPE 16:0/22:5 [% of total PLPE]	1.30 ± 0.18	---	0.99 ± 0.30	0.74 ± 0.20	---	0.80 ± 0.15	---
PLPE 18:0/18:2 [% of total PLPE]	1.09 ± 0.33	---	0.97 ± 0.31	1.18 ± 0.60	---	1.25 ± 0.58	---
PLPE 16:0/22:3 [% of total PLPE]	0.82 ± 0.29	---	0.91 ± 0.46	0.61 ± 0.11	---	0.72 ± 0.11	---
PLPE 16:0/16:0 [% of total PLPE]	0.64 ± 0.05	**	0.85 ± 0.05	0.86 ± 0.06	---	0.83 ± 0.11	---
PLPE 18:0/16:1 [% of total PLPE]	0.93 ± 0.11	---	0.83 ± 0.17	0.98 ± 0.10	---	0.96 ± 0.06	---
PLPE 18:1/18:3 [% of total PLPE]	0.54 ± 0.20	---	0.79 ± 0.35	0.55 ± 0.15	---	0.59 ± 0.19	---
PLPE 16:0/22:4 [% of total PLPE]	0.68 ± 0.14	---	0.66 ± 0.20	0.49 ± 0.08	---	0.62 ± 0.17	---
PLPE 18:0/22:6 [% of total PLPE]	1.11 ± 0.24	**	0.63 ± 0.27	0.39 ± 0.14	---	0.63 ± 0.14	---
PLPE 18:1/22:6 [% of total PLPE]	0.86 ± 0.19	---	0.61 ± 0.11	0.43 ± 0.13	---	0.57 ± 0.14	---
PLPE 16:0/18:0 [% of total PLPE]	0.26 ± 0.13	---	0.41 ± 0.09	0.36 ± 0.07	---	0.41 ± 0.13	---
PLPE 18:1/18:0 [% of total PLPE]	0.36 ± 0.14	---	0.38 ± 0.10	0.40 ± 0.11	---	0.45 ± 0.12	---
PLPE 18:0/18:3 [% of total PLPE]	0.25 ± 0.06	---	0.28 ± 0.09	0.19 ± 0.03	---	0.23 ± 0.02	---
PLPE 18:0/22:5 [% of total PLPE]	0.29 ± 0.06	---	0.24 ± 0.05	0.16 ± 0.04	---	0.20 ± 0.03	---
PLPE 18:0/16:0 [% of total PLPE]	0.20 ± 0.04	---	0.23 ± 0.01	0.24 ± 0.03	---	0.26 ± 0.06	---
PLPE 18:0/22:3 [% of total PLPE]	0.19 ± 0.07	---	0.20 ± 0.07	0.13 ± 0.03	---	0.16 ± 0.04	---
PLPE 18:1/22:3 [% of total PLPE]	0.18 ± 0.09	---	0.20 ± 0.07	0.15 ± 0.04	---	0.17 ± 0.05	---
PLPE 18:1/22:5 [% of total PLPE]	0.19 ± 0.06	---	0.18 ± 0.02	0.14 ± 0.04	---	0.16 ± 0.03	---
PLPE 18:1/22:4 [% of total PLPE]	0.16 ± 0.06	---	0.17 ± 0.05	0.13 ± 0.03	---	0.15 ± 0.02	---
PLPE 18:0/22:4 [% of total PLPE]	0.18 ± 0.05	---	0.16 ± 0.04	0.13 ± 0.03	---	0.16 ± 0.02	---
PLPE 18:0/18:0 [% of total PLPE]	0.08 ± 0.06	---	0.10 ± 0.05	0.08 ± 0.04	---	0.09 ± 0.06	---
PLPE 16:0 sum [% of total PLPE]	67.75 ± 1.21	---	61.88 ± 4.70	60.60 ± 4.92	---	60.72 ± 4.70	---
PLPE 18:0 sum [% of total PLPE]	14.05 ± 2.40	---	13.49 ± 3.29	12.13 ± 3.11	---	14.59 ± 4.26	---
PLPE 18:1 sum [% of total PLPE]	18.20 ± 2.15	*	24.62 ± 4.71	27.27 ± 6.24	---	24.68 ± 3.87	---

SD – standard deviation, P – P-value compared to WT, PLPE – plasmenylethanolamine. *P<0.05, **P<0.01, ***P<0.001.

Table 7.3: Cellular chololesterol composition.

	A549 [mean±SD]	P (A549) ANOVA	WT [mean±SD]	Q215K [mean±SD]	P (p.Q215K) ANOVA	E292V [mean±SD]	P (p.E292V) ANOVA
TC [nmol/mg protein]	49.15 ± 25.55	---	38.90 ± 21.37	52.94 ± 27.36	*	47.52 ± 23.33	---
TC[% of total lipids]	22.97 ± 0.77	---	21.55 ± 0.77	22.58 ± 2.31	---	22.56 ± 1.53	---
CE [nmol/mg protein]	3.08 ± 0.77	---	4.75 ± 3.58	7.78 ± 2.96	*	6.83 ± 2.94	*
CE [% of total lipids]	1.70 ± 0.79	---	2.72 ± 1.17	3.60 ± 0.97	---	3.39 ± 0.79	---
FC [nmol/mg protein]	46.07 ± 25.14	*	34.14 ± 19.81	45.15 ± 25.50	---	40.70 ± 21.53	---
FC [% of total lipids]	21.22 ± 1.30	*	18.67 ± 1.90	18.96 ± 2.52	---	19.05 ± 2.14	---
CE 18:1 [% of total CE]	28.73 ± 2.74	---	33.35 ± 6.64	37.70 ± 2.14	---	36.30 ± 2.99	---
CE 16:0 [% of total CE]	15.40 ± 1.01	---	14.40 ± 2.76	15.23 ± 2.39	---	16.60 ± 2.59	---
CE 16:1 [% of total CE]	13.20 ± 1.41	---	12.28 ± 2.00	11.98 ± 1.67	---	11.53 ± 1.79	---
CE 20:0 [% of total CE]	10.03 ± 2.34	---	7.68 ± 3.21	4.38 ± 0.59	---	4.85 ± 1.05	---
CE 18:2 [% of total CE]	5.63 ± 0.56	---	6.18 ± 1.55	5.43 ± 0.80	---	5.75 ± 0.85	---
CE 22:6 [% of total CE]	5.33 ± 1.35	---	4.85 ± 1.02	5.93 ± 0.33	---	4.90 ± 0.55	---
CE 18:0 [% of total CE]	5.75 ± 0.48	**	4.50 ± 0.49	4.23 ± 0.46	---	4.78 ± 0.62	---
CE 14:0 [% of total CE]	2.80 ± 0.47	---	2.38 ± 0.24	2.15 ± 0.34	---	2.30 ± 0.36	---
CE 20:1 [% of total CE]	1.90 ± 0.33	---	2.43 ± 1.11	2.30 ± 0.99	---	2.10 ± 1.18	---
CE 20:4 [% of total CE]	2.18 ± 0.39	---	2.25 ± 0.39	2.68 ± 0.57	---	3.03 ± 0.56	*
CE 15:0 [% of total CE]	2.63 ± 0.67	---	2.10 ± 0.67	1.43 ± 0.17	---	1.65 ± 0.26	---
CE 22:5 [% of total CE]	1.13 ± 0.21	---	1.28 ± 0.68	1.25 ± 0.65	---	1.00 ± 0.67	---
CE 20:2 [% of total CE]	0.98 ± 0.31	---	1.25 ± 0.31	0.93 ± 0.30	---	0.83 ± 0.50	---
CE 20:3 [% of total CE]	1.30 ± 0.18	---	1.23 ± 0.30	1.13 ± 0.25	---	1.05 ± 0.24	---
CE 20:5 [% of total CE]	1.15 ± 0.24	---	1.18 ± 0.43	1.03 ± 0.13	---	1.25 ± 0.21	---
CE 22:1 [% of total CE]	0.83 ± 0.59	---	1.13 ± 0.51	1.03 ± 0.43	---	0.90 ± 0.76	---
CE 18:3 [% of total CE]	0.98 ± 0.17	---	1.03 ± 0.28	0.85 ± 0.17	---	0.95 ± 0.13	---
CE 22:4 [% of total CE]	0.18 ± 0.24	---	0.55 ± 0.25	0.35 ± 0.24	---	0.20 ± 0.28	---
CE saturated [% of total CE]	36.55 ± 3.38	---	31.08 ± 6.64	27.45 ± 2.94	---	30.23 ± 3.96	---
CE monounsaturated [% of total CE]	44.63 ± 3.59	---	49.20 ± 6.79	52.98 ± 3.35	---	50.80 ± 3.33	---
CE polyunsaturated [% of total CE]	18.83 ± 1.37	---	19.73 ± 0.95	19.60 ± 1.52	---	18.98 ± 1.17	---
CE sum of unsaturated [% of total CE]	63.45 ± 3.38	---	68.93 ± 6.64	72.55 ± 2.94	---	69.78 ± 3.96	---
CE [% of total cholesterol]	7.45 ± 3.52	*	12.85 ± 5.80	16.08 ± 4.37	---	15.29 ± 4.10	---
FC [% of total cholesterol]	92.56 ± 3.52	*	87.15 ± 5.80	83.93 ± 4.37	---	84.71 ± 4.10	---

SD – standard deviation, P – P-value compared to WT, TC – total cholesterol, FC – free cholesterol, CE – cholesterol esters. *P<0.05, **P<0.01.

Table 7.4: Cellular lipid composition of PI.

	A549 [mean±SD]	P (A549) ANOVA	WT [mean±SD]	Q215K [mean±SD]	P (p.Q215K) ANOVA	E292V [mean±SD]	P (p.E292V) ANOVA
PI [ng/mg protein]	18.90 ± 8.64	---	16.50 ± 7.49	21.18 ± 8.87	*	18.55 ± 7.45	---
PI [% of total lipids]	9.11 ± 0.93	---	9.50 ± 1.08	9.23 ± 1.08	---	9.02 ± 1.04	---
PI (% of PL]	15.40 1.47	---	15.68 1.92	15.45 1.59	---	15.04 1.56	---
PI 38:3 [% of total PI]	26.13 ± 6.00	---	31.37 ± 8.74	23.12 ± 4.64	*	24.03 ± 3.41	*
PI 38:4 [% of total PI]	27.39 ± 3.71	---	24.18 ± 7.45	29.44 ± 6.72	---	28.10 ± 7.08	---
PI 34:0 [% of total PI]	23.91 ± 11.36	---	26.49 ± 11.24	22.04 ± 11.29	---	24.06 ± 10.79	---
PI 36:2 [% of total PI]	9.20 ± 0.41	---	10.46 ± 0.85	11.16 ± 1.51	---	11.19 ± 1.89	---
PI 36:1 [% of total PI]	4.91 ± 1.33	---	5.68 ± 1.20	4.69 ± 1.19	---	4.62 ± 0.62	---
PI 38:2 [% of total PI]	3.77 ± 0.70	---	4.52 ± 1.32	3.85 ± 1.51	---	4.40 ± 1.29	---
PI 38:5 [% of total PI]	5.05 ± 0.80	*	3.88 ± 1.42	6.68 ± 1.36	***	6.53 ± 0.97	***
PI 36:3 [% of total PI]	4.07 ± 0.89	---	3.79 ± 1.21	3.80 ± 1.14	---	3.60 ± 0.92	---
PI 34:1 [% of total PI]	3.27 ± 0.72	---	2.94 ± 0.37	2.40 ± 0.36	---	2.30 ± 0.51	---
PI 34:2 [% of total PI]	2.23 ± 0.32	---	2.53 ± 0.76	3.23 ± 0.78	---	2.37 ± 0.68	---
PI 40:6 [% of total PI]	4.60 ± 1.52	*	2.26 ± 1.33	3.33 ± 1.28	---	4.34 ± 1.75	---
PI 40:4 [% of total PI]	1.95 ± 0.11	---	2.12 ± 0.18	1.95 ± 0.15	---	2.16 ± 0.25	---
PI 40:3 [% of total PI]	1.57 ± 0.56	---	2.07 ± 0.76	1.21 ± 0.47	---	1.38 ± 0.43	*
PI 36:4 [% of total PI]	2.13 ± 0.38	**	1.35 ± 0.43	1.68 ± 0.38	---	1.42 ± 0.34	---
PI 40:5 [% of total PI]	1.85 ± 0.41	---	1.47 ± 0.66	1.78 ± 0.42	---	1.88 ± 0.29	---
PI 38:6 [% of total PI]	1.12 ± 0.31	---	0.64 ± 0.25	0.96 ± 0.28	---	1.04 ± 0.30	---
PI 36:0 [% of total PI]	0.24 ± 0.13	---	0.24 ± 0.07	0.25 ± 0.13	---	0.21 ± 0.10	---
PI 34:3 [% of total PI]	0.27 ± 0.08	---	0.26 ± 0.13	0.26 ± 0.09	---	0.21 ± 0.09	---
PI saturated [% of total PI]	0.53 ± 0.16	---	0.51 ± 0.12	0.47 ± 0.18	---	0.45 ± 0.15	---
PI monounsaturated [% of total PI]	8.18 ± 2.04	---	8.62 ± 1.50	7.09 ± 1.45	---	6.92 ± 1.05	---
PI polyunsaturated [% of total PI]	91.30 ± 1.98	---	90.88 ± 1.40	92.44 ± 1.35	---	92.63 ± 1.09	---
PI unsaturated [% of total PI]	99.48 ± 0.16	---	99.50 ± 0.12	99.53 ± 0.18	---	99.55 ± 0.15	---

SD – standard deviation, P – P-value compared to WT, PI – phosphatidylinositol. *P<0.05, **P<0.01, ***P<0.001.

Table 7.5: Cellular lipid composition of PE.

	A549 [mean±SD]	P (A549) ANOVA	WT [mean±SD]	Q215K [mean±SD]	P (p.Q215K) ANOVA	E292V [mean±SD]	P (p.E292V) ANOVA
PE [ng/mg protein]	16.11 ± 9.34	---	15.62 ± 9.34	18.24 ± 9.69	---	16.29 ± 8.97	---
PE [% of total lipids]	7.29 ± 0.86	*	8.35 ± 1.07	7.49 ± 1.29	*	7.41 ± 1.13	*
PE (% of PL]	12.32 ± 1.47	*	13.75 ± 1.62	12.49 ± 1.71	---	12.35 ± 1.70	*
PE 36:2 [% of total PE]	15.51 ± 0.93	---	19.45 ± 2.60	23.00 ± 3.58	---	21.33 ± 1.95	---
PE 38:4 [% of total PE]	12.58 ± 3.40	---	13.27 ± 4.18	11.69 ± 4.83	---	11.79 ± 4.72	---
PE 34:1 [% of total PE]	12.98 ± 0.49	*	11.53 ± 1.06	11.73 ± 0.99	---	11.69 ± 1.54	---
PE 36:1 [% of total PE]	8.36 ± 1.21	---	8.12 ± 1.08	7.78 ± 1.21	---	8.28 ± 1.23	---
PE 34:2 [% of total PE]	6.59 ± 1.81	---	6.67 ± 2.14	9.34 ± 2.98	**	6.88 ± 2.29	---
PE 38:5 [% of total PE]	5.47 ± 1.43	*	6.25 ± 1.68	6.20 ± 1.59	---	6.05 ± 1.82	---
PE O 40:3 [% of total PE]	6.81 ± 1.93	---	5.92 ± 1.94	4.94 ± 2.18	---	5.79 ± 2.33	---
PE 38:3 [% of total PE]	3.31 ± 0.48	---	4.03 ± 1.11	2.56 ± 0.23	*	3.15 ± 0.52	---
PE 36:3 [% of total PE]	2.83 ± 0.16	---	3.08 ± 0.17	3.35 ± 0.16	---	3.20 ± 0.20	---
PE 40:6 [% of total PE]	5.23 ± 0.90	***	2.75 ± 1.05	1.89 ± 0.53	---	2.68 ± 0.56	---
PE 32:1 [% of total PE]	3.24 ± 0.80	**	2.61 ± 0.80	2.56 ± 0.67	---	2.50 ± 0.81	---
PE 36:4 [% of total PE]	2.34 ± 0.33	---	2.26 ± 0.35	1.76 ± 0.38	***	1.89 ± 0.28	***
PE 38:6 [% of total PE]	2.49 ± 0.38	*	2.19 ± 0.36	1.91 ± 0.29	*	2.13 ± 0.17	---
PE 38:2 [% of total PE]	1.52 ± 0.12	---	1.91 ± 0.34	2.16 ± 0.56	---	2.39 ± 0.47	---
PE 40:5 [% of total PE]	1.45 ± 0.10	---	1.61 ± 0.19	1.50 ± 0.24	---	1.66 ± 0.24	---
PE 40:4 [% of total PE]	1.54 ± 0.19	---	1.45 ± 0.19	1.06 ± 0.12	---	1.51 ± 0.23	---
PE 40:3 [% of total PE]	1.00 ± 0.28	---	1.11 ± 0.36	0.72 ± 0.19	*	0.98 ± 0.21	---
PE O 38:7 [% of total PE]	1.16 ± 0.18	**	0.82 ± 0.18	0.67 ± 0.16	---	0.90 ± 0.24	---
PE 36:5 [% of total PE]	0.84 ± 0.15	---	0.78 ± 0.16	0.71 ± 0.14	---	0.69 ± 0.07	---
PE 42:7 [% of total PE]	0.90 ± 0.19	---	0.72 ± 0.29	0.64 ± 0.17	---	0.73 ± 0.20	---
PE 32:2 [% of total PE]	0.68 ± 0.28	---	0.61 ± 0.31	0.98 ± 0.46	**	0.60 ± 0.29	---
PE 34:0 [% of total PE]	0.64 ± 0.05	---	0.57 ± 0.03	0.53 ± 0.08	---	0.68 ± 0.04	---
PE 42:5 [% of total PE]	0.54 ± 0.05	---	0.55 ± 0.06	0.46 ± 0.12	---	0.57 ± 0.08	---
PE 34:3 [% of total PE]	0.61 ± 0.15	---	0.54 ± 0.17	0.67 ± 0.15	*	0.52 ± 0.14	---
PE 32:0 [% of total PE]	0.45 ± 0.06	*	0.39 ± 0.07	0.40 ± 0.07	---	0.50 ± 0.09	***
PE 42:6 [% of total PE]	0.56 ± 0.04	*	0.42 ± 0.08	0.44 ± 0.04	---	0.53 ± 0.08	---
PE 38:1 [% of total PE]	0.42 ± 0.05	---	0.43 ± 0.06	0.34 ± 0.06	---	0.44 ± 0.04	---
PE saturated [% of total PE]	1.08 ± 0.11	---	0.96 ± 0.08	0.93 ± 0.02	---	1.17 ± 0.10	**
PE monounsaturated [% of total PE]	24.57 ± 0.64	*	22.26 ± 1.36	22.07 ± 1.43	---	22.46 ± 1.89	---
PE polyunsaturated [% of total PE]	66.38 ± 2.26	*	70.04 ± 3.40	71.40 ± 2.93	---	69.68 ± 3.56	---
PE sum of unsaturated [% of total PE]	90.95 ± 2.22	---	92.30 ± 2.19	93.46 ± 2.31	---	92.14 ± 2.64	---
PE alkylated [% of total PE]	7.97 ± 2.12	---	6.74 ± 2.11	5.61 ± 2.32	---	6.69 ± 2.57	---

SD – standard deviation, P – P-value compared to WT, PE – phosphatidylethanolamine. *P<0.05, **P<0.01, ***P<0.001.

Table 7.6: Cellular lipid composition of PS.

	A549 [mean±SD]	P (A549) ANOVA	WT [mean±SD]	Q215K [mean±SD]	P (p.Q215K) ANOVA	E292V [mean±SD]	P (p.E292V) ANOVA
PS [ng/mg protein]	15.36 ± 8.11	*	11.60 ± 6.31	13.78 ± 7.46	---	13.32 ± 6.56	---
PS [% of total lipids]	7.13 ± 0.20	*	6.44 ± 0.52	5.83 ± 0.66	---	6.32 ± 0.59	---
PS (% of PL]	12.05 ± 0.45	*	10.63 ± 0.99	9.80 ± 1.42	**	10.56 ± 1.21	*
PS 36:1 [% of total PS]	42.96 ± 1.12	*	48.51 ± 2.85	47.74 ± 2.96	---	49.23 ± 2.54	---
PS 34:1 [% of total PS]	15.61 ± 1.99	---	15.99 ± 1.66	16.49 ± 1.78	---	14.35 ± 2.11	*
PS 36:2 [% of total PS]	11.16 ± 0.73	---	12.46 ± 1.02	14.40 ± 1.11	*	14.05 ± 1.12	---
PS 40:7 [% of total PS]	9.79 ± 5.02	---	11.13 ± 5.44	9.15 ± 3.80	---	9.50 ± 3.81	---
PS 38:4 [% of total PS]	3.93 ± 0.91	---	4.67 ± 1.89	4.96 ± 1.76	---	3.90 ± 1.99	---
PS 38:3 [% of total PS]	2.02 ± 0.84	---	2.33 ± 0.69	1.01 ± 0.72	**	1.58 ± 1.06	---
PS 38:5 [% of total PS]	1.23 ± 0.42	---	1.72 ± 0.18	1.60 ± 0.04	---	1.41 ± 0.14	---
PS 40:6 [% of total PS]	7.07 ± 3.71	*	1.12 ± 2.24	0.00 ± 0.00	---	0.79 ± 1.57	---
PS 34:2 [% of total PS]	0.93 ± 0.26	---	0.78 ± 0.58	2.02 ± 0.55	*	1.58 ± 0.56	---
PS 38:1 [% of total PS]	0.97 ± 0.84	---	0.71 ± 0.85	0.46 ± 0.68	---	1.20 ± 0.36	---
PS 32:1 [% of total PS]	2.05 ± 0.69	---	0.61 ± 0.71	1.66 ± 1.17	---	0.90 ± 0.77	---
PS 38:2 [% of total PS]	0.87 ± 0.24	---	0.49 ± 0.60	0.74 ± 0.33	---	1.46 ± 0.24	*
PS 36:3 [% of total PS]	0.63 ± 0.54	---	0.36 ± 0.53	0.49 ± 0.56	---	0.68 ± 0.55	---
PS saturated [% of total PS]	0.00		0.00	0.24		0.43	
PS monounsaturated [% of total PS]	61.59 ± 2.37	---	65.82 ± 2.13	66.34 ± 2.46	---	65.67 ± 0.68	---
PS polyunsaturated [% of total PS]	38.42 ± 2.37	---	34.19 ± 2.13	33.60 ± 2.58	---	34.23 ± 0.90	---
PS unsaturated [% of total PS]	100.00 ± 0.00	---	100.00 ± 0.00	99.94 ± 0.12	---	99.89 ± 0.22	---

SD – standard deviation, P – P-value compared to WT, PS – phosphatidylserine. *P<0.05, **P<0.01.

Table 7.7: Cellular lipid composition of SPM and dihydro SPM.

	A549 [mean±SD]	P (A549) ANOVA	WT [mean±SD]	Q215K [mean±SD]	P (p.Q215K) ANOVA	E292V [mean±SD]	P (p.E292V) ANOVA
SPM [nmol/mg protein]	8.08 ± 4.60	---	6.53 ± 4.13	9.06 ± 5.85	---	8.83 ± 5.10	---
SPM [% of total lipids]	3.69 ± 0.40	---	3.50 ± 0.54	3.67 ± 0.73	---	4.05 ± 0.63	**
SPM (% of PL)	6.24 ± 0.73	---	5.78 ± 0.90	6.16 ± 1.27	---	6.78 ± 1.12	*
SPM 16:0 [% of total SPM]	58.82 ± 2.01	***	46.23 ± 3.26	54.55 ± 2.45	***	52.07 ± 2.39	***
SPM 24:1 [% of total SPM]	13.37 ± 0.46	***	22.38 ± 2.08	16.75 ± 1.95	***	17.79 ± 1.45	**
SPM 24:0 [% of total SPM]	8.71 ± 2.23	***	11.49 ± 2.39	7.27 ± 1.92	***	8.23 ± 2.18	***
SPM 18:0 [% of total SPM]	2.23 ± 0.57	*	3.59 ± 0.53	3.72 ± 0.61	---	4.50 ± 0.49	---
SPM 14:0 [% of total SPM]	3.02 ± 0.14	*	2.73 ± 0.06	2.87 ± 0.20	---	2.71 ± 0.13	---
SPM 24:2 [% of total SPM]	2.04 ± 0.13	*	2.66 ± 0.48	2.73 ± 0.17	---	2.55 ± 0.22	---
SPM 16:1 [% of total SPM]	3.17 ± 0.16	***	2.38 ± 0.34	2.58 ± 0.24	---	2.31 ± 0.07	---
SPM 16:1-OH [% of total SPM]	2.37 ± 0.38	---	2.01 ± 0.32	2.45 ± 0.50	---	2.22 ± 0.32	---
SPM 22:1 [% of total SPM]	1.45 ± 0.27	---	1.93 ± 0.39	2.01 ± 0.26	---	2.10 ± 0.32	---
SPM 15:0 [% of total SPM]	2.34 ± 0.10	*	1.87 ± 0.14	2.26 ± 0.27	---	2.04 ± 0.18	---
SPM 18:1 [% of total SPM]	1.05 ± 0.07	*	1.22 ± 0.09	1.17 ± 0.13	---	1.10 ± 0.12	---
SPM 16:0-OH [% of total SPM]	0.80 ± 0.25	---	0.47 ± 0.16	0.72 ± 0.11	---	0.97 ± 0.46	---
SPM 22:2 [% of total SPM]	0.21 ± 0.12	---	0.26 ± 0.10	0.32 ± 0.10	---	0.28 ± 0.12	---
SPM 20:1 [% of total SPM]	0.20 ± 0.14	---	0.25 ± 0.05	0.30 ± 0.07	---	0.17 ± 0.07	---
SPM 24:3 [% of total SPM]	0.07 ± 0.07	---	0.11 ± 0.08	0.05 ± 0.02	---	0.07 ± 0.06	---
SPM saturated [% of total SPM]	76.07 ± 1.01	***	66.82 ± 3.06	71.64 ± 2.07	**	71.44 ± 2.01	**
SPM monounsaturated [% of total SPM]	21.61 ± 1.02	***	30.16 ± 2.74	25.26 ± 2.08	**	25.67 ± 1.77	**
SPM polyunsaturated [% of total SPM]	2.32 ± 0.06	*	3.03 ± 0.44	3.10 ± 0.18	---	2.90 ± 0.27	---
SPM unsaturated [% of total SPM]	23.93 ± 1.01	***	33.19 ± 3.06	28.36 ± 2.07	**	28.57 ± 2.01	**
dih-SPM [nmol/mg protein]	1.27 ± 0.72	---	1.14 ± 0.84	1.76 ± 1.21	*	1.47 ± 0.83	---
dih-SPM [% of total lipids]	0.58 ± 0.10	---	0.57 ± 0.18	0.68 ± 0.20	---	0.66 ± 0.10	---
dih-SPM (% of PL)	0.98 ± 0.17	---	0.93 ± 0.27	1.13 ± 0.32	---	1.11 ± 0.16	---
dih-SPM 16:0 [% of total dih-SPM]	47.79 ± 5.24	---	52.25 ± 5.63	50.46 ± 3.08	---	56.00 ± 8.22	---
dih-SPM 20:0 [% of total dih-SPM]	26.70 ± 2.74	---	27.61 ± 2.15	31.89 ± 11.42	---	25.72 ± 7.31	---
dih-SPM 18:0 [% of total dih-SPM]	20.99 ± 9.87	---	14.64 ± 6.46	13.52 ± 9.36	---	13.40 ± 2.60	---
dih-SPM 22:0 [% of total dih-SPM]	4.51 ± 2.54	---	5.50 ± 1.15	4.13 ± 1.74	---	4.90 ± 2.10	---

SD – standard deviation, P – P-value compared to WT, SPM – sphingomyelin, dih – dihydro. *P<0.05, **P<0.01, ***P<0.001.

Table 7.8: Cellular lipid composition of LPC.

	A549 [mean±SD]	P (A549) ANOVA	WT [mean±SD]	Q215K [mean±SD]	P (p.Q215K) ANOVA	E292V [mean±SD]	P (p.E292V) ANOVA
LPC [nmol/mg protein]	0.99 ± 0.34	---	0.86 ± 0.23	1.27 ± 0.46	---	1.13 ± 0.32	---
LPC [% of total lipids]	0.52 ± 0.17	---	0.55 ± 0.19	0.62 ± 0.28	---	0.61 ± 0.24	---
LPC (% of PL)	0.88 ± 0.28	---	0.90 ± 0.33	1.04 ± 0.47	---	1.02 ± 0.40	---
LPC 18:1 [% of total LPC]	45.57 ± 11.34	---	42.54 ± 12.83	46.41 ± 11.45	---	44.59 ± 11.34	---
LPC 16:0 [% of total LPC]	15.59 ± 5.97	---	15.64 ± 5.10	15.01 ± 5.63	---	15.69 ± 5.10	---
LPC 16:1 [% of total LPC]	10.93 ± 3.65	---	11.56 ± 4.93	11.11 ± 5.48	---	9.62 ± 4.19	---
LPC 18:0 [% of total LPC]	10.10 ± 8.01	---	10.67 ± 10.08	10.40 ± 8.24	---	12.17 ± 8.71	---
LPC 18:2 [% of total LPC]	3.28 ± 0.57	---	3.45 ± 0.76	3.62 ± 0.63	---	3.35 ± 0.66	---
LPC 20:4 [% of total LPC]	2.25 ± 0.24	---	2.47 ± 0.70	2.21 ± 0.39	---	2.44 ± 0.43	---
LPC 20:3 [% of total LPC]	2.20 ± 0.25	---	2.49 ± 0.14	2.04 ± 0.06	*	2.05 ± 0.14	*
LPC 22:0 [% of total LPC]	1.93 ± 0.31	---	2.09 ± 0.54	1.51 ± 0.52	---	1.65 ± 0.57	---
LPC 22:6 [% of total LPC]	1.84 ± 0.27	---	1.75 ± 0.56	1.53 ± 0.64	---	1.82 ± 0.41	---
LPC 22:5 [% of total LPC]	1.30 ± 0.45	---	1.57 ± 0.48	1.36 ± 0.50	---	1.54 ± 0.37	---
LPC 22:4 [% of total LPC]	1.14 ± 0.24	---	1.46 ± 0.35	1.18 ± 0.38	---	1.27 ± 0.31	---
LPC 20:0 [% of total LPC]	1.19 ± 0.33	---	1.22 ± 0.40	1.12 ± 0.36	---	1.15 ± 0.40	---
LPC 20:5 [% of total LPC]	0.85 ± 0.20	---	1.13 ± 0.22	0.88 ± 0.17	---	0.97 ± 0.08	---
LPC 15:0 [% of total LPC]	1.11 ± 0.21	---	1.08 ± 0.21	0.95 ± 0.26	---	0.94 ± 0.20	---
LPC 18:3 [% of total LPC]	0.75 ± 0.23	---	0.90 ± 0.18	0.68 ± 0.14	---	0.76 ± 0.13	---
SPC [% of total LPC]	0.44 ± 0.09	---	0.66 ± 0.25	0.44 ± 0.31	---	0.32 ± 0.19	---
LPC saturated [% of total LPC]	29.92 ± 14.58	---	30.69 ± 16.07	29.00 ± 14.63	---	31.60 ± 14.53	---
LPC monounsaturated [% of total LPC]	56.49 ± 14.79	---	54.10 ± 17.38	57.52 ± 16.67	---	54.21 ± 15.29	---
LPC polyunsaturated [% of total LPC]	13.60 ± 0.85	---	15.21 ± 1.67	13.48 ± 2.06	---	14.20 ± 0.98	---
LPC unsaturated [% of total LPC]	70.09 ± 14.58	---	69.31 ± 16.07	71.01 ± 14.63	---	68.40 ± 14.53	---

SD – standard deviation, P – P-value compared to WT, LPC – lysophosphatidylcholine, SPC - .sphingosylphosphorylcholine. *P<0.05.

Table 7.9: Cellular lipid composition of Cer and GluCer.

	A549 [mean±SD]	P (A549) ANOVA	WT [mean±SD]	Q215K [mean±SD]	P (p.Q215K) ANOVA	E292V [mean±SD]	P (p.E292V) ANOVA
Cer [nmol/mg protein]	0.82 ± 0.42	---	0.81 ± 0.52	1.44 ± 1.00	---	1.08 ± 0.48	---
Cer [% of total lipids]	0.38 ± 0.02	---	0.43 ± 0.08	0.58 ± 0.23	---	0.51 ± 0.02	---
GluCer [nmol/mg protein]	0.14 ± 0.07	---	0.14 ± 0.09	0.30 ± 0.20	*	0.20 ± 0.10	---
GluCer [% of total lipids]	0.07 ± 0.01	---	0.07 ± 0.01	0.12 ± 0.04	*	0.09 ± 0.01	---
Cer 24:1 [% of total Cer]	34.08 ± 3.18	**	42.99 ± 4.15	40.17 ± 6.90	---	36.63 ± 4.10	---
Cer 24:0 [% of total Cer]	39.58 ± 7.51	*	31.89 ± 8.48	30.04 ± 8.14	---	30.32 ± 6.22	---
Cer 16:0 [% of total Cer]	17.71 ± 3.87	---	15.15 ± 3.54	20.16 ± 2.44	**	21.21 ± 2.90	***
Cer 22:0 [% of total Cer]	3.21 ± 0.08	----	3.84 ± 0.20	3.79 ± 0.46	---	5.11 ± 0.39	***
Cer 23:0 [% of total Cer]	3.40 ± 0.32	---	3.01 ± 0.36	2.80 ± 0.19	---	2.99 ± 0.11	---
Cer 18:0 [% of total Cer]	1.44 ± 0.36	**	2.26 ± 0.64	2.27 ± 0.41	---	2.84 ± 0.36	*
Cer 20:0 [% of total Cer]	0.60 ± 0.23	*	0.86 ± 0.30	0.77 ± 0.20	---	0.92 ± 0.14	---
GluCer 24:1 [% of Glu Cer]	84.98 ± 2.87	**	90.41 ± 2.07	81.84 ± 1.90	***	83.99 ± 3.40	**
GluCer 16:0 [% of Glu Cer]	15.03 ± 2.87	**	9.59 ± 2.07	18.16 ± 1.90	***	16.01 ± 3.40	**
Cer saturated [% of total Cer]	65.92 ± 3.18	**	57.01 ± 4.15	59.83 ± 6.90	---	63.38 ± 4.10	---
Cer unsaturated [% of total Cer]	34.08 ± 3.18	**	42.99 ± 4.15	40.17 ± 6.90	---	36.63 ± 4.10	---

SD – standard deviation, P – P-value compared to WT, Cer – ceramide, Glu – glucosyl. *P<0.05, **P<0.01, ***P<0.001.

Table 7.10: Cellular lipid composition of PG.

	A549 [mean±SD]	P (A549) ANOVA	WT [mean±SD]	Q215K [mean±SD]	P (p.Q215K) ANOVA	E292V [mean±SD]	P (p.E292V) ANOVA
PG [ng/mg protein]	0.37 ± 0.26	*	0.28 ± 0.21	0.44 ± 0.26	***	0.37 ± 0.26	*
PG [% of total lipids]	0.16 ± 0.04	---	0.14 ± 0.05	0.18 ± 0.03	**	0.16 ± 0.06	---
PG (% of PL]	0.26 ± 0.07	---	0.22 ± 0.07	0.30 ± 0.04	**	0.26 ± 0.09	---
PG 34:1 [% of total PG]	83.43 ± 4.36	---	91.21 ± 10.92	65.55 ± 7.60	**	85.96 ± 10.11	---
PG 36:1 [% of total PG]	16.58 ± 4.36	---	6.37 ± 7.36	12.56 ± 5.17	---	10.49 ± 7.01	---
PG 36:2 [% of total PG]	0.00 ± 0.00	---	2.43 ± 4.85	10.86 ± 2.80	*	3.55 ± 4.70	---
PG 34:2 [% of total PG]	0.00 ± 0.00	---	0.00 ± 0.00	11.04 ± 4.37	***	0.00 ± 96.46	---
PG monunsaturated [% of total PG]	100.00 ± 0.00	---	97.58 ± 4.85	78.11 ± 6.55	**	± 4.70	---
PG polyunsaturated [% of total PG]	0.00 ± 0.00	---	2.43 ± 4.85	21.89 ± 6.55	**	3.55 ± 4.70	---

SD – standard deviation, P – P-value compared to WT, PG – phosphatidylglycerol. *P<0.05, **P<0.01, ***P<0.001.

7.1.2 Microarray analysis

In the following data tables, all regulated genes of regulated KEGG pathways with an EASE score (P value) of 0.05 and below are presented for each comparison that was performed.

7.1.2.1 p.Q215K vs. WT (non-infected)

Table 7.11: Regulated genes in regulated KEGG pathways, comparison p.Q215K vs. WT

hsa00140	Steroid hormone biosynthesis				
GeneName	**Description**	**logFC**	**AveExpr**	**adj.P.Val**	**B**
UGT2B11	UDP glucuronosyltransferase 2 family, polypeptide B11 (UGT2B11)	-2.18	3.95	2.69E-04	0.89
UGT2B15	UDP glucuronosyltransferase 2 family, polypeptide B15 (UGT2B15)	-3.76	3.38	2.83E-06	6.38
UGT2B7	UDP glucuronosyltransferase 2 family, polypeptide B7	-1.69	4.64	1.39E-04	1.67
AKR1C4	aldo-keto reductase family 1, member C4 (chlordecone reductase; 3-alpha hydroxysteroid dehydrogenase, type I; dihydrodiol dehydrogenase 4) (AKR1C4)	-2.15	2.82	1.49E-05	4.36
CYP3A5	cytochrome P450, family 3, subfamily A, polypeptide 5 (CYP3A5)	-1.74	9.89	1.13E-07	10.36
CYP3A7	cytochrome P450, family 3, subfamily A, polypeptide 7 (CYP3A7)	-1.76	10.23	5.25E-10	17.03
HSD11B1	hydroxysteroid (11-beta) dehydrogenase 1 (HSD11B1)	-2.81	4.23	2.54E-02	-4.40
HSD17B2	hydroxysteroid (17-beta) dehydrogenase 2 (HSD17B2)	-1.37	3.14	2.14E-02	-4.11
STS	steroid sulfatase (microsomal), isozyme S (STS)	-1.17	6.07	2.64E-02	-4.44
SRD5A2	steroid-5-alpha-reductase, alpha polypeptide 2 (3-oxo-5 alpha-steroid delta 4-dehydrogenase alpha 2) (SRD5A2)	1.57	4.28	7.78E-03	-3.04
UGT1A6	UDP glucuronosyltransferase 1 family, polypeptide A6 (UGT1A6)	1.33	9.34	2.36E-08	12.30
CYP7B1	cytochrome P450, family 7, subfamily B, polypeptide 1 (CYP7B1)	2.55	4.72	5.30E-06	5.61
HSD17B3	hydroxysteroid (17-beta) dehydrogenase 3 (HSD17B3)	2.57	3.65	1.08E-02	-3.42
SULT2B1	sulfotransferase family, cytosolic, 2B, member 1 (SULT2B1)	1.57	8.88	6.78E-12	22.36

hsa00982	Drug metabolism - Cytochrome P450				
GeneName	**Description**	**logFC**	**AveExpr**	**adj.P.Val**	**B**
UGT2B11	UDP glucuronosyltransferase 2 family, polypeptide B11 (UGT2B11)	-2.18	3.95	2.69E-04	0.89
UGT2B15	UDP glucuronosyltransferase 2 family, polypeptide B15 (UGT2B15)	-3.76	3.38	2.83E-06	6.38
UGT2B7	UDP glucuronosyltransferase 2 family, polypeptide B7 (UGT2B7)	-1.69	4.64	1.39E-04	1.67
AOX1	aldehyde oxidase 1 (AOX1)	-1.02	8.62	7.53E-08	10.86
CYP3A5	cytochrome P450, family 3, subfamily A, polypeptide 5 (CYP3A5)	-1.74	9.89	1.13E-07	10.36
CYP3A7	cytochrome P450, family 3, subfamily A, polypeptide 7 (CYP3A7)	-1.76	10.23	5.25E-10	17.03
GSTA2	glutathione S-transferase alpha 2 (GSTA2)	-1.21	4.98	9.26E-03	-3.24
GSTM2	glutathione S-transferase mu 2 (muscle) (GSTM2)	-1.53	2.7	1.17E-02	-3.51
GSTT2	glutathione S-transferase theta 2 (GSTT2)	-3.94	5.82	7.73E-10	16.55
MAOB	monoamine oxidase B (MAOB), nuclear gene encoding mitochondrial protein	-2.61	2.98	3.81E-06	6.01
UGT1A6	UDP glucuronosyltransferase 1 family, polypeptide A6 (UGT1A6)	1.33	9.34	2.36E-08	12.30
ALDH1A3	aldehyde dehydrogenase 1 family, member A3 (ALDH1A3)	1.24	11.29	3.54E-09	14.67
CYP2C18	cytochrome P450, family 2, subfamily C, polypeptide 18 (CYP2C18)	2.07	2.79	1.32E-03	-0.98
CYP2C9	cytochrome P450, family 2, subfamily C, polypeptide 9 (CYP2C9)	1.26	3.42	3.06E-02	-4.61
GSTA4	glutathione S-transferase alpha 4 (GSTA4)	1.06	9.75	7.15E-09	13.80
GSTO2	glutathione S-transferase omega 2 (GSTO2)	1.27	5.96	5.42E-05	2.80

hsa00980	Metabolism of xenobiotics by cytochrome P450				
GeneName	**Description**	**logFC**	**AveExpr**	**adj.P.Val**	**B**
UGT2B11	UDP glucuronosyltransferase 2 family, polypeptide B11 (UGT2B11)	-2.18	3.95	2.69E-04	0.89
UGT2B15	UDP glucuronosyltransferase 2 family, polypeptide B15 (UGT2B15)	-3.76	3.38	2.83E-06	6.38
UGT2B7	UDP glucuronosyltransferase 2 family, polypeptide B7 (UGT2B7)	-1.69	4.64	1.39E-04	1.67
AKR1C4	aldo-keto reductase family 1, member C4 (chlordecone reductase; 3-alpha hydroxysteroid dehydrogenase, type I; dihydrodiol dehydrogenase 4) (AKR1C4)	-2.27	3.11	5.75E-04	0.00
CYP2S1	cytochrome P450, family 2, subfamily S, polypeptide 1 (CYP2S1)	-1.08	10.65	8.25E-07	7.89
CYP3A5	cytochrome P450, family 3, subfamily A, polypeptide 5 (CYP3A5)	-1.74	9.89	1.13E-07	10.36
CYP3A7	cytochrome P450, family 3, subfamily A, polypeptide 7 (CYP3A7)	-1.76	10.23	5.25E-10	17.03
GSTA2	glutathione S-transferase alpha 2 (GSTA2)	-1.21	4.98	9.26E-03	-3.24
GSTM2	glutathione S-transferase mu 2 (muscle) (GSTM2)	-1.53	2.7	1.17E-02	-3.51
GSTT2	glutathione S-transferase theta 2 (GSTT2)	-3.94	5.82	7.73E-10	16.55
UGT1A6	UDP glucuronosyltransferase 1 family, polypeptide A6 (UGT1A6)	1.33	9.34	2.36E-08	12.30
ALDH1A3	aldehyde dehydrogenase 1 family, member A3 (ALDH1A3)	1.24	11.29	3.54E-09	14.67
CYP2C18	cytochrome P450, family 2, subfamily C, polypeptide 18 (CYP2C18)	1.78	3.02	9.95E-04	-0.65
CYP2C9	cytochrome P450, family 2, subfamily C, polypeptide 9 (CYP2C9)	1.26	3.42	3.06E-02	-4.61
GSTA4	glutathione S-transferase alpha 4 (GSTA4)	1.06	9.75	7.15E-09	13.80
GSTO2	glutathione S-transferase omega 2 (GSTO2)	1.27	5.96	5.42E-05	2.80

hsa04610	Complement and coagulation cascades				
GeneName	**Description**	**logFC**	**AveExpr**	**adj.P.Val**	**B**
BDKRB2	bradykinin receptor B2 (BDKRB2)	-1.39	10.5	4.94E-11	19.90
F2	coagulation factor II (thrombin) (F2)	-4.75	6.32	3.93E-13	25.93
F10	coagulation factor X (F10)	-1.17	4.5	8.04E-03	-3.08
C1R	complement component 1, r subcomponent (C1R)	-1.28	14.43	7.06E-13	25.20
C4BPA	complement component 4 binding protein, alpha (C4BPA)	-2.70	7.07	3.88E-13	25.97
CFH	complement factor H (CFH)	-4.44	6.77	1.30E-09	15.91

CFI	complement factor I (CFI)	-3.56	4.29	4.51E-10	17.23
FGA	fibrinogen alpha chain (FGA)	-4.82	5.36	4.79E-07	8.56
FGB	fibrinogen beta chain (FGB)	-5.63	4.89	6.81E-15	31.28
FGG	fibrinogen gamma chain (FGG)	-5.38	6.52	1.41E-08	12.93
KNG1	kininogen 1 (KNG1)	-1.23	2.47	1.85E-02	-4.04
SERPINE1	serpin peptidase inhibitor, clade E (nexin, plasminogen activator inhibitor type 1), member 1 (SERPINE1)	-1.14	10.6	4.83E-07	8.55
THBD	thrombomodulin (THBD)	-1.06	13.06	1.11E-08	13.24
C5AR1	complement component 5a receptor 1 (C5AR1)	1.00	6	5.42E-05	2.80
PROS1	protein S (alpha) (PROS1)	1.58	8.99	5.71E-11	19.73
TFPI	tissue factor pathway inhibitor (lipoprotein-associated coagulation inhibitor) (TFPI)	1.24	8.09	2.58E-09	15.06

hsa00150 Androgen and estrogen metabolism

GeneName	Description	logFC	AveExpr	adj.P.Val	B
UGT2B11	UDP glucuronosyltransferase 2 family, polypeptide B11 (UGT2B11)	-2.18	3.95	2.69E-04	0.89
UGT2B15	UDP glucuronosyltransferase 2 family, polypeptide B15 (UGT2B15)	-3.76	3.38	2.83E-06	6.38
UGT2B7	UDP glucuronosyltransferase 2 family, polypeptide B7 (UGT2B7)	-1.69	4.64	1.39E-04	1.67
AKR1C4	aldo-keto reductase family 1, member C4 (chlordecone reductase; 3-alpha hydroxysteroid dehydrogenase, type I; dihydrodiol dehydrogenase 4) (AKR1C4)	-2.27	3.11	5.75E-04	0.00
HSD11B1	hydroxysteroid (11-beta) dehydrogenase 1 (HSD11B1)	-2.81	4.23	2.54E-02	-4.40
HSD17B2	hydroxysteroid (17-beta) dehydrogenase 2 (HSD17B2)	-1.37	3.14	2.14E-02	-4.11
STS	steroid sulfatase (microsomal), isozyme S (STS)	-1.06	6.17	1.36E-04	1.70
SRD5A2	steroid-5-alpha-reductase, alpha polypeptide 2 (3-oxo-5 alpha-steroid delta 4-dehydrogenase alpha 2) (SRD5A2)	1.57	4.28	7.78E-03	-3.04
UGT1A6	UDP glucuronosyltransferase 1 family, polypeptide A6 (UGT1A6)	1.33	9.34	2.36E-08	12.30
HSD17B3	hydroxysteroid (17-beta) dehydrogenase 3 (HSD17B3)	2.22	5.66	3.12E-07	9.09
SULT2B1	sulfotransferase family, cytosolic, 2B, member 1 (SULT2B1)	1.57	8.88	6.78E-12	22.36

hsa00830 Retinol metabolism

GeneName	Description	logFC	AveExpr	adj.P.Val	B
UGT2B11	UDP glucuronosyltransferase 2 family, polypeptide B11 (UGT2B11)	-2.18	3.95	2.69E-04	0.89
UGT2B15	UDP glucuronosyltransferase 2 family, polypeptide B15 (UGT2B15)	-3.76	3.38	2.83E-06	6.38
UGT2B7	UDP glucuronosyltransferase 2 family, polypeptide B7 (UGT2B7)	-1.69	4.64	1.39E-04	1.67
BCMO1	beta-carotene 15,15'-monooxygenase 1 (BCMO1)	-2.03	6.26	3.11E-10	17.69
CYP3A5	cytochrome P450, family 3, subfamily A, polypeptide 5 (CYP3A5)	-1.74	9.89	1.13E-07	10.36
CYP3A7	cytochrome P450, family 3, subfamily A, polypeptide 7 (CYP3A7)	-1.76	10.23	5.25E-10	17.03
DHRS9	dehydrogenase/reductase (SDR family) member 9 (DHRS9)	-2.20	6.01	1.63E-07	9.89
UGT1A6	UDP glucuronosyltransferase 1 family, polypeptide A6 (UGT1A6)	1.33	9.34	2.36E-08	12.30
CYP2C18	cytochrome P450, family 2, subfamily C, polypeptide 18 (CYP2C18)	2.07	2.79	1.32E-03	-0.98
CYP2C9	cytochrome P450, family 2, subfamily C, polypeptide 9 (CYP2C9)	1.26	3.42	3.06E-02	-4.61
CYP26A1	cytochrome P450, family 26, subfamily A, polypeptide 1 (CYP26A1)	1.04	8.56	3.16E-08	11.92
CYP26B1	cytochrome P450, family 26, subfamily B, polypeptide 1 (CYP26B1)	2.16	4.25	2.19E-04	1.13
DGAT2	diacylglycerol O-acyltransferase 2 (DGAT2)	1.22	7.35	1.01E-07	10.50

hsa0460 Cytokine-cytokine receptor interaction

GeneName	Description	logFC	AveExpr	adj.P.Val	B
CCL26	chemokine (C-C motif) ligand 26 (CCL26)	-1.23	8.5	2.05E-09	15.34
CCL28	chemokine (C-C motif) ligand 28 (CCL28)	-1.43	3.49	3.15E-03	-2.00
CCL3L3	chemokine (C-C motif) ligand 3-like 3 (CCL3L3)	-1.82	8.28	2.40E-02	-4.33
CXCL1	chemokine (C-X-C motif) ligand 1 (melanoma growth stimulating activity, alpha) (CXCL1)	-1.71	13.24	7.46E-13	25.12
CXCL3	chemokine (C-X-C motif) ligand 3 (CXCL3)	-1.33	10.07	1.41E-07	10.08
CXCL5	chemokine (C-X-C motif) ligand 5 (CXCL5)	-1.31	15.27	2.75E-09	14.98
CSF2	colony stimulating factor 2 (granulocyte-macrophage) (CSF2)	-1.53	7.04	1.37E-03	-1.03
CSF2RA	colony stimulating factor 2 receptor, alpha, low-affinity (granulocyte-macrophage) (CSF2RA)	-2.42	6.95	1.23E-09	15.98
INHBB	inhibin, beta B (INHBB)	-3.34	11.04	5.55E-14	28.48
IL1R2	interleukin 1 receptor, type II (IL1R2)	-2.09	3.27	1.05E-03	-0.72
IL1B	interleukin 1, beta (IL1B)	-1.60	7.67	2.35E-02	-4.22
IL10RA	interleukin 10 receptor, alpha (IL10RA)	-1.05	5.46	4.44E-02	-5.03
IL22	interleukin 22 (IL22)	-1.94	1.95	2.15E-02	-4.21
IL28A	interleukin 28A (interferon, lambda 2) (IL28A)	-1.30	10.8	3.09E-02	-4.62
IL6	interleukin 6 (interferon, beta 2) (IL6)	-1.01	9.23	8.89E-03	-3.20
IL7R	interleukin 7 receptor (IL7R)	-5.77	6.92	5.02E-09	14.25
IL8	interleukin 8 (IL8)	-1.49	7.01	2.94E-02	-4.56
PDGFC	platelet derived growth factor C (PDGFC)	-1.44	7.8	8.18E-09	13.62
PF4	platelet factor 4 (PF4)	-1.42	7.18	1.51E-08	12.85
PDGFA	platelet-derived growth factor alpha polypeptide (PDGFA)	-1.11	9	1.70E-08	12.71
PDE9A	phosphodiesterase 9A (PDE9A)	-1.70	7.76	4.81E-08	11.40
PDGFB	platelet-derived growth factor beta polypeptide (simian sarcoma viral (v-sis) oncogene homolog) (PDGFB)	-3.63	6.29	4.98E-09	14.26
TNFSF10	tumor necrosis factor (ligand) superfamily, member 10 (TNFSF10)	-2.04	6.1	1.72E-05	4.18
TNFSF15	tumor necrosis factor (ligand) superfamily, member 15 (TNFSF15)	-3.27	3.36	4.59E-08	11.46
TNFRSF21	tumor necrosis factor receptor superfamily, member 21 (TNFRSF21)	-1.28	12.46	3.78E-13	26.00
CD40	CD40 molecule, TNF receptor superfamily member 5 (CD40)	1.43	8.1	8.16E-09	13.63
FAS	Fas (TNF receptor superfamily, member 6) (FAS)	1.17	9.94	1.34E-07	10.14
BMP7	bone morphogenetic protein 7 (BMP7)	4.49	7.6	6.83E-11	19.51
CCL1	chemokine (C-C motif) ligand 1 (CCL1)	1.11	3.03	2.74E-02	-4.48
CCL20	chemokine (C-C motif) ligand 20 (CCL20)	2.81	6.6	1.21E-07	10.27
CCL3	chemokine (C-C motif) ligand 3 (CCL3)	1.22	9.58	5.68E-05	2.75
CCL5	chemokine (C-C motif) ligand 5 (CCL5)	3.26	10.29	1.69E-10	18.41
CXCR4	chemokine (C-X-C motif) receptor 4 (CXCR4)	7.30	7.15	3.93E-13	25.94
CX3CR1	chemokine (C-X3-C motif) receptor 1 (CX3CR1)	1.99	3.02	1.90E-03	-1.41
INHBA	inhibin, beta A (INHBA)	3.42	7.8	7.86E-05	2.35
INHBE	inhibin, beta E (INHBE)	1.01	4.68	2.56E-04	0.95
IL13	interleukin 13 (IL13)	2.75	3.3	9.73E-07	7.69
IL18R1	interleukin 18 receptor 1 (IL18R1)	2.15	5.4	3.65E-05	3.27
IL6ST	interleukin 6 signal transducer (gp130, oncostatin M receptor) (IL6ST)	1.06	8.07	4.39E-07	8.67

OSM	oncostatin M (OSM)	1.57	4.82	5.70E-04	0.01
TNFSF4	tumor necrosis factor (ligand) superfamily, member 4 (TNFSF4)	2.40	4.01	2.21E-05	3.88
TNFRSF8	tumor necrosis factor receptor superfamily, member 8 (TNFRSF8)	1.32	6.42	5.43E-05	2.80
TNFRSF10D	tumor necrosis factor receptor superfamily, member 10d, decoy with truncated death domain (TNFRSF10D)	1.40	11.16	2.70E-11	20.62
VEGFC	vascular endothelial growth factor C (VEGFC)	1.33	12.57	6.17E-11	19.63

hsa04514 Cell adhesion molecules

GeneName	Description	logFC	AveExpr	adj.P.Val	B
CD274	CD274 molecule (CD274)	-1.50	6.51	3.68E-05	3.26
CD99	CD99 molecule (CD99)	-1.72	12.25	4.46E-11	20.02
CDH2	cadherin 2, type 1, N-cadherin (neuronal) (CDH2)	-7.51	8.7	1.20E-11	21.62
CLDN2	claudin 2 (CLDN2)	-2.93	10.02	6.83E-14	28.16
CLDN4	claudin 4 (CLDN4)	-2.25	10.72	6.58E-13	25.30
CLDN7	claudin 7 (CLDN7)	-1.17	5.55	1.09E-03	-0.76
CNTN1	contactin 1 (CNTN1)	-3.16	7.14	3.68E-12	23.11
ITGB2	integrin, beta 2 (complement component 3 receptor 3 and 4 subunit) (ITGB2)	-3.25	5.97	3.94E-10	17.40
ITGB8	integrin, beta 8 (ITGB8)	-1.10	6.15	2.36E-04	1.04
ICAM2	intercellular adhesion molecule 2 (ICAM2)	-1.27	5.18	5.92E-03	-2.73
HLA-DMA	major histocompatibility complex, class II, DM alpha (HLA-DMA)	-1.45	7.03	5.95E-08	11.15
HLA-DMB	major histocompatibility complex, class II, DM beta (HLA-DMB)	-3.81	7.91	5.24E-06	5.62
PECAM1	platelet/endothelial cell adhesion molecule (PECAM1)	-2.36	2.96	2.70E-02	-4.47
SELE	selectin E (SELE)	-2.19	3.49	1.03E-02	-3.37
VCAN	versican (VCAN)	-4.65	9.33	2.31E-15	32.91
CD40	CD40 molecule, TNF receptor superfamily member 5 (CD40)	1.43	8.1	8.16E-09	13.63
CD86	CD86 molecule (CD86)	1.64	9.26	5.32E-04	0.12
CLDN14	claudin 14 (CLDN14)	1.11	4.55	4.48E-02	-5.04
CLDN19	claudin 19 (CLDN19)	1.72	2.62	1.95E-02	-4.10
ITGA4	integrin, alpha 4 (antigen CD49D, alpha 4 subunit of VLA-4 receptor) (ITGA4)	2.03	4.49	1.71E-05	4.19
ICAM1	intercellular adhesion molecule 1 (ICAM1)	1.32	7.68	4.33E-03	-2.37
MADCAM1	mucosal vascular addressin cell adhesion molecule 1 (MADCAM1)	2.08	4.8	7.33E-04	-0.29
NLGN3	neuroligin 3 (NLGN3)	1.87	3.5	2.72E-03	-1.83

hsa04080 Neuroactive ligand-receptor interaction

GeneName	Description	logFC	AveExpr	adj.P.Val	B
HTR1E	5-hydroxytryptamine (serotonin) receptor 1E (HTR1E)	-1.98	2.34	2.36E-02	-4.31
ADRA1B	adrenergic, alpha-1B-, receptor (ADRA1B)	-1.76	10.45	6.82E-10	16.71
ADRB2	adrenergic, beta-2-, receptor, surface (ADRB2)	-2.34	8.33	1.85E-12	23.96
AGTR1	angiotensin II receptor, type 1 (AGTR1)	-2.95	4.24	1.39E-05	4.44
BDKRB2	bradykinin receptor B2 (BDKRB2)	-1.39	10.5	4.94E-11	19.90
CHRM3	cholinergic receptor, muscarinic 3 (CHRM3)	-1.42	3.05	1.62E-02	-3.88
CNR1	cannabinoid receptor 1 (brain) (CNR1)	-3.37	2.82	2.42E-06	6.57
F2	coagulation factor II (thrombin) (F2)	-4.75	6.32	3.93E-13	25.93
DRD1	dopamine receptor D1 (DRD1)	-2.66	4.75	2.39E-07	9.41
DRD3	dopamine receptor D3 (DRD3)	-1.00	3.53	3.10E-02	-4.62
FPR1	formyl peptide receptor 1 (FPR1)	-2.27	4.59	4.82E-05	2.94
GABRE	gamma-aminobutyric acid (GABA) A receptor, epsilon (GABRE)	-1.40	11.97	1.41E-09	15.81
GLP2R	glucagon-like peptide 2 receptor (GLP2R)	-1.61	4.57	1.24E-03	-0.90
HRH3	histamine receptor H3 (HRH3)	-1.57	5.95	2.77E-04	0.86
NPY1R	neuropeptide Y receptor Y1 (NPY1R)	-2.34	2.95	5.80E-06	5.50
NPY5R	neuropeptide Y receptor Y5 (NPY5R)	-1.53	3.66	1.41E-02	-3.72
PTGER1	prostaglandin E receptor 1 (subtype EP1), 42kDa (PTGER1)	-1.60	2.9	1.57E-02	-3.85
PTGER4	prostaglandin E receptor 4 (subtype EP4) (PTGER4)	-1.10	9.33	3.00E-07	9.13
PRSS2	protease, serine, 2 (trypsin 2) (PRSS2)	-1.47	8.94	7.51E-09	13.74
PRSS3	protease, serine, 3 (PRSS3)	-1.52	7.87	3.06E-10	17.71
P2RY2	purinergic receptor P2Y, G-protein coupled, 2 (P2RY2)	-1.08	9.53	8.32E-11	19.27
P2RY6	pyrimidinergic receptor P2Y, G-protein coupled, 6 (P2RY6)	-1.55	10.53	6.92E-11	19.50
SSTR1	somatostatin receptor 1 (SSTR1)	-2.43	2.15	2.12E-02	-4.19
THRA	thyroid hormone receptor, alpha (erythroblastic leukemia viral (v-erb-a) oncogene homolog, avian) (THRA)	-1.11	7.92	2.13E-06	6.73
VIPR1	vasoactive intestinal peptide receptor 1 (VIPR1)	-2.67	3.23	3.05E-05	3.49
CNR2	cannabinoid receptor 2 (macrophage) (CNR2)	1.48	3.69	4.43E-02	-5.03
F2RL2	coagulation factor II (thrombin) receptor-like 2 (F2RL2)	2.40	8.83	1.52E-12	24.22
C5AR1	complement component 5a receptor 1 (C5AR1)	1.00	6	5.42E-05	2.80
GABRD	gamma-aminobutyric acid (GABA) A receptor, delta (GABRD)	1.94	3.93	4.47E-02	-5.03
GRIN2C	glutamate receptor, ionotropic, N-methyl D-aspartate 2C (GRIN2C)	2.00	6.9	3.63E-10	17.50
GRID1	glutamate receptor, ionotropic, delta 1 (GRID1)	1.76	4.94	3.77E-04	0.49
CGA	glycoprotein hormones, alpha polypeptide (CGA)	2.03	2.49	1.64E-04	1.48
NTSR1	neurotensin receptor 1 (high affinity) (NTSR1)	1.61	5.05	8.88E-03	-3.20
PTGER2	prostaglandin E receptor 2 (subtype EP2), 53kDa (PTGER2)	2.15	6.44	6.13E-04	-0.08
PTGIR	prostaglandin I2 (prostacyclin) receptor (IP) (PTGIR)	1.89	5.8	3.28E-03	-2.05
P2RY1	purinergic receptor P2Y, G-protein coupled, 1 (P2RY1)	2.89	5.57	5.78E-08	11.18
TBXA2R	thromboxane A2 receptor (TBXA2R)	1.07	7.05	1.86E-04	1.33

hsa04621 NOD-like receptor signaling

GeneName	Description	logFC	AveExpr	adj.P.Val	B
CASP1	caspase 1, apoptosis-related cysteine peptidase (interleukin 1, beta, convertase) (CASP1)	-1.59	6.22	5.94E-05	2.69
CASP5	caspase 5, apoptosis-related cysteine peptidase (CASP5)	-3.01	9.11	4.28E-14	28.85
CARD6	caspase recruitment domain family, member 6 (CARD6)	-1.14	7.72	5.51E-06	5.56
CXCL1	chemokine (C-X-C motif) ligand 1 (melanoma growth stimulating activity, alpha) (CXCL1)	-1.71	13.24	7.46E-13	25.12
IL1B	interleukin 1, beta (IL1B)	-1.60	7.67	2.35E-02	-4.22
IL6	interleukin 6 (interferon, beta 2) (IL6)	-1.01	9.23	8.89E-03	-3.20
IL8	interleukin 8 (IL8)	-1.49	7.01	2.94E-02	-4.56
MAPK13	mitogen-activated protein kinase 13 (MAPK13)	1.46	6.57	8.82E-07	7.81
TNFAIP3	tumor necrosis factor, alpha-induced protein 3 (TNFAIP3)	1.09	9.71	2.56E-08	12.19
NLRP3	NLR family, pyrin domain containing 3 (NLRP3)	1.37	4.25	2.54E-04	0.96

BIRC3	baculoviral IAP repeat-containing 3 (BIRC3)	1.72	12.88	2.42E-12	23.61
CASP8	caspase 8, apoptosis-related cysteine peptidase (CASP8)	1.44	6.88	4.65E-07	8.60
CARD9	caspase recruitment domain family, member 9 (CARD9)	2.10	7.44	1.62E-10	18.47
CCL5	chemokine (C-C motif) ligand 5 (CCL5)	3.26	10.29	1.69E-10	18.41

hsa04670 Leukocyte transendothelial migration

GeneName	Description	logFC	AveExpr	adj.P.Val	B
CD99	CD99 molecule (CD99)	-1.72	12.25	4.46E-11	20.02
NOX1	NADPH oxidase 1 (NOX1)	-1.17	3.91	1.23E-02	-3.57
RASSF5	Ras association (RalGDS/AF-6) domain family member 5 (RASSF5)	-1.11	3.46	3.14E-02	-4.64
CLDN4	claudin 4 (CLDN4)	-2.25	10.72	6.58E-13	25.30
CLDN2	claudin 2 (CLDN2)	-2.93	10.02	6.83E-14	28.16
CLDN7	claudin 7 (CLDN7)	-1.17	5.55	1.09E-03	-0.76
ITGB2	integrin, beta 2 (complement component 3 receptor 3 and 4 subunit) (ITGB2)	-3.25	5.97	3.94E-10	17.40
MYL9	myosin, light chain 9, regulatory (MYL9)	-1.59	6.91	4.88E-06	5.71
PECAM1	platelet/endothelial cell adhesion molecule (PECAM1)	-2.36	2.96	2.70E-02	-4.47
VAV3	vav 3 guanine nucleotide exchange factor (VAV3)	-1.34	8.57	4.21E-05	3.10
RAPGEF3	Rap guanine nucleotide exchange factor (GEF) 3 (RAPGEF3)	1.38	4.44	1.20E-03	-0.87
TXK	TXK tyrosine kinase (TXK)	1.45	4.21	1.25E-03	-0.92
CXCR4	chemokine (C-X-C motif) receptor 4 (CXCR4)	7.30	7.15	3.93E-13	25.94
CLDN14	claudin 14 (CLDN14)	1.11	4.55	4.48E-02	-5.04
CLDN19	claudin 19 (CLDN19)	1.72	2.62	1.95E-02	-4.10
ITGA4	integrin, alpha 4 (antigen CD49D, alpha 4 subunit of VLA-4 receptor) (ITGA4)	2.03	4.49	1.71E-05	4.19
ICAM1	intercellular adhesion molecule 1 (ICAM1)	1.32	7.68	4.33E-03	-2.37
MMP2	matrix metallopeptidase 2 (gelatinase A, 72kDa gelatinase, 72kDa type IV collagenase) (MMP2)	3.22	4.15	2.34E-03	-1.65
MMP9	matrix metallopeptidase 9 (gelatinase B, 92kDa gelatinase, 92kDa type IV collagenase) (MMP9)	1.57	9.19	2.39E-11	20.78
MAPK13	mitogen-activated protein kinase 13 (MAPK13)	1.46	6.57	8.82E-07	7.81
NCF1	neutrophil cytosolic factor 1 (NCF1)	1.54	3.02	6.59E-03	-2.85
PLCG2	phospholipase C, gamma 2 (phosphatidylinositol-specific) (PLCG2)	1.18	8.92	1.56E-09	15.68

hsa04512 ECM-receptor interaction

GeneName	Description	logFC	AveExpr	adj.P.Val	B
AGRN	agrin (AGRN)	-1.15	12.28	6.58E-06	5.35
COL5A1	collagen, type V, alpha 1 (COL5A1)	-2.64	11.8	1.78E-13	26.90
FN1	fibronectin 1 (FN1)	-1.23	6.7	5.61E-05	2.76
ITGB6	integrin, beta 6 (ITGB6)	-3.50	3.33	5.92E-06	5.48
ITGB8	integrin, beta 8 (ITGB8)	-1.10	6.15	2.36E-04	1.04
LAMA2	laminin, alpha 2 (LAMA2)	-1.18	5.27	4.24E-03	-2.34
LAMC2	laminin, gamma 2 (LAMC2)	-1.35	9.96	4.71E-08	11.43
TNC	tenascin C (TNC)	-3.32	5.51	1.48E-09	15.75
COMP	cartilage oligomeric matrix protein (COMP)	1.92	3.27	9.43E-03	-3.26
ITGA2	integrin, alpha 2 (CD49B, alpha 2 subunit of VLA-2 receptor) (ITGA2)	1.63	7.17	2.81E-06	6.38
ITGA4	integrin, alpha 4 (antigen CD49D, alpha 4 subunit of VLA-4 receptor) (ITGA4)	2.03	4.49	1.71E-05	4.19
LAMC3	laminin, gamma 3 (LAMC3)	2.52	6.27	1.83E-08	12.61
SPP1	secreted phosphoprotein 1 (SPP1)	1.37	12.69	1.68E-10	18.42
TNXB	tenascin XB (TNXB)	1.43	8.08	9.48E-10	16.30
THBS4	thrombospondin 4 (THBS4)	2.38	4.16	5.83E-04	-0.02

hsa02010 ABC transporter

GeneName	Description	logFC	AveExpr	adj.P.Val	B
ABCB8	ATP-binding cassette, sub-family B (MDR/TAP), member 8 (ABCB8), nuclear gene encoding mitochondrial protein	-1.53	7.34	3.22E-07	9.05
ABCC6	ATP-binding cassette, sub-family C (CFTR/MRP), member 6 (ABCC6)	-1.28	5.32	3.84E-05	3.30
CFTR	cystic fibrosis transmembrane conductance regulator (ATP-binding cassette sub-family C, member 7) (CFTR)	-2.93	2.8	1.41E-06	7.23
ABCA1	ATP-binding cassette, sub-family A (ABC1), member 1 (ABCA1)	1.89	7.91	4.59E-08	11.46
ABCA5	ATP-binding cassette, sub-family A (ABC1), member 5 (ABCA5)	1.14	8.82	1.39E-09	15.83
ABCA6	ATP-binding cassette, sub-family A (ABC1), member 6 (ABCA6)	2.66	3.62	4.32E-05	3.07
ABCC8	ATP-binding cassette, sub-family C (CFTR/MRP), member 8 (ABCC8)	1.89	9.5	7.56E-12	22.21
ABCG4	ATP-binding cassette, sub-family G (WHITE), member 4 (ABCG4)	1.03	5.63	7.19E-05	2.46
TAP1	transporter 1, ATP-binding cassette, sub-family B (MDR/TAP) (TAP1)	1.28	13.98	1.52E-10	18.54
TAP2	transporter 2, ATP-binding cassette, sub-family B (MDR/TAP) (TAP2)	1.33	3.51	1.43E-03	-1.07

hsa00983 Drug metabolism - other enzymes

GeneName	Description	logFC	AveExpr	adj.P.Val	B
UGT2B11	UDP glucuronosyltransferase 2 family, polypeptide B11 (UGT2B11)	-2.18	3.95	2.69E-04	0.89
UGT2B15	UDP glucuronosyltransferase 2 family, polypeptide B15 (UGT2B15)	-3.76	3.38	2.83E-06	6.38
UGT2B7	UDP glucuronosyltransferase 2 family, polypeptide B7 (UGT2B7)	-1.69	4.64	1.39E-04	1.67
CYP3A5	cytochrome P450, family 3, subfamily A, polypeptide 5 (CYP3A5)	-1.74	9.89	1.13E-07	10.36
CYP3A7	cytochrome P450, family 3, subfamily A, polypeptide 7 (CYP3A7)	-1.76	10.23	5.25E-10	17.03
DPYD	dihydropyrimidine dehydrogenase (DPYD)	-1.38	8.06	7.16E-09	13.80
UPB1	ureidopropionase, beta (UPB1)	-1.09	3.98	1.01E-02	-3.31
CES1	carboxylesterase 1 (CES1)	8.75	12.86	9.89E-21	43.36
UGT1A6	UDP glucuronosyltransferase 1 family, polypeptide A6 (UGT1A6)	1.33	9.34	2.36E-08	12.30

7.1.2.2 p.Q215K vs. WT (RSV-infected)

Table 7.12: Regulated genes in regulated KEGG pathways, comparison p.Q215K vs. WT in the presence of virus.

hsa4060	Cytokine-cytokine receptor interaction				
GeneName	**Description**	**logFC**	**AveExpr**	**adj.P.Val**	**B**
KITLG	KIT ligand (KITLG)	-1.11	8.78	5.12E-08	10.68
CCL2	chemokine (C-C motif) ligand 2 (CCL2)	-1.61	11.11	4.15E-12	22.56
CCL26	chemokine (C-C motif) ligand 26 (CCL26)	-2.22	8.5	2.66E-13	26.12
CCL28	chemokine (C-C motif) ligand 28 (CCL28)	-4.49	3.39	4.27E-08	10.90
CXCL1	chemokine (C-X-C motif) ligand 1 (melanoma growth stimulating activity, alpha) (CXCL1)	-2.02	13.24	2.34E-14	29.35
CXCL5	chemokine (C-X-C motif) ligand 5 (CXCL5)	-1.14	15.29	1.49E-09	15.06
CXCL6	chemokine (C-X-C motif) ligand 6 (granulocyte chemotactic protein 2) (CXCL6)	-3.58	3.08	8.84E-10	15.70
CX3CL1	chemokine (C-X3-C motif) ligand 1 (CX3CL1)	-1.24	3.71	2.05E-02	-4.42
CSF2	colony stimulating factor 2 (granulocyte-macrophage) (CSF2)	-1.47	7.12	3.01E-04	0.34
CSF2RA	colony stimulating factor 2 receptor, alpha, low-affinity (granulocyte-macrophage) (CSF2RA)	-2.46	6.95	1.53E-10	17.94
CRLF2	cytokine receptor-like factor 2 (CRLF2)	-1.79	6.2	1.16E-08	12.50
INHBB	inhibin, beta B (INHBB)	-3.44	11.04	7.75E-15	30.64
IL10	interleukin 10 (IL10)	-1.18	2.67	4.40E-02	-5.20
IL15RA	interleukin 15 receptor, alpha (IL15RA)	-1.14	8.05	8.53E-08	10.06
IL21R	interleukin 21 receptor (IL21R)	-1.42	4.56	2.35E-04	0.63
IL21	interleukin 21 (IL21)	-1.30	2.68	5.85E-02	-5.56
IL6	interleukin 6 (interferon, beta 2) (IL6)	-2.32	9.19	5.79E-08	10.53
IL7R	interleukin 7 receptor (IL7R)	-3.14	6.92	1.14E-06	6.92
IL8	interleukin 8 (IL8)	-0.89	7.01	1.32E-01	-6.42
PF4	platelet factor 4 (PF4)	-1.51	7.18	1.09E-09	15.45
PDGFB	platelet-derived growth factor beta polypeptide (simian sarcoma viral (v-sis) oncogene homolog) (PDGFB)	-2.92	6.29	1.08E-08	12.59
PPBP	pro-platelet basic protein (chemokine (C-X-C motif) ligand 7) (PPBP)	-1.43	3.5	6.95E-03	-3.17
TGFB2	transforming growth factor, beta 2 (TGFB2)	-1.12	9	2.66E-07	8.67
TNFSF10	tumor necrosis factor (ligand) superfamily, member 10 (TNFSF10)	-2.75	6.86	5.45E-09	13.44
TNFSF15	tumor necrosis factor (ligand) superfamily, member 15 (TNFSF15)	-1.13	3.37	1.60E-02	-4.14
TNFRSF14	tumor necrosis factor receptor superfamily, member 14 (herpesvirus entry mediator) (TNFRSF14)	-2.04	5.43	2.78E-08	11.43
TNFRSF1B	tumor necrosis factor receptor superfamily, member 1B (TNFRSF1B)	-2.09	3.94	2.03E-05	3.50
TNFRSF21	tumor necrosis factor receptor superfamily, member 21 (TNFRSF21)	-1.53	12.48	1.91E-12	23.59
ACVR2A	activin A receptor, type IIA (ACVR2A)	1.04	6.55	5.25E-06	5.10
BMP7	bone morphogenetic protein 7 (BMP7)	3.85	7.49	8.29E-14	27.71
FIGF	c-fos induced growth factor (vascular endothelial growth factor D) (FIGF)	1.13	6.91	1.29E-08	12.37
CCL1	chemokine (C-C motif) ligand 1 (CCL1)	2.17	2.97	3.58E-04	0.15
CCL17	chemokine (C-C motif) ligand 17 (CCL17)	2.44	8.04	1.09E-07	9.76
CCL4	chemokine (C-C motif) ligand 4 (CCL4)	1.59	7.18	7.19E-11	18.88
CCR7	chemokine (C-C motif) receptor 7 (CCR7)	1.24	8.78	2.00E-09	14.69
CXCR4	chemokine (C-X-C motif) receptor 4 (CXCR4)	4.12	7.25	3.22E-13	25.86
EDA	ectodysplasin A (EDA)	1.12	4.94	7.72E-02	-5.85
EDA2R	ectodysplasin A2 receptor (EDA2R)	1.19	8.78	4.52E-12	22.43
EPOR	erythropoietin receptor (EPOR)	1.32	8.7	2.00E-09	14.70
INHBA	inhibin, beta A (INHBA)	2.54	7.76	1.43E-11	20.96
IL13	interleukin 13 (IL13)	1.56	3.52	1.34E-03	-1.36
IL18R1	interleukin 18 receptor 1 (IL18R1)	2.31	5.4	3.65E-06	5.53
IL23A	interleukin 23, alpha subunit p19 (IL23A)	1.41	8.94	7.80E-11	18.79
LEPR	leptin receptor (LEPR)	1.23	2.06	9.43E-03	-3.56
OSM	oncostatin M (OSM)	1.49	5.13	7.49E-03	-3.30
PDGFRA	platelet-derived growth factor receptor, alpha polypeptide (PDGFRA)	3.61	3.34	3.80E-06	5.48
PRLR	prolactin receptor (PRLR)	1.63	2.21	7.62E-06	4.65
TNFSF4	tumor necrosis factor (ligand) superfamily, member 4 (TNFSF4)	1.30	3.84	6.12E-03	-3.08

hsa04610	Complement and coagulation cascades				
GeneName	**Description**	**logFC**	**AveExpr**	**adj.P.Val**	**B**
F2	coagulation factor II (thrombin) (F2)	-3.03	6.35	4.47E-10	16.57
C1R	complement component 1, r subcomponent (C1R)	-1.81	12.02	1.09E-14	30.23
C3	complement component 3 (C3)	-1.08	10.81	2.03E-06	6.23
C4BPA	complement component 4 binding protein, alpha (C4BPA)	-3.43	7.07	4.78E-15	31.28
C4BPB	complement component 4 binding protein, beta (C4BPB)	-2.57	5.89	2.10E-06	6.19
C4B	complement component 4B (Chido blood group) (C4B)	-1.89	7.07	2.14E-12	23.44
CFB	complement factor B (CFB)	-1.23	9.99	2.24E-07	8.88
CFH	complement factor H (CFH)	-4.22	6.77	3.70E-10	16.80
CFI	complement factor I (CFI)	-3.28	4.29	1.91E-10	17.64
FGA	fibrinogen alpha chain (FGA)	-5.12	5.36	4.11E-08	10.95
FGB	fibrinogen beta chain (FGB)	-3.26	4.89	7.78E-13	24.76
FGG	fibrinogen gamma chain (FGG)	-5.89	6.52	7.29E-10	15.95
PLAT	plasminogen activator, tissue (PLAT)	-1.72	8.58	2.67E-11	20.14
SERPING1	serpin peptidase inhibitor, clade G (C1 inhibitor), member 1 (SERPING1)	-1.39	3.46	3.54E-03	-2.46
PROC	protein C (inactivator of coagulation factors Va and VIIIa) (PROC)	1.31	5.25	2.47E-02	-4.62
PROS1	protein S (alpha) (PROS1)	1.80	6.24	7.90E-09	12.98
SERPINA1	serpin peptidase inhibitor, clade A (alpha-1 antiproteinase, antitrypsin), member 1 (SERPINA1)	1.48	7.73	3.74E-07	8.26

hsa04110	Cell cycle				
GeneName	**Description**	**logFC**	**AveExpr**	**adj.P.Val**	**B**
CDC45	cell division cycle 45 homolog (S. cerevisiae) (CDC45)	-1.47	12.59	1.05E-11	21.37
DBF4	DBF4 homolog (S. cerevisiae) (DBF4)	-1.05	9.5	2.98E-08	11.34
E2F1	E2F transcription factor 1 (E2F1)	-1.06	10.6	2.63E-09	14.35

E2F2	E2F transcription factor 2 (E2F2)	-1.10	10.86	9.15E-11	18.57
MAD2L1	MAD2 mitotic arrest deficient-like 1 (yeast) (MAD2L1)	-1.47	11.06	1.89E-09	14.77
SKP2	S-phase kinase-associated protein 2 (p45) (SKP2)	-1.02	8.65	7.84E-09	12.99
TTK	TTK protein kinase (TTK)	-1.26	9.68	3.43E-10	16.90
CDK1	cyclin-dependent kinase 1 (CDK1)	-1.86	11.93	2.87E-10	17.21
CDC25A	cell division cycle 25 homolog A (S. pombe) (CDC25A)	-1.47	8.98	7.20E-11	18.88
CDC25C	cell division cycle 25 homolog C (S. pombe) (CDC25C)	-1.24	9.27	8.59E-11	18.65
CCNA2	cyclin A2 (CCNA2)	-1.59	10.18	5.06E-12	22.29
CCNB1	cyclin B1 (CCNB1)	-1.26	13.41	6.15E-12	22.09
CCNB2	cyclin B2 (CCNB2)	-1.26	13.42	3.43E-12	22.80
MCM4	minichromosome maintenance complex component 4 (MCM4)	-1.08	11.43	1.41E-08	12.25
ORC6	origin recognition complex, subunit 6 (ORC6)	-1.28	10.23	1.25E-09	15.28
PTTG1	pituitary tumor-transforming 1 (PTTG1)	-1.17	14.8	1.02E-11	21.40
PTTG2	pituitary tumor-transforming 2 (PTTG2)	-1.18	12.89	2.67E-11	20.14
PLK1	polo-like kinase 1 (PLK1)	-1.27	7.96	7.34E-08	10.24
PCNA	proliferating cell nuclear antigen (PCNA)	-1.30	13.38	7.10E-11	18.90
RBL1	retinoblastoma-like 1 (p107) (RBL1)	-1.37	5.77	7.86E-07	7.36
TGFB2	transforming growth factor, beta 2 (TGFB2)	-1.12	9	2.66E-07	8.67
CDC14A	CDC14 cell division cycle 14 homolog A (S. cerevisiae) (CDC14A)	1.16	4.05	9.33E-03	-3.55
CCNB3	cyclin B3 (CCNB3)	1.05	7.29	1.02E-08	12.66
CDKN1C	cyclin-dependent kinase inhibitor 1C (p57, Kip2) (CDKN1C)	1.69	9.55	1.10E-12	24.30
GADD45A	growth arrest and DNA-damage-inducible, alpha (GADD45A)	1.17	12.32	4.41E-10	16.59
GADD45B	growth arrest and DNA-damage-inducible, beta (GADD45B)	1.11	12.17	1.40E-09	15.14
GADD45G	growth arrest and DNA-damage-inducible, gamma (GADD45G)	2.55	7.12	6.96E-13	24.92

hsa03030 **DNA replication**

GeneName	Description	logFC	AveExpr	adj.P.Val	B
FEN1	flap structure-specific endonuclease 1 (FEN1)	-1.40	10.73	6.07E-10	16.18
MCM4	minichromosome maintenance complex component 4 (MCM4)	-1.08	11.43	1.41E-08	12.25
POLA2	polymerase (DNA directed), alpha 2 (70kD subunit) (POLA2)	-1.56	9.65	3.24E-08	11.24
POLE2	polymerase (DNA directed), epsilon 2 (p59 subunit) (POLE2)	-1.16	9.39	1.99E-07	9.02
PRIM1	primase, DNA, polypeptide 1 (49kDa) (PRIM1)	-1.53	10.8	6.61E-13	24.98
PRIM2	primase, DNA, polypeptide 2 (58kDa) (PRIM2)	-1.13	6.81	7.30E-06	4.70
PCNA	proliferating cell nuclear antigen (PCNA)	-1.30	13.38	7.10E-11	18.90
RFC2	replication factor C (activator 1) 2, 40kDa (RFC2)	-1.02	10.73	1.60E-09	14.98
RFC3	replication factor C (activator 1) 3, 38kDa (RFC3)	-1.38	9.65	1.20E-09	15.34
RFC5	replication factor C (activator 1) 5, 36.5kDa (RFC5)	-1.29	12.69	4.80E-12	22.36
RPA4	replication protein A4, 30kDa (RPA4)	1.21	7.17	6.57E-07	7.58

hsa04672 **Intestinal immune network for IgA production**

GeneName	Description	logFC	AveExpr	adj.P.Val	B
AICDA	activation-induced cytidine deaminase (AICDA)	-1.97	2.92	1.73E-03	-1.66
CCL28	chemokine (C-C motif) ligand 28 (CCL28)	-4.49	3.39	4.27E-08	10.90
IL10	interleukin 10 (IL10)	-1.18	2.67	4.40E-02	-5.20
IL15RA	interleukin 15 receptor, alpha (IL15RA)	-1.14	8.05	8.53E-08	10.06
IL6	interleukin 6 (interferon, beta 2) (IL6)	-2.32	9.19	5.79E-08	10.53
HLA-DMB	major histocompatibility complex, class II, DM beta (HLA-DMB)	-3.15	7.84	1.76E-11	20.70
PIGR	polymeric immunoglobulin receptor (PIGR)	-2.75	2.88	7.05E-12	21.86
TGFB2	transforming growth factor, beta 2 (TGFB2)	-1.12	9	2.66E-07	8.67
CD86	CD86 molecule (CD86)	2.67	9.21	2.89E-08	11.38
CXCR4	chemokine (C-X-C motif) receptor 4 (CXCR4)	4.12	7.25	3.22E-13	25.86
ICOS	inducible T-cell co-stimulator (ICOS)	1.57	3.12	2.00E-03	-1.82
ITGA4	integrin, alpha 4 (antigen CD49D, alpha 4 subunit of VLA-4 receptor) (ITGA4)	2.01	3.2	7.07E-10	15.99
MADCAM1	mucosal vascular addressin cell adhesion molecule 1 (MADCAM1)	1.66	4.6	1.79E-04	0.95

hsa05217 **Basal cell carcinoma**

GeneName	Description	logFC	AveExpr	adj.P.Val	B
AXIN2	axin 2 (AXIN2)	-1.33	7.99	1.59E-09	14.98
BMP4	bone morphogenetic protein 4 (BMP4)	-2.67	6.61	1.18E-07	9.67
FZD2	frizzled homolog 2 (Drosophila) (FZD2)	-1.25	12.81	3.92E-10	16.73
FZD5	frizzled homolog 5 (Drosophila) (FZD5)	-1.26	8.86	2.94E-09	14.32
HHIP	hedgehog interacting protein (HHIP)	-4.65	5.74	8.57E-11	18.66
SHH	sonic hedgehog (SHH)	-1.12	3.79	3.63E-02	-5.04
WNT10A	wingless-type MMTV integration site family, member 10A (WNT10A)	-1.32	3.05	6.30E-02	-5.55
GLI1	GLI family zinc finger 1 (GLI1)	1.08	10.62	1.09E-08	12.58
APC2	adenomatosis polyposis coli 2 (APC2)	1.99	8.6	7.23E-11	18.88
FZD8	frizzled homolog 8 (Drosophila) (FZD8)	2.62	9.56	4.47E-15	31.36
LEF1	lymphoid enhancer-binding factor 1 (LEF1)	1.64	2.18	2.45E-03	-2.05
WNT11	wingless-type MMTV integration site family, member 11 (WNT11)	1.08	5.74	8.06E-06	4.58
WNT5B	wingless-type MMTV integration site family, member 5B (WNT5B)	1.30	5.48	4.50E-05	2.55

hsa04512 **ECM-receptor interaction**

GeneName	Description	logFC	AveExpr	adj.P.Val	B
CD36	CD36 molecule (thrombospondin receptor) (CD36)	-1.76	2.8	1.03E-03	-1.07
COL5A1	collagen, type V, alpha 1 (COL5A1)	-1.78	11.8	4.17E-12	22.55
FN1	fibronectin 1 (FN1)	-1.01	6.68	5.30E-05	2.36
HMMR	hyaluronan-mediated motility receptor (RHAMM) (HMMR)	-1.68	11.8	2.01E-11	20.52
ITGB6	integrin, beta 6 (ITGB6)	-2.77	3.33	1.54E-05	3.83
LAMB1	laminin, beta 1 (LAMB1)	-1.09	13.8	8.59E-11	18.65
TNC	tenascin C (TNC)	-4.09	5.51	1.82E-11	20.65
COMP	cartilage oligomeric matrix protein (COMP)	2.08	3.27	1.97E-03	-1.80
ITGA4	integrin, alpha 4 (antigen CD49D, alpha 4 subunit of VLA-4 receptor) (ITGA4)	2.01	3.2	7.07E-10	15.99
ITGB3	integrin, beta 3 (platelet glycoprotein IIIa, antigen CD61) (ITGB3)	1.65	7.86	1.48E-06	6.60
LAMC3	laminin, gamma 3 (LAMC3)	2.42	6.27	4.64E-09	13.64
SPP1	secreted phosphoprotein 1 (SPP1)	1.33	12.69	6.69E-11	19.00

TNN	tenascin N (TNN)	1.98	3.19	3.33E-02	-4.95
TNXB	tenascin XB (TNXB)	1.80	8.08	9.43E-12	21.50
THBS4	thrombospondin 4 (THBS4)	2.30	4.23	1.23E-06	6.82
COL11A2	collagen, type XI, alpha 2 (COL11A2)	1.46	6.34	2.91E-02	-4.80

hsa04514 Cell adhesion molecules

GeneName	Description	logFC	AveExpr	adj.P.Val	B
CD99	CD99 molecule (CD99)	-1.65	12.28	5.30E-12	22.23
CDH1	cadherin 1, type 1, E-cadherin (epithelial) (CDH1)	-3.90	10.04	3.21E-17	37.47
CDH2	cadherin 2, type 1, N-cadherin (neuronal) (CDH2)	-4.28	10.19	4.76E-17	37.07
CDH3	cadherin 3, type 1, P-cadherin (placental) (CDH3)	-1.24	5.88	1.55E-07	9.33
CLDN2	claudin 2 (CLDN2)	-3.96	10.02	5.99E-16	34.22
CLDN7	claudin 7 (CLDN7)	-1.24	5.54	1.70E-05	3.71
CNTN1	contactin 1 (CNTN1)	-3.94	7.05	7.52E-12	21.78
ITGB2	integrin, beta 2 (complement component 3 receptor 3 and 4 subunit) (ITGB2)	-4.09	5.85	8.13E-08	10.12
HLA-DMB	major histocompatibility complex, class II, DM beta (HLA-DMB)	-3.15	7.84	1.76E-11	20.70
PECAM1	platelet/endothelial cell adhesion molecule (PECAM1)	-2.66	2.67	1.45E-09	15.09
VCAM1	vascular cell adhesion molecule 1 (VCAM1)	-3.21	2.82	5.14E-07	7.87
VCAN	versican (VCAN)	-4.44	9.33	6.24E-16	33.93
CD86	CD86 molecule (CD86)	2.67	9.21	2.89E-08	11.38
CD8A	CD8a molecule (CD8A)	1.39	4.41	1.07E-03	-1.11
CDH15	cadherin 15, type 1, M-cadherin (myotubule) (CDH15)	1.19	4.93	8.31E-05	1.84
CDH4	cadherin 4, type 1, R-cadherin (retinal) (CDH4)	1.25	10.11	1.27E-10	18.17
CLDN14	claudin 14 (CLDN14)	6.32	4.55	7.26E-10	15.96
ICOS	inducible T-cell co-stimulator (ICOS)	1.57	3.12	2.00E-03	-1.82
ITGA4	integrin, alpha 4 (antigen CD49D, alpha 4 subunit of VLA-4 receptor) (ITGA4)	2.01	3.2	7.07E-10	15.99
ICAM3	intercellular adhesion molecule 3 (ICAM3)	1.25	10.35	3.34E-12	22.84
MADCAM1	mucosal vascular addressin cell adhesion molecule 1 (MADCAM1)	1.66	4.6	1.79E-04	0.95
NLGN3	neuroligin 3 (NLGN3)	1.78	3.12	8.44E-06	4.53

hsa05200 Pathways in cancer

GeneName	Description	logFC	AveExpr	adj.P.Val	B
CKS1B	CDC28 protein kinase regulatory subunit 1B (CKS1B)	-1.24	11.96	9.25E-12	21.53
E2F1	E2F transcription factor 1 (E2F1)	-1.06	10.6	2.63E-09	14.35
E2F2	E2F transcription factor 2 (E2F2)	-1.10	10.86	9.15E-11	18.57
KITLG	KIT ligand (KITLG)	-1.11	8.78	5.12E-08	10.68
RAD51	RAD51 homolog (RecA homolog, E. coli) (S. cerevisiae) (RAD51)	-1.31	11.12	2.71E-12	23.11
SKP2	S-phase kinase-associated protein 2 (p45) (SKP2)	-1.07	8.66	2.84E-05	3.10
AR	androgen receptor (AR)	-2.53	9.76	1.24E-13	27.15
AXIN2	axin 2 (AXIN2)	-1.33	7.99	1.59E-09	14.98
BIRC5	baculoviral IAP repeat-containing 5 (BIRC5)	-1.22	14.28	1.71E-12	23.74
BMP4	bone morphogenetic protein 4 (BMP4)	-2.67	6.61	1.18E-07	9.67
CDH1	cadherin 1, type 1, E-cadherin (epithelial) (CDH1)	-3.90	10.04	3.21E-17	37.47
CSF2RA	colony stimulating factor 2 receptor, alpha, low-affinity (granulocyte-macrophage) (CSF2RA)	-2.46	6.95	1.53E-10	17.94
FN1	fibronectin 1 (FN1)	-1.01	6.68	5.30E-05	2.36
FZD2	frizzled homolog 2 (Drosophila) (FZD2)	-1.25	12.81	3.92E-10	16.73
FZD5	frizzled homolog 5 (Drosophila) (FZD5)	-1.26	8.86	2.94E-09	14.32
HHIP	hedgehog interacting protein (HHIP)	-4.65	5.74	8.57E-11	18.66
HIF1A	hypoxia inducible factor 1, alpha subunit (basic helix-loop-helix transcription factor) (HIF1A)	-1.02	11.81	2.36E-07	8.82
IL6	interleukin 6 (interferon, beta 2) (IL6)	-2.32	9.19	5.79E-08	10.53
LAMB1	laminin, beta 1 (LAMB1)	-1.12	13.76	1.49E-10	17.97
MITF	microphthalmia-associated transcription factor (MITF)	-1.04	6.55	1.86E-05	3.60
PPARG	peroxisome proliferator-activated receptor gamma (PPARG)	-1.27	10.92	7.45E-10	15.92
PDGFB	platelet-derived growth factor beta polypeptide (simian sarcoma viral (v-sis) oncogene homolog) (PDGFB)	-2.92	6.29	1.08E-08	12.59
PML	promyelocytic leukemia (PML)	-1.12	6.63	7.70E-07	7.39
PTGS2	prostaglandin-endoperoxide synthase 2 (prostaglandin G/H synthase and cyclooxygenase) (PTGS2)	-1.10	9.89	1.32E-07	9.53
RAC2	ras-related C3 botulinum toxin substrate 2 (rho family, small GTP binding protein Rac2) (RAC2)	-1.06	7.42	6.26E-05	2.17
RARB	retinoic acid receptor, beta (RARB)	-1.09	4.99	3.83E-03	-2.55
SLC2A1	solute carrier family 2 (facilitated glucose transporter), member 1 (SLC2A1)	-1.48	12.05	8.32E-14	27.68
SHH	sonic hedgehog (SHH)	-1.12	3.79	3.63E-02	-5.04
TGFB2	transforming growth factor, beta 2 (TGFB2)	-1.12	9	2.66E-07	8.67
WNT10A	wingless-type MMTV integration site family, member 10A (WNT10A)	-1.32	3.05	6.30E-02	-5.55
GLI1	GLI family zinc finger 1 (GLI1)	1.08	10.62	1.09E-08	12.58
RASSF5	Ras association (RalGDS/AF-6) domain family member 5 (RASSF5)	1.16	3.46	1.08E-02	-3.71
TRAF1	TNF receptor-associated factor 1 (TRAF1)	1.34	8.82	1.91E-10	17.65
ACVR1C	activin A receptor, type IC (ACVR1C)	2.09	2.6	2.17E-05	3.42
APC2	adenomatosis polyposis coli 2 (APC2)	1.99	8.6	7.23E-11	18.88
FIGF	c-fos induced growth factor (vascular endothelial growth factor D) (FIGF)	1.13	6.91	1.29E-08	12.37
CASP8	caspase 8, apoptosis-related cysteine peptidase (CASP8)	1.14	6.83	1.24E-06	6.81
CTNNA2	catenin (cadherin-associated protein), alpha 2 (CTNNA2)	2.06	3.13	1.27E-04	1.35
FGF13	fibroblast growth factor 13 (FGF13)	1.00	3.88	6.60E-03	-3.16
FZD8	frizzled homolog 8 (Drosophila) (FZD8)	2.62	9.56	4.47E-15	31.36
LAMC3	laminin, gamma 3 (LAMC3)	2.42	6.27	4.64E-09	13.64
LEF1	lymphoid enhancer-binding factor 1 (LEF1)	1.64	2.18	2.45E-03	-2.05
MMP1	matrix metallopeptidase 1 (interstitial collagenase) (MMP1)	2.61	7.37	6.90E-08	10.32
MMP2	matrix metallopeptidase 2 (gelatinase A, 72kDa gelatinase, 72kDa type IV collagenase) (MMP2)	3.18	4.02	9.30E-06	4.41
MMP9	matrix metallopeptidase 9 (gelatinase B, 92kDa gelatinase, 92kDa type IV collagenase) (MMP9)	1.75	9.23	1.71E-12	23.72
PDGFRA	platelet-derived growth factor receptor, alpha polypeptide (PDGFRA)	3.61	3.34	3.80E-06	5.48
RUNX1	runt-related transcription factor 1 (RUNX1)	1.25	5.9	7.70E-07	7.39
ETS1	v-ets erythroblastosis virus E26 oncogene homolog 1 (avian) (ETS1)	1.16	6.23	3.47E-07	8.35
FOS	FBJ murine osteosarcoma viral oncogene homolog (FOS)	1.03	9.49	1.41E-04	1.22
WNT11	wingless-type MMTV integration site family, member 11 (WNT11)	1.08	5.74	8.06E-06	4.58
WNT5B	wingless-type MMTV integration site family, member 5B (WNT5B)	1.36	5.1	1.98E-02	-4.38

7.1.2.3 p.E292V vs. WT (non-infected)

Table 7.13: Regulated genes in regulated KEGG pathways, comparison p.E292V vs. WT

hsa0460	Cytokine-cytokine receptor interaction				
GeneName	**Description**	**logFC**	**AveExpr**	**adj.P.Val**	**B**
ACVRL1	activin A receptor type II-like 1 (ACVRL1)	-1.42	4.96	2.27E-03	-1.19
CCL28	chemokine (C-C motif) ligand 28 (CCL28)	-1.15	3.49	1.72E-02	-3.58
CCL2	chemokine (C-C motif) ligand 2 (CCL2)	-2.66	11.18	6.46E-13	25.87
CCL3L3	chemokine (C-C motif) ligand 3-like 3 (CCL3L3)	-1.88	8.28	2.47E-02	-4.00
CXCL1	chemokine (C-X-C motif) ligand 1 (melanoma growth stimulating activity, alpha) (CXCL1)	-2.30	13.24	3.35E-14	29.50
CXCL12	chemokine (C-X-C motif) ligand 12 (CXCL12)	-1.61	2.71	2.84E-02	-4.08
CSF2RA	colony stimulating factor 2 receptor, alpha, low-affinity (granulocyte-macrophage) (CSF2RA)	-1.52	6.95	4.38E-07	9.23
EGF	epidermal growth factor (EGF)	-1.76	3.49	1.06E-02	-3.00
IL1RAP	interleukin 1 receptor accessory protein (IL1RAP)	-1.03	7.57	2.88E-06	6.93
IL1R2	interleukin 1 receptor, type II (IL1R2)	-1.47	3.27	1.60E-02	-3.49
IL1B	interleukin 1, beta (IL1B)	-1.12	7.37	1.10E-05	5.27
IL10RA	interleukin 10 receptor, alpha (IL10RA)	-1.15	5.6	3.75E-03	-1.78
IL18	interleukin 18 (interferon-gamma-inducing factor) (IL18)	-1.09	11.19	1.94E-11	21.76
IL21R	interleukin 21 receptor (IL21R)	-1.66	4.56	2.76E-04	1.35
IL22	interleukin 22 (IL22)	-1.90	1.95	2.91E-02	-4.19
IL6	interleukin 6 (interferon, beta 2) (IL6)	-2.07	9.3	7.36E-08	11.45
IL7	interleukin 7 (IL7)	-1.41	4.32	1.50E-01	-6.10
IL8	interleukin 8 (IL8)	-2.43	7.01	1.53E-03	-0.71
PDGFC	platelet derived growth factor C (PDGFC)	-1.41	7.8	1.44E-08	13.48
TGFBR2	transforming growth factor, beta receptor II (70/80kDa) (TGFBR2)	-1.14	13.25	4.01E-10	18.00
TNFSF10	tumor necrosis factor (ligand) superfamily, member 10 (TNFSF10)	-2.95	6.1	4.08E-07	9.32
TNFSF14	tumor necrosis factor (ligand) superfamily, member 14 (TNFSF14)	-4.17	7.02	1.11E-08	13.81
TNFSF15	tumor necrosis factor (ligand) superfamily, member 15 (TNFSF15)	-2.68	3.36	6.55E-07	8.73
TNFSF9	tumor necrosis factor (ligand) superfamily, member 9 (TNFSF9)	-1.26	10.04	9.08E-11	19.88
TNFRSF14	tumor necrosis factor receptor superfamily, member 14 (herpesvirus entry mediator) (TNFRSF14)	-1.81	5.43	9.78E-07	8.24
TNFRSF21	tumor necrosis factor receptor superfamily, member 21 (TNFRSF21)	-1.53	12.46	6.83E-14	28.62
VEGFA	vascular endothelial growth factor A (VEGFA)	-1.13	8.32	4.93E-06	6.26
BMP7	bone morphogenetic protein 7 (BMP7)	1.39	3.45	6.16E-03	-2.37
CCL5	chemokine (C-C motif) ligand 5 (CCL5)	3.01	10.29	7.02E-10	17.27
CXCR4	chemokine (C-X-C motif) receptor 4 (CXCR4)	3.78	7.23	1.81E-10	19.00
INHBA	inhibin, beta A (INHBA)	1.48	7.74	8.72E-08	11.24
INHBE	inhibin, beta E (INHBE)	1.48	4.68	7.72E-06	5.70
IL18R1	interleukin 18 receptor 1 (IL18R1)	1.81	5.4	2.73E-04	1.37
IL3RA	interleukin 3 receptor, alpha (low affinity) (IL3RA)	1.02	6.1	8.06E-04	0.06
PDGFRA	platelet-derived growth factor receptor, alpha polypeptide (PDGFRA)	2.00	3.34	4.74E-03	-2.06
TNFSF4	tumor necrosis factor (ligand) superfamily, member 4 (TNFSF4)	1.48	4.01	2.45E-03	-1.28

hsa00980	Metabolism of xenobiotics by cytochrome P450				
GeneName	**Description**	**logFC**	**AveExpr**	**adj.P.Val**	**B**
ALDH3A1	aldehyde dehydrogenase 3 family, member A1 (ALDH3A1)	-1.06	14.21	1.90E-06	7.43
UGT1A6	UDP glucuronosyltransferase 1 family, polypeptide A6 (UGT1A6)	-1.35	6.99	7.13E-07	8.62
UGT1A8	UDP glucuronosyltransferase 1 family, polypeptide A8 (UGT1A8)	-1.30	6.71	1.27E-06	7.93
UGT2B10	UDP glucuronosyltransferase 2 family, polypeptide B10 (UGT2B10)	-1.26	7.04	1.40E-06	7.80
UGT2B11	UDP glucuronosyltransferase 2 family, polypeptide B11 (UGT2B11)	-1.79	3.95	1.84E-03	-0.94
UGT2B15	UDP glucuronosyltransferase 2 family, polypeptide B15 (UGT2B15)	-2.71	3.38	1.20E-04	2.35
UGT2B7	UDP glucuronosyltransferase 2 family, polypeptide B7 (UGT2B7)	-1.82	4.64	8.98E-05	2.70
AKR1C4	aldo-keto reductase family 1, member C4 (chlordecone reductase; 3-alpha hydroxysteroid dehydrogenase, type I; dihydrodiol dehydrogenase 4) (AKR1C4)	-2.43	2.82	5.55E-06	6.11
CYP3A5	cytochrome P450, family 3, subfamily A, polypeptide 5 (CYP3A5)	-1.03	9.91	1.56E-06	7.66
CYP3A7	cytochrome P450, family 3, subfamily A, polypeptide 7 (CYP3A7)	-1.02	10.23	4.86E-07	9.10
EPHX1	epoxide hydrolase 1, microsomal (xenobiotic) (EPHX1)	-1.39	10.88	4.25E-07	9.27
GSTA2	glutathione S-transferase alpha 2 (GSTA2)	-1.54	4.57	1.20E-03	-0.43
GSTM2	glutathione S-transferase mu 2 (muscle) (GSTM2)	-1.37	5.16	1.74E-07	10.38
GSTT2B	glutathione S-transferase theta 2B (gene/pseudogene) (GSTT2B)	-2.90	5.13	1.42E-05	4.95
GSTT2	glutathione S-transferase theta 2 (GSTT2)	-3.03	5.82	2.66E-08	12.72
GSTO2	glutathione S-transferase omega 2 (GSTO2)	1.52	5.96	1.12E-05	5.24

hsa00140	Steroid hormone biosynthesis				
GeneName	**Description**	**logFC**	**AveExpr**	**adj.P.Val**	**B**
UGT1A6	UDP glucuronosyltransferase 1 family, polypeptide A6 (UGT1A6)	-1.35	6.99	7.13E-07	8.62
UGT1A8	UDP glucuronosyltransferase 1 family, polypeptide A8 (UGT1A8)	-1.30	6.71	1.27E-06	7.93
UGT2B10	UDP glucuronosyltransferase 2 family, polypeptide B10 (UGT2B10)	-1.26	7.04	1.40E-06	7.80
UGT2B11	UDP glucuronosyltransferase 2 family, polypeptide B11 (UGT2B11)	-1.79	3.95	1.84E-03	-0.94
UGT2B15	UDP glucuronosyltransferase 2 family, polypeptide B15 (UGT2B15)	-2.71	3.38	1.20E-04	2.35
UGT2B7	UDP glucuronosyltransferase 2 family, polypeptide B7 (UGT2B7)	-1.82	4.64	8.98E-05	2.70
AKR1C4	aldo-keto reductase family 1, member C4 (chlordecone reductase; 3-alpha hydroxysteroid dehydrogenase, type I; dihydrodiol dehydrogenase 4) (AKR1C4)	-2.43	2.82	5.55E-06	6.11
CYP3A5	cytochrome P450, family 3, subfamily A, polypeptide 5 (CYP3A5)	-1.03	9.91	1.56E-06	7.66
CYP3A7	cytochrome P450, family 3, subfamily A, polypeptide 7 (CYP3A7)	-1.02	10.23	4.86E-07	9.10
HSD11B1	hydroxysteroid (11-beta) dehydrogenase 1 (HSD11B1)	-2.74	4.23	3.46E-02	-4.40
STS	steroid sulfatase (microsomal), isozyme S (STS)	-1.67	6.17	1.62E-06	7.62
CYP7B1	cytochrome P450, family 7, subfamily B, polypeptide 1 (CYP7B1)	1.76	4.72	3.16E-04	1.19
HSD17B2	hydroxysteroid (17-beta) dehydrogenase 2 (HSD17B2)	1.51	2.95	2.79E-02	-4.15

hsa00982	Drug metabolism-Cytochrome P450				
GeneName	**Description**	**logFC**	**AveExpr**	**adj.P.Val**	**B**
ALDH3A1	aldehyde dehydrogenase 3 family, member A1 (ALDH3A1)	-1.06	14.21	1.90E-06	7.43

UGT1A6	UDP glucuronosyltransferase 1 family, polypeptide A6 (UGT1A6)	-1.35	6.99	7.13E-07	8.62
UGT1A8	UDP glucuronosyltransferase 1 family, polypeptide A8 (UGT1A8)	-1.30	6.71	1.27E-06	7.93
UGT2B10	UDP glucuronosyltransferase 2 family, polypeptide B10 (UGT2B10)	-1.26	7.04	1.40E-06	7.80
UGT2B11	UDP glucuronosyltransferase 2 family, polypeptide B11 (UGT2B11)	-1.79	3.95	1.84E-03	-0.94
UGT2B15	UDP glucuronosyltransferase 2 family, polypeptide B15 (UGT2B15)	-2.71	3.38	1.20E-04	2.35
UGT2B7	UDP glucuronosyltransferase 2 family, polypeptide B7 (UGT2B7)	-1.82	4.64	8.98E-05	2.70
CYP3A5	cytochrome P450, family 3, subfamily A, polypeptide 5 (CYP3A5)	-1.03	9.91	1.56E-06	7.66
CYP3A7	cytochrome P450, family 3, subfamily A, polypeptide 7 (CYP3A7)	-1.02	10.23	4.86E-07	9.10
GSTA2	glutathione S-transferase alpha 2 (GSTA2)	-1.54	4.57	1.20E-03	-0.43
GSTM2	glutathione S-transferase mu 2 (muscle) (GSTM2)	-1.37	5.16	1.74E-07	10.38
GSTT2B	glutathione S-transferase theta 2B (gene/pseudogene) (GSTT2B)	-2.90	5.13	1.42E-05	4.95
GSTT2	glutathione S-transferase theta 2 (GSTT2)	-3.03	5.82	2.66E-08	12.72
MAOB	monoamine oxidase B (MAOB), nuclear gene encoding mitochondrial protein	-2.34	2.98	1.77E-05	4.68
GSTO2	glutathione S-transferase omega 2 (GSTO2)	1.52	5.96	1.12E-05	5.24

hsa00983 Drug metabolism-other enzymes

GeneName	Description	logFC	AveExpr	adj.P.Val	B
UGT1A6	UDP glucuronosyltransferase 1 family, polypeptide A6 (UGT1A6)	-1.35	6.99	7.13E-07	8.62
UGT1A8	UDP glucuronosyltransferase 1 family, polypeptide A8 (UGT1A8)	-1.30	6.71	1.27E-06	7.93
UGT2B10	UDP glucuronosyltransferase 2 family, polypeptide B10 (UGT2B10)	-1.26	7.04	1.40E-06	7.80
UGT2B11	UDP glucuronosyltransferase 2 family, polypeptide B11 (UGT2B11)	-1.79	3.95	1.84E-03	-0.94
UGT2B15	UDP glucuronosyltransferase 2 family, polypeptide B15 (UGT2B15)	-2.71	3.38	1.20E-04	2.35
UGT2B7	UDP glucuronosyltransferase 2 family, polypeptide B7 (UGT2B7)	-1.82	4.64	8.98E-05	2.70
CYP3A5	cytochrome P450, family 3, subfamily A, polypeptide 5 (CYP3A5)	-1.03	9.91	1.56E-06	7.66
CYP3A7	cytochrome P450, family 3, subfamily A, polypeptide 7 (CYP3A7)	-1.02	10.23	4.86E-07	9.10
DPYD	dihydropyrimidine dehydrogenase (DPYD)	-1.67	8.06	2.62E-08	12.74
UPB1	ureidopropionase, beta (UPB1)	1.22	4.17	3.07E-02	-4.26
CES1	carboxylesterase 1 (CES1)	8.99	12.86	3.20E-20	42.45

hsa00053 Ascorbate and aldarate metabolism

GeneName	Description	logFC	AveExpr	adj.P.Val	B
UGT1A6	UDP glucuronosyltransferase 1 family, polypeptide A6 (UGT1A6)	-1.35	6.99	7.13E-07	8.62
UGT1A8	UDP glucuronosyltransferase 1 family, polypeptide A8 (UGT1A8)	-1.30	6.71	1.27E-06	7.93
UGT2B10	UDP glucuronosyltransferase 2 family, polypeptide B10 (UGT2B10)	-1.26	7.04	1.40E-06	7.80
UGT2B11	UDP glucuronosyltransferase 2 family, polypeptide B11 (UGT2B11)	-1.79	3.95	1.84E-03	-0.94
UGT2B15	UDP glucuronosyltransferase 2 family, polypeptide B15 (UGT2B15)	-2.71	3.38	1.20E-04	2.35
UGT2B7	UDP glucuronosyltransferase 2 family, polypeptide B7 (UGT2B7)	-1.82	4.64	8.98E-05	2.70
ALDH2	aldehyde dehydrogenase 2 family (mitochondrial) (ALDH2), nuclear gene encoding mitochondrial protein	-1.19	12.05	1.79E-10	19.02

hsa04621 NOD-like receptor signaling

GeneName	Description	logFC	AveExpr	adj.P.Val	B
PYCARD	PYD and CARD domain containing (PYCARD)	-1.09	12.48	8.53E-10	17.05
CASP1	caspase 1, apoptosis-related cysteine peptidase (interleukin 1, beta, convertase) (CASP1)	-1.59	6.22	7.69E-05	2.89
CASP5	caspase 5, apoptosis-related cysteine peptidase (CASP5)	-2.40	9.11	9.92E-13	25.39
CCL2	chemokine (C-C motif) ligand 2 (CCL2)	-2.66	11.18	6.46E-13	25.87
CXCL1	chemokine (C-X-C motif) ligand 1 (melanoma growth stimulating activity, alpha) (CXCL1)	-2.30	13.24	3.35E-14	29.50
IL1B	interleukin 1, beta (IL1B)	-1.12	7.37	1.10E-05	5.27
IL18	interleukin 18 (interferon-gamma-inducing factor) (IL18)	-1.15	11.24	4.11E-07	9.39
IL6	interleukin 6 (interferon, beta 2) (IL6)	-2.07	9.3	7.36E-08	11.45
IL8	interleukin 8 (IL8)	-2.43	7.01	1.53E-03	-0.71
CASP8	caspase 8, apoptosis-related cysteine peptidase (CASP8)	1.29	6.88	2.46E-06	7.12
CCL5	chemokine (C-C motif) ligand 5 (CCL5)	2.61	10.49	1.38E-07	10.67
MAPK13	mitogen-activated protein kinase 13 (MAPK13)	1.02	6.57	5.96E-05	3.21
TNFAIP3	tumor necrosis factor, alpha-induced protein 3 (TNFAIP3)	1.15	9.71	1.86E-08	13.16

hsa00830 Retinol metabolism

GeneName	Description	logFC	AveExpr	adj.P.Val	B
UGT1A6	UDP glucuronosyltransferase 1 family, polypeptide A6 (UGT1A6)	-1.35	6.99	7.13E-07	8.62
UGT1A8	UDP glucuronosyltransferase 1 family, polypeptide A8 (UGT1A8)	-1.30	6.71	1.27E-06	7.93
UGT2B10	UDP glucuronosyltransferase 2 family, polypeptide B10 (UGT2B10)	-1.26	7.04	1.40E-06	7.80
UGT2B11	UDP glucuronosyltransferase 2 family, polypeptide B11 (UGT2B11)	-1.79	3.95	1.84E-03	-0.94
UGT2B15	UDP glucuronosyltransferase 2 family, polypeptide B15 (UGT2B15)	-2.71	3.38	1.20E-04	2.35
UGT2B7	UDP glucuronosyltransferase 2 family, polypeptide B7 (UGT2B7)	-1.82	4.64	8.98E-05	2.70
BCMO1	beta-carotene 15,15'-monooxygenase 1 (BCMO1)	-1.43	6.26	3.29E-08	12.45
CYP3A5	cytochrome P450, family 3, subfamily A, polypeptide 5 (CYP3A5)	-1.03	9.91	1.56E-06	7.66
CYP3A7	cytochrome P450, family 3, subfamily A, polypeptide 7 (CYP3A7)	-1.02	10.23	4.86E-07	9.10
DHRS9	dehydrogenase/reductase (SDR family) member 9 (DHRS9)	-3.34	6.01	1.62E-09	16.22
CYP26B1	cytochrome P450, family 26, subfamily B, polypeptide 1 (CYP26B1)	1.60	4.25	3.49E-03	-1.70
DGAT2	diacylglycerol O-acyltransferase 2 (DGAT2)	1.46	7.35	1.65E-08	13.32

hsa04610 Complement and coagulation cascades

GeneName	Description	logFC	AveExpr	adj.P.Val	B
CD55	CD55 molecule, decay accelerating factor for complement (Cromer blood group) (CD55)	-1.36	11.64	1.44E-10	19.29
C4BPA	complement component 4 binding protein, alpha (C4BPA)	-3.45	7.07	3.27E-14	29.56
C4BPB	complement component 4 binding protein, beta (C4BPB)	-1.00	5.98	7.58E-05	2.91
CFB	complement factor B (CFB)	-2.30	9.99	1.06E-09	16.78
CFD	complement factor D (adipsin) (CFD)	-1.40	13.39	1.01E-09	16.83
CFH	complement factor H (CFH)	-3.00	9.92	1.24E-12	25.14
CFI	complement factor I (CFI)	-5.42	4.29	3.85E-12	23.76
FGA	fibrinogen alpha chain (FGA)	-4.57	5.44	9.46E-11	19.83
FGB	fibrinogen beta chain (FGB)	-5.66	4.89	1.01E-14	31.20
FGG	fibrinogen gamma chain (FGG)	-7.15	6.48	2.22E-12	24.44
KNG1	kininogen 1 (KNG1)	-1.54	2.47	5.68E-03	-2.27
C3	complement component 3 (C3)	-3.21	12.72	7.44E-12	22.98

TFPI	tissue factor pathway inhibitor (lipoprotein-associated coagulation inhibitor) (TFPI)	1.70	8.09	8.67E-11	19.94

hsa04670	**Leukocyte transendothelial migration**				
GeneName	**Description**	**logFC**	**AveExpr**	**adj.P.Val**	**B**
CD99	CD99 molecule (CD99)	-1.04	12.25	3.43E-08	12.40
NOX1	NADPH oxidase 1 (NOX1)	-1.30	3.63	2.86E-02	-4.18
RASSF5	Ras association (RalGDS/AF-6) domain family member 5 (RASSF5)	-1.21	3.46	2.37E-02	-3.95
CXCL12	chemokine (C-X-C motif) ligand 12 (CXCL12)	-1.61	2.71	2.84E-02	-4.08
CLDN7	claudin 7 (CLDN7)	-1.20	5.55	1.14E-03	-0.36
ITGB2	integrin, beta 2 (complement component 3 receptor 3 and 4 subunit) (ITGB2)	-1.51	5.95	7.49E-05	2.92
MYL9	myosin, light chain 9, regulatory (MYL9)	-3.74	6.91	3.22E-10	18.29
RAPGEF3	Rap guanine nucleotide exchange factor (GEF) 3 (RAPGEF3)	1.10	4.44	8.23E-03	-2.71
CTNNA2	catenin (cadherin-associated protein), alpha 2 (CTNNA2)	2.72	3.13	4.54E-05	3.53
CXCR4	chemokine (C-X-C motif) receptor 4 (CXCR4)	3.78	7.23	1.81E-10	19.00
ITGA4	integrin, alpha 4 (antigen CD49D, alpha 4 subunit of VLA-4 receptor) (ITGA4)	1.96	4.49	3.38E-05	3.89
ICAM1	intercellular adhesion molecule 1 (ICAM1)	2.44	7.68	2.42E-05	4.29
MAPK13	mitogen-activated protein kinase 13 (MAPK13)	1.02	6.57	5.96E-05	3.21
NCF1	neutrophil cytosolic factor 1 (NCF1)	1.18	3.02	3.73E-02	-4.49
PLCG2	phospholipase C, gamma 2 (phosphatidylinositol-specific) (PLCG2)	1.77	8.92	2.10E-10	18.83
RHOH	ras homolog gene family, member H (RHOH)	1.33	4.18	2.37E-02	-3.95
VCAM1	vascular cell adhesion molecule 1 (VCAM1)	1.34	2.76	1.00E-03	-0.21

hsa00512	**Mucin type O-glycan biosynthesis**				
GeneName	**Description**	**logFC**	**AveExpr**	**adj.P.Val**	**B**
ST3GAL1	ST3 beta-galactoside alpha-2,3-sialyltransferase 1 (ST3GAL1)	-1.22	9.47	1.97E-07	10.23
ST6GALNAC1	ST6 (alpha-N-acetyl-neuraminyl-2,3-beta-galactosyl-1,3)-N-acetylgalactosaminide alpha-2,6-sialyltransferase 1 (ST6GALNAC1)	-4.56	3.36	3.71E-07	9.45
B4GALT5	UDP-Gal:betaGlcNAc beta 1,4- galactosyltransferase, polypeptide 5 (B4GALT5)	-1.03	12.99	3.80E-09	15.15
GALNT5	UDP-N-acetyl-alpha-D-galactosamine:polypeptide N-acetylgalactosaminyltransferase 5 (GalNAc-T5) (GALNT5)	-2.34	5.69	2.30E-06	7.20
GALNT6	UDP-N-acetyl-alpha-D-galactosamine:polypeptide N-acetylgalactosaminyltransferase 6 (GalNAc-T6) (GALNT6)	-1.41	7.96	6.64E-10	17.36
GALNT5	UDP-N-acetyl-alpha-D-galactosamine:polypeptide N-acetylgalactosaminyltransferase 5 (GalNAc-T5) (GALNT5)	-2.34	5.69	2.30E-06	7.20
GALNT13	UDP-N-acetyl-alpha-D-galactosamine:polypeptide N-acetylgalactosaminyltransferase 13 (GalNAc-T13) (GALNT13)	1.56	3.9	2.82E-02	-4.16
GALNT14	UDP-N-acetyl-alpha-D-galactosamine:polypeptide N-acetylgalactosaminyltransferase 14 (GalNAc-T14) (GALNT14)	1.16	14.13	1.30E-09	16.51
GALNTL2	UDP-N-acetyl-alpha-D-galactosamine:polypeptide N-acetylgalactosaminyltransferase-like 2 (GALNTL2)	2.38	2.4	1.06E-05	5.32
GCNT4	glucosaminyl (N-acetyl) transferase 4, core 2 (GCNT4)	1.66	3.45	6.95E-03	-2.51

hsa00150	**Androgen and estrogen metabolism**				
GeneName	**Description**	**logFC**	**AveExpr**	**adj.P.Val**	**B**
UGT1A6	UDP glucuronosyltransferase 1 family, polypeptide A6 (UGT1A6)	-1.35	6.99	7.13E-07	8.62
UGT1A8	UDP glucuronosyltransferase 1 family, polypeptide A8 (UGT1A8)	-1.30	6.71	1.27E-06	7.93
UGT2B10	UDP glucuronosyltransferase 2 family, polypeptide B10 (UGT2B10)	-1.26	7.04	1.40E-06	7.80
UGT2B11	UDP glucuronosyltransferase 2 family, polypeptide B11 (UGT2B11)	-1.79	3.95	1.84E-03	-0.94
UGT2B15	UDP glucuronosyltransferase 2 family, polypeptide B15 (UGT2B15)	-2.71	3.38	1.20E-04	2.35
UGT2B7	UDP glucuronosyltransferase 2 family, polypeptide B7 (UGT2B7)	-1.82	4.64	8.98E-05	2.70
AKR1C4	aldo-keto reductase family 1, member C4 (chlordecone reductase; 3-alpha hydroxysteroid dehydrogenase, type I; dihydrodiol dehydrogenase 4) (AKR1C4)	-2.43	2.82	5.55E-06	6.11
HSD11B1	hydroxysteroid (11-beta) dehydrogenase 1 (HSD11B1)	-2.74	4.23	3.46E-02	-4.40
STS	steroid sulfatase (microsomal), isozyme S (STS)	-1.67	6.17	1.62E-06	7.62
HSD17B2	hydroxysteroid (17-beta) dehydrogenase 2 (HSD17B2)	1.51	2.95	2.79E-02	-4.15

hsa 00500	**Starch and sucrose metabolism**				
GeneName	**Description**	**logFC**	**AveExpr**	**adj.P.Val**	**B**
UGT1A6	UDP glucuronosyltransferase 1 family, polypeptide A6 (UGT1A6)	-1.35	6.99	7.13E-07	8.62
UGT1A8	UDP glucuronosyltransferase 1 family, polypeptide A8 (UGT1A8)	-1.30	6.71	1.27E-06	7.93
UGT2B10	UDP glucuronosyltransferase 2 family, polypeptide B10 (UGT2B10)	-1.26	7.04	1.40E-06	7.80
UGT2B11	UDP glucuronosyltransferase 2 family, polypeptide B11 (UGT2B11)	-1.79	3.95	1.84E-03	-0.94
UGT2B15	UDP glucuronosyltransferase 2 family, polypeptide B15 (UGT2B15)	-2.71	3.38	1.20E-04	2.35
UGT2B7	UDP glucuronosyltransferase 2 family, polypeptide B7 (UGT2B7)	-1.82	4.64	8.98E-05	2.70
MGAM	maltase-glucoamylase (alpha-glucosidase) (MGAM)	-3.91	4.59	1.29E-10	19.43
AMY1C	amylase, alpha 1C (salivary) (AMY1C)	1.40	7.04	1.50E-07	10.57
HK2	hexokinase 2 (HK2)	2.23	8.08	7.40E-12	22.99

hsa04640	**Hematopoietic cell lineage**				
GeneName	**Description**	**logFC**	**AveExpr**	**adj.P.Val**	**B**
CD19	CD19 molecule (CD19)	-1.35	3.03	1.66E-02	-3.53
CD38	CD38 molecule (CD38)	-3.16	10.69	1.40E-13	27.78
CD55	CD55 molecule, decay accelerating factor for complement (Cromer blood group) (CD55)	-1.36	11.64	1.44E-10	19.29
CSF2RA	colony stimulating factor 2 receptor, alpha, low-affinity (granulocyte-macrophage) (CSF2RA)	-1.52	6.95	4.38E-07	9.23
IL1R2	interleukin 1 receptor, type II (IL1R2)	-1.47	3.27	1.60E-02	-3.49
IL1B	interleukin 1, beta (IL1B)	-1.12	7.37	1.10E-05	5.27
IL6	interleukin 6 (interferon, beta 2) (IL6)	-2.07	9.3	7.36E-08	11.45
IL7R	interleukin 7 receptor (IL7R)	-2.05	6.99	2.36E-07	10.01
CD33	CD33 molecule (CD33)	2.09	2.91	5.41E-07	8.97
ITGA4	integrin, alpha 4 (antigen CD49D, alpha 4 subunit of VLA-4 receptor) (ITGA4)	1.96	4.49	3.38E-05	3.89
ITGB3	integrin, beta 3 (platelet glycoprotein IIIa, antigen CD61) (ITGB3)	1.32	7.86	1.01E-04	2.56
IL3RA	interleukin 3 receptor, alpha (low affinity) (IL3RA)	1.02	6.1	8.06E-04	0.06

hsa00040	Pentose and glucuronate interconversions				
GeneName	**Description**	**logFC**	**AveExpr**	**adj.P.Val**	**B**
UGT1A6	UDP glucuronosyltransferase 1 family, polypeptide A6 (UGT1A6)	-1.35	6.99	7.13E-07	8.62
UGT1A8	UDP glucuronosyltransferase 1 family, polypeptide A8 (UGT1A8)	-1.30	6.71	1.27E-06	7.93
UGT2B10	UDP glucuronosyltransferase 2 family, polypeptide B10 (UGT2B10)	-1.26	7.04	1.40E-06	7.80
UGT2B11	UDP glucuronosyltransferase 2 family, polypeptide B11 (UGT2B11)	-1.79	3.95	1.84E-03	-0.94
UGT2B15	UDP glucuronosyltransferase 2 family, polypeptide B15 (UGT2B15)	-2.71	3.38	1.20E-04	2.35
UGT2B7	UDP glucuronosyltransferase 2 family, polypeptide B7 (UGT2B7)	-1.82	4.64	8.98E-05	2.70

hsa04514	Cell adhesion molecules				
GeneName	**Description**	**logFC**	**AveExpr**	**adj.P.Val**	**B**
CD99	CD99 molecule (CD99)	-1.04	12.25	3.43E-08	12.40
CLDN7	claudin 7 (CLDN7)	-1.20	5.55	1.14E-03	-0.36
CNTN1	contactin 1 (CNTN1)	-4.01	7.14	3.37E-13	26.72
ITGB2	integrin, beta 2 (complement component 3 receptor 3 and 4 subunit) (ITGB2)	-1.51	5.95	7.49E-05	2.92
ICAM2	intercellular adhesion molecule 2 (ICAM2)	-1.62	5.18	1.19E-03	-0.42
HLA-DMA	major histocompatibility complex, class II, DM alpha (HLA-DMA)	-1.95	7.93	1.25E-11	22.33
HLA-DMB	major histocompatibility complex, class II, DM beta (HLA-DMB)	-2.97	7.84	3.58E-10	18.17
SELE	selectin E (SELE)	-2.09	3.49	1.70E-02	-3.56
VCAN	versican (VCAN)	-4.86	9.33	2.07E-15	33.29
CDH4	cadherin 4, type 1, R-cadherin (retinal) (CDH4)	1.54	10.12	4.36E-09	14.98
ITGA4	integrin, alpha 4 (antigen CD49D, alpha 4 subunit of VLA-4 receptor) (ITGA4)	1.96	4.49	3.38E-05	3.89
ICAM1	intercellular adhesion molecule 1 (ICAM1)	2.44	7.68	2.42E-05	4.29
MADCAM1	mucosal vascular addressin cell adhesion molecule 1 (MADCAM1)	1.19	4.8	3.86E-02	-4.52
NLGN3	neuroligin 3 (NLGN3)	1.24	3.5	4.12E-02	-4.60
VCAM1	vascular cell adhesion molecule 1 (VCAM1)	1.34	2.76	1.00E-03	-0.21

hsa00590	Arachidonic acid metabolism				
GeneName	**Description**	**logFC**	**AveExpr**	**adj.P.Val**	**B**
ALOX5	arachidonate 5-lipoxygenase (ALOX5)	-5.10	5.41	1.67E-11	21.98
CYP4F2	cytochrome P450, family 4, subfamily F, polypeptide 2 (CYP4F2)	-1.70	5.63	2.87E-05	4.08
GPX2	glutathione peroxidase 2 (gastrointestinal) (GPX2)	-4.21	11.1	5.77E-14	28.85
PLA2G4A	phospholipase A2, group IVA (cytosolic, calcium-dependent) (PLA2G4A)	-2.02	9.91	4.44E-09	14.97
PLA2G5	phospholipase A2, group V (PLA2G5)	-2.04	3.3	3.37E-02	-4.37
PTGES	prostaglandin E synthase (PTGES)	-1.22	9.94	1.73E-08	13.25
PTGS2	prostaglandin-endoperoxide synthase 2 (prostaglandin G/H synthase and cyclooxygenase) (PTGS2)	-1.50	9.91	2.45E-08	12.81
CBR3	carbonyl reductase 3 (CBR3)	1.06	9.57	1.26E-08	13.65
CYP2J2	cytochrome P450, family 2, subfamily J, polypeptide 2 (CYP2J2)	2.22	6.33	6.19E-10	17.47

hsa04620	Toll-like receptor signaling pathway				
GeneName	**Description**	**logFC**	**AveExpr**	**adj.P.Val**	**B**
IL1B	interleukin 1, beta (IL1B)	-1.12	7.37	1.10E-05	5.27
IL6	interleukin 6 (interferon, beta 2) (IL6)	-2.07	9.3	7.36E-08	11.45
IL8	interleukin 8 (IL8)	-2.06	6.91	1.46E-03	-0.66
LBP	lipopolysaccharide binding protein (LBP)	-1.32	3.77	1.51E-02	-3.42
SPP1	secreted phosphoprotein 1 (SPP1)	-1.14	12.88	3.54E-10	18.23
TLR2	toll-like receptor 2 (TLR2)	-1.37	4.14	5.61E-07	8.92
TLR3	toll-like receptor 3 (TLR3)	-2.88	6.15	4.68E-06	6.32
TLR4	toll-like receptor 4 (TLR4)	-3.41	3.58	4.78E-07	9.12
FOS	FBJ murine osteosarcoma viral oncogene homolog (FOS)	-1.21	9.68	3.51E-08	12.37
CASP8	caspase 8, apoptosis-related cysteine peptidase (CASP8)	1.29	6.88	2.46E-06	7.12
CCL5	chemokine (C-C motif) ligand 5 (CCL5)	3.01	10.29	7.02E-10	17.27
MAPK13	mitogen-activated protein kinase 13 (MAPK13)	1.02	6.57	5.96E-05	3.21
MAP3K8	mitogen-activated protein kinase kinase kinase 8 (MAP3K8)	1.07	10.55	1.59E-08	13.36

7.1.2.4 p.E292V vs. WT (RSV-infected)

Table 7.14: Regulated genes in regulated KEGG pathways, comparison p.E292V vs. WT in the presence of virus.

hsa04610	Complement and coagulation cascades				
GeneName	**Description**	**logFC**	**AveExpr**	**adj.P.Val**	**B**
CD55	CD55 molecule, decay accelerating factor for complement (Cromer blood group) (CD55)	-1.28	11.71	6.95E-11	20.30
F2	coagulation factor II (thrombin) (F2)	-1.01	6.35	5.50E-04	0.38
C4BPA	complement component 4 binding protein, alpha (C4BPA)	-3.09	7.1	1.95E-10	19.00
C4BPB	complement component 4 binding protein, beta (C4BPB)	-4.47	5.98	1.95E-12	24.60
C4B	complement component 4B (Chido blood group) (C4B)	-1.97	7.07	1.16E-11	22.40
CFB	complement factor B (CFB)	-1.88	9.99	1.19E-08	13.70
CFD	complement factor D (adipsin) (CFD)	-1.24	13.39	4.39E-09	15.00
CFH	complement factor H (CFH)	-2.10	9.92	9.34E-11	19.90
CFI	complement factor I (CFI)	-3.30	4.29	1.72E-09	16.20
FGA	fibrinogen alpha chain (FGA)	-5.31	5.36	2.09E-07	10.10
FGB	fibrinogen beta chain (FGB)	-3.25	4.89	7.06E-12	23.10
FGG	fibrinogen gamma chain (FGG)	-6.44	6.48	8.21E-12	22.90
SERPING1	serpin peptidase inhibitor, clade G (C1 inhibitor), member 1 (SERPING1)	-1.32	3.35	4.78E-03	-2.19
C3	complement component 3 (C3)	-1.13	12.67	1.44E-06	7.68
PROS1	protein S (alpha) (PROS1)	1.36	8.99	6.39E-10	17.50
TFPI	tissue factor pathway inhibitor (lipoprotein-associated coagulation inhibitor) (TFPI)	1.14	8.06	6.78E-07	8.61

hsa04060	Cytokine-cytokine receptor interaction				
GeneName	**Description**	**logFC**	**AveExpr**	**adj.P.Val**	**B**
CCL2	chemokine (C-C motif) ligand 2 (CCL2)	-2.32	11.18	5.32E-13	26.30
CCL20	chemokine (C-C motif) ligand 20 (CCL20)	-1.22	6.53	7.21E-05	2.84
CCL25	chemokine (C-C motif) ligand 25 (CCL25)	-1.03	3.39	1.35E-02	-3.40
CCL28	chemokine (C-C motif) ligand 28 (CCL28)	-4.58	3.49	3.12E-08	12.50
CXCL10	chemokine (C-X-C motif) ligand 10 (CXCL10)	-1.41	4.62	4.20E-08	12.10
CXCL6	chemokine (C-X-C motif) ligand 6 (granulocyte chemotactic protein 2) (CXCL6)	-2.84	3.08	1.22E-07	10.80
CSF2RA	colony stimulating factor 2 receptor, alpha, low-affinity (granulocyte-macrophage) (CSF2RA)	-1.32	6.95	1.96E-06	7.30
INHBB	inhibin, beta B (INHBB)	-1.40	11.04	3.52E-09	15.30
IL13	interleukin 13 (IL13)	-2.08	3.3	2.54E-05	4.11
IL18	interleukin 18 (interferon-gamma-inducing factor) (IL18)	-1.17	11.19	8.60E-12	22.80
IL21R	interleukin 21 receptor (IL21R)	-1.64	4.56	2.65E-04	1.26
IL28A	interleukin 28A (interferon, lambda 2) (IL28A)	-1.61	10.46	2.49E-07	9.84
IL28B	interleukin 28B (interferon, lambda 3) (IL28B)	-1.80	7.4	3.16E-08	12.50
IL6	interleukin 6 (interferon, beta 2) (IL6)	-2.20	9.33	5.95E-08	11.70
PPBP	pro-platelet basic protein (chemokine (C-X-C motif) ligand 7) (PPBP)	-2.61	3.78	1.78E-04	1.78
TNF	tumor necrosis factor (TNF)	-1.58	6.49	3.72E-03	-1.90
TNFSF10	tumor necrosis factor (ligand) superfamily, member 10 (TNFSF10)	-2.56	7.03	8.34E-07	8.36
TNFSF14	tumor necrosis factor (ligand) superfamily, member 14 (TNFSF14)	-1.70	7.12	2.53E-06	6.98
TNFRSF14	tumor necrosis factor receptor superfamily, member 14 (herpesvirus entry mediator) (TNFRSF14)	-3.45	5.43	4.78E-10	17.80
TNFRSF21	tumor necrosis factor receptor superfamily, member 21 (TNFRSF21)	-1.02	12.48	2.53E-09	15.70
ACVR1	activin A receptor, type I (ACVR1)	1.19	8.52	1.70E-07	10.30
CCL1	chemokine (C-C motif) ligand 1 (CCL1)	1.14	3.03	2.60E-02	-4.16
CCL19	chemokine (C-C motif) ligand 19 (CCL19)	1.91	4.64	8.37E-05	2.65
CCL17	chemokine (C-C motif) ligand 17 (CCL17)	1.89	7.88	2.64E-08	12.70
CCL14	chemokine (C-C motif) ligand 14 (CCL14)	1.72	2.23	3.72E-02	-4.58
CCL3L3	chemokine (C-C motif) ligand 3-like 3 (CCL3L3)	1.79	8.28	2.10E-02	-3.92
CCL3	chemokine (C-C motif) ligand 3 (CCL3)	1.21	9.58	7.41E-05	2.80
CCL5	chemokine (C-C motif) ligand 5 (CCL5)	1.18	10.49	4.93E-04	0.51
CCR7	chemokine (C-C motif) receptor 7 (CCR7)	1.50	8.78	2.02E-09	16.00
CXCR4	chemokine (C-X-C motif) receptor 4 (CXCR4)	1.68	7.24	2.15E-06	7.18
CSF1R	colony stimulating factor 1 receptor (CSF1R)	2.01	4.38	5.73E-06	5.95
EPOR	erythropoietin receptor (EPOR)	1.44	8.68	1.54E-08	13.40
IL1R1	interleukin 1 receptor, type I (IL1R1)	1.38	6.57	1.33E-08	13.60
IL1A	interleukin 1, alpha (IL1A)	1.37	5.85	1.41E-05	4.83
IL10RA	interleukin 10 receptor, alpha (IL10RA)	1.35	5.6	9.20E-04	-0.25
IL18R1	interleukin 18 receptor 1 (IL18R1)	1.97	5.13	4.44E-02	-4.78
IL2RG	interleukin 2 receptor, gamma (IL2RG)	1.42	4.29	2.31E-03	-1.33
PDGFRA	platelet-derived growth factor receptor, alpha polypeptide (PDGFRA)	3.30	3.34	5.52E-05	3.16
PRLR	prolactin receptor (PRLR)	3.06	2.21	4.03E-08	12.20
TNFRSF8	tumor necrosis factor receptor superfamily, member 8 (TNFRSF8)	1.19	6.42	1.74E-04	1.77

hsa04514	Cell adhesion molecules (CAMs)				
GeneName	**Description**	**logFC**	**AveExpr**	**adj.P.Val**	**B**
CDH1	cadherin 1, type 1, E-cadherin (epithelial) (CDH1)	-3.36	10.1	1.25E-13	28.20
CNTN1	contactin 1 (CNTN1)	-4.12	7.05	4.27E-11	20.80
ITGB2	integrin, beta 2 (complement component 3 receptor 3 and 4 subunit) (ITGB2)	-1.92	5.97	2.87E-07	9.66
ICAM2	intercellular adhesion molecule 2 (ICAM2)	-1.14	5.12	1.29E-02	-3.36
HLA-DMB	major histocompatibility complex, class II, DM beta (HLA-DMB)	-4.31	7.91	1.77E-06	7.43
PECAM1	platelet/endothelial cell adhesion molecule (PECAM1)	-2.70	2.67	1.15E-08	13.80
SELE	selectin E (SELE)	2.11	2.94	3.40E-04	0.95
VCAM1	vascular cell adhesion molecule 1 (VCAM1)	-3.19	2.82	3.81E-06	6.46
VCAN	versican (VCAN)	-4.28	9.33	9.25E-15	31.50
CD22	CD22 molecule (CD22)	2.21	3.69	1.70E-03	-0.97
L1CAM	L1 cell adhesion molecule (L1CAM)	1.76	5.87	1.39E-05	4.85
CDH15	cadherin 15, type 1, M-cadherin (myotubule) (CDH15)	2.00	4.93	2.03E-06	7.25

CDH4	cadherin 4, type 1, R-cadherin (retinal) (CDH4)	1.67	10.12	1.71E-09	16.20
ITGA4	integrin, alpha 4 (antigen CD49D, alpha 4 subunit of VLA-4 receptor) (ITGA4)	1.77	3.2	3.03E-08	12.50
ITGAV	integrin, alpha V (vitronectin receptor, alpha polypeptide, antigen CD51) (ITGAV)	1.07	12.66	6.71E-10	17.40
ICAM1	intercellular adhesion molecule 1 (ICAM1)	1.45	7.79	1.10E-04	2.32
ICAM3	intercellular adhesion molecule 3 (ICAM3)	1.25	10.35	3.20E-11	21.20
MADCAM1	mucosal vascular addressin cell adhesion molecule 1 (MADCAM1)	1.33	4.8	1.96E-02	-3.84
NLGN3	neuroligin 3 (NLGN3)	1.27	3.12	1.04E-03	-0.39
PDCD1LG2	programmed cell death 1 ligand 2 (PDCD1LG2)	1.47	2.73	5.25E-04	0.44

hsa04062 Chemokine signaling pathway

GeneName	Description	logFC	AveExpr	adj.P.Val	B
ROCK2	Rho-associated, coiled-coil containing protein kinase 2 (ROCK2)	-1.03	10.34	1.91E-09	16.10
SHC4	SHC (Src homology 2 domain containing) family, member 4 (SHC4)	-1.56	4.32	2.70E-03	-1.52
CCL2	chemokine (C-C motif) ligand 2 (CCL2)	-2.32	11.18	5.32E-13	26.30
CCL20	chemokine (C-C motif) ligand 20 (CCL20)	-1.22	6.53	7.21E-05	2.84
CCL25	chemokine (C-C motif) ligand 25 (CCL25)	-1.03	3.39	1.35E-02	-3.40
CCL28	chemokine (C-C motif) ligand 28 (CCL28)	-4.58	3.49	3.12E-08	12.50
CXCL6	chemokine (C-X-C motif) ligand 6 (granulocyte chemotactic protein 2) (CXCL6)	-2.84	3.08	1.22E-07	10.80
CXCL10	chemokine (C-X-C motif) ligand 10 (CXCL10)	-1.41	4.62	4.20E-08	12.10
CXCR3	chemokine (C-X-C motif) receptor 3 (CXCR3)	-1.33	7.58	1.16E-05	5.08
GNG2	guanine nucleotide binding protein (G protein), gamma 2 (GNG2)	-1.24	3.22	4.81E-02	-4.87
NCF1	neutrophil cytosolic factor 1 (NCF1)	-1.51	3.02	8.17E-03	-2.82
PPBP	pro-platelet basic protein (chemokine (C-X-C motif) ligand 7) (PPBP)	-2.61	3.78	1.78E-04	1.78
VAV3	vav 3 guanine nucleotide exchange factor (VAV3)	-1.20	8.62	6.97E-07	8.57
GRK4	G protein-coupled receptor kinase 4 (GRK4)	1.43	3.05	1.76E-02	-3.72
SHC3	SHC (Src homology 2 domain containing) transforming protein 3 (SHC3)	1.58	4.43	1.38E-02	-3.43
CCL1	chemokine (C-C motif) ligand 1 (CCL1)	1.14	3.03	2.60E-02	-4.16
CCL14	chemokine (C-C motif) ligand 14 (CCL14)	1.72	2.23	3.72E-02	-4.58
CCL17	chemokine (C-C motif) ligand 17 (CCL17)	1.91	8.04	1.21E-05	5.03
CCL19	chemokine (C-C motif) ligand 19 (CCL19)	1.91	4.64	8.37E-05	2.65
CCL3	chemokine (C-C motif) ligand 3 (CCL3)	1.21	9.58	7.41E-05	2.80
CCL3L3	chemokine (C-C motif) ligand 3-like 3 (CCL3L3)	1.79	8.28	2.10E-02	-3.92
CCL5	chemokine (C-C motif) ligand 5 (CCL5)	1.18	10.49	4.93E-04	0.51
CCR7	chemokine (C-C motif) receptor 7 (CCR7)	1.50	8.78	2.02E-09	16.00
CXCR4	chemokine (C-X-C motif) receptor 4 (CXCR4)	1.68	7.24	2.15E-06	7.18
ELMO1	engulfment and cell motility 1 (ELMO1)	1.24	6.12	1.21E-05	5.02
GNG8	guanine nucleotide binding protein (G protein), gamma 8 (GNG8)	1.77	6.83	4.70E-06	6.19
PLCB1	phospholipase C, beta 1 (phosphoinositide-specific) (PLCB1)	1.53	5.97	2.47E-06	7.01
RAC2	ras-related C3 botulinum toxin substrate 2 (rho family, small GTP binding protein Rac2) (RAC2)	1.20	7.88	2.32E-05	4.22

hsa04360 Axon guidance

GeneName	Description	logFC	AveExpr	adj.P.Val	B
EPHA4	EPH receptor A4 (EPHA4)	-1.05	7.24	1.05E-05	5.28
ROCK2	Rho-associated, coiled-coil containing protein kinase 2 (ROCK2)	-1.03	10.34	1.91E-09	16.10
ABLIM1	actin binding LIM protein 1 (ABLIM1)	-1.09	12.01	6.98E-10	17.40
EFNB2	ephrin-B2 (EFNB2)	-1.49	8.93	1.23E-08	13.70
FES	feline sarcoma oncogene (FES)	-1.25	5.69	9.92E-07	8.14
RGS3	regulator of G-protein signaling 3 (RGS3)	-1.84	3.87	5.80E-04	0.32
SEMA3B	sema domain, immunoglobulin domain (Ig), short basic domain, secreted, (semaphorin) 3B (SEMA3B)	-1.41	11.52	1.24E-08	13.70
SEMA4G	sema domain, immunoglobulin domain (Ig), transmembrane domain (TM) and short cytoplasmic domain, (semaphorin) 4G (SEMA4G)	-1.62	8.58	8.06E-10	17.20
UNC5D	unc-5 homolog D (C. elegans) (UNC5D)	-2.19	2.9	1.52E-05	4.74
EPHA5	EPH receptor A5 (EPHA5)	2.39	4.15	3.26E-07	9.50
EPHB3	EPH receptor B3 (EPHB3)	1.83	4.08	5.65E-03	-2.39
EPHB6	EPH receptor B6 (EPHB6)	1.42	4.08	2.58E-03	-1.47
FYN	FYN oncogene related to SRC, FGR, YES (FYN)	1.52	8.78	2.23E-08	12.90
L1CAM	L1 cell adhesion molecule (L1CAM)	1.76	5.87	1.39E-05	4.85
ABLIM3	actin binding LIM protein family, member 3 (ABLIM3)	1.20	6.43	5.91E-06	5.91
CXCR4	chemokine (C-X-C motif) receptor 4 (CXCR4)	1.68	7.24	2.15E-06	7.18
NFATC2	nuclear factor of activated T-cells, cytoplasmic, calcineurin-dependent 2 (NFATC2)	1.99	2.57	9.63E-03	-3.01
RAC2	ras-related C3 botulinum toxin substrate 2 (rho family, small GTP binding protein Rac2) (RAC2)	1.20	7.88	2.32E-05	4.22
SEMA3D	sema domain, immunoglobulin domain (Ig), short basic domain, secreted, (semaphorin) 3D (SEMA3D)	2.25	4.16	5.17E-10	17.70
SLIT3	slit homolog 3 (Drosophila) (SLIT3)	1.10	12.72	3.68E-10	18.20

hsa04623 Cytosolic DNA-sensing pathway

GeneName	Description	logFC	AveExpr	adj.P.Val	B
PYCARD	PYD and CARD domain containing (PYCARD)	-1.00	12.48	2.53E-09	15.70
ZBP1	Z-DNA binding protein 1 (ZBP1)	-3.51	3.32	6.72E-07	8.62
CASP1	caspase 1, apoptosis-related cysteine peptidase (interleukin 1, beta, convertase) (CASP1)	-2.07	6.22	4.46E-06	6.26
CXCL10	chemokine (C-X-C motif) ligand 10 (CXCL10)	-1.41	4.62	4.20E-08	12.10
IL18	interleukin 18 (interferon-gamma-inducing factor) (IL18)	-1.17	11.19	8.60E-12	22.80
IL6	interleukin 6 (interferon, beta 2) (IL6)	-2.20	9.33	5.95E-08	11.70
TMEM173	transmembrane protein 173 (TMEM173), nuclear gene encoding mitochondrial protein	-1.41	7.86	9.53E-10	16.90
AIM2	absent in melanoma 2 (AIM2)	2.87	2.71	2.31E-05	4.23
CCL5	chemokine (C-C motif) ligand 5 (CCL5)	1.18	10.49	4.93E-04	0.51
IL33	interleukin 33 (IL33)	1.14	5.52	5.97E-03	-2.46

hsa04640 Hematopoietic cell lineage

GeneName	Description	logFC	AveExpr	adj.P.Val	B
CD38	CD38 molecule (CD38)	-1.50	10.64	2.42E-10	18.70
CD55	CD55 molecule, decay accelerating factor for complement (Cromer blood group) (CD55)	-1.28	11.71	6.95E-11	20.30
CSF2RA	colony stimulating factor 2 receptor, alpha, low-affinity (granulocyte-macrophage) (CSF2RA)	-1.32	6.95	1.96E-06	7.30
IL6	interleukin 6 (interferon, beta 2) (IL6)	-2.20	9.33	5.95E-08	11.70

TNF	tumor necrosis factor (TNF)	-1.58	6.49	3.72E-03	-1.90
CD22	CD22 molecule (CD22)	2.21	3.69	1.70E-03	-0.97
ANPEP	alanyl (membrane) aminopeptidase (ANPEP)	2.11	9.64	2.46E-10	18.70
CSF1R	colony stimulating factor 1 receptor (CSF1R)	2.01	4.38	5.73E-06	5.95
EPOR	erythropoietin receptor (EPOR)	1.44	8.68	1.54E-08	13.40
ITGA4	integrin, alpha 4 (antigen CD49D, alpha 4 subunit of VLA-4 receptor) (ITGA4)	1.77	3.2	3.03E-08	12.50
ITGB3	integrin, beta 3 (platelet glycoprotein IIIa, antigen CD61) (ITGB3)	2.25	7.86	2.89E-07	9.65
IL1R1	interleukin 1 receptor, type I (IL1R1)	1.38	6.57	1.33E-08	13.60
IL1A	interleukin 1, alpha (IL1A)	1.37	5.85	1.41E-05	4.83

hsa04670	**Leukocyte transendothelial migration**				
GeneName	**Description**	**logFC**	**AveExpr**	**adj.P.Val**	**B**
ROCK2	Rho-associated, coiled-coil containing protein kinase 2 (ROCK2)	-1.03	10.34	1.91E-09	16.10
ITGB2	integrin, beta 2 (complement component 3 receptor 3 and 4 subunit) (ITGB2)	-1.89	5.89	5.57E-06	5.98
MYL9	myosin, light chain 9, regulatory (MYL9)	-2.75	6.91	1.28E-08	13.60
NCF1	neutrophil cytosolic factor 1 (NCF1)	-1.51	3.02	8.17E-03	-2.82
PECAM1	platelet/endothelial cell adhesion molecule (PECAM1)	-2.70	2.67	1.15E-08	13.80
VCAM1	vascular cell adhesion molecule 1 (VCAM1)	-3.19	2.82	3.81E-06	6.46
VAV3	vav 3 guanine nucleotide exchange factor (VAV3)	-1.20	8.62	6.97E-07	8.57
RAPGEF3	Rap guanine nucleotide exchange factor (GEF) 3 (RAPGEF3)	1.77	4.44	1.51E-04	1.94
CTNNA2	catenin (cadherin-associated protein), alpha 2 (CTNNA2)	3.03	3.13	1.31E-05	4.93
CXCR4	chemokine (C-X-C motif) receptor 4 (CXCR4)	1.68	7.24	2.15E-06	7.18
ITGA4	integrin, alpha 4 (antigen CD49D, alpha 4 subunit of VLA-4 receptor) (ITGA4)	1.77	3.2	3.03E-08	12.50
ICAM1	intercellular adhesion molecule 1 (ICAM1)	1.45	7.79	1.10E-04	2.32
MMP9	matrix metallopeptidase 9 (gelatinase B, 92kDa gelatinase, 92kDa type IV collagenase) (MMP9)	1.21	9.28	6.54E-11	20.30
PLCG2	phospholipase C, gamma 2 (phosphatidylinositol-specific) (PLCG2)	1.27	8.92	8.04E-09	14.20
RHOH	ras homolog gene family, member H (RHOH)	1.37	4.06	2.22E-02	-3.99
RAC2	ras-related C3 botulinum toxin substrate 2 (rho family, small GTP binding protein Rac2) (RAC2)	1.20	7.88	2.32E-05	4.22

7.1.2.5 RSV vs. non-infected (n.i.)

Table 7.15: Regulated genes in regulated KEGG pathways, comparison RSV vs. non-infected (n.i.).

hsa04060	**Cytokine-cytokine receptor interactions**				
GeneName	**Description**	**logFC**	**AveExpr**	**adj.P.Val**	**B**
BMP7	bone morphogenetic protein 7 (BMP7)	-1.14	7.49	1.48E-11	17.93
CX3CR1	chemokine (C-X3-C motif) receptor 1 (CX3CR1)	-1.18	3.02	1.03E-04	-0.02
EDA	ectodysplasin A (EDA)	-1.03	4.94	2.42E-03	-3.44
INHBB	inhibin, beta B (INHBB)	-2.55	11.04	6.17E-18	35.74
IL17RB	interleukin 17 receptor B (IL17RB)	-1.58	4.65	8.38E-11	15.88
TNFSF15	tumor necrosis factor (ligand) superfamily, member 15 (TNFSF15)	-1.18	3.37	3.63E-05	1.13
CLCF1	cardiotrophin-like cytokine factor 1 (CLCF1)	1.06	11.04	1.27E-13	23.65
CD40	CD40 molecule, TNF receptor superfamily member 5 (CD40)	1.71	8.21	1.92E-13	23.15
RELT	RELT tumor necrosis factor receptor (RELT)	1.05	11.77	3.07E-16	31.01
ACVRL1	activin A receptor type II-like 1 (ACVRL1)	3.71	4.75	5.41E-09	11.03
ACVR1	activin A receptor, type I (ACVR1)	1.40	10.29	8.73E-16	29.74
AMHR2	anti-Mullerian hormone receptor, type II (AMHR2)	1.32	5.74	7.88E-08	7.99
CCL17	chemokine (C-C motif) ligand 17 (CCL17)	7.22	7.88	4.35E-21	44.51
CCL19	chemokine (C-C motif) ligand 19 (CCL19)	1.37	4.64	1.94E-07	6.97
CCL2	chemokine (C-C motif) ligand 2 (CCL2)	3.38	11.15	2.20E-20	42.54
CCL20	chemokine (C-C motif) ligand 20 (CCL20)	7.23	6.53	1.46E-19	40.21
CCL28	chemokine (C-C motif) ligand 28 (CCL28)	1.29	3.49	2.36E-06	4.16
CCL3	chemokine (C-C motif) ligand 3 (CCL3)	14.90	9.58	2.05E-23	50.68
CCL3L3	chemokine (C-C motif) ligand 3-like 3 (CCL3L3)	12.30	8.28	3.01E-16	31.03
CCL4	chemokine (C-C motif) ligand 4 (CCL4)	10.20	7.18	6.57E-25	55.10
CCL5	chemokine (C-C motif) ligand 5 (CCL5)	11.70	10.29	1.00E-22	49.00
CCL7	chemokine (C-C motif) ligand 7 (CCL7)	2.60	3.36	4.78E-10	13.84
CXCL1	chemokine (C-X-C motif) ligand 1 (melanoma growth stimulating activity, alpha) (CXCL1)	6.02	13.17	6.71E-24	51.99
CXCL10	chemokine (C-X-C motif) ligand 10 (CXCL10)	5.22	4.62	1.08E-20	43.41
CXCL11	chemokine (C-X-C motif) ligand 11 (CXCL11)	7.05	5.57	2.17E-22	48.12
CXCL2	chemokine (C-X-C motif) ligand 2 (CXCL2)	4.84	13.11	2.43E-22	47.92
CXCL3	chemokine (C-X-C motif) ligand 3 (CXCL3)	4.71	10.07	9.16E-20	40.75
CXCL5	chemokine (C-X-C motif) ligand 5 (CXCL5)	2.45	15.27	5.01E-18	35.98
CXCL6	chemokine (C-X-C motif) ligand 6 (granulocyte chemotactic protein 2) (CXCL6)	2.08	3.08	5.53E-11	16.37
CXCR3	chemokine (C-X-C motif) receptor 3 (CXCR3)	1.66	2.89	2.76E-06	4.00
CXCR4	chemokine (C-X-C motif) receptor 4 (CXCR4)	2.09	7.15	2.69E-11	17.23
CX3CL1	chemokine (C-X3-C motif) ligand 1 (CX3CL1)	2.28	3.71	7.42E-08	8.06
CSF1R	colony stimulating factor 1 receptor (CSF1R)	4.22	4.26	7.99E-15	27.04
CSF2	colony stimulating factor 2 (granulocyte-macrophage) (CSF2)	8.78	7.04	2.01E-17	34.33
CSF2RA	colony stimulating factor 2 receptor, alpha, low-affinity (granulocyte-macrophage)	1.42	8.41	3.99E-08	8.76
CSF3	colony stimulating factor 3 (granulocyte) (CSF3)	11.20	7.4	1.73E-24	53.57
CRLF2	cytokine receptor-like factor 2 (CRLF2)	2.59	6.2	5.34E-15	27.51
FLT3LG	fms-related tyrosine kinase 3 ligand (FLT3LG)	1.92	7.05	1.42E-15	29.14
INHBA	inhibin, beta A (INHBA)	6.71	7.64	1.51E-16	31.87
IFNAR2	interferon (alpha, beta and omega) receptor 2 (IFNAR2)	1.25	7.9	2.12E-10	14.79
IFNGR1	interferon gamma receptor 1 (IFNGR1)	1.52	12.2	4.57E-15	27.71
IFNGR2	interferon gamma receptor 2 (interferon gamma transducer 1) (IFNGR2)	1.46	10.62	9.86E-15	26.75
IFNB1	interferon, beta 1, fibroblast (IFNB1)	8.54	6.24	7.16E-19	38.25

IL1RAP	interleukin 1 receptor accessory protein (IL1RAP)	1.38	7.57	6.80E-13	21.62
IL1A	interleukin 1, alpha (IL1A)	7.92	5.87	1.29E-21	45.94
IL1B	interleukin 1, beta (IL1B)	6.19	7.43	3.83E-20	41.81
IL10RA	interleukin 10 receptor, alpha (IL10RA)	6.45	5.46	1.22E-14	26.49
IL12A	interleukin 12A (natural killer cell stimulatory factor 1, cytotoxic lymphocyte maturation factor 1, p35) (IL12A)	2.01	5.19	9.82E-11	15.69
IL13	interleukin 13 (IL13)	1.03	3.52	9.92E-05	0.02
IL15RA	interleukin 15 receptor, alpha (IL15RA)	2.51	4.91	6.35E-11	16.21
IL18R1	interleukin 18 receptor 1 (IL18R1)	1.25	5.13	4.31E-03	-4.05
IL2RG	interleukin 2 receptor, gamma (IL2RG)	2.00	4.63	1.09E-07	7.63
IL20RB	interleukin 20 receptor beta (IL20RB)	1.64	8.51	1.79E-15	28.85
IL21R	interleukin 21 receptor (IL21R)	1.94	4.56	1.45E-09	12.54
IL23A	interleukin 23, alpha subunit p19 (IL23A)	3.57	8.9	3.58E-19	39.14
IL28RA	interleukin 28 receptor, alpha (interferon, lambda receptor) (IL28RA)	1.23	8.01	2.74E-13	22.71
IL28A	interleukin 28A (interferon, lambda 2) (IL28A)	9.31	10.46	3.18E-22	47.60
IL28B	interleukin 28B (interferon, lambda 3) (IL28B)	10.60	7.4	3.08E-23	50.26
IL29	interleukin 29 (interferon, lambda 1) (IL29)	11.20	9	2.34E-21	45.21
IL3RA	interleukin 3 receptor, alpha (low affinity) (IL3RA)	2.56	6.1	3.13E-13	22.55
IL4R	interleukin 4 receptor (IL4R)	1.62	13.43	2.65E-18	36.73
IL6	interleukin 6 (interferon, beta 2) (IL6)	8.57	9.19	1.89E-19	39.92
IL6ST	interleukin 6 signal transducer (gp130, oncostatin M receptor) (IL6ST)	1.35	12.41	2.14E-15	28.63
IL7R	interleukin 7 receptor (IL7R)	5.07	6.92	1.99E-13	23.10
IL7	interleukin 7 (IL7)	3.30	4.32	1.24E-06	4.88
IL8	interleukin 8 (IL8)	6.84	6.91	1.87E-14	25.97
LIF	leukemia inhibitory factor (cholinergic differentiation factor) (LIF)	1.56	12.32	2.26E-15	28.56
NGFR	nerve growth factor receptor (NGFR)	2.43	3.63	1.00E-08	10.33
OSMR	oncostatin M receptor (OSMR)	2.33	9.22	1.21E-18	37.65
OSM	oncostatin M (OSM)	1.17	4.82	1.78E-06	4.48
PDGFRA	platelet-derived growth factor receptor, alpha polypeptide (PDGFRA)	1.34	4.3	3.43E-04	-1.33
PPBP	pro-platelet basic protein (chemokine (C-X-C motif) ligand 7) (PPBP)	1.98	3.73	8.00E-10	13.24
PRLR	prolactin receptor (PRLR)	1.14	2.21	1.09E-07	7.62
TNF	tumor necrosis factor (TNF)	6.26	6.24	2.90E-13	22.64
TNFSF10	tumor necrosis factor (ligand) superfamily, member 10 (TNFSF10)	4.92	6.1	3.80E-15	27.93
TNFSF13B	tumor necrosis factor (ligand) superfamily, member 13b (TNFSF13B)	4.56	7.35	4.83E-17	33.28
TNFSF14	tumor necrosis factor (ligand) superfamily, member 14 (TNFSF14)	3.36	7.02	9.58E-13	21.20
TNFSF4	tumor necrosis factor (ligand) superfamily, member 4 (TNFSF4)	1.78	3.84	2.52E-07	6.67
TNFRSF10B	tumor necrosis factor receptor superfamily, member 10b (TNFRSF10B)	1.12	13.94	4.44E-17	33.37
TNFRSF12A	tumor necrosis factor receptor superfamily, member 12A (TNFRSF12A)	1.16	15.75	3.79E-13	22.32
TNFRSF14	tumor necrosis factor receptor superfamily, member 14 (herpesvirus entry mediator) (TNFRSF14)	2.13	5.43	9.38E-10	13.05
TNFRSF1B	tumor necrosis factor receptor superfamily, member 1B (TNFRSF1B)	3.79	3.88	4.47E-17	33.36
TNFRSF25	tumor necrosis factor receptor superfamily, member 25 (TNFRSF25)	2.01	10.49	1.54E-17	34.65
TNFRSF8	tumor necrosis factor receptor superfamily, member 8 (TNFRSF8)	4.62	6.42	1.15E-16	32.19
TNFRSF9	tumor necrosis factor receptor superfamily, member 9 (TNFRSF9)	4.29	7.9	3.35E-19	39.22
VEGFA	vascular endothelial growth factor A (VEGFA)	1.37	9.62	3.68E-12	19.59
VEGFC	vascular endothelial growth factor C (VEGFC)	1.85	12.57	4.70E-18	36.06

hsa04630 JAK-STAT signaling pathway

GeneName	Description	logFC	AveExpr	adj.P.Val	B
CCND3	cyclin D3 (CCND3)	-1.15	12.62	3.97E-14	25.05
PIAS4	protein inhibitor of activated STAT, 4	-2.21	4.44	1.07E-05	2.48
STAT4	signal transducer and activator of transcription 4 (STAT4)	-1.36	8.7	7.56E-15	27.09
CLCF1	cardiotrophin-like cytokine factor 1 (CLCF1)	1.06	11.04	1.27E-13	23.65
CSF2	colony stimulating factor 2 (granulocyte-macrophage) (CSF2)	8.78	7.04	2.01E-17	34.33
CSF2RA	colony stimulating factor 2 receptor, alpha, low-affinity (granulocyte-macrophage)	1.42	8.41	3.99E-08	8.76
CSF3	colony stimulating factor 3 (granulocyte) (CSF3)	11.20	7.4	1.73E-24	53.57
CRLF2	cytokine receptor-like factor 2 (CRLF2)	2.59	6.2	5.34E-15	27.51
IFNAR2	interferon (alpha, beta and omega) receptor 2 (IFNAR2)	1.25	7.9	2.12E-10	14.79
IFNGR1	interferon gamma receptor 1 (IFNGR1)	1.52	12.2	4.57E-15	27.71
IFNGR2	interferon gamma receptor 2 (interferon gamma transducer 1) (IFNGR2)	1.46	10.62	9.86E-15	26.75
IRF9	interferon regulatory factor 9 (IRF9)	3.04	10.33	1.56E-18	37.34
IFNB1	interferon, beta 1, fibroblast (IFNB1)	8.54	6.24	7.16E-19	38.25
IL10RA	interleukin 10 receptor, alpha (IL10RA)	6.45	5.46	1.22E-14	26.49
IL12A	interleukin 12A (natural killer cell stimulatory factor 1, cytotoxic lymphocyte maturation factor 1, p35) (IL12A)	2.01	5.19	9.82E-11	15.69
IL13	interleukin 13 (IL13)	1.03	3.52	9.92E-05	0.02
IL13RA2	interleukin 13 receptor, alpha 2 (IL13RA2)	1.88	3.13	8.37E-07	5.32
IL15RA	interleukin 15 receptor, alpha (IL15RA)	2.51	4.91	6.35E-11	16.21
IL2RG	interleukin 2 receptor, gamma (IL2RG)	2.00	4.63	1.09E-07	7.63
IL21R	interleukin 21 receptor (IL21R)	1.94	4.56	1.45E-09	12.54
IL23A	interleukin 23, alpha subunit p19 (IL23A)	3.57	8.9	3.58E-19	39.14
IL28RA	interleukin 28 receptor, alpha (interferon, lambda receptor) (IL28RA)	1.23	8.01	2.74E-13	22.71
IL28A	interleukin 28A (interferon, lambda 2) (IL28A)	9.31	10.46	3.18E-22	47.60
IL28B	interleukin 28B (interferon, lambda 3) (IL28B)	10.60	7.4	3.08E-23	50.26
IL29	interleukin 29 (interferon, lambda 1) (IL29)	11.70	8.75	6.53E-19	38.36
IL3RA	interleukin 3 receptor, alpha (low affinity) (IL3RA)	2.56	6.1	3.13E-13	22.55
IL4R	interleukin 4 receptor (IL4R)	1.62	13.43	2.65E-18	36.73
IL6	interleukin 6 (interferon, beta 2) (IL6)	8.57	9.19	1.89E-19	39.92
IL6ST	interleukin 6 signal transducer (gp130, oncostatin M receptor) (IL6ST)	1.35	12.41	2.14E-15	28.63
IL7	interleukin 7 (IL7)	3.30	4.32	1.24E-06	4.88
IL7R	interleukin 7 receptor (IL7R)	5.07	6.92	1.99E-13	23.10
LIF	leukemia inhibitory factor (cholinergic differentiation factor) (LIF)	1.56	12.32	2.26E-15	28.56
OSMR	oncostatin M receptor (OSMR)	2.33	9.22	1.21E-18	37.65
OSM	oncostatin M (OSM)	1.17	4.82	1.78E-06	4.48
PIK3CD	phosphoinositide-3-kinase, catalytic, delta polypeptide (PIK3CD)	1.02	8.73	1.29E-11	18.09
PRLR	prolactin receptor (PRLR)	1.14	2.21	1.09E-07	7.62

STAT1	signal transducer and activator of transcription 1, 91kDa (STAT1)	2.79	12.71	1.22E-19	40.44
STAT2	signal transducer and activator of transcription 2, 113kDa (STAT2)	2.76	13.14	6.93E-20	41.10
STAT5A	signal transducer and activator of transcription 5A (STAT5A)	2.31	8	5.66E-19	38.54
SPRY2	sprouty homolog 2 (Drosophila) (SPRY2)	1.63	10.61	1.08E-15	29.48
SPRY4	sprouty homolog 4 (Drosophila) (SPRY4)	2.40	8.44	2.05E-15	28.69
SOCS1	suppressor of cytokine signaling 1 (SOCS1)	3.85	7.96	2.03E-19	39.83
SOCS3	suppressor of cytokine signaling 3 (SOCS3)	2.91	11.23	1.92E-21	45.48

hsa04620 TLR signaling

GeneName	Description	logFC	AveExpr	adj.P.Val	B
MAPK10	mitogen-activated protein kinase 10 (MAPK10)	-1.45	3.7	7.32E-04	-2.15
MAP2K6	mitogen-activated protein kinase kinase 6 (MAP2K6)	-1.37	9.62	3.25E-16	30.94
CD40	CD40 molecule, TNF receptor superfamily member 5 (CD40)	1.71	8.21	1.92E-13	23.15
CCL4	chemokine (C-C motif) ligand 4 (CCL4)	10.20	7.18	6.57E-25	55.10
CCL5	chemokine (C-C motif) ligand 5 (CCL5)	11.70	10.29	1.00E-22	49.00
CXCL10	chemokine (C-X-C motif) ligand 10 (CXCL10)	5.22	4.62	1.08E-20	43.41
CXCL11	chemokine (C-X-C motif) ligand 11 (CXCL11)	7.05	5.57	2.17E-22	48.12
IKBKE	inhibitor of kappa light polypeptide gene enhancer in B-cells, kinase epsilon (IKBKE)	1.24	6.63	8.34E-11	15.89
IFNAR2	interferon (alpha, beta and omega) receptor 2 (IFNAR2)	1.25	7.9	2.12E-10	14.79
IRF7	interferon regulatory factor 7 (IRF7)	5.15	12.88	1.67E-23	50.92
IFNB1	interferon, beta 1, fibroblast (IFNB1)	8.54	6.24	7.16E-19	38.25
IL1B	interleukin 1, beta (IL1B)	6.19	7.43	3.83E-20	41.81
IL12A	interleukin 12A (natural killer cell stimulatory factor 1, cytotoxic lymphocyte maturation factor 1, p35) (IL12A)	2.01	5.19	9.82E-11	15.69
IL6	interleukin 6 (interferon, beta 2) (IL6)	8.57	9.19	1.89E-19	39.92
IL8	interleukin 8 (IL8)	6.84	6.91	1.87E-14	25.97
LBP	lipopolysaccharide binding protein (LBP)	2.50	3.6	1.39E-08	9.96
LY96	lymphocyte antigen 96 (LY96)	2.09	4.29	2.78E-08	9.17
MAPK13	mitogen-activated protein kinase 13 (MAPK13)	3.08	6.49	1.92E-11	17.62
MAP2K3	mitogen-activated protein kinase kinase 3 (MAP2K3)	1.07	10.68	7.26E-14	24.31
MAP3K8	mitogen-activated protein kinase kinase kinase 8 (MAP3K8)	1.59	10.59	7.68E-15	27.07
MYD88	myeloid differentiation primary response gene (88) (MYD88)	1.97	11.57	2.21E-15	28.59
NFKB1	nuclear factor of kappa light polypeptide gene enhancer in B-cells 1 (NFKB1)	1.71	11.47	3.00E-16	31.11
NFKBIA	nuclear factor of kappa light polypeptide gene enhancer in B-cells inhibitor, alpha (NFKBIA)	2.47	14.79	8.84E-21	43.65
PIK3CD	phosphoinositide-3-kinase, catalytic, delta polypeptide (PIK3CD)	1.02	8.73	1.29E-11	18.09
STAT1	signal transducer and activator of transcription 1, 91kDa (STAT1)	2.79	12.71	1.22E-19	40.44
TLR2	toll-like receptor 2 (TLR2)	2.61	4.14	9.71E-16	29.60
TLR3	toll-like receptor 3 (TLR3)	3.30	6.24	1.08E-12	21.06
TICAM1	toll-like receptor adaptor molecule 1 (TICAM1)	1.74	12.52	1.06E-17	35.10
TNF	tumor necrosis factor (TNF)	6.26	6.24	2.90E-13	22.64
FOS	FBJ murine osteosarcoma viral oncogene homolog (FOS)	3.16	9.68	6.86E-19	38.30

hsa04612 Antigen processing and presentation

GeneName	Description	logFC	AveExpr	adj.P.Val	B
CD8A	CD8a molecule (CD8A)	-1.06	4.41	1.60E-05	2.03
HSPA2	heat shock 70kDa protein 2 (HSPA2)	-1.01	12.52	1.64E-15	28.97
HLA-DMB	major histocompatibility complex, class II, DM beta (HLA-DMB)	-3.70	7.84	7.50E-17	32.72
NFYA	nuclear transcription factor Y, alpha (NFYA)	-1.84	7.69	5.41E-16	30.33
NFYB	nuclear transcription factor Y, beta (NFYB)	-1.24	9.13	8.01E-15	27.01
TAPBP	TAP binding protein (tapasin) (TAPBP)	1.55	9.66	1.56E-15	29.03
B2M	beta-2-microglobulin (B2M)	2.66	15.14	3.03E-19	39.35
CTSL1	cathepsin L1 (CTSL1)	1.37	15.82	3.97E-13	22.26
CTSS	cathepsin S (CTSS)	3.62	5.59	1.64E-12	20.56
HSPA1A	heat shock 70kDa protein 1A (HSPA1A)	1.14	14.75	8.85E-17	32.52
HSPA1B	heat shock 70kDa protein 1B (HSPA1B)	1.28	13	1.73E-15	28.90
HSPA6	heat shock 70kDa protein 6 (HSP70B') (HSPA6)	3.43	6.9	6.22E-18	35.73
IFI30	interferon, gamma-inducible protein 30 (IFI30)	1.27	12.37	6.82E-15	27.21
KIR2DL4	killer cell immunoglobulin-like receptor, two domains, long cytoplasmic tail, 4 (KIR2DL4)	1.49	3.85	1.13E-06	4.98
KIR2DL5A	killer cell immunoglobulin-like receptor, two domains, long cytoplasmic tail, 5A (KIR2DL5A)	2.80	3.39	1.39E-12	20.76
KLRC1	killer cell lectin-like receptor subfamily C, member 1 (KLRC1)	2.05	3.86	5.50E-11	16.38
KLRC3	killer cell lectin-like receptor subfamily C, member 3 (KLRC3)	1.45	2.87	3.23E-09	11.62
KLRC4	killer cell lectin-like receptor subfamily C, member 4 (KLRC4)	1.46	4.78	3.39E-06	3.75
LGMN	legumain (LGMN)	1.07	10.08	1.35E-12	20.80
HLA-A	major histocompatibility complex, class I, A (HLA-A)	3.07	13.25	2.44E-20	42.41
HLA-E	major histocompatibility complex, class I, E (HLA-E)	3.02	13.8	6.19E-20	41.22
HLA-DOB	major histocompatibility complex, class II, DO beta (HLA-DOB)	2.37	6.5	4.61E-13	22.09
PSME2	proteasome (prosome, macropain) activator subunit 2 (PA28 beta) (PSME2)	1.01	16.55	7.31E-17	32.75
TAP1	transporter 1, ATP-binding cassette, sub-family B (MDR/TAP) (TAP1)	2.34	13.98	3.33E-19	39.23
TAP2	transporter 2, ATP-binding cassette, sub-family B (MDR/TAP) (TAP2)	1.60	10.44	9.85E-17	32.38

hsa04621 NOD-like receptor signaling

GeneName	Description	logFC	AveExpr	adj.P.Val	B
MAPK10	mitogen-activated protein kinase 10 (MAPK10)	-1.45	3.7	7.32E-04	-2.15
NLRP3	NLR family, pyrin domain containing 3 (NLRP3)	4.80	4.28	3.16E-15	28.16
BIRC3	baculoviral IAP repeat-containing 3 (BIRC3)	2.86	12.88	1.81E-20	42.78
CASP1	caspase 1, apoptosis-related cysteine peptidase (interleukin 1, beta, convertase) (CASP1)	4.36	6.22	3.40E-15	28.07
CASP5	caspase 5, apoptosis-related cysteine peptidase (CASP5)	2.60	9.07	8.50E-19	38.05
CARD6	caspase recruitment domain family, member 6 (CARD6)	1.66	7.72	6.93E-13	21.59
CCL2	chemokine (C-C motif) ligand 2 (CCL2)	3.38	11.15	2.20E-20	42.54
CCL5	chemokine (C-C motif) ligand 5 (CCL5)	11.70	10.29	1.00E-22	49.00
CCL7	chemokine (C-C motif) ligand 7 (CCL7)	2.60	3.36	4.78E-10	13.84
CXCL1	chemokine (C-X-C motif) ligand 1 (melanoma growth stimulating activity, alpha) (CXCL1)	6.02	13.17	6.71E-24	51.99
CXCL2	chemokine (C-X-C motif) ligand 2 (CXCL2)	4.84	13.11	2.43E-22	47.92
IL1B	interleukin 1, beta (IL1B)	6.19	7.43	3.83E-20	41.81
IL6	interleukin 6 (interferon, beta 2) (IL6)	8.57	9.19	1.89E-19	39.92

IL8	interleukin 8 (IL8)	6.84	6.91	1.87E-14	25.97
MAPK13	mitogen-activated protein kinase 13 (MAPK13)	3.08	6.49	1.92E-11	17.62
TAB3	TGF-beta activated kinase 1/MAP3K7 binding protein 3 (TAB3)	1.36	7.26	5.21E-07	5.85
NFKB1	nuclear factor of kappa light polypeptide gene enhancer in B-cells 1 (NFKB1)	1.71	11.47	3.00E-16	31.11
NFKBIA	nuclear factor of kappa light polypeptide gene enhancer in B-cells inhibitor, alpha (NFKBIA)	2.47	14.79	8.84E-21	43.65
NFKBIB	nuclear factor of kappa light polypeptide gene enhancer in B-cells inhibitor, beta (NFKBIB)	1.24	10.52	5.14E-13	21.96
NOD2	nucleotide-binding oligomerization domain containing 2 (NOD2)	3.55	3.65	1.64E-15	28.97
RIPK2	receptor-interacting serine-threonine kinase 2 (RIPK2)	1.98	12.52	1.36E-10	15.31
TNF	tumor necrosis factor (TNF)	6.26	6.24	2.90E-13	22.64

hsa04610 Complement and coagulation cascades

GeneName	Description	logFC	AveExpr	adj.P.Val	B
F2	coagulation factor II (thrombin) (F2)	-1.48	6.35	4.20E-10	14.02
F7	coagulation factor VII (serum prothrombin conversion accelerator) (F7)	-1.27	3.58	1.27E-05	2.28
C4BPB	complement component 4 binding protein, beta (C4BPB)	-1.55	5.98	5.52E-12	19.11
C5	complement component 5 (C5)	-2.34	9.38	3.91E-17	33.52
CFI	complement factor I (CFI)	-1.21	4.59	4.03E-10	14.03
PROC	protein C (inactivator of coagulation factors Va and VIIIa) (PROC)	-3.18	4.97	3.12E-09	11.66
SERPINF2	serpin peptidase inhibitor, clade F (alpha-2 antiplasmin, pigment epithelium derived factor), member 2 (SERPINF2)	-1.35	4.1	3.42E-04	-1.33
CD55	CD55 molecule, decay accelerating factor for complement (Cromer blood group) (CD55)	1.91	11.71	1.21E-18	37.64
BDKRB1	bradykinin receptor B1 (BDKRB1)	2.24	9.85	6.81E-19	38.32
BDKRB2	bradykinin receptor B2 (BDKRB2)	1.44	10.5	1.70E-16	31.72
F3	coagulation factor III (thromboplastin, tissue factor) (F3)	2.01	8.05	5.28E-16	30.36
C1R	complement component 1, r subcomponent (C1R)	3.26	12.02	1.35E-22	48.67
C1S	complement component 1, s subcomponent (C1S)	2.87	8.91	2.52E-15	28.43
C4B	complement component 4B (Chido blood group) (C4B)	2.25	7.07	6.16E-18	35.74
CFB	complement factor B (CFB)	7.07	9.99	2.27E-21	45.25
CFH	complement factor H (CFH)	1.01	9.2	9.80E-12	18.42
PLAT	plasminogen activator, tissue (PLAT)	1.74	8.72	3.20E-16	31.01
PLAUR	plasminogen activator, urokinase receptor (PLAUR)	4.19	12.64	4.73E-21	44.40
PLAU	plasminogen activator, urokinase (PLAU)	2.71	11.61	2.21E-17	34.21
SERPINA1	serpin peptidase inhibitor, clade A (alpha-1 antiproteinase, antitrypsin), member 1 (SERPINA1)	4.67	7.73	8.63E-18	35.35
SERPINE1	serpin peptidase inhibitor, clade E (nexin, plasminogen activator inhibitor type 1), member 1 (SERPINE1)	2.07	10.56	4.09E-16	30.67
SERPING1	serpin peptidase inhibitor, clade G (C1 inhibitor), member 1 (SERPING1)	3.41	3.46	4.82E-11	16.53
THBD	thrombomodulin (THBD)	2.06	13.14	9.35E-17	32.45

hsa04640 Hematopoietic cell lineage

GeneName	Description	logFC	AveExpr	adj.P.Val	B
CD33	CD33 molecule (CD33)	-1.96	3.48	9.83E-04	-2.47
CD8A	CD8a molecule (CD8A)	-1.06	4.41	1.60E-05	2.03
ITGA4	integrin, alpha 4 (antigen CD49D, alpha 4 subunit of VLA-4 receptor) (ITGA4)	-1.46	4.59	4.02E-07	6.15
CD22	CD22 molecule (CD22)	1.09	3.69	4.61E-04	-1.65
CD36	CD36 molecule (thrombospondin receptor) (CD36)	1.10	2.49	8.91E-05	0.15
CD38	CD38 molecule (CD38)	2.99	10.69	6.16E-19	38.43
CD55	CD55 molecule, decay accelerating factor for complement (Cromer blood group) (CD55)	1.91	11.71	1.21E-18	37.64
ANPEP	alanyl (membrane) aminopeptidase (ANPEP)	3.11	9.64	5.26E-18	35.93
CSF1	colony stimulating factor 1 (macrophage) (CSF1)	2.04	8.24	1.38E-13	23.54
CSF2	colony stimulating factor 2 (granulocyte-macrophage) (CSF2)	8.78	7.04	2.01E-17	34.33
CSF3	colony stimulating factor 3 (granulocyte) (CSF3)	11.20	7.4	1.73E-24	53.57
CSF2RA	colony stimulating factor 2 receptor, alpha, low-affinity (granulocyte-macrophage)	1.42	8.41	3.99E-08	8.76
FLT3LG	fms-related tyrosine kinase 3 ligand (FLT3LG)	1.92	7.05	1.42E-15	29.14
ITGA2	integrin, alpha 2 (CD49B, alpha 2 subunit of VLA-2 receptor) (ITGA2)	1.69	7.17	2.90E-11	17.13
ITGA5	integrin, alpha 5 (fibronectin receptor, alpha polypeptide) (ITGA5)	3.91	10.59	6.06E-19	38.46
ITGB3	integrin, beta 3 (platelet glycoprotein IIIa, antigen CD61) (ITGB3)	2.57	7.86	4.19E-13	22.20
IL1A	interleukin 1, alpha (IL1A)	7.92	5.87	1.29E-21	45.94
IL1B	interleukin 1, beta (IL1B)	6.19	7.43	3.83E-20	41.81
IL11	interleukin 11 (IL11)	2.46	12.56	5.26E-17	33.16
IL3RA	interleukin 3 receptor, alpha (low affinity) (IL3RA)	2.56	6.1	3.13E-13	22.55
IL4R	interleukin 4 receptor (IL4R)	1.62	13.43	2.65E-18	36.73
IL6	interleukin 6 (interferon, beta 2) (IL6)	8.57	9.19	1.89E-19	39.92
IL7	interleukin 7 (IL7)	3.30	4.32	1.24E-06	4.88
IL7R	interleukin 7 receptor (IL7R)	5.07	6.92	1.99E-13	23.10
TNF	tumor necrosis factor (TNF)	6.26	6.24	2.90E-13	22.64

hsa04110 Cell cycle

GeneName	Description	logFC	AveExpr	adj.P.Val	B
DBF4	DBF4 homolog (S. cerevisiae) (DBF4)	-1.62	4	6.53E-07	5.60
E2F1	E2F transcription factor 1 (E2F1)	-1.23	10.59	3.73E-16	30.78
E2F2	E2F transcription factor 2 (E2F2)	-1.82	10.86	4.89E-18	36.02
MAD2L1	MAD2 mitotic arrest deficient-like 1 (yeast) (MAD2L1)	-1.23	11	9.94E-14	23.93
SKP2	S-phase kinase-associated protein 2 (p45) (SKP2)	-1.28	8.65	2.11E-14	25.82
SMAD2	SMAD family member 2 (SMAD2)	-1.17	7.75	3.14E-12	19.78
TTK	TTK protein kinase (TTK)	-1.16	9.67	3.54E-13	22.41
BUB1B	budding uninhibited by benzimidazoles 1 homolog beta (yeast) (BUB1B)	-1.11	10.74	2.61E-13	22.77
CDK1	cyclin-dependent kinase 1 (CDK1)	-1.09	11.93	1.73E-11	17.85
CDC20	cell division cycle 20 homolog (S. cerevisiae) (CDC20)	-1.15	11.64	4.90E-15	27.62
CDC25C	cell division cycle 25 homolog C (S. pombe) (CDC25C)	-1.07	9.27	2.43E-14	25.65
CDC7	cell division cycle 7 homolog (S. cerevisiae) (CDC7)	-1.53	9.45	1.04E-15	29.52
CCNA2	cyclin A2 (CCNA2)	-1.18	10.18	7.44E-15	27.11
CCNB1	cyclin B1 (CCNB1)	-1.51	13.2	1.70E-16	31.72
CCNB2	cyclin B2 (CCNB2)	-1.40	13.31	7.17E-17	32.78
CCND3	cyclin D3 (CCND3)	-1.15	12.62	3.97E-14	25.05
CCNE2	cyclin E2 (CCNE2)	-1.09	5.58	5.61E-09	10.99

MCM2	minichromosome maintenance complex component 2 (MCM2)	-1.02	12.27	2.19E-14	25.78
MCM3	minichromosome maintenance complex component 3 (MCM3)	-1.04	13.45	9.79E-17	32.39
MCM4	minichromosome maintenance complex component 4 (MCM4)	-1.18	11.43	2.52E-13	22.82
MCM5	minichromosome maintenance complex component 5 (MCM5)	-1.13	12.32	6.05E-15	27.36
MCM6	minichromosome maintenance complex component 6 (MCM6)	-1.37	12.69	5.16E-16	30.39
MCM7	minichromosome maintenance complex component 7 (MCM7)	-1.04	9.55	1.75E-08	9.70
ORC1	origin recognition complex, subunit 1 (ORC1)	-1.06	8.42	2.37E-09	11.98
PTTG1	pituitary tumor-transforming 1 (PTTG1)	-1.04	14.8	1.56E-15	29.03
PLK1	polo-like kinase 1 (PLK1)	-1.26	7.96	5.91E-12	19.02
PCNA	proliferating cell nuclear antigen (PCNA)	-1.16	13.84	6.72E-15	27.23
RBL1	retinoblastoma-like 1 (p107) (RBL1)	-1.09	5.77	1.49E-09	12.51
SMC1A	structural maintenance of chromosomes 1A (SMC1A)	-1.13	8.23	6.72E-14	24.41
TP53	tumor protein p53 (TP53)	-1.14	8.68	1.26E-10	15.40
CDC14A	CDC14 cell division cycle 14 homolog A (S. cerevisiae) (CDC14A)	1.20	4.05	1.60E-05	2.03
GADD45A	growth arrest and DNA-damage-inducible, alpha (GADD45A)	1.86	12.22	6.20E-19	38.42
GADD45G	growth arrest and DNA-damage-inducible, gamma (GADD45G)	1.33	7.12	8.81E-14	24.08

hsa04623 Cytosolic DNA sensing pathway

GeneName	Description	logFC	AveExpr	adj.P.Val	B
ZBP1	Z-DNA binding protein 1 (ZBP1)	1.76	3.32	5.43E-08	8.41
AIM2	absent in melanoma 2 (AIM2)	2.35	2.75	2.63E-13	22.76
CASP1	caspase 1, apoptosis-related cysteine peptidase (interleukin 1, beta, convertase) (CASP1)	4.36	6.22	3.40E-15	28.07
CCL4	chemokine (C-C motif) ligand 4 (CCL4)	10.20	7.18	6.57E-25	55.10
CCL5	chemokine (C-C motif) ligand 5 (CCL5)	11.70	10.29	1.00E-22	49.00
CXCL10	chemokine (C-X-C motif) ligand 10 (CXCL10)	5.22	4.62	1.08E-20	43.41
IKBKE	inhibitor of kappa light polypeptide gene enhancer in B-cells, kinase epsilon (IKBKE)	1.24	6.63	8.34E-11	15.89
IRF7	interferon regulatory factor 7 (IRF7)	5.15	12.88	1.67E-23	50.92
IFNB1	interferon, beta 1, fibroblast (IFNB1)	8.54	6.24	7.16E-19	38.25
IL1B	interleukin 1, beta (IL1B)	6.19	7.43	3.83E-20	41.81
IL33	interleukin 33 (IL33)	1.45	5.52	8.45E-08	7.91
IL6	interleukin 6 (interferon, beta 2) (IL6)	8.57	9.19	1.89E-19	39.92
NFKB1	nuclear factor of kappa light polypeptide gene enhancer in B-cells 1 (NFKB1)	1.71	11.47	3.00E-16	31.11
NFKBIA	nuclear factor of kappa light polypeptide gene enhancer in B-cells inhibitor, alpha (NFKBIA)	2.47	14.79	8.84E-21	43.65
TREX1	three prime repair exonuclease 1 (TREX1)	1.58	11.71	4.13E-15	27.83
TMEM173	transmembrane protein 173 (TMEM173), nuclear gene encoding mitochondrial protein	1.49	7.86	1.83E-15	28.82

hsa03030 DNA replication

GeneName	Description	logFC	AveExpr	adj.P.Val	B
MCM2	minichromosome maintenance complex component 2 (MCM2)	-1.02	12.27	2.19E-14	25.78
MCM3	minichromosome maintenance complex component 3 (MCM3)	-1.04	13.45	9.79E-17	32.39
MCM4	minichromosome maintenance complex component 4 (MCM4)	-1.18	11.43	2.52E-13	22.82
MCM5	minichromosome maintenance complex component 5 (MCM5)	-1.13	12.32	6.05E-15	27.36
MCM6	minichromosome maintenance complex component 6 (MCM6)	-1.37	12.69	5.16E-16	30.39
POLA1	polymerase (DNA directed), alpha 1, catalytic subunit (POLA1)	-1.10	11.3	3.85E-15	27.92
POLE2	polymerase (DNA directed), epsilon 2 (p59 subunit) (POLE2)	-1.54	9.39	3.62E-14	25.16
PRIM1	primase, DNA, polypeptide 1 (49kDa) (PRIM1)	-1.36	10.8	7.82E-17	32.67
PCNA	proliferating cell nuclear antigen (PCNA)	-1.14	13.38	1.58E-14	26.17
RFC3	replication factor C (activator 1) 3, 38kDa (RFC3)	-1.20	9.65	5.39E-13	21.90
RFC4	replication factor C (activator 1) 4, 37kDa (RFC4)	-1.00	12.22	3.26E-15	28.12
RFC5	replication factor C (activator 1) 5, 36.5kDa (RFC5)	-1.05	12.63	4.87E-14	24.80
RPA1	replication protein A1, 70kDa (RPA1)	-1.74	12.85	9.18E-02	-7.18

hsa04062 Chemokine signaling pathway

GeneName	Description	logFC	AveExpr	adj.P.Val	B
ADCY9	adenylate cyclase 9 (ADCY9)	-1.14	9.75	3.45E-15	28.05
ARRB1	arrestin, beta 1 (ARRB1)	-1.04	6.07	9.89E-09	10.34
CX3CR1	chemokine (C-X3-C motif) receptor 1 (CX3CR1)	-1.18	3.02	1.03E-04	-0.02
ELMO1	engulfment and cell motility 1 (ELMO1)	-1.01	6.12	4.24E-09	11.33
PRKX	protein kinase, X-linked (PRKX)	-1.04	9.13	8.01E-15	27.01
PRKACG	protein kinase, cAMP-dependent, catalytic, gamma (PRKACG)	-1.37	2.77	3.84E-07	6.20
VAV3	vav 3 guanine nucleotide exchange factor (VAV3)	-3.20	8.57	1.32E-14	26.39
FGR	Gardner-Rasheed feline sarcoma viral (v-fgr) oncogene homolog (FGR)	1.14	4.49	6.78E-04	-2.03
SHC2	SHC (Src homology 2 domain containing) transforming protein 2 (SHC2)	1.97	7.99	1.30E-15	29.24
CCL17	chemokine (C-C motif) ligand 17 (CCL17)	7.22	7.88	4.35E-21	44.51
CCL19	chemokine (C-C motif) ligand 19 (CCL19)	1.37	4.64	1.94E-07	6.97
CCL2	chemokine (C-C motif) ligand 2 (CCL2)	3.38	11.15	2.20E-20	42.54
CCL28	chemokine (C-C motif) ligand 28 (CCL28)	1.29	3.49	2.36E-06	4.16
CCL3	chemokine (C-C motif) ligand 3 (CCL3)	14.90	9.58	2.05E-23	50.68
CCL3L3	chemokine (C-C motif) ligand 3-like 3 (CCL3L3)	12.30	8.28	3.01E-16	31.03
CCL4	chemokine (C-C motif) ligand 4 (CCL4)	10.20	7.18	6.57E-25	55.10
CCL5	chemokine (C-C motif) ligand 5 (CCL5)	11.70	10.29	1.00E-22	49.00
CCL7	chemokine (C-C motif) ligand 7 (CCL7)	2.60	3.36	4.78E-10	13.84
CCR7	chemokine (C-C motif) receptor 7 (CCR7)	1.18	8.71	1.38E-12	20.77
CXCL1	chemokine (C-X-C motif) ligand 1 (melanoma growth stimulating activity, alpha) (CXCL1)	6.02	13.17	6.71E-24	51.99
CXCL10	chemokine (C-X-C motif) ligand 10 (CXCL10)	5.22	4.62	1.08E-20	43.41
CXCL11	chemokine (C-X-C motif) ligand 11 (CXCL11)	7.05	5.57	2.17E-22	48.12
CXCL2	chemokine (C-X-C motif) ligand 2 (CXCL2)	4.84	13.11	2.43E-22	47.92
CXCL3	chemokine (C-X-C motif) ligand 3 (CXCL3)	4.71	10.07	9.16E-20	40.75
CXCL5	chemokine (C-X-C motif) ligand 5 (CXCL5)	2.45	15.27	5.01E-18	35.98
CXCL6	chemokine (C-X-C motif) ligand 6 (granulocyte chemotactic protein 2) (CXCL6)	2.08	3.08	5.53E-11	16.37
CXCR3	chemokine (C-X-C motif) receptor 3 (CXCR3)	1.66	2.89	2.76E-06	4.00
CXCR4	chemokine (C-X-C motif) receptor 4 (CXCR4)	2.09	7.15	2.69E-11	17.23
CX3CL1	chemokine (C-X3-C motif) ligand 1 (CX3CL1)	2.28	3.71	7.42E-08	8.06
GNG8	guanine nucleotide binding protein (G protein), gamma 8 (GNG8)	1.61	6.83	2.13E-10	14.78

GNGT2	guanine nucleotide binding protein (G protein), gamma transducing activity polypeptide 2 (GNGT2)	1.83	3.99	4.95E-09	11.13
IL8	interleukin 8 (IL8)	6.84	6.91	1.87E-14	25.97
NFKB1	nuclear factor of kappa light polypeptide gene enhancer in B-cells 1 (NFKB1)	1.71	11.47	3.00E-16	31.11
NFKBIA	nuclear factor of kappa light polypeptide gene enhancer in B-cells inhibitor, alpha (NFKBIA)	2.47	14.79	8.84E-21	43.65
PIK3CD	phosphoinositide-3-kinase, catalytic, delta polypeptide (PIK3CD)	1.02	8.73	1.29E-11	18.09
PLCB1	phospholipase C, beta 1 (phosphoinositide-specific) (PLCB1)	1.93	5.1	4.55E-09	11.23
PPBP	pro-platelet basic protein (chemokine (C-X-C motif) ligand 7) (PPBP)	1.98	3.73	8.00E-10	13.24
PRKCD	protein kinase C, delta (PRKCD)	1.24	9.84	1.16E-13	23.83
RAC2	ras-related C3 botulinum toxin substrate 2 (rho family, small GTP binding protein Rac2) (RAC2)	1.32	7.77	2.66E-12	19.98
STAT1	signal transducer and activator of transcription 1, 91kDa (STAT1)	2.79	12.71	1.22E-19	40.44
LYN	v-yes-1 Yamaguchi sarcoma viral related oncogene homolog (LYN)	1.41	12.18	2.69E-16	31.18

hsa04622 RIG-I-like receptor signaling pathway

GeneName	Description	logFC	AveExpr	adj.P.Val	B
MAPK10	mitogen-activated protein kinase 10 (MAPK10)	-1.45	3.7	7.32E-04	-2.15
DHX58	DEXH (Asp-Glu-X-His) box polypeptide 58 (DHX58)	6.47	9.06	6.63E-22	46.73
ISG15	ISG15 ubiquitin-like modifier (ISG15)	7.38	14	5.43E-24	52.25
TANK	TRAF family member-associated NFKB activator (TANK)	1.10	11.22	5.10E-13	21.97
CASP10	caspase 10, apoptosis-related cysteine peptidase (CASP10)	1.94	8.91	6.23E-17	32.95
CXCL10	chemokine (C-X-C motif) ligand 10 (CXCL10)	5.22	4.62	1.08E-20	43.41
IKBKE	inhibitor of kappa light polypeptide gene enhancer in B-cells, kinase epsilon (IKBKE)	1.24	6.63	8.34E-11	15.89
IFIH1	interferon induced with helicase C domain 1 (IFIH1)	6.00	10.94	5.43E-24	52.21
IRF7	interferon regulatory factor 7 (IRF7)	5.15	12.88	1.67E-23	50.92
IFNB1	interferon, beta 1, fibroblast (IFNB1)	8.54	6.24	7.16E-19	38.25
IL12A	interleukin 12A (natural killer cell stimulatory factor 1, cytotoxic lymphocyte maturation factor 1, p35) (IL12A)	2.01	5.19	9.82E-11	15.69
IL8	interleukin 8 (IL8)	6.84	6.91	1.87E-14	25.97
MAPK13	mitogen-activated protein kinase 13 (MAPK13)	3.08	6.49	1.92E-11	17.62
NFKB1	nuclear factor of kappa light polypeptide gene enhancer in B-cells 1 (NFKB1)	1.71	11.47	3.00E-16	31.11
NFKBIA	nuclear factor of kappa light polypeptide gene enhancer in B-cells inhibitor, alpha (NFKBIA)	2.47	14.79	8.84E-21	43.65
TMEM173	transmembrane protein 173 (TMEM173), nuclear gene encoding mitochondrial protein	1.49	7.86	1.83E-15	28.82
TNF	tumor necrosis factor (TNF)	6.26	6.24	2.90E-13	22.64

hsa04650 Natural killer cell mediated cytotoxicity

GeneName	Description	logFC	AveExpr	adj.P.Val	B
CD247	CD247 molecule (CD247)	-1.09	3.82	1.02E-03	-2.51
VAV3	vav 3 guanine nucleotide exchange factor (VAV3)	-3.20	8.57	1.32E-14	26.39
FYN	FYN oncogene related to SRC, FGR, YES (FYN)	1.63	8.86	1.72E-14	26.14
MICB	MHC class I polypeptide-related sequence B (MICB)	1.34	10.74	4.96E-16	30.43
SH2D1B	SH2 domain containing 1B (SH2D1B)	2.61	3.64	1.06E-08	10.27
SHC2	SHC (Src homology 2 domain containing) transforming protein 2 (SHC2)	1.97	7.99	1.30E-15	29.24
ULBP2	UL16 binding protein 2 (ULBP2)	3.29	8.81	6.98E-18	35.59
CSF2	colony stimulating factor 2 (granulocyte-macrophage) (CSF2)	8.78	7.04	2.01E-17	34.33
ICAM1	intercellular adhesion molecule 1 (ICAM1)	7.88	7.68	9.96E-17	32.37
ICAM2	intercellular adhesion molecule 2 (ICAM2)	1.93	5.12	1.03E-08	10.30
IFNAR2	interferon (alpha, beta and omega) receptor 2 (IFNAR2)	1.25	7.9	2.12E-10	14.79
IFNGR1	interferon gamma receptor 1 (IFNGR1)	1.52	12.2	4.57E-15	27.71
IFNGR2	interferon gamma receptor 2 (interferon gamma transducer 1) (IFNGR2)	1.46	10.62	9.86E-15	26.75
IFNB1	interferon, beta 1, fibroblast (IFNB1)	8.54	6.24	7.16E-19	38.25
KIR2DL4	killer cell immunoglobulin-like receptor, two domains, long cytoplasmic tail, 4 (KIR2DL4)	1.49	3.85	1.13E-06	4.98
KIR2DL5A	killer cell immunoglobulin-like receptor, two domains, long cytoplasmic tail, 5A (KIR2DL5A)	2.80	3.39	1.39E-12	20.76
KLRC1	killer cell lectin-like receptor subfamily C, member 1 (KLRC1)	2.05	3.86	5.50E-11	16.38
KLRC3	killer cell lectin-like receptor subfamily C, member 3 (KLRC3)	1.45	2.87	3.23E-09	11.62
HLA-A	major histocompatibility complex, class I, A (HLA-A)	3.07	13.25	2.44E-20	42.41
HLA-E	major histocompatibility complex, class I, E (HLA-E)	3.02	13.8	6.19E-20	41.22
HLA-G	major histocompatibility complex, class I, G (HLA-G)	3.36	15.23	1.34E-20	43.11
PIK3CD	phosphoinositide-3-kinase, catalytic, delta polypeptide (PIK3CD)	1.02	8.73	1.29E-11	18.09
PLCG2	phospholipase C, gamma 2 (phosphatidylinositol-specific) (PLCG2)	1.47	8.94	6.33E-15	27.31
RAC2	ras-related C3 botulinum toxin substrate 2 (rho family, small GTP binding protein Rac2) (RAC2)	1.32	7.77	2.66E-12	19.98
SYK	spleen tyrosine kinase (SYK)	1.75	3.43	6.31E-07	5.64
TNF	tumor necrosis factor (TNF)	6.26	6.24	2.90E-13	22.64
TNFSF10	tumor necrosis factor (ligand) superfamily, member 10 (TNFSF10)	4.92	6.1	3.80E-15	27.93
TNFRSF10B	tumor necrosis factor receptor superfamily, member 10b (TNFRSF10B)	1.12	13.94	4.44E-17	33.37

hsa05322 Systemic lupus erythematosus

GeneName	Description	logFC	AveExpr	adj.P.Val	B
H2AFV	H2A histone family, member V (H2AFV)	-1.70	5.85	4.34E-11	16.65
H2AFX	H2A histone family, member X (H2AFX)	-1.41	13.24	5.61E-15	27.45
H2AFZ	H2A histone family, member Z (H2AFZ)	-1.12	14.28	3.48E-14	25.21
H3F3A	H3 histone, family 3A (H3F3A)	-1.01	14.66	5.74E-15	27.42
C5	complement component 5 (C5)	-2.34	9.38	3.91E-17	33.52
ELANE	elastase, neutrophil expressed (ELANE)	-1.06	4.12	1.02E-04	-0.01
HIST1H2AA	histone cluster 1, H2aa (HIST1H2AA)	-1.47	4.98	1.57E-07	7.21
HIST1H2AB	histone cluster 1, H2ab (HIST1H2AB)	-1.45	9.72	3.99E-12	19.50
HIST1H2AH	histone cluster 1, H2ah (HIST1H2AH)	-1.11	13.15	1.27E-12	20.87
HIST1H2AM	histone cluster 1, H2am (HIST1H2AM)	-1.26	10.25	1.42E-11	17.97
HIST1H2AI	histone cluster 1, H2ai (HIST1H2AI)	-2.48	9.6	1.76E-16	31.68
HIST1H3J	histone cluster 1, H3j (HIST1H3J)	-1.85	8.37	1.03E-09	12.95
HIST1H3H	histone cluster 1, H3h (HIST1H3H)	-1.16	9.18	3.75E-12	19.57
HIST1H3F	histone cluster 1, H3f (HIST1H3F)	-1.06	9.46	8.91E-10	13.11
HIST1H3E	histone cluster 1, H3e (HIST1H3E)	-1.49	11.98	9.89E-12	18.40
HIST1H3D	histone cluster 1, H3d (HIST1H3D)	-1.28	11.09	9.65E-10	13.02
HIST1H3B	histone cluster 1, H3b (HIST1H3B)	-1.81	12	4.81E-14	24.82
HIST1H3A	histone cluster 1, H3a (HIST1H3A)	-1.01	12.65	2.19E-12	20.21

HIST1H4L	histone cluster 1, H4l (HIST1H4L)	-2.10	7.11	2.38E-12	20.11
HIST1H4E	histone cluster 1, H4e (HIST1H4E)	-1.54	11.76	8.21E-12	18.63
HIST1H4D	histone cluster 1, H4d (HIST1H4D)	-2.09	11.07	4.90E-14	24.79
HIST1H4C	histone cluster 1, H4c (HIST1H4C)	-1.44	16.57	5.71E-18	35.83
HIST1H4B	histone cluster 1, H4b (HIST1H4B)	-1.76	13.16	7.36E-09	10.68
HIST1H4A	histone cluster 1, H4a (HIST1H4A)	-1.35	10.47	4.82E-11	16.53
HIST2H2AC	histone cluster 2, H2ac (HIST2H2AC)	-1.01	12.1	2.24E-11	17.44
HLA-DMB	major histocompatibility complex, class II, DM beta (HLA-DMB)	-3.70	7.84	7.50E-17	32.72
HLA-DOB	major histocompatibility complex, class II, DO beta (HLA-DOB)	2.37	6.5	4.61E-13	22.09
C2	complement component 2 (C2)	1.67	3.84	2.28E-07	6.79
C4B	complement component 4B (Chido blood group) (C4B)	2.25	7.07	6.16E-18	35.74
CD40	CD40 molecule, TNF receptor superfamily member 5 (CD40)	1.71	8.21	1.92E-13	23.15
C1R	complement component 1, r subcomponent (C1R)	3.26	12.02	1.35E-22	48.67
C1S	complement component 1, s subcomponent (C1S)	2.87	8.91	2.52E-15	28.43
HIST2H2AA4	histone cluster 2, H2aa4 (HIST2H2AA4)	1.53	10.43	5.60E-16	30.28
TRIM21	tripartite motif-containing 21 (TRIM21)	2.62	9.24	5.09E-18	35.97
TNF	tumor necrosis factor (TNF)	6.26	6.24	2.90E-13	22.64

7.2 Abbreviations

ABC	ATP-binding cassette
Apo	apolipoprotein
ATII	alveolar type II cells
ATF	activating transcription factor
ATP	adenosine triphosphate
BAL	bronchoalveolar lavage
BiP	binding immunoglobulin protein
BSA	bovine serum albumine
CE	cholesterol ester
Cer	ceramide
CFTR	cystic fibrosis transmembrane conductance regulater
COX	cyclooxygenase
Da	Dalton
DIP	desquamative interstitial pneumonia
DSMZ	Deutsche Sammlung von Mikroorganismen und Zellkulturen (German Collection of Microorganisms and Cell Cultures)
DNA	desoxyribonucleic acid
DPLD	diffuse parenchymal lung disease
DPPC	dipalmitoylphosphatidylcholine
ECM	extracellular matrix
EEA	early endosomal antigen
ELISA	enzyme-linked immunosorbent assay
EM	electron microscopy
EMT	epithelial-mesenchymal transition
ER	endoplasmic reticulum
ERK	extracellular signal-regulated kinase
ESI	electrospray ionization
ET	endothelin
FBS	fetal bovine serum
FC	free cholesterol or fold change
FSP	fibroblast-specific protein
g	earth’s gravitational accelaration
GluCer	glucosyl ceramide

GM-CSF	granulocyte macrophage colony-stimulating factor
HA	hemagglutinin
HDL	high density lipoprotein
HRP	horseradish peroxidase
IL	interleukin
ILD	interstitial lung disease
IPF	idiopathic pulmonary fibrosis
JNK	c-Jun N-terminal kinases
LAMP	lysosomal-associated membrane glycoprotein
LB	lamellar body
LPC	lysophosphatidylcholine
LPS	lipopolysaccharide
LXR	liver X receptor
MAPK	mitogen-activated protein kinase
MMP	matrix metalloproteinase
MOI	multiplicity of infection
mRNA	messenger ribonucleic acid
MTT	3-(4,5-Dimethylthiazol-2-yl)-2,5-diphenyltetrazoliumbromid
MS	mass spectrometry
MVB	multivesicular body
NBD	nucleotide binding domain
NF	nuclear factor
NSIP	non-specific interstitial pneumonia
p.	protein sequence
PAP	pulmonary alveolar proteinosis
PBS	phosphate buffered saline
PC	phosphatidylcholine
PE	phosphatidylethanolamine
PG	phosphatidylglycerol
PGE	prostaglandin E
PI	phosphatidylinositol
PLPE	plasmenylethanolamine
PPAR	peroxisome proliferator-activated receptor
PS	phosphatidylserine

PL	phospholipid
qPCR	quantitative polymerase chain reaction
RANTES	regulated upon activation, normal T-cell expressed, and secreted
RDS	respiratory distress syndrome
RIPA	radioimmunoprecipitation assay buffer
RSV	respiratory syncytial virus
SD	standard deviation
SMA	smooth muscle actin
SP	surfactant protein
SPM	sphingomyelin
TC	total cholesterol
TEM	transmission electron microscopy
TGF	transforming growth factor
TLR	toll-like receptor
TMD	transmembrane domain
TNF	tumor necrosis factor
TTF	thyroid transcription factor
UIP	usual interstitial pneumonia
UPR	unfolded protein response
UV	ultraviolet
WT	wildtype
ZO	zonula occludens

7.3 List of publications

Peer reviewed original papers

Thurm T, **Kaltenborn E**, Kern S, Griese M and Zarbock R
SFTPC mutations cause SP-C degradation and aggregate formation without increasing ER stress.
Eur J Clin Invest. 2013 Aug;43(8):791-800.

Zarbock R, Woischnik M, Sparr C, Thurm T, Kern S, **Kaltenborn E**, Hector A, Hartl D, Liebisch G, Schmitz G and Griese M.
The surfactant protein C mutation A116D alters cellular processing, stress tolerance, surfactant lipid composition, and immune cell activation.
BMC Pulm Med. 2012 Mar 29;12:15

Kaltenborn E, Kern S, Frixel S, Fragnet L, Conzelmann KK, Zarbock R and Griese M.
Respiratory syncytial virus potentiates ABCA3 mutation-induced loss of lung epithelial cell differentiation.
Hum Mol Genet. (Oxford University Press) 2012 Jun 15;21(12):2793-806

Hellmich UA, Lyubenova S, **Kaltenborn E**, Doshi R, van Veen HW, Prisner TF and Glaubitz C.
Probing the ATP hydrolysis cycle of the ABC multidrug transporter LmrA by pulsed EPR spectroscopy.
J Am Chem Soc. 2012 Apr 4;134(13):5857-62

Weichert N*, **Kaltenborn E***, Hector A, Woischnik M, Schams A, Holzinger A, Kern S and Griese M. *** equally contributed**
Some ABCA3 mutations elevate ER stress and initiate apoptosis of lung epithelial cells.
Respir Res. 2011 Jan 7;12:4

Engelbrecht S*, **Kaltenborn E***, Griese M and Kern S. *** equally contributed**
The surfactant lipid transporter ABCA3 is N-terminally cleaved inside LAMP3-positive vesicles.
FEBS Lett. 2010 Oct 22;584(20):4306-12

Kaltenborn E, Frixel S, Zarbock R and Griese M.
ABCA3 mutations interfere with ATII cholesterol homeostasis and immune response
Manuscript in preparation